Towards Non-Invasive Health Diagnostics – Profiling the Human Skin Volatile Emissions

Dominik Walkowiak, BSc.

Submitted for the award of MSc.

Supervisor:

Dr Aoife Morrin

School of Chemical Sciences

August 2025

Declaration

I hereby certify that this material, which I now submit for assessment on the programme of study leading to the award of Master of Science is entirely my work, and that I have exercised reasonable care to ensure that the work is original, and does not to the best of my knowledge breach any law of copyright, and has not been taken from the work of others save and to the extent that such work has been cited and acknowledged within the text of my work.

Signed: Dominik Walkowiak

ID No: 23275461

Date: 25.08.2025

Acknowledgements

I'd like to acknowledge my supervisor, Dr Aoife Morrin, for providing me an opportunity to develop my passion in skin research, for continually supporting me and for facilitating my professional growth. I wish you the best going forward and I hope to make you proud in the future!

Special thank you to Mary Ross, Ambrose May and Veronica Dobbyn of the chemistry technical team in DCU. Your time dedicated to all my queries will never be forgotten. More importantly, your support, smiles and attitudes in work have empowered me to keep pushing forward, even during the toughest days.

Thank you to Dr Melissa Finnegan, from my very first year ever in university, to my last day of postgrad, you've always supported me unconditionally and passed down your knowledge. You've shaped me into the researcher I am today and I'm blessed I've you to look up to!

Thanks to all my postgraduate friends in DCU, Aicha, Sophie, Miguel, Rinki, Shalini, Róisín and Helen. Thank you for reminding me what kindness and collaboration really mean.

To my chosen family, Eve, Róisín and Seóna, thank you for your unshakeable loyalty, love, guidance and support. Who would've guessed myself to be at DCU the longest!

Special thank you from the bottom of my heart to Gabby, Jade, Kenza, Sara, Wiktoria, Ciara and Jack. I wouldn't have been able to live a beautiful life without your blessings.

Lastly, thank you to my parents, whose lives of endeavour provided me with the opportunity and privilege of education.

List of Publications and Presentations

Poster Presentations

Walkowiak D. and Morrin A. **Exploring the Healthy Human Volatile Profile,** 9th Annual Chemistry Symposium, Dublin City University, Dublin, Ireland (2024)

Walkowiak D. and Morrin A. **Exploring the Human Skin Volatilome for Wearable Biodiagnostic Applications**, EUChemS 2024 Conference, Dublin, Ireland (2024)

Walkowiak D. and Morrin A. **Exploring the Human Skin Volatilome for Wearable Biodiagnostic Applications**, Insight Scientific Plenary, University College Dublin, Dublin, Ireland (2024)

Walkowiak D. and Morrin A. **Exploring Sorbent Materials Towards Wearable Human Skin VOC Collection**, Conference for Analytical Science in Ireland (CASi), University College Cork, Cork, Ireland (2025)

Table of Contents

DECLARATION II
ACKNOWLEDGEMENTS III
LIST OF PUBLICATIONS AND PRESENTATIONS IV
LIST OF ABBREVIATIONS VIII
LIST OF FIGURES XI
LIST OF TABLES XVII

TOWARDS NON-INVASIVE HEALTH DIAGNOSTICS – PROFILING THE HUMAN SKIN VOLATILE EMISSIONS XIX

CHAPTER 1: HUMAN SKIN EMITTED VOLATILE ORGANIC COMPOUNDS— AETIOLOGY, INTERPLAY, SAMPLING AND ANALYSIS APPROACHES 1

1.1. INTRODUCTION 3

1.2. COMPOSITION OF HUMAN SKIN DERIVED VOLATILE EMISSIONS 6
1.2.1. Transcutaneous movement 7
1.2.2. Cutaneous cellular activity 8
1.2.3. Skin glandular secretions 10
1.2.3.1. Sweat 11
1.2.3.2. Sebum 12
1.2.3.3. Residual skin surface components 13
1.2.4. Skin microbiome 14
1.2.4.1. Bacteria 15
1.2.4.2. Fungi 16
1.2.4.3. Archaea 17
1.2.4.4. Viruses 18
1.2.5. The human exposome 18
1.2.5.1. Nutrition 19
1.2.5.2. Hygienic habits 20
1.2.5.3. Stressor stimuli 21
1.2.5.4. Personal care products 23

1.3. BIOCHEMICAL SIGNIFICANCE OF HUMAN SKIN DERIVED VOLATILE ORGANIC COMPOUNDS 24
1.3.1 Aldehydes 25
1.3.2. Carboxylic acids 27
1.3.3. Ketones 29
1.3.4. Alcohols 30
1.3.5. Aliphatic hydrocarbons 31
1.3.6. Aromatic volatile compounds 32
1.3.7. Nitrogen containing compounds 32
1.3.8. Sulphur containing volatiles 33

1.4. APPROACHES FOR CAPTURING SKIN DERIVED VOLATILE EMISSIONS 34
1.4.1 Direct contact sampling 34
1.4.1.1. Cotton fabrics and swabs 35
1.4.1.2. Silica materials 35
1.4.1.3. Tape Stripping 36

1.4.1.4. Biocompatible polymers 36
1.4.2. Contactless volatile emissions sampling 37
1.4.2.1. Static headspace solid phase microextraction fibres 38
1.4.2.2. Passive flux samplers 39
1.4.2.3. Patch type sampling 39
1.4.2.3.1. Tenax Trapping Agent 40
1.4.2.3.2. Metal organic frameworks 40
1.4.3. Plethysmography chambers 41

1.5. ANALYSIS WORKFLOWS FOR SKIN DERIVED VOLATILE ORGANIC COMPOUND EMISSIONS 42
1.5.1. Offline analysis 42
1.5.1.1. Gas chromatography-mass spectrometry 43
1.5.1.2. Thermal desorption gas chromatography mass spectrometry 44
1.5.1.3. Two dimensional gas chromatography mass spectrometry 44
1.5.2. Online analysis 45
1.5.2.1. Proton transfer reaction time of flight mass spectrometry 46
1.5.3. Data pre-processing 46
1.5.4. Biological interpretation 47

1.6 CONCLUSION 48

1.7 REFERENCES 49

THESIS OUTLINE 67

CHAPTER 2: EXPLORING THE STABILITY OF THE HEALTHY HUMAN SKIN VOLATILE PROFILE 69

2.1. INTRODUCTION 71

2.2. MATERIALS AND METHODS 74
2.2.1. Chemicals 74
2.2.2. Participant recruitment 74
2.2.3. Participant biophysical skin barrier function assessment 74
2.2.4. Participant skin volatile emission sampling 75
2.2.5. 2% salicylic acid solution preparation and application 76
2.2.6. Gas chromatography-mass spectrometry 77
2.2.7. Data analysis 77

2.3. RESULTS AND DISCUSSION 78
2.3.1. Characterising the healthy human skin barrier function 78
2.3.2. Characterising skin volatile emissions across the 3 healthy participants 81
2.3.3. Correlation and cluster analysis of temporal skin VOC and barrier function data 84
2.3.4. Influence of acidic compounds on skin volatile profiles 89
2.3.5. Influence of carbonyl compounds on skin volatile profiles 91
2.3.6. Influence of 2% salicylic acid skin treatments on the skin volatile profile 92
2.3.6.1. Characterising the skin volatile profile after 2% (w/w) SA treatment 94
2.3.6.2. Influence of salicylic acid on the skin barrier function and volatile emissions 97
2.3.6.3. Characterising salicylic acid treated skin volatile emissions over time 98

2.4.CONCLUSION **101**

2.5. REFERENCES **102**

CHAPTER 3: EXPLORING SORBENT MATERIALS AS PLANAR FILMS TOWARDS WEARABLE SKIN VOC SAMPLING PLATFORMS WITH GC-MS ANALYSIS **109**

3.1. INTRODUCTION **111**

3.2. MATERIALS AND METHODS **114**
3.2.1. Materials 114
3.2.2. HS-SPME of skin volatiles 114
3.2.3. Neat VOC standard solution preparation 114
3.2.4. Standard calibration solutions preparation for HS-SPME sampling 115
3.2.5. Standard calibration solutions preparation for liquid injection 117
3.2.6. Tenax TA and Tenax TA/divinylbenzene planar film preparation 120
3.2.7. Polydimethylsiloxane film preparation 120
3.2.8. Sorbent film evaluation in the HS of standard VOC solutions 121
3.2.9. Solvent extraction 124
3.2.10. Skin VOC sampling using sorbent films 124
3.2.11. Gas chromatography-mass spectrometry 125
3.2.12. Data analysis 126

3.3. RESULTS AND DISCUSSION **127**
3.3.1. HS-SPME standard VOC sampling 127
3.3.2. GC-MS analysis of skin emitted compounds 130
3.3.3. Tenax TA sorbent film testing 133
3.3.4. Tenax TA/divinylbenzene sorbent film testing 137
3.3.5. PDMS planar film sorption testing 141
3.3.6. Comparison of film sorption between Tenax TA and Tenax TA/DVB 142
3.3.7. Sorbent film testing on skin 144

3.4 CONCLUSION **146**

3.5. REFERENCES **147**

CHAPTER 4: CONCLUSIONS AND FUTURE WORK **151**

4.1. CONCLUSION AND FUTURE WORK **152**

4.2. REFERENCES **154**

APPENDIX **A1**

List of Abbreviations

% (v/v)	Percentage volume by volume
% (w/w)	Percentage weight by weight
%RSD	Relative standard deviation percentage
°C	Degrees Celsius
2-EH	2-ethyl-1-hexanol
4-OPA	4-oxopentanal
6-MHO	6-methyl-5-hepten-2-one
ALS	Automatic liquid sampler
AM/PM	Morning/Evening
AMS	Allyl methyl sulphide
ATP	Adenosine triphosphate
atm	Atmosphere
C. acnes	*Cutibacterium acnes*
CAR	Carboxen
CO_2	Carbon dioxide
DADS	Diallyl disulphide
DCM	Dichloromethane
DNA	Deoxyribonucleic acid
DVB	Divinylbenzene
ECM	Extracellular matrix
EtOH	Ethanol
FFAs	Free fatty acids
fmol	Femtomole
GA	Geranyl acetone (6,10-dimethyl-5,9-undecadien-2-one)
GC x GC	Two dimensional gas chromatography
GC-MS	Gas chromatography
H^+	Hydrogen ion
HS-SPME	Headspace solid-phase microextraction
kHz	Kilohertz
K_{OA}	Octanol-air partition co-efficient
kPa	Kilopascal
LOD	Limit of detection

LOQ	Limit of quantification
Log_P	Molecular lipophilicity measure
MAR	Missing at random
MCAR	Missing completely at random
MCFAs	Medium chain fatty acids
MHz	Megahertz
MNAR	Missing not at random
MOF	Metal-organic framework
mg	Micrograms
NH_3	Ammonia
NIST	National Institute of Standards and Technology
NMF	Natural Moisturising Factor
NO_2	Nitrogen dioxide
NS_{VOC}	Neat standard compound solution
n	Number of samples
ng	Nanograms
O_3	Ozone
PAHs	Polyaromatic hydrocarbons
PC	Principle component
PCA	Principle component analysis
PCP	Personal care product
PCR	Principle component regression
PDMS	Polydimethylsiloxane
PFS	Passive flux sampler
ppb	Parts per billion
ppt	Parts per trillion
PTR	Proton transfer reaction
R^2	Co-efficient of determination
RH	Relative humidity
RI	Retention index
ROS	Reactive oxygen species
r	Spearman correlation co-efficient
rRNA	Ribosomal ribonucleic acid

S. *epidermis*	*Staphylococcus epidermis*
SA	Salicylic acid
SBS	Sick building syndrome
SC	Stratum corneum
SCFAs	Short chain fatty acids
SCH	Stratum corneum hydration
SD	Standard deviation
SLR	Simple linear regression
SQ	Squalene
SspH	Skin surface potential hydrogen
SS_{aq}	Stock solution (aqueous)
SS_{Hex}	Stock solution (hexane)
TAcids	Total carboxylic acids
TCA	Citric acid cycle (glycolysis)
TD	Thermal desorption
TDC	Tissue dielectric constant
TEWL	Trans-epidermal water loss
TIC	Total ion count
TOF	Time-of-flight
TVOCs	Total volatile organic compounds
UV	Ultraviolet radiation
VOCs	Volatile organic compounds
µg	Micrograms
µL	Microliters

List of Figures

Figure 1.1. Schematic representation of human skin derived volatile organic compound emissions and their concentration gradient between a human body and encompassing atmosphere.

Figure 1.2. Sweat rate, SC thickness (in cell layers) and transcutaneous skin ethanol emissions for the dorsum hand, fingers, toe and ear. Darker colour represents lower ethanol emission rates while brighter colour represents higher emission rates. Figure reproduced from Iitani et al.

Figure 1.3. Schematic of young skin, aged skin and photodamaged skin features, including the shedding of skin cells, skin lipid peroxidation processes and VOC breakdown products. Figure adapted from Orioli and Dellambra.

Figure 1.4. Contribution of glandular secretions and microbiome metabolism to skin volatile formation, excreted during physical exercise or during increased skin perspiration. Figure reproduced from Chang and Wang.

Figure 1.5. Schematic of skin lipid peroxidation on **(a)** fatty acids and **(b)** SQ. The primary reactions are shown in red while secondary reactions are in blue (Cis-hexadec-6-enoic acid is synonymous with sapienic acid). Figure adapted from Morrison et al.

Figure 1.6. The range of available biochemical pathways the skin microbiome may access towards formation of volatile compounds. Figure reproduced from Vesalova et al.

Figure 1.7. Depiction of fungi induced VOC formation events through metabolism mechanisms of substrates metabolised by *Malassezia* species. Figure adapted from Rios Navaro et al.

Figure 1.8. Factors of the human exposome (host characteristics and external factors) influencing the skin microenvironment. Figure reproduced from Moitinho-Silva et al.

Figure 1.9. Frequency of showering altering breath and skin volatile emission rates due to the effects of personal hygiene on the skin microenvironment. Figure reproduced from Wang et al.

Figure 1.10. The influence of airborne pollutant species and photoactivated airborne species initiating a chain of ROS induced effects such as lipid peroxidation, antioxidant depletion and accumulation of skin cellular damage over time. Figure reproduced from Araviiskaia et al.

Figure 1.11. Schematic of chemical transport model of compounds contacting the skin showing resulting in direct dermal uptake, then transfer to systemic circulation, given high enough partition co-efficient, K. Figure reproduced from Wang et al.

Figure 1.12. Schematic of the biochemical pathways for volatile C_9 compound formation using triglyceride of oleic acid as a substrate and atmospheric ozone as the initiator. Figure reproduced from Zhou et al.

Figure 1.13. The saturated and monounsaturated FFAs found in the human skin. Figure reproduced from Knox and O'Boyle.

Figure 1.14. General structures of phospholipid membrane subclasses, phosphoglycerides and sphingomyelins. Figure reproduced from Knox and O'Boyle.

Figure 1.15. Chemical structures of Alliin (ingested in garlic), converting to allicin which may be emitted from the skin as AMS. DADS can also be converted into this volatile compound and emitted from the skin. Figure adapted from Hiramoto et al.

Figure 1.16. (a) PDMS sampling loop attached to the wrist (left) and ankle (centre) reproduced from Roodt et al. **(b)** Modified silicone rubber band for skin VOC sampling towards GC based identification of tuberculosis associated compounds (right), reproduced from Makhubela et al.

Figure 1.17. (a) Plethysmography chamber design schematic for sampling of whole body VOC emissions. Adaptations also exist for isolation of breath VOCs. **(b)** Image of the plethysmography chamber. Figure reproduced from Rankin-Turner and McMeniman.

Figure 1.18. A GC x GC chromatograph of a skin sample obtained from the hand of a 25 year old male. Figure reproduced from Cuzuel et al.

Figure 2.1. Schematic of human skin viewed in cross-section, with skin resident microbiota inhabiting the invaginations and appendages of the skin (right). Microorganism propagated skin VOC formation from available substrates found on the skin (left). Figure adapted from Grice and Segre (left)[8] and Rios-Navarro et al. (right)[9].

Figure 2.2. (a) Hanna Instruments HALO flat glass probe measuring skin surface pH at the volar forearm and **(b)** SPME fibre housed in a glass headspace affixed to the volar forearm.

Figure 2.3. (a) Volar forearm sspH measurements, **(b)** TDC measurements, **(c)** TEWL measurements and **(d)** SCH measurements in box plots comparing every AM and every PM sample, per participant. Box and whiskers are calculated using the Tukey method. P values are shown in **Table A2.1.** due to no significant trends shared across all participants.

Figure 2.4. (a) Volar forearm sspH measurements, **(b)** TDC measurements, **(c)** TEWL measurements and **(d)** SCH measurements per participant collected on volar forearm daily over 10 days of study. Error bars represent the SD of the replicate data within each sampling day.

Figure 2.5. Bar charts of (**a)** % frequency of each VOC recovered (n=20) recovered from P1, P2 and P3, **(b)** Mean abundance of each recovered VOC per participant (log scale). Bar chart **(b)** only displays abundances for VOCs detected > 30% frequency. Error bars represent the SD of mean abundances recovered.

Figure 2.6. Box and whisker plot of each recovered VOC abundance from Figure 2.5 that was considered endogenous (log scale). Box and whisker plots calculated using the Tukey method.

Figure 2.7. (a) Correlation matrix for each variable collected from P1 skin (n=20) **(b)** Correlation matrix for each variable collected from P2 skin (n=20) **(c)** Correlation matrix for each variable collected from P3 skin (n=20). Blue indicates a positive correlation and red indicates a negative correlation, with spearman correlation co-efficient (*r*) inside each box. Boxes with X represent missing indicating an absence of correlation analysis.

Figure 2.8. (a) Scores plot PC1 and PC2 for collected skin data of each participant (n=60) and **(b)** its corresponding loadings plot. Normalised data and the correlation matrix were used for the PCA. Each sample in **(a)** is coloured and labelled according to the participant from which the data is collected. The length and direction of the arrows in **(b)** represent the contribution of each variable onto each point in the scores plot. The tabulated output is provided in Table A2.2.

Figure 2.9. Heatmap showing the normalised peak area of each acid VOC recovered from the volar forearm in AM samples (LHS) and PM samples (RHS) across days of the study, for each participant (n=60). SspH and its SD across the 3 participants is shown above each heatmap. The legend shows a bright colour as the maximum abundance recovered in the study for that compound while a darker colour indicates a lower or absent abundance value for that compound, within a day.

Figure 2.10. (a) Scatter plots of acetic acid abundance as a function of sspH per each participant. **(b)** Scatter plots of total acid abundance as a function of sspH per each participant. Simple regression analysis output is shown in Table A2.3. and Table A2.4.

Figure 2.11. Heatmap showing the normalised peak area of each labelled VOC recovered from the volar forearm in AM samples (LHS) and PM samples (RHS) across the 3 participants (n=60). The legend shows a bright colour as the maximum abundance recovered in the study for that compound while a darker colour indicates a lower or absent abundance value for that compound, within a day.

Figure 2.12. (a) % Frequency of each VOC recovered from laboratory HS air control samples (red, n=9) and SA solution HS (orange, n=3) samples. **(b)** Abundance of each VOC recovered from laboratory HS air control samples (red, n=9) and SA solution HS (orange, n=3) samples (log scale). Error bars represent SD of mean abundances per each compound recovered.

Figure 2.13. (a) % Frequency of each VOC recovered from P1 skin samples (blue, n=9), skin samples 5 min after carrier solution (light brown, n=6) and 5 min after 2% (w/w) SA treatment (dark brown, n=6). **(b)** Mean abundance of each VOC recovered from P1 skin samples (blue, n=9), skin samples collected 5 min after carrier solution (light brown, n=6) and skin samples collected 5 min after 2% (w/w) SA treatment (dark brown, n=6), in log scale. Error bars represent SD of mean abundances for each compound.

Figure 2.14. Box and whisker plots comparing skin volatile emissions and skin barrier function before and 5 min after 2% (w/w) SA treatment. **(a)** Compared to unperturbed skin, 2% (w/w) SA treatment significantly decreases sspH ($p=0.0001$), **(b)** significantly up-regulates total acid (TAcid) VOC emissions ($p=0.0021$) **(c)** up-regulates volatile acids recovery (abundances), particularly for acetic acid, significant up-regulation in emissions ($p=0.0131$) is observed. **(d)** Volatile aldehydes, ketones and alcohol VOC emissions remained undisturbed with no significant differences before and after 2% (w/w) SA application. Boxes and whiskers were calculated using the Tukey method.

Figure 2.15. (a) Connected scatterplots of SspH measurements over time for P1 untreated skin (grey, n=6) and during 2% (w/w) SA treatments (red, n=6). **(b)** Acetic acid abundance during 2% (w/w) SA treatments (n=6). **(c)** TAcid abundance during 2% (w/w) SA treatments (n=6), in log scale. **(d)** TVOC abundance during 2% (w/w) SA treatments (n=6), in log scale. Each unique colour represents data collected during each of the n=6 SA treatment experiments.

Figure 3.1. SEM micrographs of Tenax TA beads, highlighting high surface areas optimised for VOC adsorption capabilities. Figure reproduced from Alfeeli et al.

Figure 3.2. Freshly prepared **(a)** Tenax TA film cutting, **(b)** Tenax TA/DVB film cutting and **(c)** PDMS film cutting. All were cut using a 38 mm diameter circular stamping press.

Figure 3.3. (a) Experimental set-up in chamber for testing sorbent films and **(b)** glass HS vial (20 cm^3) used for solvent extraction from the sorbent films following exposure. Solvent: 2 cm^3 hexane.

Figure 3.4. Image of the VOC sampler worn on the participant volar forearm during the study (left) for wearable skin VOC collection and the corresponding schematic of the VOC sampler structure underneath the worn plaster (right).

Figure 3.5. A representative raw chromatograph obtained from P1 volar forearm HS-SPME skin sample. Table 3.5. lists the identified compounds from (n=3) SPME P1 skin samples.

Figure 3.6. Overlaid raw chromatographs obtained for 5 lowest concentrations prepared from dilutions of SS_{Hex}. Upper concentrations were excluded for clarity in the lower range of the Y-axis.

Figure 3.7. Scatterplots and applied linear regressions for VOC abundances recovered from mixed VOC solutions prepared from SS_{Hex} at 7 different concentrations.

Figure 3.8. Bar charts of each VOC abundance recovered from each of the NS_{aq} solutions (10 cm^3) used to test Tenax TA sorbent film (n=3). Solutions (10 cm^3) were added to the chamber (850 cm^3) with a specified sorbent film. Films were left for 2 h in the chamber before solvent extraction and GC-MS analysis.

Figure 3.9. Bar charts of each VOC abundance recovered from each of the NS_{aq} solutions (10 cm^3) used to test Tenax TA/DVB sorbent film (n=3). Solutions (10 cm^3) were added to the chamber (850 cm^3) with a specified sorbent film. Films were left for 2 h in the chamber before solvent extraction and GC-MS analysis.

Figure 3.10. A representative raw chromatograph obtained from P1 volar forearm wearable Tenax TA skin sample (black) and P1 volar forearm wearable PDMS skin sample (red). The sampling duration used for both films was 8 h. The films were solvent extracted immediately after sampling using 2 cm^3 hexane for ALS-GC-MS analysis (n=3).

List of Tables

Table 3.1. Densities and masses of each VOC in the SS_{aq}. Using serial dilutions, 1/3375 dilution and 1/50,625 dilutions of the SS_{aq} were selected for triplicate 20 cm^3 HS-SPME analysis and comparison to HS-SPME skin samples. Bolded values represent importance towards results.

Table 3.2. Densities and calculated masses of VOC in NS_{VOC} and SS_{Hex}, and concentrations of all VOCs in SS_{Hex}.

Table 3.3. Masses of each VOC/L for each specified dilution of SS_{Hex}.

Table 3.4. Masses of each VOC in each of the NS_{aq} solutions (10 cm^3) used to test the different sorbent films. Solutions (10 cm^3) were added to the chamber (850 cm^3) with a specified sorbent film. Films were left for 2 h in the chamber before solvent extraction and GC-MS analysis.

Table 3.5. Average abundances and SD of VOCs recovered from the HS above skin, collected via HS-SPME sampling (HS volume 3cm^3; n=3), and average abundances of VOCs recovered from the HS above NS_{aq} solutions (1 cm^3) at 2 dilutions (HS volume 20 cm^3; n=3).

Table 3.6. Average abundances and SD of VOCs recovered from each of the NS_{aq} solutions (10 cm^3) used to test Tenax TA sorbent film (n=3). Solutions (10 cm^3) were added to the chamber (850 cm^3) with a specified sorbent film. Films were left for 2 h in the chamber before solvent extraction and GC-MS analysis. n/d=not detected.

Table 3.7. Average abundances and SD of VOCs recovered from each of the NS_{aq} solutions (10 cm^3) used to test Tenax TA/DVB sorbent film (n=3). Solutions (10 cm^3) were added to the chamber (850 cm^3) with a specified sorbent film. Films were left for 2 h in the chamber before solvent extraction and GC-MS analysis. n/d=not detected.

Table 3.8. Comparison of average abundances of recovered compound, between the prepared Tenax TA and Tenax TA/DVB films. PDMS films are not shown, due to lack of compound identifications from their chromatographs.

Table 3.9. Comparison of recovered isopropyl palmitate from P1 volar forearm HS-SPME skin and from the solvent extraction of a PDMS film worn on P1 volar forearm. GC chromatographs were obtained through a 2 min SPME desorption in the GC inlet or through direct liquid injections with ALS. No SD is shown due to n=2 samples.

Towards Non-Invasive Health Diagnostics – Profiling the Human Skin Volatile Emissions

Dominik Walkowiak

Human skin constantly emits volatile organic compounds (VOCs) reflecting underlying biochemical processes, resident microbial activity and environmental influences. Current literature highlights need for standardisation of skin VOC collection and analysis. The myriad of approaches employed adds to variability of skin VOC profiles reported. Addressing this, the present work explores skin derived VOCs, where Chapter 1 highlights interplay amongst metabolic processes, microbial activity, environmental conditions and their impacts on recovered VOC profiles.

Chapter 2 explores skin VOC profile stability within and across different participants over time, towards understanding factors influencing healthy skin VOC profiles. Headspace solid-phase microextraction (HS-SPME) fibres were used for non-invasive volar forearm VOC collection with gas-chromatography mass-spectrometry (GC-MS) analysis. Biophysical parameters (skin surface pH, tissue dielectric constant, transepidermal water loss) were collected alongside VOC samples to investigate correlations. Resulting data highlighted stability within a single participant over the sampling duration whilst showing a greater variance between different participants.

Chapter 3 introduces a new skin VOC sampling method using planar films (instead of SPME fibres) with solvent extraction for GC-MS analysis. Merits include ‘cost-effectiveness’ and ‘ease of use’ compared to HS-SPME unit used by our group to date. Three free-standing sorbents (polydimethylsiloxane, Tenax-TA, divinylbenzene) were explored for their ability to retain VOCs from gas HS containing VOC standards. Skin VOC collection using these samplers was explored by integrating these into a wearable format and applying on volar forearm.

Chapter 4 evaluates conclusions from this thesis, summarising key findings and offering fresh perspectives for this field. This work provides foundation for evaluating VOC capture material performance, with high specificity and reproducibility, whilst addressing critical gaps in current skin VOC workflows. Furthermore, this work introduces a wearable and scalable skin VOC collection platform, allowing decentralised VOC collection, towards increasing skin VOC study cohorts for high quality results within this emerging field.

Chapter 1: Human skin emitted volatile organic compounds— aetiology, interplay, sampling and analysis approaches

Abstract

The skin is a constant source of volatile organic compounds (VOCs) that can be used as non-invasive probes, containing valuable physiochemical information about an individual's health or environment. Formed near or at the skin surface through an array of diverse and dynamic biochemical processes, over 600 compounds have been reported to be emitted as volatile from the skin. Even though the skin presents an easily accessible and large surface area for VOC sampling, it remains unknown to which extent these compounds can be signatures of health and disease. When considered together, these compounds emanating from the skin are collectively known as a skin volatilome. Based on these skin VOC profiles, an application for wearable monitoring or diagnostic devices becomes apparent. However, the complexity of the skin volatilome, influenced by both endogenous and exogenous sources, poses challenges for accurate analysis and interpretation. Addressing these areas, this review aims to outline the recent advancements in the knowledge of biochemical origin for commonly reported skin VOCs, as well as their capture, or sampling approaches, while outlining analysis techniques, along with possible opportunities to harness their tremendous utility as non-invasive health cues.

1.1. Introduction

Skin serves as a protective barrier which interfaces the internal organism with the external environment, alongside concomitant homeostatic functions[1]. Recently, human skin has garnered attention as a valuable source of physiochemical information, not only pertaining to cutaneous status but also, more recently, to local and systemic metabolic states[2–5]. A recent approach to harnessing this biochemical information involves examining low molecular weight, by- and end- stage metabolic molecules known as volatile organic compounds (VOCs)[6].

A defining characteristic of VOCs is their high vapour pressure at ambient room temperatures and pressures (i.e., >0.01 kPa at 20°C)[7,8], favouring conversion into the gas phase at these conditions[9]. Currently, it is known living organisms continuously produce a diverse range of VOCs, originating from different metabolic and environmental processes collectively known as a volatilome[10]. Driven by Gibbs free energy gradient, VOCs tend to diffuse from regions of high partial pressures toward regions of lower partial pressure, in a stochastic manner[11,12] as depicted in Figure 1.1.

Generally, for skin VOC emissions and within the context of this review, the organism is considered to be the area of high concentration of these small metabolic molecules, while the encompassing atmosphere is regarded as the area of lower concentration. While the total human skin volatilome is thought to have some similarities across individuals, it is also proposed to possess person-to-person variance, specifically in terms of the variety of unique compounds and their relative abundances[13,14].

Reported skin-derived VOCs encompass a diverse range of by- and end-products, including aldehydes, carboxylic acids, ketones, alcohols, esters, ethers, aliphatic and aromatic hydrocarbons, nitrous and sulphurous VOCs[4,10,13,15–27]. Differentiation in volatile profiles observed amongst individuals is thought to be attributed to both endogenous factors (genetic predisposition, biological age[16], gender[18], ethnicity) and exogenous factors (environmental conditions, dietary habits[22], physical and psychological stress states[21], pollutant incidences[23] or personal care product (PCP) use[28]), where these variables collectively make up the human exposome[21,29].

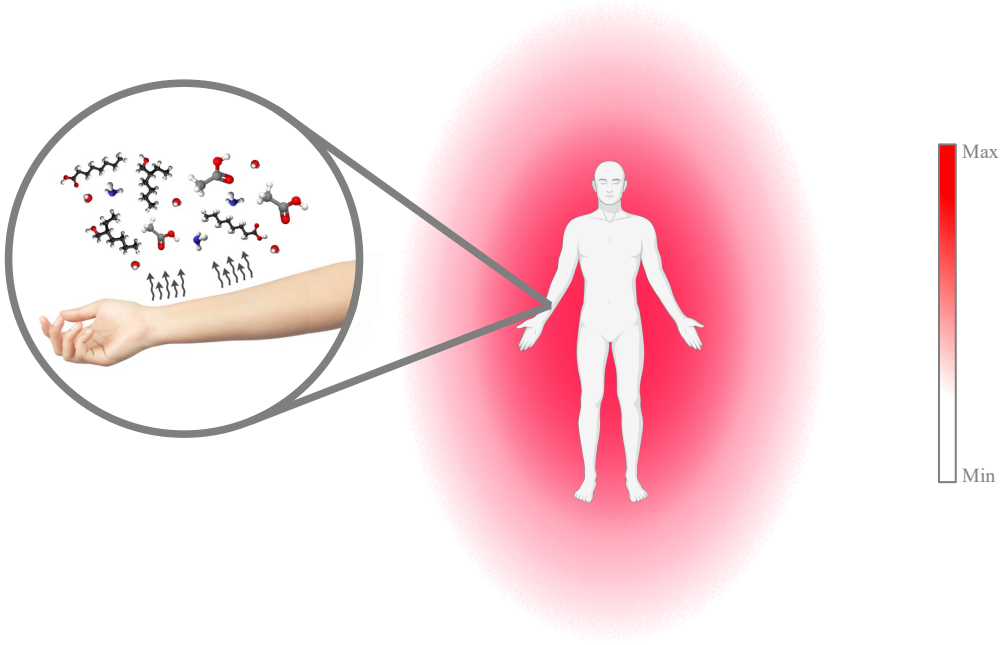

Figure 1.1. Schematic representation of human skin derived volatile organic compound emissions and their concentration gradient between a human body and encompassing atmosphere.

The human integumentary system forms the largest organ of the body, composed of three main skin layers, pilosebaceous units, sweat glands, and nails[20,30]. The skin, itself composed of superficial epidermis, dermis and hypodermis, undertakes a diverse set of critical roles including pathogen and radiation defence, thermal homeostasis, vitamin D synthesis, and prevention of systemic water loss[1,31]. This organ system is closely interlinked with all other systems in the body, functioning as the body's most sophisticated stimuli responsive biosensor. Other functions include chemo-signalling roles[24,32], immunological modulations[1] and reactive oxygen species (ROS) mitigation[33].

Skin secretions from these pores and glands support the skin, towards maintaining its integrity and function[1]. Together, these superficial irregularities with glandular secretions form into a rough surface called the stratum corneum (SC) which is colonised by microorganisms shortly after birth[24,32]. Interacting with these are residual skin surface components (RSSCs), a collective term used to address superficial layers of skin, sebum, residues of sweat, small quantities of intercellular lipids, corneocyte debris, proteolytic products of filaggrin and components of natural moisturising factor (NMF) present on the skin surface[34–36].

Skin VOC emissions occur as by- and end-products from these aforementioned processes, compounded by the interplay of these variables amongst each other. Moreover, external stimuli such as PCP usage may exceed endogenous skin volatile emissions, by several orders of magnitude[10,17]. These factors are important to understand in the context of endogenous volatile emission profiling. Towards this, inter-participant and intra-participant differentiation, along with meaningful future prospects are discussed throughout the text.

Approaches to skin VOC collection range from direct contact sampling using biocompatible materials[26], to employing contactless (non-invasive) VOC collection using organic adsorbent materials. For analysis, analytical instrumentation used by most researchers are gas chromatographic systems, with most approaches varying analyte separation parameters and concurrent types of detectors employed. Gas chromatography-mass spectrometry (GC-MS) is currently a gold standard for separation and analysis of these complex gaseous mixtures derived from the skin.

A large experimental procedural disparity exists within the published literature resulting from these varied collection and analysis approaches. Therefore, a main consideration for this literature review is the human skin VOC aetiology for each relevant compound. Subsequent considerations include the types of capture materials and methods employed currently, in combination with instrumentation used for separation and analysis. Future multi-omics based perspectives taking skin VOC emissions into account may prove to be an invaluable aid to improve medical outcomes.

1.2. Composition of human skin derived volatile emissions

While human skin is commonly recognised as a continuous source of VOC emissions[23], a closer examination reveals complex interplay and feedback loops contributing to overall skin volatile emissions. The metabolic origins of many VOCs remain contested and differentiation between exogenous, mixed or endogenous sources remains a challenge. This difficulty arises from advancements uncovering complex interplay between endogenous and environmental variables implicated in skin VOC emissions. A 2022 review found 40% of identified 'disease associated' skin derived VOCs overlapped with compounds associated with pollutant or external sources[37]. This is strong incentive to examine the different mechanisms and pathways through which these skin volatile emissions arise.

Moving up through the skin layers, the transcutaneous movement of compounds is a notable contributor to small metabolite emissions. Small compounds from systemic circulation may diffuse through blood vessels (vasculature) moving through the skin layers, releasing into the environment in the form of skin volatile emissions[38].

Volatile emissions may also arise from constant cutaneous cellular activity within the skin. Viable skin cells continually metabolise available substrate for energy. This process is tightly interlinked with skin cellular desquamation, or the constant process of shedding dead skin cells. Desquamation contributes further to overall skin VOC emissions as viable cells differentiate, move through the skin layers releasing their breakdown products as substrate for volatile compounds[2,39].

Skin glandular secretions, particularly from eccrine, sebaceous, and apocrine glands, contribute substantially to skin volatile profiles[16]. Constituents of the skin microbiome then metabolise these secretions, further generating VOCs at the skin surface. This significantly impacts the overall skin volatile emissions[10].

Understanding these different contributing matrices to the skin VOC emissions unlocks potential to harness these small molecules for bio-diagnostic applications. At present, VOC-based discriminations is difficult as VOC abundances and compositions are highly dependent on individual systemic, microbial and behavioural conditions[2,10]. Furthermore, each of the discrete sources contribute to the perceived total volatile profile in varying proportions, based on sampling area[6], ambient conditions, VOC capture materials and their subsequent analysis workflows.

1.2.1. Transcutaneous movement

The entire skin surface area of approximately 1.8 m^2 may release VOCs where the number of SC layers, vasculature density and activity of skin glands affect the amount of compounds from a transcutaneous origin[38]. VOCs may passively diffuse from blood and red blood cells, across skin layers, involving transfer from the systemic circulation followed by a bioaccumulation in dermal and epidermal tissues, before being emitted from the skin surface[12,40]. Inversely, exogenous compounds may bioaccumulate and then undergo subsequent re-emission from the skin.

Small molecules such as acetone, acetic acid, CO_2, NH_3, ethanol (EtOH) have been reported to be part of the healthy skin emissions. These may be delivered to the surface transcutaneously via skin layer diffusion from capillary rich dermal layers within the skin[38].

Furthermore, in 2021 Longo et al. identified 324 unique VOCs in blood samples, where 80 were common across participants[41]. Of these, abundant VOCs found emanating from human blood included acetic acid, acetone, hexane, hexanal, heptanal, 2-heptanone. These compounds overlap with those commonly identified as 'skin-derived'.

Generally, the larger the compound is the less likely it is to originate from the systemic circulation. Figure 1.2 shows the distribution of EtOH gas emitted from the skin of dorsal hand, fingers, toe and ear. An increase in EtOH emissions from the skin appears to be inversely proportional to sweat gland activity, while following up-regulating with decreasing SC layers.

	dorsum	fingers	toe	ear
sweat rate ($g \times m^{-2} \times h^{-1}$)	126	86	149	N.D.
stratum corneum (cell layer)	25±11	50±10	55±14	7±2
skin gas EtOH distribution	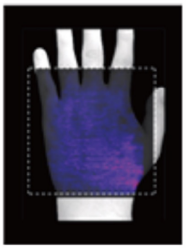			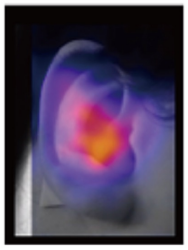

Figure 1.2. Sweat rate, SC thickness (in cell layers) and transcutaneous skin ethanol emissions for the dorsum hand, fingers, toe and ear. Darker colour represents lower ethanol emission rates while brighter colour represents higher emission rates. Figure reproduced from Iitani et al.[38]

Toma et al. corroborated these findings showing the skin sampling location significantly impacts the abundances of ethanol recovered. The external ears and eyelids showed promising stability for systemic ethanol monitoring due to their lower sweat gland density (≈140 spots/cm²) compared to forearms (≈225 spots/cm²)[40]. Low densities of sweat glands in the external ear area were proposed as monitoring sites for transcutaneous ethanol emissions as response to alcohol intake. In contrast to the ears and eyelids sampling areas with thicker skin have lower potential for monitoring compounds in systemic circulation, such as the arms, legs and upper back.

Understanding these dermal variations is crucial for developing robust VOC-based monitoring/diagnostic tools, as transcutaneous emissions may provide continuous, non-invasive insights into systemic metabolic processes and disease states[2,38,40,41]. Addressing this, it is paramount that examined areas of the skin selected for VOC analysis should be supported by measurements of SC thickness, skin surface pH (sspH), SC hydration (SCH) and local tissue dielectric constant (TDC) values. This probe-based information helps take into account skin structure at the sampling site.

1.2.2. Cutaneous cellular activity

Desquamation, a constant 'shedding' of the epidermis involving cell proliferation and differentiation[42], impacts VOC emissions by maintaining a steady release of cellular metabolites and RSSC based materials. Furthermore, all viable cells present in the skin undergo their own range of cellular metabolism, where their excrements may be recovered as volatile compounds. An example of this is VOC production as by- and end-products of ATP utilisation. Of these living cells, keratinocytes and melanocytes are the most understood contributors, albeit this field is currently in its infancy.

The avascular epidermis consists of a basal layer of epithelial cells (keratinocytes) producing keratin, a fibrous protein that gives hair, nails, and skin their structure, along its hydrophobic properties[42]. Over time those keratinocytes migrate towards SC and differentiate into corneocytes, which are non-nucleated cutaneous cells enriched by sebaceous and intercellular lipids[33]. This cellular migration contributes to VOC production through both active and passive processes. During this process, excreted intercellular fatty compounds are composed of squalene (SQ), triglycerides, ceramides and free fatty acids (FFAs)[1,43], often referred to collectively as the human skin surface lipids. These deposited materials enrich the SC with RSSCs as available substrates towards VOC emissions as depicted in Figure 1.3.

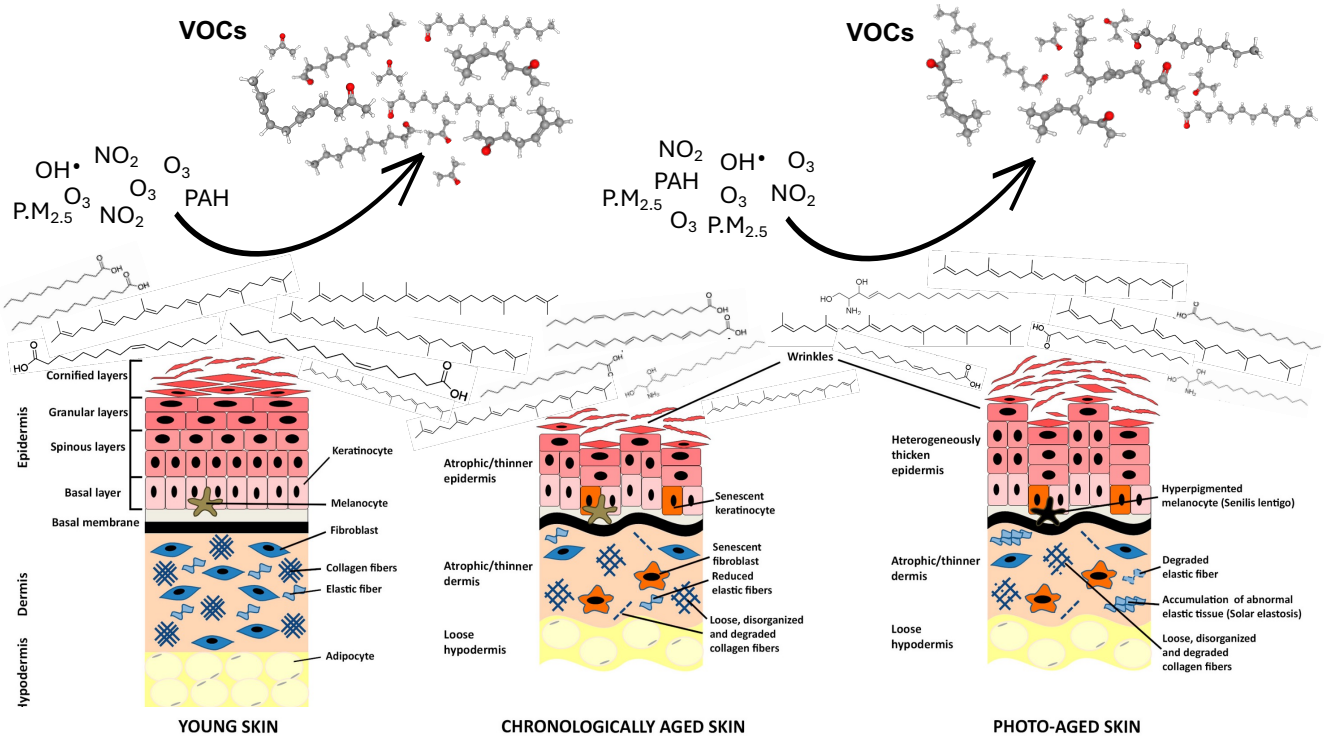

Figure 1.3. Schematic of young skin, aged skin and photodamaged skin features, including the shedding of skin cells, skin lipid peroxidation processes and VOC breakdown products. Figure adapted from Orioli and Dellambra[44].

Amongst these keratinocyte intercellular lipids, which are expelled to the extracellular matrix (ECM) of stratum lucidium, are arachidonic acid and linoleic acid. These FFAs have been reported to undergo lipid peroxidation into the ageing associated VOC, 4-hydroxynonenal[45].

A disturbed desquamation rate is often associated with skin damage such as sunburn or alkalinisation of the skin barrier (pathophysiology for psoriasis, atopic dermatitis, amongst other skin conditions)[1,30,46]. These changes in the skin can also be attributed to chronological ageing. Keratinocytes exhibit high sensitivity to these stresses, leading to altered keratolysis rates and thus enhanced emissions of ROS related VOCs as a consequence[47]. To mitigate ROS as a potent source of damage, skin also contains melanocytes, specialised melanin (skin pigment) producing cells[48].

While these cells are situated in the hypodermis and usually do not undergo cutaneous migration, melanocytes distribute melanin (a skin pigment) to keratinocytes in response to genetics or photoirradiation[31]. Melanocytes are a key interest for researchers as melanoma is the deadliest form of skin cancer, albeit VOC related research is limited. The most recent study

by Kwak et al. examined in-vitro differences in volatile emissions between normal melanocytes and melanoma cells[49], observing volatile organo-sulphur compounds emitted from melanoma cells, not identified in healthy melanocytes. More studies are essential to address this potential.

Unfortunately, VOCs from growth media and cell cultures dominated the chromatographs, therefore elucidation of any potential VOC cancer-related biomarkers deemed unreliable. Nonetheless preliminary differences observed in these studies show promise for skin cancer diagnosis and biomonitoring using VOCs[50]. Melanocytes actively produce intermediaries during their metabolic pathways, particularly during melanin synthesis[48], or during glycolysis[51], further enhancing small molecule VOC emissions from the skin.

1.2.3. Skin glandular secretions

Humans are thought to have evolved the ability to excrete substances onto the skin to support its homeostatic and defence roles, with recent research highlighting the potential of secretions for human health applications[1,36]. Studies suggest sweat and sebum to have qualitative and quantitative differences, with respect to biological age and sexual maturity, based on analysed volatile profiles[16,20]. Both sweat and sebum have been shown to partially mix at the skin surface, interacting with RSSCs and their microenvironment in Figure 1.4., contributing to skin VOC emissions. These emitted VOCs may also transfer and adsorb onto clothing.

Sweat (apocrine and eccrine) glands secrete aqueous fluid containing small amounts of glycoproteins, water soluble acids, sugars, amino acids, and electrolytes[1,52]. These saturate the epidermis inducing perspiration, or sweating. This aqueous fluid may serve as a medium for the dissolution and transport of various compounds that may become airborne as VOCs[36].

Sebaceous glands, a sub-structure of the pilosebaceous unit, produces sebum. Sebum is a lipid-rich substance composed of triglycerides, wax esters, SQ and FFAs[20]. These are compounds with large octanol-water co-efficients (Log P). The log P describes the lipophilicity of a compound. Higher values usually indicate greater solubility in non-polar solvents compared to water.

The release of sebum occurs through sebocyte holocrine secretion (when a cell expels its intercellular contents)[53]. additionally contributing intracellular components to the skin surface, enriching substrate available for local microbiome metabolism further inducing skin surface VOC production.

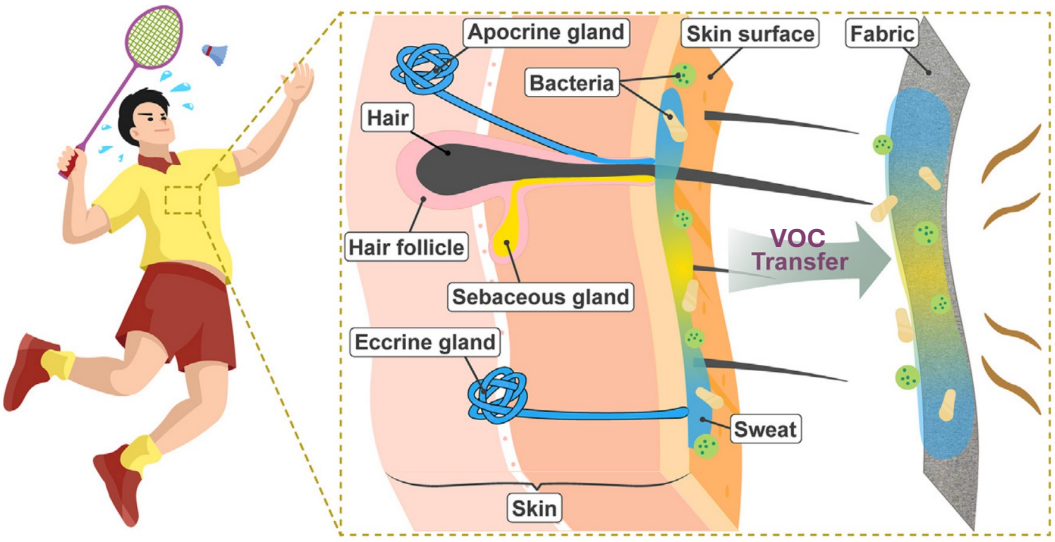

Figure 1.4. Contribution of glandular secretions and microbiome metabolism to skin volatile formation, excreted during physical exercise or during increased skin perspiration. Figure reproduced from Chang and Wang[54].

1.2.3.1. Sweat

Sweat secretions are a source of protons for the skin surface, containing lactic acid, contributing to healthy keratinocyte function[1,55] and upkeep of the SC acid mantle[56]. Lactic acid and glycerol are converted to pyruvate for glycolysis[57], contributing to VOC emissions. The composition of local excreted sweat and associated local microbiome significantly influence the abundance and variety of the emitted skin derived VOCs[54].

Skin surface salinity, interlinked with sweat, was also shown to alter local skin microbiome composition. Resident skin microbes were observed to show preference towards physiological salinity levels[52]. Human sweat has been described to be ‘odourless’ containing ‘odour precursors’ (lactic acid, leucine, valine, isoleucine)[57]. As sweat interacts with RSSCs and resident microbiota, biochemical transformations occur forming malodour associated VOCs (such as acetic and isovaleric acids)[20].

1.2.3.2. Sebum

Sebaceous lipids are estimated to represent 90% of skin surface lipids and are crucial for balancing micro-environments of the skin[53,58]. Human sebum is a complex mixture of FFAs, sphingosines, triglycerides, wax esters, squalene and cholesterols[36,43,52], primarily non-volatile compounds. Palmitic acid (C_{16}), sapienic acid (C_{16}), myristic acid (C_{14}) and oleic acid (C_{18}) are thought to be abundant components of these FFAs[34,59]. The breakdown products of these longer chained, non-volatile FFAs are readily identified in skin volatile emissions. The oxidation target for oleic acid and its corresponding product, nonanal is shown in Figure 1.5. (a).

Shetewi et al. probed emitted volatile FFA, as non-invasive measures of skin surface pH[17]. This work captured skin emitted volatile FFA (including nonanoic acid), with abundances generally higher amongst sampling sites of higher sebaceous gland density (forehead) compared to lower gland density (forearm), exploring if these captured VOCs (C_9 to C_{16} saturated acids) are also present as natural FFA of sebum with healthy skin function.

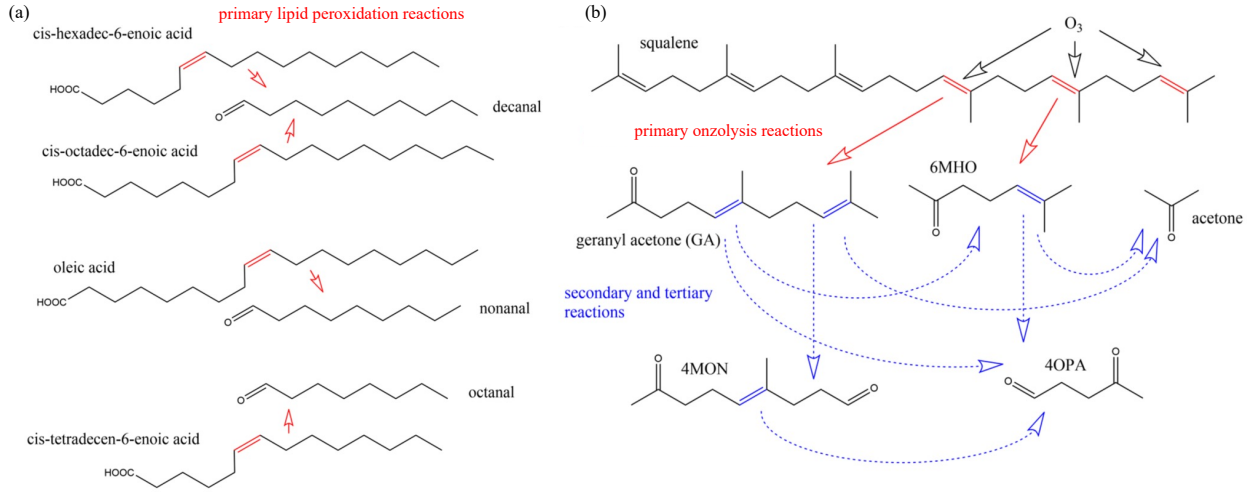

Figure 1.5. Schematic of skin lipid peroxidation on **(a)** fatty acids and **(b)** SQ. The primary reactions are shown in red while secondary reactions are in blue (Cis-hexadec-6-enoic acid is synonymous with sapienic acid). Figure adapted from Morrison et al.[60]

Human sebum is composed of 10–15% SQ[43]. SQ is a C_{18} triterpene lipid, intermediate of cholesterol and precursor to several human steroids[32]. With 6 C=C bonds per molecule, this lipid alone constitutes approximately 50% of double bonds present at the skin surface, making it a highly susceptible target for oxidation[36].

Based on a study by Owsienko et al., SQ concentrations in the skin were found to be higher amongst post-pubertal children (14-18 years), compared to infants (0-3 years)[20], indicating sebaceous gland activity and oxidation susceptibility differences, comparatively, across these age groups. As SQ reacts with ROS, oxidative cleavage induces carbonyl VOC formation of 6-methyl-5-hepten-2-one (6-MHO), 4-oxopentanal (4-OPA) and geranyl acetone (GA)[19,23,60–62], unanimous for human skin VOC emissions.

Recently, sebum and VOC analysis has been gaining attention for Parkinson's disease research, where 4 key metabolites (perillic anhydride, hippuric acid, eicosane and octadecanal) have been found to correlate with Parkinson's patients' sebum[63].

1.2.3.3. Residual skin surface components

RSSCs represent a complex mixture of substances present on the skin surface, including sebum and sweat residues, desquamated corneocytes, ECM components, microbial matter and metabolites[1,35]. The lipophilic nature of RSSCs, derived from sebaceous gland secretions and cutaneous cellular components, provide a matrix for dissolution, retention and re-emission of volatile compounds (principle of bioaccumulation)[64].

Specifically, unsaturated acyl groups of FFA, tri-, di-, monoglycerides, glycerols and wax esters are all active sites for further binding of RSSCs or could be oxidation attack sites, susceptible to ROS-modulated VOC production[43,47]. As secretions are liberated onto the skin surface, they interact with these RSSCs, altering their composition and facilitating the release of VOCs with perspiration and subsequent SC drying. The interplay between RSSCs and skin derived VOCs is dynamic and responsive to various physiological and environmental factors.

Furthermore, the relationship between these components is bidirectional. While sweat influences the production of certain VOC emissions, the presence of certain VOCs on the skin surface can also affect glandular activity through chemo-signalling. Some studies have suggested VOCs may act as chemo-signalling molecules[32,65], potentially even modulating glandular activity or influencing the skin microbiome[10]. These processes can form feedback loops likely in an effort to support general skin homeostasis.

1.2.4. Skin microbiome

The overarching human skin microbiome typically consists of trillions of anthropophilic bacteria, fungi, archaea, and viruses and even small arthropods[10,30,66,67]. All of these living biological systems present at or near the skin surface contribute to overall skin VOC emissions. The range of these biochemical pathways is shown in Figure 1.6.

These microbiota may be grouped into resident microbes (routinely found on the skin, re-establish their population after skin perturbations, often considered commensal) and transient microbes (arise from the environment and persist for hours to days at maximum)[54]. Current literature suggests skin microbiota is predominantly comprised of a small number of consistent residents, with rare and transitory species filling in the gaps to account for differences across individuals in the skin microbiome. Indeed, interparticipant variation is consistently found to be a higher magnitude difference than intraparticipant variation, for sebum analysis[36,68], skin microbiome analysis[10,67,69] and for resulting skin VOC analysis[5,70].

Dysbiosis has recently gained significant traction within the literature, defined as "changes to the composition of resident commensal communities relative to the communities found in healthy individuals"[69]. A number of skin conditions have been associated with dysbiosis of the skin microbiome, inclusive of atopic dermatitis, acne vulgaris and psoriasis[1,3,30]. Furthermore, dysbiosis is becoming increasingly relevant to overall systemic disease states.

Probing for skin dysbiosis typically involves complex 16S rRNA sequencing[10]. Importantly, these snapshot-style sequencing methods lack information about real time microbial metabolism. As such, time-consuming culturomics methods are preferred for a more comprehensive insight[30]. VOCs emitted from skin are a promising non-invasive alternative as a probe for skin dysbiosis. Furthermore, skin VOCs are increasingly identified to exhibit antimicrobial[71] and even chemo-communication roles[72]. Antimicrobial effects have been reported for ubiquitous skin derived aldehyde decanal[73], therefore there is a possibility certain skin-emitted VOCs are involved in both systemic and cutaneous immunomodulation.

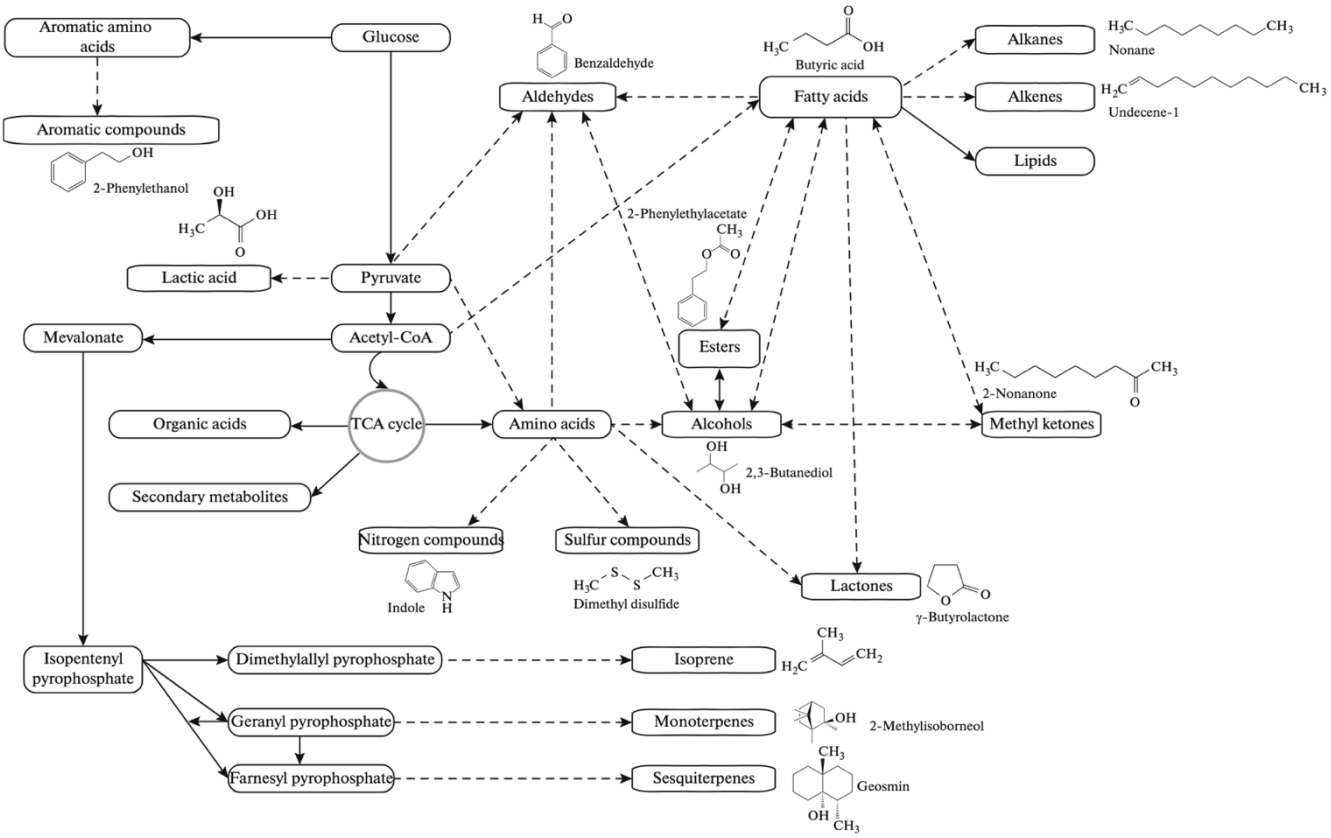

Figure 1.6. The range of available biochemical pathways the skin microbiome may access towards formation of volatile compounds. Figure reproduced from Vesalova et al.[74]

1.2.4.1. Bacteria

Commensal cutaneous bacteria prefer physiological sspH (4 – 6) along with healthy desquamation and barrier function[1,43]. The most common phyla on human skin are *Actinobacteria*, *Bacillota*, *Proteobacteria*, and *Bacteroidetes*[10,57,66,67,75,76]. Their distribution varies by body site, skin hydration, sebum-to-sweat gland ratio and human exposomal factors[52]. *Cutibacteria*, *Corynebacteria*, and *Staphylococci* are the most abundant skin commensal species[10]. Sebaceous sites are dominated by Cutibacterium (e.g., C. *acnes*) and Staphylococcus (e.g., S. *epidermis*), while humid sites like the axilla are dominated by Corynebacterium (e.g., C. *diphtheriae*). Skin commensal bacteria capable of coinhabiting surfaces have been reported. Dry sites have mixed populations of β-*Proteobacteria* and *Flavobacteriales*.

Higher bacterial colony counts in apocrine and sebaceous glands are reflected in skin emitted VOCs. Bacterial metabolism of longer-chained FFAs can produce short chain fatty acids (SCFAs) and medium chain fatty acids (MCFAs), including compounds with C_2-C_{12} chain lengths[77,78]. These compounds are reported to have broad bactericidal effects, which could be

emitted by bacteria to support their proliferation. For example, C. *acnes* secretes lipases and peroxidases that metabolise sebaceous triglycerides excreting FFAs onto the skin surface.

Through the living organisms of the skin utilising glycolysis (TCA cycle)[79], acetic acid may be emitted as a signature VOC of the skin. The conversion of acetyl-CoA to acetate occurs readily, then favouring conversion to its conjugate acid (acetic acid), in the presence of the acidic skin barrier. Acetic acid emissions from the skin are frequently reported in studies[14,37,57]. Notably, acetic acid is also reported to be toxic to *M. tuberculosis* due to its acidic nature and strong bactericidal effect[80],

1.2.4.2. Fungi

The skin fungi are often less studied than its bacterial counterpart however play important roles in the skin microenvironment[81]. Fungal metabolism, similar to bacterial metabolism, has common pathways per phyla with inter-species and growth phase variations, identified using collected VOCs[82]. Fungal VOCs may be generated from glycolytic, mevalonate, shikimate, and oxylipin metabolic pathways[83,84], shown in Figure 1.7. *Malassezia* species, a prevalent and resident skin fungi, contributes to the overall skin microbiome where its over proliferation may be associated with adverse skin conditions.

Rios-Navarro et al. identified 54 compounds emitted by *Malassezia* species during growth phases including alcohols, polyols, fatty alcohols, and unsaturated aliphatic hydrocarbons[82]. The metabolic hallmark of *Malassezia* species is lipid catabolism. Secreted lipases, phospholipases, and sphingomyelinases metabolise skin surface lipids[9], producing VOCs during their proliferation.

Skin resident microbial VOC emissions are dynamic, influenced by nutrient availability, growth phase, skin surface pH, collaborative or competitive microorganism interactions, and human exposomal factors. VOCs (decanal, 2-undecanone, 3-undecanone, undecanal) produced by *Bacillus* genus were shown by Li et al. to have high anti-fungal activity. This builds on reported evidence of fungi-bacteria and fungi-host interactions, likely also taking place at the skin surface[73]. VOCs have been shown to play significant roles for host-insect attraction, demonstrated by studies showing VOCs produced by the skin microbiome can even significantly attract mosquitoes[9,75,85,86].

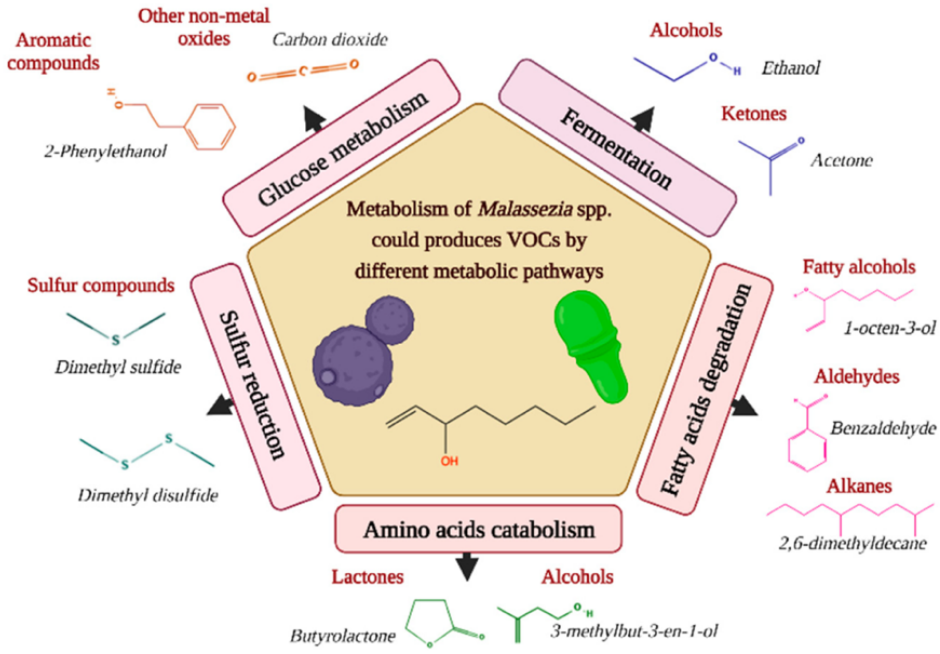

Figure 1.7. Depiction of fungi induced VOC formation events through metabolism mechanisms of substrates metabolised by *Malassezia* species. Figure adapted from Rios Navaro et al.[9]

1.2.4.3. Archaea

Archaea, initially identified in extreme environments, have been found ubiquitously in nature, including as part of human skin microbiota[87–89]. Though less abundant than other skin microorganisms[90], archaea are increasingly recognised as involved in the skin microbiome.

Moissl-Eichinger et al. established the first archaeome of human skin, predominantly composed of *Nitrososphaeria*, with signals of *Euryarchaeota* as well[89]. Moreover, they observed a triphasic distribution of skin archaea across age groups, with higher abundances in younger and older individuals compared to middle-aged subjects. This variance may be linked to age-dependent skin physiology changes involving sebum composition and sspH[16,42,91]. Mahnert et al. explored the commensal presence of *Nitrosocosmicus* signatures on human skin, observing a higher prevalence in sebaceous areas[92], suggesting reliance for lipid rich substrate.

Elucidating the presence or absence of archaea compared to other microbiota is important to understand for overall skin health and its VOC emissions. Similar to cutaneous or sebaceous cells, presence of archaeal extra- and inter-cellular compounds may lead to the release of unique VOCs associated with their presence.

1.2.4.4. Viruses

While endogenous viral VOC production is unlikely, research on virus-specific VOCs is emerging. Recent studies show that viral presence significantly alters VOCs emitted from affected cells and tissues[66,86,93,94]. Unlike former skin residents, whose VOC production is catabolic, viruses induce certain VOCs through host manipulation. Giraldo et al. examined how different human skin VOC compositions guided attractiveness for anthropophilic *An. gambiae*. This is a malaria vector and found increased abundances of SCFAs including butyric, isobutyric and isovaleric acids in attractive individuals, compared to less attractive individuals[95].

Zhang et al. sampled skin VOCs emitted by infected mice models as probes for skin mosquito interactions[86]. The 2022 study corroborated evidence[72] of viral influence on mice skin microbiome, upregulating VOCs that favoured mosquito attraction. Moreover, *Flavivirus* infections were found to upregulate acetophenone emissions. Clinically, VOC emissions were upregulated for *Dengue* infected patients, compared to healthy individuals[86].

1.2.5. The human exposome

VOC emission from the skin-air interface contains information about their formation. The diagnostic utility of these VOCs hinges on disentangling endogenous and exogenous contributions. Person-to-person variability of the human exposome include nutrition[22], personal hygienic habits[33] and other stimuli, shown in Figure 1.8. These factors influence the composition and abundance of skin emitted VOCs. It has been described that approximately 40% of skin VOCs show mixed origins, resulting in a 'VOC fingerprint' sensitive to lifestyle and environmental events[37].

This plasticity mirrors principles of microbial dysbiosis but functions through biochemical pathways such as oxidative stress cascades[45,47], xenobiotic metabolism processes[1,28] and epidermal barrier insults[10,96]. PCPs are widely used as response to various medical or cosmetic concerns[97]. These include topically applied cleansing products, lotions and sunscreens.

Crucially, skin VOCs used as probes of intra- and inter- participant exposomal variability is challenging, as human control measurements without sources of variability is difficult[20]. Even if adequate controls could be acquired for patients, cross-participant validation against a specific personal control could be inaccurate. To address these challenges, personal VOC profile collection is advised to be performed regularly, as early in life as possible, for a patient of healthy functioning cutaneous and systemic functions.

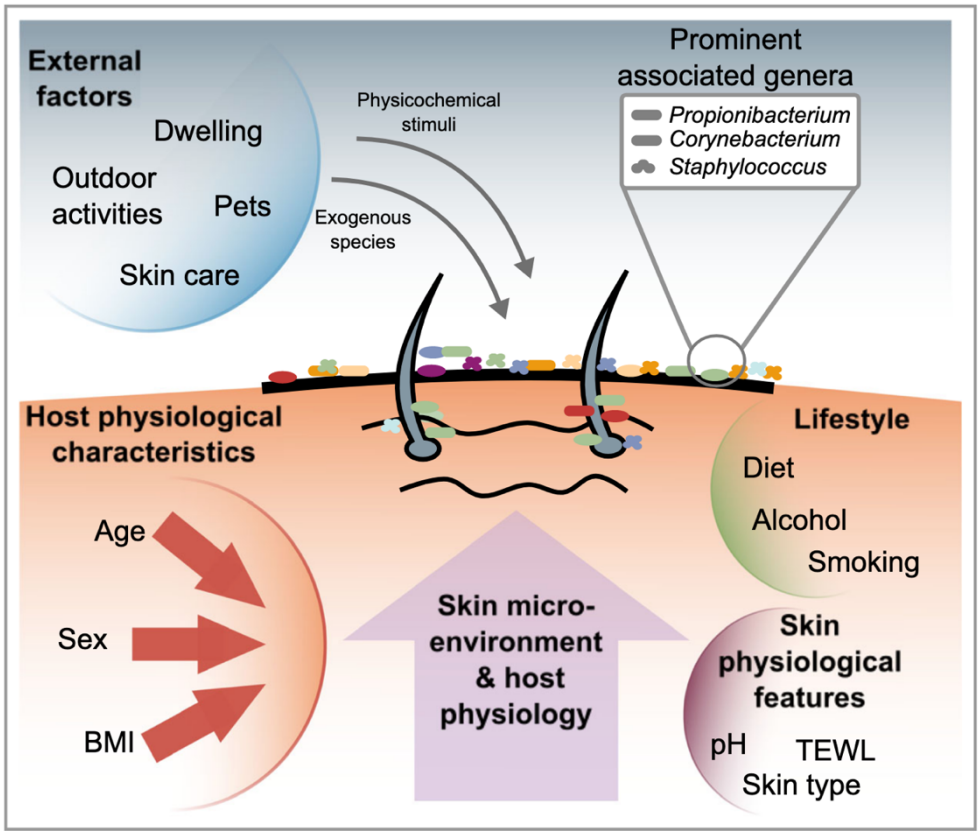

Figure 1.8. Factors of the human exposome influencing the skin microenvironment, including downstream VOC emissions originating from, or at the skin surface. Figure reproduced from Moitinho-Silva et al.[96]

1.2.5.1. Nutrition

Dietary intake has been shown to directly influence RSSC composition[35,96] and skin-derived VOC emissions, from postprandial effects such as garlic ingestion[22], to longer term effects, such as altering the antimicrobial peptide composition of the skin[86]. A 2022 study showed 7-day supplementation with New Zealand blackcurrant powder downregulated emissions of 2-nonenal and allyl methyl sulfide by >25%, while upregulating γ-lactones, changes attributed to antioxidant based modulation of lipid peroxidation pathways[98]. Certain compounds readily identified as skin derived may also be identified in food products. Heptanoic and octanoic acids are naturally abundant in castor and coconut oils may be attributed to dietary origins[99]. In cooking oils, unsaturated triglycerides are highly abundant, and have been reported to oxidise over time, where their consumption may be linked to certain FFAs of the skin, transported in sebum as substrate for skin emissions[100].

1.2.5.2. Hygienic habits

Hygienic practices and their frequency, play a crucial role in shaping the skin VOC profile[33,61]. Frequent washings may reduce the abundance or variety of emitted VOCs through accumulated RSSC and applied PCP removal from the skin surface[97], as shown in Figure 1.9. Additionally, showering may induce perturbation of the skin microbiome, leading to changes in VOCs produced by resident microbiota[54]. Wang et al. found when using a neutral and uniform cleansing regimen, a cutaneous microbiome exhibits stability over time, concurrently corroborating interparticipant variation to be of a greater magnitude than intraparticipant variation[67].

The use of certain PCPs for hygiene may introduce VOCs to the skin surface, with likely concomitant bio-accumulative effects, temporarily altering a volatile profile[12,101]. Abstention from showering for 48 hours found to upregulate C_4-C_{10} carboxylic acid emissions (for example, heptanoic acid, upregulated 184% from the baseline emissions) likely due to microbial re-establishment exhibiting enhanced sebum catabolism[33]. This increase in volatile acid emissions is thought to emerge from proliferating *Cutibacterium* and *Staphylococcus* species strains metabolising RSSCs into volatile FFA[54], a process suppressed by daily washing.

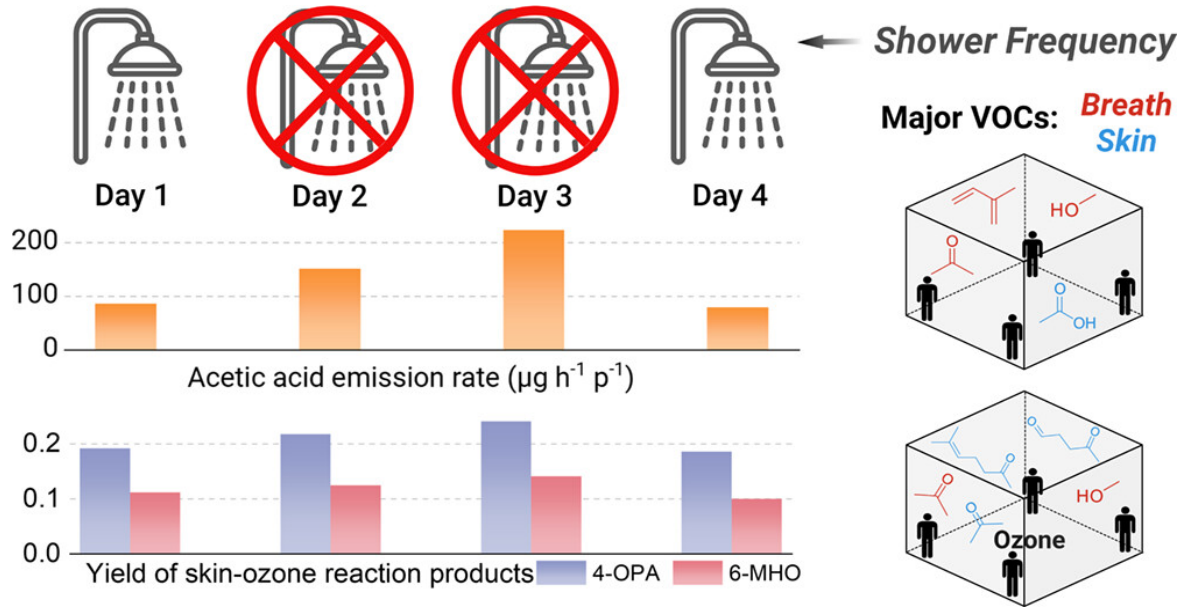

Figure 1.9. The frequency of showering altering breath and skin volatile emission rates due to the effects of personal hygiene on the skin microenvironment. Figure reproduced from Wang et al.[33]

Volatile ketone emissions (6-MHO, GA) were also upregulated on no shower days[33]. This suggests accumulation of skin lipids over time, which can enrich the substrate available for downstream emissions of skin ozonolysis products. Excessive hygiene practices may elevate exogenous VOC uptake as stripped skin exhibits higher intercellular lipid exposure[102], increasing permeability coefficients for lipophilic substances.

Freshly exposed skin is a reservoir for pollutant-derived volatiles[12,55,64], likely due to a high abundance of newly oxidisable targets. This bidirectional relationship between hygiene frequency and VOC diversity, if extrapolated and robustly verified, could indicate cleaning guidelines in the future, to optimally balance the skin microbiome and barrier function, for maintaining optimal skin homeostasis. These considerations are especially relevant towards reliably probing person-to-person variance in VOC profiles, disentangling external contributions from host metabolism, and eventually developing reliable wearable sensors.

1.2.5.3. Stressor stimuli

A range of stressor stimuli, including airborne pollutants and even psychological stress, can lead to ROS upregulation and oxidative damage[47]. These stressors were shown to induce sebum hypersecretion, increase trans-epidermal water loss (TEWL), and up-regulate sebum secretion[21]. Environmental pollutants such as ozone (O_3) or polyaromatic hydrocarbons (PAHs), compound to stressors leading to skin ECM breakdown, potentially elevating VOC production.

Airborne oxidative stressor stimuli originate from atmospheric pollutants (O_3, PAHs, VOCs) and is further amplified by solar radiation exposure[100,103], as shown in Figure 1.10. Further amplification of pollutant induced VOC production can occur in urban areas due to reduced ventilation, elevated secondary aerosol formation and increased population densities[104]. This is referred to as sick building syndrome (SBS) and often associated with VOC exposure, such as described for airborne 2-ethyl-1-hexanol (2-EH)[29,105]. Environmental pollutants compound to these negative health risks[69,106].

Rapid SQ oxidisation occurs due to a lack of dietary vitamin E, or through exposures to sunlight, cigarette smoke, dust, ozone, and other airborne pollutants[36], indicating it is naturally present as a mitigation to oxidative assaults. UV-induced photo-oxidation from sunlight exposure amplifies these mentioned mechanisms, often up-regulating VOC production at or near the skin surface[31,43,107]. UV radiation generates ROS at or near the skin surface,

capable of oxidising skin lipids, proteins, and even DNA, leading to accumulated cellular damages and premature ageing over time as shown in Figure 1.10.

Psychological stressor events are usually defined as overwhelming cognitive experiences of a self-measurable response to a host's environment[21,108–110]. Research has found acute psychological stress events to induce rapid sympathetic nervous system activation with sebum hypersecretion[111]. The 35 subject trial also identified stress up-regulated squalene peroxidation products (GA) and a branched aldehyde, while downregulating ethylbenzene derivatives within 20 min of stress induction. Concurrently, upregulated sebum fatty-acyl concentration decreased sspH. This finding has tremendous monitoring potential using skin VOCs, since one of the most explored relationships is established to be between skin surface acidity and the volatile carboxylic acids of the skin[17]. Further research may result in robust psychological stress monitoring capabilities.

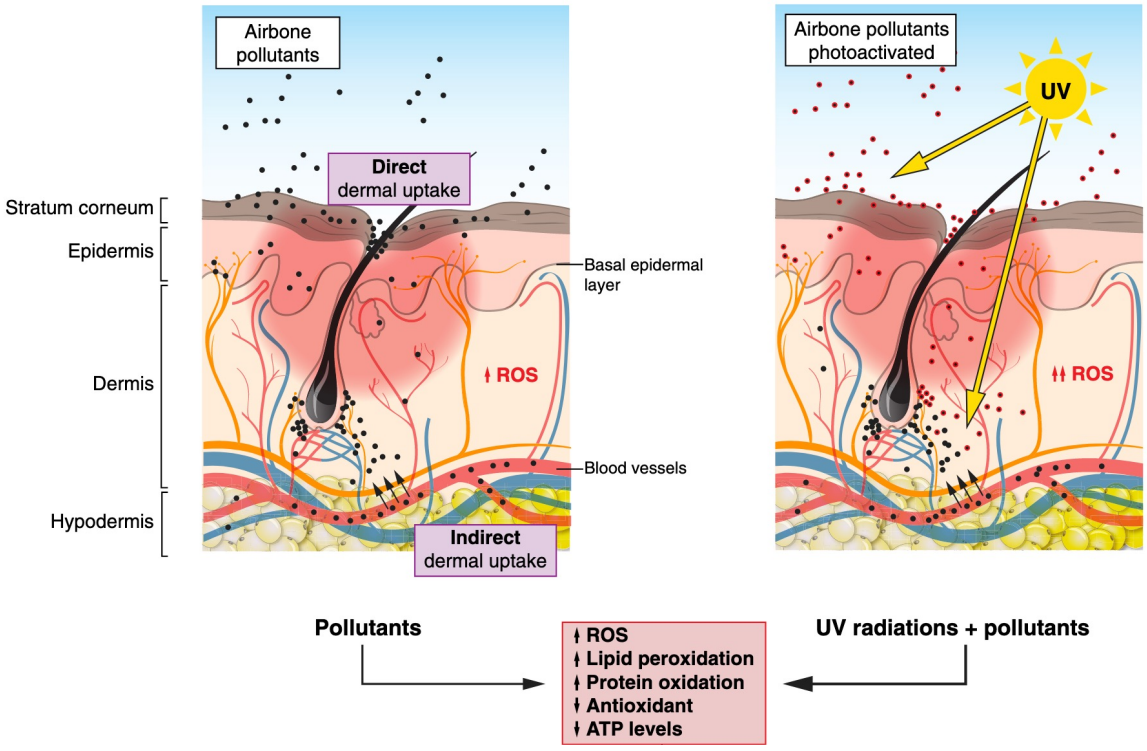

Figure 1.10. The influence of airborne pollutant species and photoactivated airborne species initiating a chain of ROS induced effects such as lipid peroxidation, antioxidant depletion and accumulation of skin cellular damage over time. Figure reproduced from Araviiskaia et al.[112]

1.2.5.4. Personal care products

PCPs are designed to mitigate these oxidative stimuli[28]. PCPs usually also aim to address barrier integrity with occlusive ingredients such as triglycerides, fatty acids and emollients, physically preventing TEWL[97]. When applied to the skin PCPs can provide an abundance of substrate towards subsequent volatile emissions[28,61,113].

Starr et al. identified persistent exogenous anionic surfactant, sodium lauryl sulfate derived from PCP usage and acting as a substrate for microbial activity contributing to skin VOC emissions[59]. Certain facial moisturisers may deposit 120-300 µg m^{-2} of exogenous monoterpenes (limonene, linalool) that dominate the immediate post application VOC profile, exceeding endogenous emission fluxes by 2-3 orders of magnitude[33,61,114]. These applied compounds can also be adsorbed through the skin and transported through systemic circulation as shown in Figure 1.11. Subsequent VOC emissions of those adsorbed compounds can occur. Wu et al. demonstrated that the interactions between solar radiation, RSSCs, and PCPs can lead to the formation of VOCs[28].

Emollients such as isopropyl myristate persist for >150 minutes, undergoing gradual ozonolysis into formaldehyde and C_6-C_9 aldehydes[14,37]. A recent study by Wu et al. showed that the use of fragranced PCPs can result in the emission of over 200 VOCs, with some reaching concentrations of several ppm in indoor environments[28].

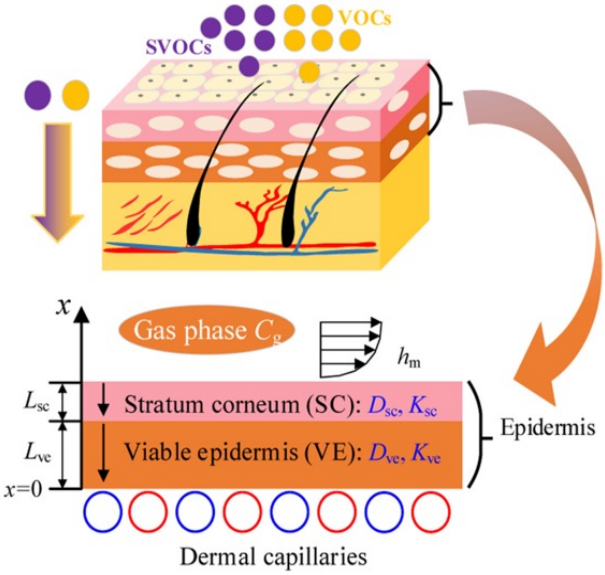

Figure 1.11. Schematic of chemical transport model of compounds contacting the skin showing resulting in direct dermal uptake, then transfer to systemic circulation, given high enough partition co-efficient, K. Figure reproduced from Wang et al.[12]

1.3. Biochemical significance of human skin derived volatile organic compounds

Skin VOC emissions arise from interplay of these source matrixes of section 3.0, encompassing wide range of VOCs of various homologous series. The sum of these emitted compounds is referred to as total volatile emissions (TVOCs).

Aldehydes, produced endogenously during oxidative stress events, are often the most abundant skin VOC series[16,37] and play roles in cellular chemo-signalling[32]. Carboxylic acids, largely generated by resident microbiota catabolising RSSCs, contribute significantly to body malodour[54,57,116] and often considered second most abundant skin VOC series[37].

Ketones, formed during fatty acid metabolism and through oxidative skin surface reactions[23], may reflect endogenous antioxidant reserves and overburdened metabolic function[14]. Alcohols, resulting from microbial fermentation within the glands and SC, or topical PCP usage, are abundant constituents of skin VOC emissions[105,117].

Short chained alkanes and alkenes, produced during lipid peroxidation, are VOCs thought to reflect upregulations in cellular division or breakdown, involved in cancer tumour growth[118–120]. Aromatic hydrocarbons, while typically of exogenous origin[104,121], could be endogenously derived from aromatic amino acid breakdown and metabolism[14,57].

Volatile nitrogen containing compounds, such as NH_3 and trimethylamine may also result from amino acid breakdown[14,116]. Otherwise, N containing compounds are associated with urban pollutants such as NO_2 car exhaust[42]. Sulfur containing compounds may be produced by resident skin microbiota[3,57]. S containing conpounds are thought to be contributors to characteristic body odours[54], derived from sulfureous precursors in sweat[52].

Instances of silicone containing VOCs (siloxanes) are observed for skin VOC studies[24], however are often determined to be exogenous compounds[122] or artefacts of experimental workflows[16,17]. Poor biochemical understanding and myriad of experimental approaches give rise to challenges for identification and classification of skin VOCs for healthy participants.

Moreover, the same recovered VOC species may be reported in literature with different names, whilst seldom including CAS numbers. For example, in 2021 Drabińska et al. reported pentanoic acid as absent in skin emissions[14], however Uebi et al. reported this VOC as skin derived in 2019, labelled as its synonym, valeric acid[24].

1.3.1 Aldehydes

Straight-chained aldehydes are often most abundant homologous series among skin derived VOC emissions[16,20], comprising an average of 26% of TVOCs for healthy skin[37]. Healthy skin emits various straight-chained aldehydes including pentanal, hexanal, heptanal, octanal, nonanal, decanal, undecanal, and dodecanal[14,16,25,123,124]. Aldehydes are formed through oxidative breakdown events at and within the skin surface[45].

Hexanal is thought to be a lipid peroxidation end product resulting from breakdown of oleic, linoleic and palmitoleic acids[45,123]. These longer chained FFAs are constituents of sebum, while forming abundant part of the skin's ECM[53]. Skin-emitted heptanal and octanal are thought to be RSSC peroxidation products[23,123]. Nonanal and decanal are amongst most frequently identified and abundant aldehydes for healthy skin emissions[14,16,37]. Current literature suggests nonanal precursors as abundant amongst exogenous sources from clothing, cooking oils to PCPs, while decanal precursors have negligible presence in consumer products, thought to be derived primarily of RSSC origin, as an endogenous, sapienic acid breakdown product[73].

2-nonenal is thought to form from oxidative degradation of omega-7 fatty acids and were observed to correlate with age[125]. These skin emitted aldehydes can be assessed as part of a multivariate function of skin biophysical parameters and skin derived VOCs to predict a subjects chronological age, to 68% accuracy, using a statistical predictive model. Upregulated skin aldehyde emissions have been observed for participants with inflammation or stress, compared to healthy individuals, suggesting a potential link between aldehyde emissions and host responses to stress[37,108,126]. Indeed, Qu et al. have highlighted interparticipant emission rates of aldehydes from human skin to vary significantly[23].

Overall, elevated skin aldehyde emissions in older individuals may be linked with excess oxidative stress based changes in their sebum compositions[47,91,98,127]. Similarly, undecanal and dodecanal are thought to arise from ROS induced breakdown, where these may be terminal products of *cis*-heptadec-6-enoic acid of skin ECM[43,128]. Longer aldehyde emissions may be associated with increasing severity of cellular insults, as emissions may derive from a build-up of cell senescence and subsequent breakdown materials[33,97]. Zhou et al. explored ozone initiated degradation of triolein (triglyceride of glycerol and oleic acid), suggesting elevated relative humidity (RH) supress secondary ozonide production and promote condensed-phase reaction pathways. In consequence, favourable formation of volatile C_9 products (nonanal and nonanoic acid)[100] occurs, shown in closer detail in Figure 1.12.

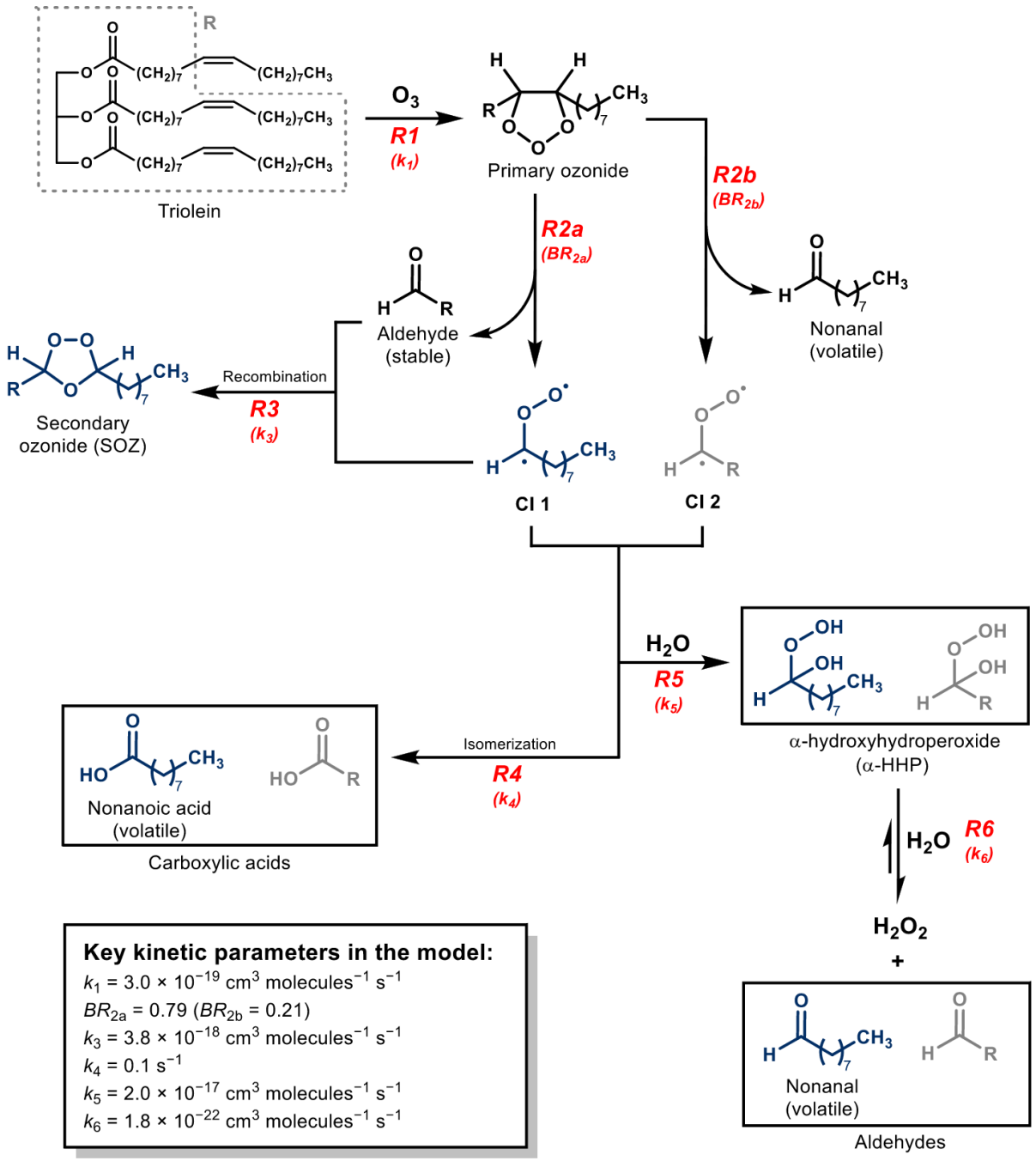

Figure 1.12. Schematic of the biochemical pathways for volatile C_9 compound formation using triglyceride of oleic acid as a substrate and atmospheric ozone as the initiator. Figure reproduced from Zhou et al.[129]

1.3.2. Carboxylic acids

Carboxylic acid emissions, the second most prevalent homologous series for skin VOC emissions, constitute 12% of TVOCs from healthy participants[14,37]. These compounds contribute to the skin's acid mantle and influence its pH. These acids, including SCFAs and MCFAs play important roles regulating the skin microbiome. Disturbances in the skin acid mantle are linked to various cutaneous and microbial diseases, making the study of these emissions relevant to understanding skin health.

These acids are derived from sebocyte activity, desquamation and subsequent microbial action of the present RSSCs[59,130]. Specifically, lipases present in the skin induce hydrolysis of sebaceous triglycerides into FFAs, further breaking down into volatile fatty acids[53]. Some fatty acids are established components of sebum while others may arise as metabolic by- and end-products from longer chained substrates[16,17]. Some of these longer chained acids of the skin are shown in Figure 1.13. Some linear correlations have been observed for skin derived acid emissions and SC H^+ concentrations, including those for some SCFAs and MCFAs[16,17,102,131].

Acetic acid (C_2) is thought to originate from microbial degradation of RSSCs, now proposed to derive from metabolism of microorganisms. Studies often find this as the most abundant skin emitted compound[33]. Other SCFAs (propanoic acid and butanoic acid) have been identified for skin emissions, albeit reported less often, compared to other aliphatic fatty acids[37]. Branched SCFAs may arise from breakdown of branched amino acids present, compared to straight chained SCFAs, more likely to originate from carbohydrate metabolism[14].

Medium chain aliphatic fatty acids (heptanoic-, octanoic-, nonanoic-, decanoic-, undecanoic- and dodecanoic acids) are have been reported as components of some cellular membranes[109] and as sebaceous lipids present within the sebocyte intercellular matrix[16,53,102,132]. For skin and its ECM, MCFAs are often esterified with glycerol and exist as MCFA-triglycerides for roles supporting the skin NMF functions[58]. These MCFAs can be emitted from the skin as RSSCs degradation products from skin-resident microbes[76], through lipid peroxidation from oxidative stress cascades[21], and initiated exogenously through human exposomal factors[12].

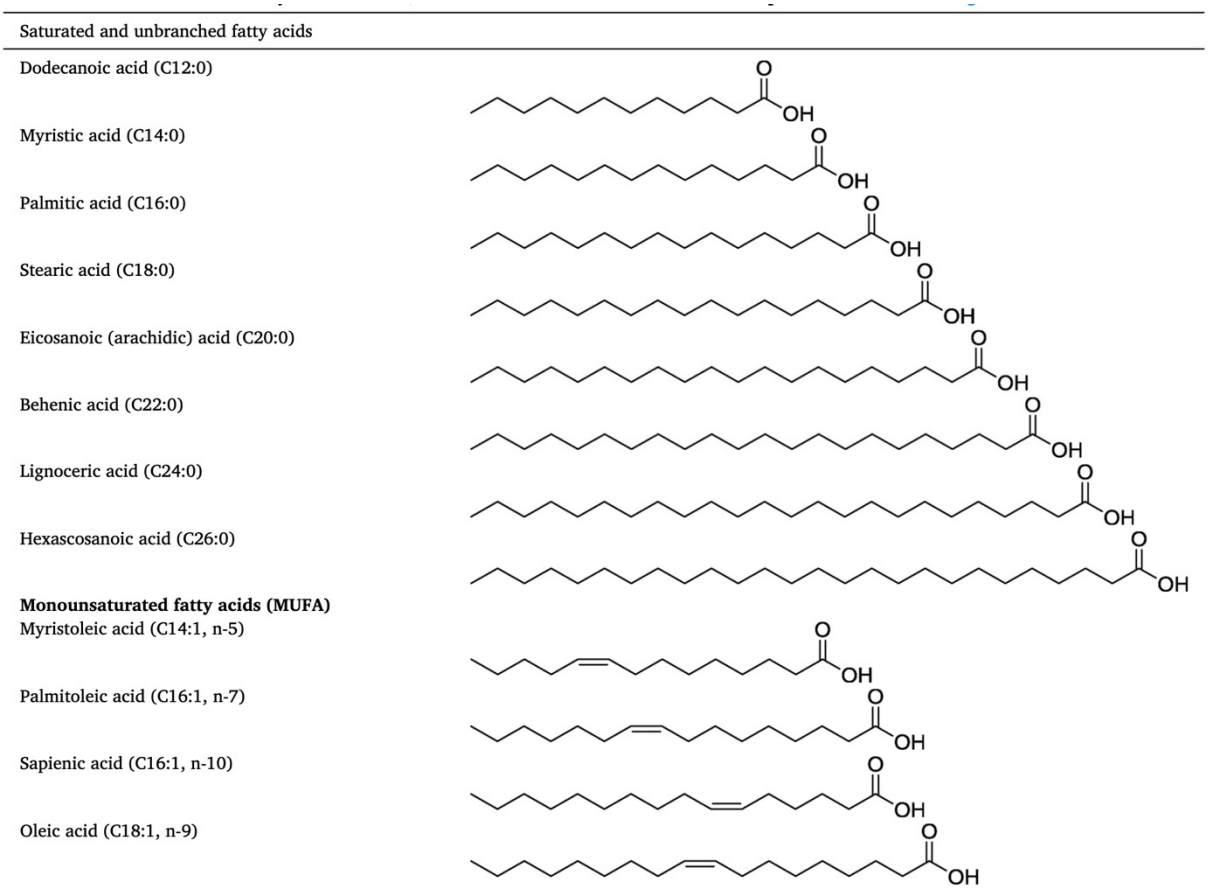

Figure 1.13. The saturated and monounsaturated FFAs found in the human skin. Figure reproduced from Knox and O'Boyle[58].

Octanoic to dodecanoic acids (C_8–C_{12}) have been shown to possess anti-microbial properties with ability to perturb microorganism cell walls[1,133,134]. Preliminary evidence has highlighted potential anticancer effects of MCFAs with octanoic, nonanoic and decanoic acids having significant inhibitory effects on human skin cancer proliferation[135]. Morrison et al.'s factor analysis correlated skin VOC abundances to fresh skin lipid compositions, oxidised skin lipid abundances, and exogenous compounds originating from cooking oils and PCPs[60]. Therefore, both endogenous and exogenous sources should not be ruled out during analysis. Importantly as these compounds may show correlation for various skin conditions, direct causation should not be assumed and instead should warrant further exploration.

1.3.3. Ketones

Ketones represent a ubiquitous class of skin derived VOC emissions fluctuating around 7-10% of healthy skin TVOC emissions[37]. These form as dominant SQ oxidation products[136], often with the highest detection frequencies amongst all skin derived VOCs. Along with C_{10}-C_{12} aliphatic aldehydes, acetone, 6-MHO and GA are considered first generation onzoloysis products of human skin lipids[23,43]. Weschler and Nazaroff have proposed six primary SQ-ozone reactions to occur on physical surfaces, while 28 out of 30 secondary reactions occur in the gas phase[43], such as the secondary aerosol formation reaction resulting in second generation product, 4-OPA[33,62,137].

Acetone is often recovered as the most abundant ketone with an estimated local skin emission flux between 140-3680 fmol cm^{-2} min^{-1} [138,139]. Whole body skin acetone emissions have been reported with an emission factor of 39.7 µg per hour per person (h^{-1} p^{-1})[124], and these could be useful towards non-invasively monitoring diabetes. Acetoin (3-hydroxy-2-butanone) is a skin resident microbially derived VOC, considered ubiquitous for many human subjects[123,130]. Shown to be emitted in-vitro by *S. epidermis* and *S. aureus* skin bacteria[10] from catabolism of pyruvate[123]. Preliminary evidence suggests acetoin to be enriched for participants deemed attractive by *An. gambiae*, a mosquito vector for malaria disease[95], compared to less attractive individuals.

6-MHO emissions reported by Wang et al. for the total body was 19 µg h^{-1} p^{-1} at near zero ozone (<1 ppb), rising to 430 µg h^{-1} p^{-1} at 36 ppb ozone, using controlled chamber experiments with human subjects[125], where 1 ppb equals 0.041 μmol O_3 m^{-3} at 1 atm and 25 °C. Furthermore, Qu et al. applied this experimental approach to a real-world office setting, controlling ozone concentrations from <3 ppb to 10–15 ppb ozone[140]. Results showed 6-MHO, GA, and C_{10}-C_{12} aliphatic aldehydes as the dominant skin oil onzoloysis products[23].

This 10-day observational study also showed that acetone room concentrations are influenced more by breath emissions, compared to skin emissions[140]. The quantified dermal 6-MHO emission ranged from 113 to 337 µg h^{-1} p^{-1}, respectively at those O_3 concentrations. Other studies report whole body 6-MHO skin emission in the ranges of 3 to 39 µg h^{-1} per person[60,123,124]. This ozone dependence helps to explain large discrepancies for emission factors observed across different studies[62,136]. Moreover, emissions rates for VOCs derived from skin oil oxidation have been reported to increase with RH[43,62], highlighting the importance of reporting ambient sampling conditions during skin VOC collection.

1.3.4. Alcohols

The origins of alcohol VOCs in skin emissions is diverse and includes microbial metabolism of RSSCs[130], lipid peroxidation[141], systemic circulation and exogenous such as PCPs[28,38,142]. Reported volatile alcohols encompass a range of fatty alcohols, branched alcohols, aromatic alcohols, distributed in a range of primary, secondary and tertiary structures including ethanol, 1-octanol and its isomer 2-ethyl-1-hexanol, 1-dodecanol, amongst others[14,25,26].

Alcohol consumption has been shown to directly affect skin EtOH emissions[38]. Endogenously, alcohols may be produced as intermediates during lipid metabolism or by reduction of aldehydes and acids through alcohol dehydrogenases[143]. Saturated aliphatic alcohols (1-hexanol, 1-octanol, 1-nonanol, 1-dodecanol) are products of skin lipid degradation[9], found frequently in studies employing direct contact based sampling[25,26], compared to contactless VOC sampling approaches[16].

Fatty branched alcohols such as 2-methyl-1-propanol and 3-methyl-1-butanol are thought to be released in planktonic and biofilm growth phases as microbes catabolise RSSCs[142,144]. These bacteria-specific VOCs are promising for monitoring differentiation of *S. aureus* biofilm maturity using volatile emissions[3,76,144]. Exogenous exposures are prevalent sources of alcohols[97], often exceeding endogenous skin VOC emissions by several orders of magnitude[10]. Among the fatty alcohols frequently emitted from healthy skin 2-EH, 2-phenoxyethanol and 1-dodecanol are often abundant but are likely exogenously sourced[2,16,105,131]. Both VOCs are frequently added to PCPs, as solvents, preservative and fragrance agents[10,28].

2-EH can adhere to skin surface due to its high lipophilicity, where it may volatilise at skin temperatures over an extended period of time post exposures. Several studies have indicated dermal uptake to be a potent and direct route of pollutant contamination[103], often leading to time delayed re-emission of a pollutant. 2-EH emissions are associated with bioaccumulation of plasticisers and their downstream microbial breakdown[14,16,105]. 2-EH's presence in indoor air has been linked to SBS characterised by irritative effects on pulmonary membranes[29], therefore its monitoring from the skin, if possible, is warranted to explore the effects on human health further.

1.3.5. Aliphatic hydrocarbons

Straight chained alkane emissions have been identified averaging 12% of TVOCs from healthy skin[37]. In general, healthy skin produces minimal volatile alkanes and alkenes, often with significant increases observed in subjects experiencing excess oxidative stress[10,141,145]. Straight chained alkanes and their corresponding alkenes are thought to originate from phospholipid cell membrane destruction during ROS attack on unsaturated membrane lipids[71,137,146].

Upregulated through pathogen presence, mechanical stresses, inflammatory processes and oxidising agents, excess lipid peroxidation induces cellular membrane collapse and fragmentation, where these alkanes can be derived from[1,3,14,146]. Alkane chains are depicted as part of these membranes shown in Figure 1.14.

Short-chained (pentane, hexane) and medium-chained (heptane to dodecane) alkanes are thought to originate from excess oxidative breakdown[14,39], compared to longer aliphatic alkanes (C_{15}–C_{30}) that are thought as environmental petroleum pollutants[10]. The detection of overexpressed alkane and alkene skin emissions offers promising applications. Elevated levels of hydrocarbons, particularly heptadecane and 2-methylpentadecane, have been proposed as potential biomarkers of psychological stress in the study described by Lucchi et al[21]. Clinically, the emission of specific alkane or alkene VOCs from the skin could serve as non-invasive probes for excessive oxidative damage or cellular membrane breakdown.

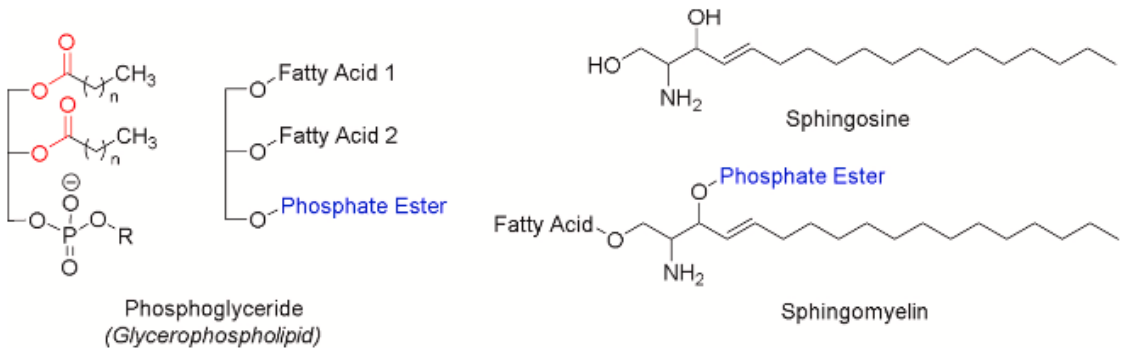

Figure 1.14. General structures of phospholipid membrane subclasses, phosphoglycerides and sphingomyelins, reproduced from Knox and O'Boyle[58].

1.3.6. Aromatic volatile compounds

Benzene and its derivatives are observed for certain healthy skin VOC emissions but this trend is less consistent compared to previously established VOC groups. Ethylbenzene and xylenes (ortho-, meta-, and para-isomers) are also frequently detected in skin emissions, likely due to environmental exposure as these are used in petroleum, car exhaust and industrial solvents[121].

Styrene (vinylbenzene) is occasionally found in skin emissions. Its presence is interesting due to its potential link to oxidative stress, as it can form through the peroxidation of unsaturated fatty acids[14]. Benzyl alcohol and toluene are commonly detected derivatives for skin emissions[123]. Endogenously, toluene may be emitted as byproduct of phenylalanine catabolism while exogenously, it's common in the environment from industrial processes and products[121]. Benzoic acid and its derivatives have also been identified in skin emissions[123].

1.3.7. Nitrogen containing compounds

N containing compounds emitted from the skin are thought to represent systemic and microbial metabolic pathways. Several groups of these compounds emitted from the skin has been reported including amines, amides, pyridines, pyrroles, and nitriles[14,37,123].

Albeit not explicitly a VOC, volatile ammonia (NH_3) is frequently detected from skin, thought to be derived from urea precursors and linked to high dietary protein (amino acid) intake[14,116]. The origins of NH_3 are contested between sources, with leading evidence supporting vascular transportation from plasma and direct secretions in eccrine sweat. Preliminary evidence suggests skin resident archaea to play a role in NH_3 removal, contributing to nitrile emissions[147].

Implicated in fish malodour syndrome, trimethylamine is a N containing volatile compound from the microbial reduction of trimethylamine N-oxide[147]. Healthy adults typically excrete approximately 1 mg of trimethylamine per day in urine[14,148]. However, individuals with genetic factors that impair removal through the urinary path exhibit significantly elevated skin emissions of trimethylamine.

Fish malodour syndrome originates from mutations in genes encoding flavin monooxygenase 3 enzyme, leading to systemic accumulation of trimethylamine[116]. Consequently, trimethylamine blood concentration is then proportional to intensity of patients' body odour. This phenomenon exemplifies interplay amongst the systemic circulation, skin microbiome and their emitted volatile compounds.

1.3.8. Sulphur containing volatiles

Emissions of S-containing volatile compounds from human skin are generally lower than those of other oxygenated compound groups[37]. However, their low olfactory thresholds make them significant contributors to perceived body odours, closely linked to skin VOC emissions[20,22,57]. S-containing volatiles are thought to be produced at skin surface through resident microbes[3], with small amounts being emitted transcutaneously via systemic circulation[22].

Hiramoto et al. observed diallyl disulphide (DADS) and allyl methyl sulphide (AMS), of ingested garlic origin, emitted persistently from skin, upregulated significantly, 30 minutes after consumption. Their chemical structures are shown in Figure 1.15. Crucially, this study showed manipulating specific skin volatile emissions through ingestion of antioxidant rich foods[22]. This is highly significant towards manipulating emissions of *trans*-2-nonenal, thought to be partially responsible for 'old person smell'[16,127].

Involved in malodourous sweating, S-containing compounds such as 3-methyl-3-sulfanylhexan-1-ol mix with branched short chain fatty acids such as *E*-3-methyl-2-hexenoic acid resulting in pungent and rancid body odours[116]. Some other examples of reported S-containing compounds emitted from skin cells include disrupted melanin synthesis (pheomelanin generation)[48] or melanoma[49,135].

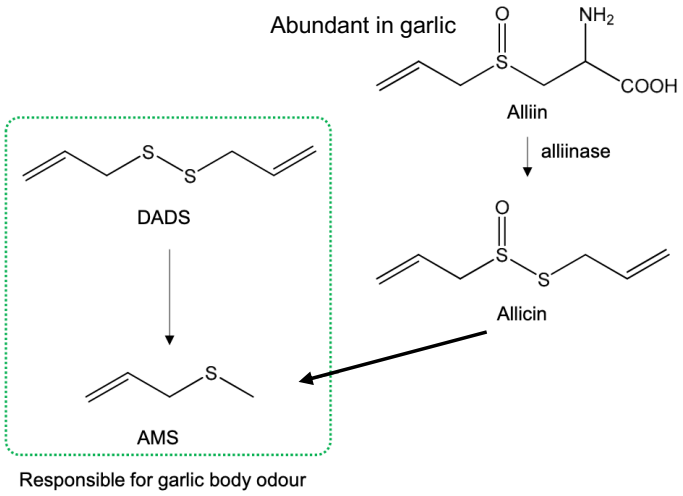

Figure 1.15. Chemical structures of Alliin (ingested in garlic), converting to allicin which may be emitted from the skin as AMS. DADS can also be converted into this volatile compound and emitted from the skin. Figure adapted from Hiramoto et al.[22]

1.4. Approaches for capturing skin derived volatile emissions

The capture of VOC emissions from skin involves a diverse array of methodologies. Capture methods differ based on targeted and untargeted analysis, the former focuses on a particular group of compounds or metabolites, while the latter focuses on a broader collection range of different analytes[3]. Sampling approaches used vary from direct skin contact sampling[26,120] and contactless headspace sampling[16,17,141] to whole body plethysmography chambers[28,123,149].

Different sampling approaches add to heterogeneity of captured VOCs as contact based sampling protocols collect lower volatility compounds more effectively compared to contactless sampling protocols[10,150]. In contrast, highly volatile species are not commonly observed for direct contact sampling protocols which may be due to competitive adsorption from more abundant, less volatile species[26]. Sampling times used range from minutes to hours with longer durations thought enhance capture of less volatile compounds[26].

The type of capture material further influences the variety and abundance of collected skin VOCs. Critical considerations are log P octanol-air partition co-efficients (K_{OA}) of each skin VOC investigated[97], along with sorbent-air partitioning equilibrium constants[151,152]. Research suggests development of standardised protocols to facilitate more robust comparisons across studies[153]. Differences of partitioning co-efficients amongst relevant VOCs indicate that one-size-fits-all approaches for skin VOC sampling is likely not suitable[150].

1.4.1 Direct contact sampling

Direct contact sampling techniques involve contacting VOC adsorbent materials onto the skin to facilitate the transfer of analytes through friction[10,20]. This approach enables immediate capture of present compounds. Conversely, some studies employ extended sampling periods to achieve detectable signals which was found particularly advantageous for compounds exhibiting low partitioning coefficients between the air and adsorbent material[26].

Common materials used for this approach include cotton based materials[25], silica beads[24,154], adhesive tapes[6,153], polymers[26] and SPME fibres[16,17,131]. These methods are often preferred for their simplicity, ease of administration, and additional potential for longer sampling durations, which can be particularly useful for capturing less volatile compounds[10]. Biocompatible wearable samplers may be applied directly onto the skin for extended periods, enabling the collection of a wide range of VOCs over a duration of time[26].

1.4.1.1. Cotton fabrics and swabs

An often omitted, potent reservoir for skin VOCs is clothing[149], where worn clothes may act as source, barrier or transient reservoir for VOCs, influencing VOC dermal absorption and emission rates[151,155]. Often used clinically, cotton swabs are good VOC sorbents due to high surface areas, rapid equilibration times, widespread availability, and ease of use[20]. This structure provides hydroxyl groups that can interact with polar headgroups via hydrogen bonding, while its fibrous structure also traps non-polar VOCs through dipole-dipole forces[156].

Studies have shown cotton to effectively adsorb wide range of VOCs including carbonyls, carboxylic acids, and aromatic hydrocarbons[20,149,151], although it is thought that VOC sorption does not occur readily past available hydrophilic binding sites, to reach internal polymer chains[156]. Yu et al. found rapid equilibration times (≤1 day) for VOCs sorbed to cotton fabrics, with interactions differing on basis of VOC polarity[151]. This observation suggests cotton based materials to be potent skin VOC reservoirs over relatively short durations. From an analytical perspective, sterile cotton based materials are consistently observed to have high contamination volumes[120,154], lower recovery rates for highly non-polar VOCs[20], therefore should be used with this in consideration.

1.4.1.2. Silica materials

Glass or silica beads are chemically inert, easy to clean and accessible, frequently used in skin VOC research. Pojmanová et al. employed these for skin VOC collection through 15 minute palm abrasion, followed by solvent extraction into hexane and analysis by GC-MS[154]. While they found glass beads advantageous for cleaning, they were observed to have relatively poor adsorption properties compared to cotton fibres of higher surface areas and porosities[156].

Addressing this, functionalised silica beads such as 'Monotrap® RGPS TD gas adsorbent', fabricated to possess superior VOC sorption capacities[110]. Uebi et al. identified 31 VOCs in samples collected from infants heads, using MonoTrap® wrapped in sterilised cotton material for sampling of volatiles[24]. MonoTrap® silica beads may be used for direct contact sampling, however as employed by Uebi et at. and Tskududa et al.[110], may also be used for near proximity VOC collection when wrapped in a porous material. This approach is advantageous for analysing skin derived gas phase VOCs, without interference from other less volatile RSSCs[150]. However sampling using silica materials is susceptible to contamination of VOC samples by siloxanes and their derivatives, as found with MonoTrap® beads, which are composed of monolithic silica[24].

1.4.1.3. Tape Stripping

Tape stripping is a collection of superficial skin samples through adhesive tape enabling access to lesional and non-lesional skin cells along with RSSCs[34,59]. This can be used for analysis of VOCs emitted from viable skin cells[30]. The depth of sampling varies based on the number of tape strips applied and individual skin characteristics[6,157]. This method may also be used to simulate impaired skin barrier to evaluate emissions for impaired skin barrier function[6].

As with other direct contact approaches, tape stripping may not be suitable for very volatile compound analysis where RSSCs of higher abundances are collected, outcompeting small VOC abundances and concentrations[10,124]. This method is however, excellent for collecting and analysing non-volatile components of the skin ECM highly applicable to lipidomics research[58]. Furthermore, tape stripping is more difficult to reproduce than other sampling approaches as standardised tape sizes and pressures are required. D-Squame™ tape disks aim to address these issues through standardising the adhesive material, SC collection area, and with their D500 pressure instrument, application pressures[34]. This could be used for reproducible skin analysis, especially coupled to thermal desorption (TD) extraction units.

1.4.1.4. Biocompatible polymers

Polydimethylsiloxane (PDMS) has emerged as a versatile, wearable and effective material for skin VOC collection[150]. Its application excels in direct contact sampling approaches such as PDMS patches and wearable loops[26]. PDMS exhibits excellent biocompatibility, thermal stability, and flexibility, making it a suitable candidate for skin-contacting sampling devices[8]. The PDMS-based skin sampling loops fabricated by Roodt et al. conformed to the contours of the body, reported to allow comfortable sampling durations exceeding 8 hours[26], shown in Figure 1.16. (a). However, the hydrophobic nature of PDMS can present challenges in high humidity environments, as is found at the skin surface[151]. Water vapor can compete with target analytes for adsorption sites on PDMS surface, potentially reducing the efficiency of VOC recoveries.

Reflecting PDMS-based direct contact sampling, SorbStar® is a commercially available VOC sorbent sampling device manufactured by Action Europe, where one to four hours of contact is necessary to transfer VOCs from a sample to the silicone binding sites[21], as stated by the manufacturer. This single-use sampling device allows for sampling of VOCs upon direct contact with the skin surface, offering advantages over traditional sampling methods[120] such as biocompatibility, handleability, and cost-effectiveness.

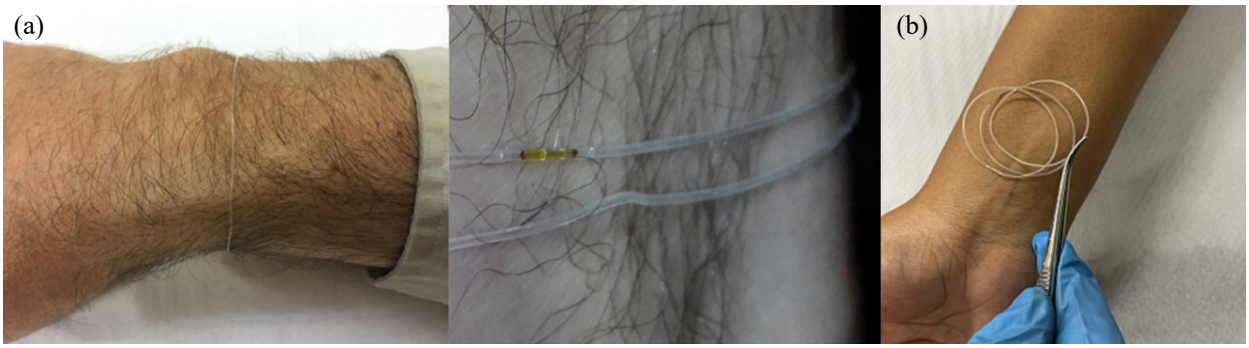

Figure 1.16. (a) PDMS sampling loop attached to the wrist (left) and ankle (centre) reproduced from Roodt et al.[26] **(b)** Modified silicone rubber band for skin VOC sampling towards GC based identification of tuberculosis associated compounds (right), reproduced from Makhubela et al.[4]

Moreover, Cuzuel et al. improved the performance of SorbStar® sampling by developing pre-concentration steps for VOCs using a Tenax TA system trap prior to GC x GC (two dimensional gas chromatography)-MS based separation and analysis[158,159]. This approach was employed in a clinical study by Leemans et al. probing collected breast cancer sweat samples while implementing GC-MS analysis workflow[120]. Figure 1.16 (b) shows another example of a modified PDMS based elastic band, applied directly onto the skin for VOC sampling[4]. Analytically, these siloxane based polymer materials tend to be 'cleaner' for analysis due to higher thermal stabilities compared sterile cotton based materials[150].

1.4.2. Contactless volatile emissions sampling

Contrasting direct contact approaches, non-invasive contactless sampling collects the gas adjacent to a region of skin, usually within a contained environment[2,6]. These techniques can include the use of glass funnels[17] or other inert chambers placed over the skin to create a headspace[22,127,155], from which VOCs are captured onto sorbent materials.

Sampled HS may be of 'static' type or 'flow through' type, where inert carrier gas is passed through the HS at a constant flow rate[16,61,102]. Typically, approaches isolating a small area of skin for sampling tend to be of the static type, while the flow through HS is more common for whole body isolation chambers used for sampling skin VOCs[16,123,124].

Contactless approaches are especially useful for exploring skin relevant microbial volatile emissions as it enables VOC collection from living specimen, without disrupting them[3,76,130]. VOCs from proliferating human cells, in vitro, may also be collected with this approach[39,49,135,146]. Furthermore, this approach reduces contamination from non-volatile RSSCs, reduces potential ethical challenges[24] while enabling non-biocompatible sorbent materials use[61]. Static HS-SPME sampling has been labelled as gold standard for skin VOC collection due to commercial availability, tuneable analyte polarity range and compatibility with GC instruments[6,9,17].

HS-SPME fibres adsorb VOCs from an equilibrated HS, governed by VOC sorbent-air partition co-efficients[17,150]. Similarly, PFS (passive flux samplers) enables in-vivo skin gas collection without disrupting typical skin VOC emissions[22,98,127]. Finally, plethysmography chambers are increasing in prevalence for skin VOC sampling[124]. Whole body skin volatile emissions can be accurately estimated using these chambers, given adequate isolation from exhaled breath[27,123,160].

1.4.2.1. Static headspace solid phase microextraction fibres

HS-SPME fibres for non-invasive skin VOC collection functions by exploiting the partitioning of VOCs between the gas adjacent to the skin and a polymer fibre coating[150]. The sorbent material is housed in a retractable needle and exposed to gas adjacent to an area of skin for a controlled period[6,17,131].

During sampling, VOCs diffuse from the skin surface into the surrounding air and adsorb onto or absorb into the fibre coating based on their physicochemical properties. Specifically, these are their tendency to volatilise, polarity and sorbent-air partitioning co-efficients[150]. For this capture approach, sufficient VOC exposure time is required for the sampled HS to establish equilibrium[16,17]. This equilibrium must also be established between the sample medium and the SPME fibre, to provide an accurate representation of analytes.

Notably, these analytes experience competitive adsorption towards available binding sites of the fibre. SPME relies on equilibrium partitioning between the headspace and fibre, where less volatile or semi-volatile compounds may not be efficiently captured due to their lower diffusion rates into the headspace. Drawbacks for VOC capture using silicon-based adsorbents is the release of siloxanes and their derivatives during extraction of the captured analyte mixture[24].

1.4.2.2. Passive flux samplers

PFS for contactless static HS skin VOC collection operate on the principle of molecular diffusion, where VOCs emitted from the skin surface diffuse through a static air layer and are captured by a sorbent material[127,139]. In 2007, Sekine et al. developed the first PFS with polytetrafluoroethylene film for collecting skin VOCs[139], later modified to use MonoTrap®, now commercially available as "Monotrap™ SG DCC18". PFS can provide time averaged VOC measurements, allowing emission rate estimation rather than instantaneous HS VOC abundances.

Researchers have determined the flux of VOCs to be proportional to VOC concentration gradient between the skin surface and the trapping medium, thereby enabling an estimation of skin emission fluxes[139]. These PFS, whether using polymer film or MonoTrap®, rely on high sorptive capacity and chemical stability for capture and release of a range of analytes efficiently. This sampling rate is governed by the effective cross-sectional area of the sorbent, the diffusion path length, and the compound-specific diffusion coefficient[127,139,150].

1.4.2.3. Patch type sampling

Patch-type sampling builds on the static HS principle by incorporating a thin sorptive layer such as a PDMS polymer membrane[150]. This approach greatly reduces the HS volume and distance between the skin and sorbent. In other words, the path which a compound must travel is shortened. This patch-type approach typically enhances available surface area for analyte capture, compared to traditional SPME fibres[109]. An increased surface area improves efficiency of analyte collection, enabling detection of VOCs for trace analysis workflows[151].

This approach is more prone to contamination from skin oils than SPME, necessitating stringent cleaning protocols to avoid carryover effects[150]. Researchers often mitigate this by introducing sacrificial layers or separate components isolating the adsorbent material from direct contact with the skin.

1.4.2.3.1. Tenax Trapping Agent

Tenax TA has emerged as a widely used adsorbent polymer for collection of skin VOCs, highly compatible and frequently used with thermal desorption techniques. Good at adsorbing and preconcentrating VOCs in the range of C_7–C_{26}, with high thermal stability and selectivity for non-polar VOCs with boiling points in the range of 60-300°C[26].

Furthermore, Tenax TA is highly hydrophobic, allowing collection of VOCs from humid samples without significant interference from water[151]. These properties make Tenax TA particularly suitable for skin VOC collection, especially for microenvironments of high humidity, as small headspace volumes and participants with high SCH and TEWL[151]. Tenax TA exhibits low recoveries for very volatile and more polar compounds such as acetic acid, isopropanol and acetone[123]. This restriction may lead to biased VOC profiles, potentially missing key VOCs that fall outside this optimal range, especially relevant for untargeted analysis workflows.

1.4.2.3.2. Metal organic frameworks

Metal-organic frameworks (MOFs) are increasing in prevalence as sorbents for non-contact skin VOC capture due to their tuneable porosities and chemical properties along with high surface areas and selectivity[161]. MOFs adsorb VOCs into their porous structures, where analytes interact with metal nodes and organic residues through mechanisms such as ligation, hydrogen bonding, or π-π stacking for aromatic molecules[162]. Two MOFs frequently highlighted in literature are MIL-101(Cr) and ZIF-8[8,161]. MIL-101(Cr) is hydrophilic and has large pore sizes which makes it good at capturing more polar grouped VOCs such as carboxylic acids.

In contrast, ZIF-8 has a hydrophobic framework with small pores making it highly selective for small, non-polar VOCs, used previously to detect gaseous acetone[161]. The synthesis of MOFs can be complex and costly, however these can be re-used to typically higher degrees than other polymer adsorbents. Moreover, while MOFs exhibit excellent performance for certain VOCs, their selectivity can limit their usage for untargeted analysis unless multiple MOFs with complementary properties are employed. Ambient conditions such as RH can influence adsorption efficiency as hydrophilic MOFs may preferentially adsorb water vapor in high-humidity conditions[161], reducing available binding sites for VOCs.

1.4.3. Plethysmography chambers

Inert material plethysmography (whole body isolation) chambers are increasingly popular for whole body skin VOC collection applications[27,95,123,124,160]. Adequate isolation from breath must be undertaken, as to not overshadow less abundant skin volatile emissions[23,33]. These chambers create a controlled, sealed environment where VOCs released from the entire skin surface can be collected efficiently. These chambers are equipped with carrier gas flow through, temperature and humidity controls and multiple sampling ports to ensure uniform VOC distribution[124]. Collecting whole body skin VOCs is both an advantage, as effects from the heterogenous skin are averaged out, for a complete look at comprehensive skin VOC emissions.

This is also a disadvantage, particularly for targeted analysis for profiling localised skin conditions and comparing involved to uninvolved skin. However, this averaging of skin VOC emissions may prove as a suitable solution for investigating systemic conditions, especially when comparing person-to-person overall healthy skin emissions. As per other outlined contactless VOC capture methods, VOCs are directed onto adsorbent materials for subsequent instrument separation and analysis workflows.

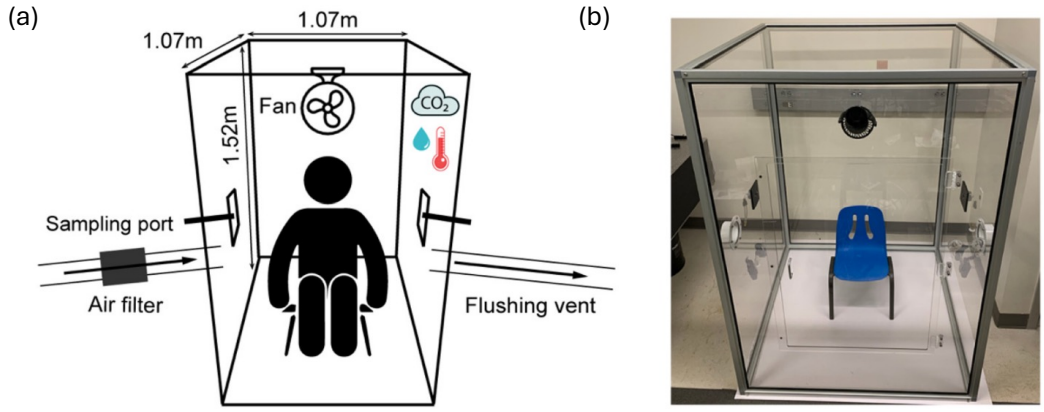

Figure 1.17. (a) Plethysmography chamber design schematic for sampling of whole body VOC emissions. Adaptations also exist for isolation of breath VOCs. **(b)** Image of the plethysmography chamber. Figure reproduced from Rankin-Turner and McMeniman[123].

1.5. Analysis workflows for skin derived volatile organic compound emissions

Compounding the outlined challenges related to skin VOC collection, difficulties in comparing VOC profiles from different participants arise due to the myriad of approaches between analytical methods and instrumentation[37,150]. Standardised sampling protocols, wider scale population profiling and unified analysis platforms will support strengthening inferences for skin volatile research[3,163].

Effective data pre-processing protocols are also essential for ensuring a GC-MS-based skin VOC analysis yields accurate and biologically meaningful results. Offline and online workflows are both employed for skin VOC analysis, however each has distinct advantages and limitations[28,150]. GC-MS was the most commonly used analytical platform, capable of a high degree of separation for complex gaseous mixtures while collecting mass spectral information for each compound[2,37]. Similar to VOC capture materials, each analytical platform has unique advantages and may offer differential results as a function of the separation material or technique employed[14,150].

1.5.1. Offline analysis

Offline analysis workflows involve sample collection followed by a temporary storage and subsequent analysis in a laboratory setting[3]. Gas chromatography-mass spectrometry is the most commonly used analytical platform[2,3,14,37,86,150], with more sophisticated techniques such as two-dimensional GC x GC-Time of Flight (ToF)-MS showing promise for improved compound separation and enhanced untargeted analysis capabilities[24]. Offline approaches usually have higher sensitivity and specificity for untargeted VOC profiling[28].

Offline instrumentation may analyse complex mixtures of VOCs with detailed chemical identification due to increased time allowed for compound separation, compared to online approaches. This is however a disadvantage when rapid results or screening are required. Offline approaches allow time to compared with available reference libraries to allow accurate biomarker identification[119,163].

1.5.1.1. Gas chromatography-mass spectrometry

GC-MS is the primary analytical technique for studying VOCs due to its suitability for analysing and identifying mixtures of chemical species at low abundances[14,20]. A sample is ionised and separated based on analyte polarity, affinities to the stationary and mobile phases, molecular weights and breakthrough volumes. Separation then occurs on a heated chromatographic column, where the selection of GC column materials affects the resultant compound retention times (RT) and perceived peak areas, also referred to as abundance.

As a result, GC-MS offers excellent performance for separation of complex mixtures and their chemical qualification. Compounds are then tentatively identified with combination of analyte retention index (RI) and mass spectral similarity scores[20]. Instrument and sample stability should be assessed for each instrument and for each target compound. Analytes tentatively identified from biological samples through mass spectral library matches should be confirmed by applying the same chromatographic methods to authentic standards to compare retention times and mass spectral features[16,17,24].

As a result, identification of chromatographic peaks solely based on mass spectral library matches without validation with synthetic standards is uncertain[28]. Owsienko et al. found GC-O (GC-olfactory detection) to have lower limits of detection (LOD) compared to traditional GC-MS[20], highlighting the importance of pre-concentration for this analysis approach. Compound misidentification can readily occur due to co-elution, compound absence from the MS library, and MS similarities[163]. Furthermore, the silicone-based composition of some GC columns gives rise to siloxane artifacts originating within the GC system[16,17,102]. These residues may form complexes with the target analytes reducing their real observed abundances. Overall, reducing reliance on RI and MS library matches and verifying with chemical standards enhances VOC identification confidence significantly[14,119,164].

1.5.1.2. Thermal desorption gas chromatography mass spectrometry

Thermal desorption (TD)-GC-MS offers significant advantages over traditional GC-MS analysis for skin VOC analysis[146]. TD-GC-MS allows pre-concentration and detection of trace-abundance VOCs with high specificity and sensitivity[28]. A thermo-desorption step is integrated, releasing adsorbed analytes onto the stationary phase for separation and detection in a single and quick burst. This strategy does not require a solvent and enhances instrumental sensitivity, detecting trace-level VOCs, where they could be below instrumental LOD without TD[28,159]. However, thermal desorption may not fully recover thermally labile compounds that decompose at elevated temperatures.

1.5.1.3. Two dimensional gas chromatography mass spectrometry

Two dimensional gas chromatography (GC x GC)-MS augments the analytical capabilities of traditional GC-MS by introducing an additional chromatographic dimension in the form of a second separation column[24]. The enhancement associated with a second dimension substantially improves separation and resolution of complex mixtures, especially useful for skin VOC analysis[4]. The technique utilises two columns with orthogonal stationary phases, typically comprising a non-polar column followed by a polar column connected through a modulator[26]. A GC x GC chromatograph of the gas emitted from a male subject's hand skin is shown in Figure 1.18.

Of further benefit to skin VOC sampling, this analysis approach is more robust when a mixture has compounds of different polarity ranges[158,159]. Especially applicable to skin, a wider range of compatible compound polarities per each chromatographic run substantially eases identification of smaller molecules containing more polar characteristic than usual, such as is the case for acetone or acetic acid. This dual-stage process can even resolve co-eluting compounds that would otherwise overlap during traditional GC-MS based separation[120], providing a more comprehensive and reliable separation and identification of skin emitted VOCs[4].

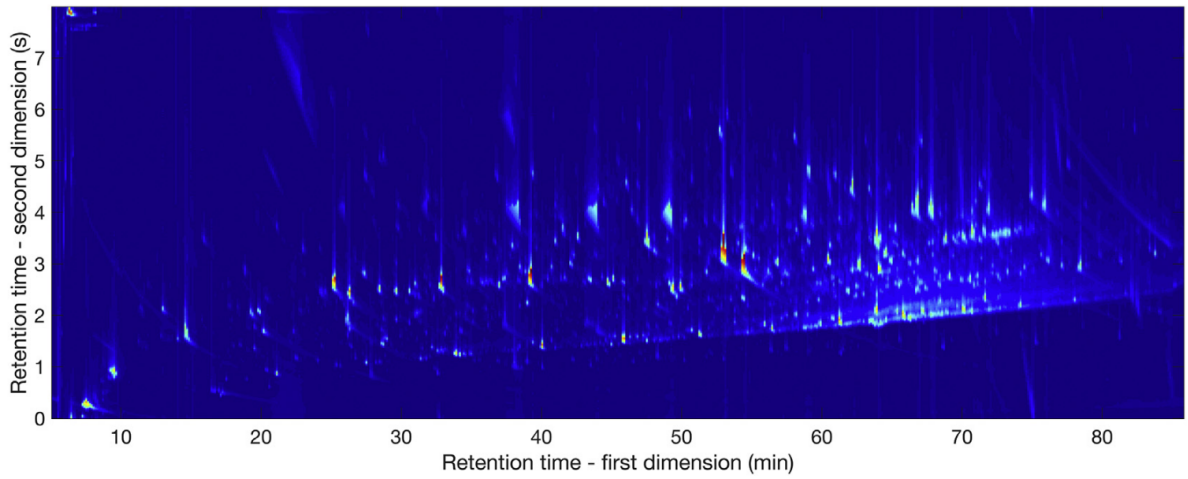

Figure 1.18. A GC x GC chromatograph of a skin sample obtained from the hand of a 25 year old male. Figure reproduced from Cuzuel et al.[158]

1.5.2. Online analysis

Online and near-participant analyses have been reported for skin derived VOC detection, especially prevalent for targeted analysis[109]. Direct detection methods offer advantages for time-resolved analysis, throughput and high sensitivity[28,61], potentially leading to end-patient operated sampling and analysis systems. Samples are analysed immediately upon collection, eliminating potential errors that could arise due to sample storage and transportation[97].

Common direct detection techniques in VOC studies include proton transfer reaction (PTR)-MS[61,97], selected ion flow tube-MS, secondary electrospray ionisation-MS and extractive electrospray ionisation-MS. Among these techniques, PTR-MS is the most frequently employed for skin VOC research as it can identify highly volatile compounds[28,33], for real time analysis. High-resolution PTR-TOF-MS can provide mass-to-charge ratios (m/z) of ionised compounds but not molecular structures[61] proving more effective for targeted analysis approaches, especially for real time analysis.

1.5.2.1. Proton transfer reaction time of flight mass spectrometry

PTR-TOF-MS is a highly sensitive, real-time analytical technique employed in skin VOC research to measure the concentration of small VOC molecules[61,141]. PTR operates by ionising VOCs through H^+ transfer with hydronium ions (H_3O^+). These selectively react with compounds possessing a higher proton affinity than water[23,28]. Resulting protonated compounds are then analysed through MS.

This method enables rapid and non-invasive monitoring of skin VOCs without a need for extensive sample preparation and sample separation. PTR-TOF-MS is particularly effective for detecting VOCs such as aldehydes, ketones, and carboxylic acids. Conversely, alkanes, which possess a proton affinity less than water are undetectable by this technique[28].

The advantages of PTR-MS include its ability to provide real-time data with high sensitivity (ppt levels) and its capacity for targeted analysis, allowing the detection of a wide range of VOCs simultaneously[97]. The soft ionisation process minimises compound fragmentation, preserving molecular ions for accurate identification[28,61]. Limitations of PTR-MS compared to GC-MS is analysing complex mixtures of VOCs, such as is the case from the skin matrix, where GC-MS has superior chromatographic separation over time. However, PTR-TOF-MS cannot distinguish structural isomers without using complementary techniques[61].

1.5.3. Data pre-processing

Data pretreatment protocols, including baseline correction, peak deconvolution, normalisation, signal alignment, and statistical preprocessing, ensure accurate reflection of biological phenomena in GC-MS skin VOC data[16]. Following rigorous sample pretreatment, noise reduction, baseline correction, and normalisation of data can improve analysis and visualisation[37].

Deconvolution of overlapping peaks in complex chromatograms, especially for skin VOC mixtures, improves identification capacity of analytes found in a chromatograph. Normalisation techniques may account for sampling conditions like temperature, skin hydration or sampling duration, scaling VOC intensities relative to other internal standards or total ion counts (TIC)[37].

Data alignment, especially for comparing samples across runs, can ensure matched peaks across datasets reducing errors in comparative analyses. RI matching is a form of data alignment used commonly to strengthen compound identification. Statistical preprocessing, such as PCA or PLS-DA, reduces the dimensionality of the data highlighting patterns in VOC

profiles over two planar dimensions. This technique helps to identify key compounds associated with physiological states or conditions while minimising noise from variables more prone to noise[146].

Overapplication of these protocols such as overcorrection during baseline subtraction or improper normalisation can distort statistical analysis. Implementing robust quality control measures, including blank samples and replicates, is essential to validate preprocessing workflows.

1.5.4. Biological interpretation

To improve the reliability of skin VOC analysis for biological and clinical applications, several workflow modifications can be implemented. Firstly, categorising collected VOC data into missing not at random (MNAR), missing at random (MAR), missing completely at random (MCAR)[165]. A frequent misconception for missing values in skin VOC data is attributing it to metabolites with low concentrations, such as those below the instrument's LOD.

While in numerous instances, missing values can be attributed to low concentrations, it has been demonstrated numerous times that missing values can also be caused by biological and/or technical variations[166]. To combat this, imputation strategies have been successfully applied to GC-MS workflows[165,166]. Integrating complementary omics data (e.g., microbiomics or proteomics) provides a holistic understanding of biochemical processes[10].

Wearable sensors for continuous monitoring capture and effectively average out temporal variations effectively[26]. Combining targeted and untargeted analytical approaches ensures detection of known and novel compounds[28]. Furthermore, well implemented machine learning algorithms have tremendous potential to improve pattern recognition and identify subtle correlations between VOC profiles and physiological states that may be missed by human data analysts[21,167,168]. Controlled studies with larger cohorts and diverse demographics validate findings and account for inter-individual variability[37,163].

1.6 Conclusion

This research explores the potential of human skin VOCs as non-invasive physiochemical probes for overall health diagnostics or monitoring. As these compounds leave the skin, they may offer systemic insight into subcutaneous biochemical processes, currently achievable through invasive methods such as biopsies or intravenous blood sampling. Furthermore, VOC composition and abundance may offer insight into localised skin conditions, even before any visual cues of disease or ailment are observed. Considering this emerging potential, devices capable of collecting VOCs from the skin are gaining traction as alternatives to the available, yet expensive commercial sampling approaches, such as the robust HS-SPME. The abundance of challenges in this field regarding stability of recovered skin VOC profiles within and across individuals highlights the influence of factors like health status and environmental conditions. Considering skin VOCs originating sources, including transcutaneous movement of compounds from systemic circulation, cutaneous cellular activity, and skin glandular secretions metabolised by the skin microbiome, person-to-person differences in recovered profiles could be taken into account for analysis.

Overall, progress in the skin volatile field is rapidly advancing, propelled through development of novel approaches for sampling VOCs directly from the skin of participants, while efforts to implement more sophisticated data analysis techniques, reveal more insightful results, guiding research towards more robust comparability across studies. However, many challenges halt skin VOC implementation as the proposed supporting physiochemical markers for overall health, governed by their intrinsic complexity and variance across subjects. Despite these challenges, the potential for decentralised sampling and further on, personalised monitoring and self-management platforms, utilising these skin volatile emissions, may be realised in the near future.

1.7 References

(1) Baker, P.; Huang, C.; Radi, R.; Moll, S. B.; Jules, E.; Arbiser, J. L. Skin Barrier Function: The Interplay of Physical, Chemical, and Immunologic Properties. *Cells* **2023**, *12* (23), 2745. https://doi.org/10.3390/cells12232745.

(2) Duffy, E.; Morrin, A. Endogenous and Microbial Volatile Organic Compounds in Cutaneous Health and Disease. *TrAC Trends Anal. Chem.* **2019**, *111*, 163–172. https://doi.org/10.1016/j.trac.2018.12.012.

(3) Fitzgerald, S.; Ahmed, W.; Piechulla, B.; Fowler, S. J.; Morrin, A. Volatilomes of Human Infection. *Anal. Bioanal. Chem.* **2024**, *416* (1), 37–53. https://doi.org/10.1007/s00216-023-04986-z.

(4) Makhubela, P. C. K.; Rohwer, E. R.; Naudé, Y. Detection of Tuberculosis-Associated Compounds from Human Skin by GCxGC-TOFMS. *J. Chromatogr. B* **2023**, *1231*, 123937. https://doi.org/10.1016/j.jchromb.2023.123937.

(5) Zhang, J. D.; Le, M. N.; Hill, K. J.; Cooper, A. A.; Stuetz, R. M.; Donald, W. A. Identifying Robust and Reliable Volatile Organic Compounds in Human Sebum for Biomarker Discovery. *Anal. Chim. Acta* **2022**, *1233*, 340506. https://doi.org/10.1016/j.aca.2022.340506.

(6) Duffy, E.; Jacobs, M. R.; Kirby, B.; Morrin, A. Probing Skin Physiology through the Volatile Footprint: Discriminating Volatile Emissions before and after Acute Barrier Disruption. *Exp. Dermatol.* **2017**, *26* (10), 919–925. https://doi.org/10.1111/exd.13344.

(7) Waring, M. S.; Wells, J. R. Volatile Organic Compound Conversion by Ozone, Hydroxyl Radicals, and Nitrate Radicals in Residential Indoor Air: Magnitudes and Impacts of Oxidant Sources. *Atmos. Environ.* **2015**, *106*, 382–391. https://doi.org/10.1016/j.atmosenv.2014.06.062.

(8) Azzouz, A.; Vikrant, K.; Kim, K.-H.; Ballesteros, E.; Rhadfi, T.; Malik, A. K. Advances in Colorimetric and Optical Sensing for Gaseous Volatile Organic Compounds. *TrAC Trends Anal. Chem.* **2019**, *118*, 502–516. https://doi.org/10.1016/j.trac.2019.06.017.

(9) Rios-Navarro, A.; Gonzalez, M.; Carazzone, C.; Celis Ramírez, A. M. Learning about Microbial Language: Possible Interactions Mediated by Microbial Volatile Organic Compounds (VOCs) and Relevance to Understanding Malassezia Spp. Metabolism. *Metabolomics* **2021**, *17* (4), 39. https://doi.org/10.1007/s11306-021-01786-3.

(10) Haertl, T.; Owsienko, D.; Schwinn, L.; Hirsch, C.; Eskofier, B. M.; Lang, R.; Wirtz, S.; Loos, H. M. Exploring the Interrelationship between the Skin Microbiome and Skin

Volatiles: A Pilot Study. *Front. Ecol. Evol.* **2023**, *11*, 1107463. https://doi.org/10.3389/fevo.2023.1107463.

(11) Wu, T.; Tasoglou, A.; Huber, H.; Stevens, P. S.; Boor, B. E. Influence of Mechanical Ventilation Systems and Human Occupancy on Time-Resolved Source Rates of Volatile Skin Oil Ozonolysis Products in a LEED-Certified Office Building. *Environ. Sci. Technol.* **2021**, *55* (24), 16477–16488. https://doi.org/10.1021/acs.est.1c03112.

(12) Wang, H.; Wang, H.; Wang, K.; Xiong, J.; Huang, S.; Wolfson, J. M.; Koutrakis, P. Characterization of Chemical Transport in Human Skin and Building Material. *J. Hazard. Mater.* **2023**, *458*, 131917. https://doi.org/10.1016/j.jhazmat.2023.131917.

(13) Zou, Z.; Yang, X. Skin Volatile Organic Compound Emissions from 14 Healthy Young Adults under Controlled Conditions. *Build. Environ.* **2022**, *222*, 109416. https://doi.org/10.1016/j.buildenv.2022.109416.

(14) Drabińska, N.; Flynn, C.; Ratcliffe, N.; Belluomo, I.; Myridakis, A.; Gould, O.; Fois, M.; Smart, A.; Devine, T.; Costello, B. D. L. A Literature Survey of All Volatiles from Healthy Human Breath and Bodily Fluids: The Human Volatilome. *J. Breath Res.* **2021**, *15* (3), 034001. https://doi.org/10.1088/1752-7163/abf1d0.

(15) Filetti, V.; Di Mizio, G.; Rendine, M.; Fortarezza, P.; Ricci, P.; Pomara, C.; Messina, G.; Riezzo, I.; Zammit, C.; Messina, A.; Salerno, M.; Sessa, F. Volatile Organic Compounds: Instrumental and Canine Detections Link an Individual to the Crime Scene. *Egypt. J. Forensic Sci.* **2019**, *9* (1), 35. https://doi.org/10.1186/s41935-019-0139-1.

(16) Finnegan, M.; Fitzgerald, S.; Duroux, R.; Attia, J.; Markey, E.; O'Connor, D.; Morrin, A. Predicting Chronological Age via the Skin Volatile Profile. *J. Am. Soc. Mass Spectrom.* **2024**, jasms.3c00315. https://doi.org/10.1021/jasms.3c00315.

(17) Shetewi, T.; Finnegan, M.; Fitzgerald, S.; Xu, S.; Duffy, E.; Morrin, A. Investigation of the Relationship between Skin-Emitted Volatile Fatty Acids and Skin Surface Acidity in Healthy Participants—a Pilot Study. *J. Breath Res.* **2021**, *15* (3), 037101. https://doi.org/10.1088/1752-7163/abf20a.

(18) Frazier, C. J. G.; Gokool, V. A.; Holness, H. K.; Mills, D. K.; Furton, K. G. Multivariate Regression Modelling for Gender Prediction Using Volatile Organic Compounds from Hand Odor Profiles via HS-SPME-GC-MS. *PLOS ONE* **2023**, *18* (7), e0286452. https://doi.org/10.1371/journal.pone.0286452.

(19) Molinier, B.; Arata, C.; Katz, E. F.; Lunderberg, D. M.; Ofodile, J.; Singer, B. C.; Nazaroff, W. W.; Goldstein, A. H. Bedroom Concentrations and Emissions of Volatile

Organic Compounds during Sleep. *Environ. Sci. Technol.* **2024**, *58* (18), 7958–7967. https://doi.org/10.1021/acs.est.3c10841.

(20) Owsienko, D.; Goppelt, L.; Hierl, K.; Schäfer, L.; Croy, I.; Loos, H. M. Body Odor Samples from Infants and Post-Pubertal Children Differ in Their Volatile Profiles. *Commun. Chem.* **2024**, *7* (1), 53. https://doi.org/10.1038/s42004-024-01131-4.

(21) Lucchi, G.; Crépin, M.; Chambaron, S.; Peltier, C.; Gilbert, L.; Guéré, C.; Vié, K. Effects of Psychological Stress on the Emission of Volatile Organic Compounds from the Skin. *Sci. Rep.* **2024**, *14* (1), 7238. https://doi.org/10.1038/s41598-024-57967-2.

(22) Hiramoto, T.; Kakumu, Y.; Sato, S.; Sekine, Y. Deodorising Garlic Body Odour by Ingesting Natural Food Additives Containing Phenolic Compounds and Polyphenol Oxidase. *Appl. Sci.* **2024**, *14* (21), 9631. https://doi.org/10.3390/app14219631.

(23) Qu, Y.; Zou, Z.; Weschler, C. J.; Liu, Y.; Yang, X. Quantifying Ozone-Dependent Emissions of Volatile Organic Compounds from the Human Body. *Environ. Sci. Technol.* **2023**, *57* (35), 13104–13113. https://doi.org/10.1021/acs.est.3c02340.

(24) Uebi, T.; Hariyama, T.; Suzuki, K.; Kanayama, N.; Nagata, Y.; Ayabe-Kanamura, S.; Yanase, S.; Ohtsubo, Y.; Ozaki, M. Sampling, Identification and Sensory Evaluation of Odors of a Newborn Baby's Head and Amniotic Fluid. *Sci. Rep.* **2019**, *9* (1), 12759. https://doi.org/10.1038/s41598-019-49137-6.

(25) Jha, S. Kr.; Marina, N.; Liu, C.; Hayashi, K. Human Body Odor Discrimination by GC-MS Spectra Data Mining. *Anal. Methods* **2015**, *7* (22), 9549–9561. https://doi.org/10.1039/C5AY02457A.

(26) Roodt, A. P.; Naudé, Y.; Stoltz, A.; Rohwer, E. Human Skin Volatiles: Passive Sampling and GC × GC-ToFMS Analysis as a Tool to Investigate the Skin Microbiome and Interactions with Anthropophilic Mosquito Disease Vectors. *J. Chromatogr. B* **2018**, *1097–1098*, 83–93. https://doi.org/10.1016/j.jchromb.2018.09.002.

(27) Zou, Z.; Yang, X. Volatile Organic Compound Emissions from the Human Body: Decoupling and Comparison between Whole-Body Skin and Breath Emissions. *Build. Environ.* **2022**, *226*, 109713. https://doi.org/10.1016/j.buildenv.2022.109713.

(28) Wu, T.; Müller, T.; Wang, N.; Byron, J.; Langer, S.; Williams, J.; Licina, D. Indoor Emission, Oxidation, and New Particle Formation of Personal Care Product Related Volatile Organic Compounds. *Environ. Sci. Technol. Lett.* **2024**, *11* (10), 1053–1061. https://doi.org/10.1021/acs.estlett.4c00353.

(29) Irga, Peter. J.; Mullen, G.; Fleck, R.; Matheson, S.; Wilkinson, Sara. J.; Torpy, Fraser. R. Volatile Organic Compounds Emitted by Humans Indoors– A Review on the

Measurement, Test Conditions, and Analysis Techniques. *Build. Environ.* **2024**, *255*, 111442. https://doi.org/10.1016/j.buildenv.2024.111442.

(30) Boxberger, M.; Cenizo, V.; Cassir, N.; La Scola, B. Challenges in Exploring and Manipulating the Human Skin Microbiome. *Microbiome* **2021**, *9* (1), 125. https://doi.org/10.1186/s40168-021-01062-5.

(31) Zamudio Díaz, D. F.; Busch, L.; Kröger, M.; Klein, A. L.; Lohan, S. B.; Mewes, K. R.; Vierkotten, L.; Witzel, C.; Rohn, S.; Meinke, M. C. Significance of Melanin Distribution in the Epidermis for the Protective Effect against UV Light. *Sci. Rep.* **2024**, *14* (1), 3488. https://doi.org/10.1038/s41598-024-53941-0.

(32) Mishor, A.; Amir, D. Sniffing the Human Body Volatile Hexadecanal Blocks Aggression in Men but Triggers Aggression in Women. *Sci. Adv.* **2021**.

(33) Wang, N.; Müller, T.; Ernle, L.; Bekö, G.; Wargocki, P.; Williams, J. How Does Personal Hygiene Influence Indoor Air Quality? *Environ. Sci. Technol.* **2024**, *58* (22), 9750–9759. https://doi.org/10.1021/acs.est.4c01698.

(34) Ludovici, M.; Kozul, N.; Materazzi, S.; Risoluti, R.; Picardo, M.; Camera, E. Influence of the Sebaceous Gland Density on the Stratum Corneum Lipidome. *Sci. Rep.* **2018**, *8* (1), 11500. https://doi.org/10.1038/s41598-018-29742-7.

(35) Shetage, S. S.; Traynor, M. J.; Brown, M. B.; Chilcott, R. P. Sebomic Identification of Sex- and Ethnicity-Specific Variations in Residual Skin Surface Components (RSSC) for Bio-Monitoring or Forensic Applications. *Lipids Health Dis.* **2018**, *17* (1), 194. https://doi.org/10.1186/s12944-018-0844-z.

(36) Géhin, C.; Tokarska, J.; Fowler, S. J.; Barran, P. E.; Trivedi, D. K. No Skin off Your Back: The Sampling and Extraction of Sebum for Metabolomics. *Metabolomics* **2023**, *19* (4), 21. https://doi.org/10.1007/s11306-023-01982-3.

(37) Mitra, A.; Choi, S.; Boshier, P. R.; Razumovskaya-Hough, A.; Belluomo, I.; Spanel, P.; Hanna, G. B. The Human Skin Volatolome: A Systematic Review of Untargeted Mass Spectrometry Analysis. *Metabolites* **2022**, *12* (9), 824. https://doi.org/10.3390/metabo12090824.

(38) Iitani, K.; Toma, K.; Arakawa, T.; Mitsubayashi, K. Transcutaneous Blood VOC Imaging System (Skin-Gas Cam) with Real-Time Bio-Fluorometric Device on Rounded Skin Surface. *ACS Sens.* **2020**, *5* (2), 338–345. https://doi.org/10.1021/acssensors.9b01658.

(39) Klemenz, A.-C.; Meyer, J.; Ekat, K.; Bartels, J.; Traxler, S.; Schubert, J. K.; Kamp, G.; Miekisch, W.; Peters, K. Differences in the Emission of Volatile Organic Compounds (VOCs) between Non-Differentiating and Adipogenically Differentiating Mesenchymal

Stromal/Stem Cells from Human Adipose Tissue. *Cells* **2019**, *8* (7), 697. https://doi.org/10.3390/cells8070697.

(40) Toma, K.; Suzuki, S.; Arakawa, T.; Iwasaki, Y.; Mitsubayashi, K. External Ears for Non-Invasive and Stable Monitoring of Volatile Organic Compounds in Human Blood. *Sci. Rep.* **2021**, *11* (1), 10415. https://doi.org/10.1038/s41598-021-90146-1.

(41) Longo, V.; Forleo, A.; Ferramosca, A.; Notari, T.; Pappalardo, S.; Siciliano, P.; Capone, S.; Montano, L. Blood, Urine and Semen Volatile Organic Compound (VOC) Pattern Analysis for Assessing Health Environmental Impact in Highly Polluted Areas in Italy. *Environ. Pollut.* **2021**, *286*, 117410. https://doi.org/10.1016/j.envpol.2021.117410.

(42) Fussell, J. C.; Kelly, F. J. Oxidative Contribution of Air Pollution to Extrinsic Skin Ageing. *Free Radic. Biol. Med.* **2020**, *151*, 111–122. https://doi.org/10.1016/j.freeradbiomed.2019.11.038.

(43) Weschler, C. J.; Nazaroff, W. W. Human Skin Oil: A Major Ozone Reactant Indoors. *Environ. Sci. Atmospheres* **2023**, *3* (4), 640–661. https://doi.org/10.1039/D3EA00008G.

(44) Orioli, D.; Dellambra, E. Epigenetic Regulation of Skin Cells in Natural Aging and Premature Aging Diseases. *Cells* **2018**, *7* (12), 268. https://doi.org/10.3390/cells7120268.

(45) Ratcliffe, N.; Wieczorek, T.; Drabińska, N.; Gould, O.; Osborne, A.; De Lacy Costello, B. A Mechanistic Study and Review of Volatile Products from Peroxidation of Unsaturated Fatty Acids: An Aid to Understanding the Origins of Volatile Organic Compounds from the Human Body. *J. Breath Res.* **2020**, *14* (3), 034001. https://doi.org/10.1088/1752-7163/ab7f9d.

(46) Montero-Vilchez, T.; Segura-Fernández-Nogueras, M.-V.; Pérez-Rodríguez, I.; Soler-Gongora, M.; Martinez-Lopez, A.; Fernández-González, A.; Molina-Leyva, A.; Arias-Santiago, S. Skin Barrier Function in Psoriasis and Atopic Dermatitis: Transepidermal Water Loss and Temperature as Useful Tools to Assess Disease Severity. *J. Clin. Med.* **2021**, *10* (2), 359. https://doi.org/10.3390/jcm10020359.

(47) Dezest, M.; Le Bechec, M.; Chavatte, L.; Desauziers, V.; Chaput, B.; Grolleau, J.-L.; Descargues, P.; Nizard, C.; Schnebert, S.; Lacombe, S.; Bulteau, A.-L. Oxidative Damage and Impairment of Protein Quality Control Systems in Keratinocytes Exposed to a Volatile Organic Compounds Cocktail. *Sci. Rep.* **2017**, *7* (1), 10707. https://doi.org/10.1038/s41598-017-11088-1.

(48) Ni, Q. Z.; Sierra, B. N.; La Clair, J. J.; Burkart, M. D. Chemoenzymatic Elaboration of the Raper–Mason Pathway Unravels the Structural Diversity within Eumelanin Pigments. *Chem. Sci.* **2020**, *11* (30), 7836–7841. https://doi.org/10.1039/D0SC02262D.

(49) Kwak, J.; Gallagher, M.; Ozdener, M. H.; Wysocki, C. J.; Goldsmith, B. R.; Isamah, A.; Faranda, A.; Fakharzadeh, S. S.; Herlyn, M.; Johnson, A. T. C.; Preti, G. Volatile Biomarkers from Human Melanoma Cells. *J. Chromatogr. B* **2013**, *931*, 90–96. https://doi.org/10.1016/j.jchromb.2013.05.007.

(50) Abaffy, T.; Duncan, R.; Riemer, D. D.; Tietje, O.; Elgart, G.; Milikowski, C.; DeFazio, R. A. Differential Volatile Signatures from Skin, Naevi and Melanoma: A Novel Approach to Detect a Pathological Process. *PLoS ONE* **2010**, *5* (11), e13813. https://doi.org/10.1371/journal.pone.0013813.

(51) Slominski, R. M.; Sarna, T.; Płonka, P. M.; Raman, C.; Brożyna, A. A.; Slominski, A. T. Melanoma, Melanin, and Melanogenesis: The Yin and Yang Relationship. *Front. Oncol.* **2022**, *12*, 842496. https://doi.org/10.3389/fonc.2022.842496.

(52) Swaney, M. H.; Nelsen, A.; Sandstrom, S.; Kalan, L. R. Sweat and Sebum Preferences of the Human Skin Microbiota. *Microbiol. Spectr.* **2023**, *11* (1), e04180-22. https://doi.org/10.1128/spectrum.04180-22.

(53) Zouboulis, C. C.; Coenye, T.; He, L.; Kabashima, K.; Kobayashi, T.; Niemann, C.; Nomura, T.; Oláh, A.; Picardo, M.; Quist, S. R.; Sasano, H.; Schneider, M. R.; Törőcsik, D.; Wong, S. Y. Sebaceous Immunobiology - Skin Homeostasis, Pathophysiology, Coordination of Innate Immunity and Inflammatory Response and Disease Associations. *Front. Immunol.* **2022**, *13*, 1029818. https://doi.org/10.3389/fimmu.2022.1029818.

(54) Chang, Y.; Wang, X. Sweat and Odor in Sportswear – A Review. *iScience* **2023**, *26* (7), 107067. https://doi.org/10.1016/j.isci.2023.107067.

(55) Gerrett, N.; Griggs, K.; Redortier, B.; Voelcker, T.; Kondo, N.; Havenith, G. Sweat from Gland to Skin Surface: Production, Transport, and Skin Absorption. *J. Appl. Physiol.* **2018**, *125* (2), 459–469. https://doi.org/10.1152/japplphysiol.00872.2017.

(56) Choi, E. H.; Kang, H. Importance of Stratum Corneum Acidification to Restore Skin Barrier Function in Eczematous Diseases. *Ann. Dermatol.* **2024**, *36* (1), 1. https://doi.org/10.5021/ad.23.078.

(57) Lam, T. H.; Verzotto, D.; Brahma, P.; Ng, A. H. Q.; Hu, P.; Schnell, D.; Tiesman, J.; Kong, R.; Ton, T. M. U.; Li, J.; Ong, M.; Lu, Y.; Swaile, D.; Liu, P.; Liu, J.; Nagarajan, N. Understanding the Microbial Basis of Body Odor in Pre-Pubescent Children and Teenagers. *Microbiome* **2018**, *6* (1), 213. https://doi.org/10.1186/s40168-018-0588-z.

(58) Knox, S.; O'Boyle, N. M. Skin Lipids in Health and Disease: A Review. *Chem. Phys. Lipids* **2021**, *236*, 105055. https://doi.org/10.1016/j.chemphyslip.2021.105055.

(59) Starr, N. J.; Khan, M. H.; Edney, M. K.; Trindade, G. F.; Kern, S.; Pirkl, A.; Kleine-Boymann, M.; Elms, C.; O'Mahony, M. M.; Bell, M.; Alexander, M. R.; Scurr, D. J. Elucidating the Molecular Landscape of the Stratum Corneum. *Proc. Natl. Acad. Sci.* **2022**, *119* (12), e2114380119. https://doi.org/10.1073/pnas.2114380119.

(60) Morrison, G. C.; Eftekhari, A.; Majluf, F.; Krechmer, J. E. Yields and Variability of Ozone Reaction Products from Human Skin. *Environ. Sci. Technol.* **2021**, *55* (1), 179–187. https://doi.org/10.1021/acs.est.0c05262.

(61) Morrison, G.; Eftekhari, A.; Fan, A.; Majluf, F.; Krechmer, J. E. The Influence of Personal Care Products on Ozone-Skin Surface Chemistry. *PLOS ONE* **2022**, *17* (9), e0268263. https://doi.org/10.1371/journal.pone.0268263.

(62) Coffaro, B.; Weisel, C. P. The Effect of Environmental Parameters on Squalene-Ozone Particle Formation. *Atmos. Environ.* **2022**, *289*, 119295. https://doi.org/10.1016/j.atmosenv.2022.119295.

(63) Drnovsek, E.; Parichenko, A.; Power Guerra, N.; Pabst, J.; Wunderlich, K.; Falkenburger, B.; Huang, S.; Cuniberti, G.; Haehner, A.; Hummel, T. Human Perception of Parkinson's Disease Body Odor in Comparison to the Volatile Organic Compounds of Parkinson's Disease. *Parkinsonism Relat. Disord.* **2024**, *127*, 107091. https://doi.org/10.1016/j.parkreldis.2024.107091.

(64) Frederick Frasch, H.; Bunge, A. L. The Transient Dermal Exposure II: Post-Exposure Absorption and Evaporation of Volatile Compounds. *J. Pharm. Sci.* **2015**, *104* (4), 1499–1507. https://doi.org/10.1002/jps.24334.

(65) Cui, J.; Li, Z.; Zhang, W.; Wang, L.; Liu, H.; Liu, H. Integrating Aromatic Plants into Indoor Biophilic Environments: Species Selection Based on Psychophysiological Effects and Bioactive Volatile Compounds. *Build. Environ.* **2025**, *267*, 112169. https://doi.org/10.1016/j.buildenv.2024.112169.

(66) Oh, J.; Byrd, A. L.; Park, M.; Kong, H. H.; Segre, J. A. Temporal Stability of the Human Skin Microbiome. *Cell* **2016**, *165* (4), 854–866. https://doi.org/10.1016/j.cell.2016.04.008.

(67) Perez Perez, G. I.; Gao, Z.; Jourdain, R.; Ramirez, J.; Gany, F.; Clavaud, C.; Demaude, J.; Breton, L.; Blaser, M. J. Body Site Is a More Determinant Factor than Human Population Diversity in the Healthy Skin Microbiome. *PLOS ONE* **2016**, *11* (4), e0151990. https://doi.org/10.1371/journal.pone.0151990.

(68) Okoro, O. E.; Adenle, A.; Ludovici, M.; Truglio, M.; Marini, F.; Camera, E. Lipidomics of Facial Sebum in the Comparison between Acne and Non-Acne Adolescents with Dark Skin. *Sci. Rep.* **2021**, *11* (1), 16591. https://doi.org/10.1038/s41598-021-96043-x.

(69) Isler, M. F.; Coates, S. J.; Boos, M. D. Climate Change, the Cutaneous Microbiome and Skin Disease: Implications for a Warming World. *Int. J. Dermatol.* **2023**, *62* (3), 337–345. https://doi.org/10.1111/ijd.16297.

(70) Trivedi, D. K.; Sinclair, E.; Xu, Y.; Sarkar, D.; Walton-Doyle, C.; Liscio, C.; Banks, P.; Milne, J.; Silverdale, M.; Kunath, T.; Goodacre, R.; Barran, P. Discovery of Volatile Biomarkers of Parkinson's Disease from Sebum. *ACS Cent. Sci.* **2019**.

(71) Almaliki, H. S.; Angela, A.; Goraya, N. J.; Yin, G.; Bennett, J. W. Volatile Organic Compounds Produced by Human Pathogenic Fungi Are Toxic to Drosophila Melanogaster. *Front. Fungal Biol.* **2021**, *1*, 629510. https://doi.org/10.3389/ffunb.2020.629510.

(72) Emami, S. N.; Lindberg, B. G.; Hua, S.; Hill, S. R.; Mozuraitis, R.; Lehmann, P.; Birgersson, G.; Borg-Karlson, A.-K.; Ignell, R.; Faye, I. A Key Malaria Metabolite Modulates Vector Blood Seeking, Feeding, and Susceptibility to Infection. *Science* **2017**, *355* (6329), 1076–1080. https://doi.org/10.1126/science.aah4563.

(73) Li, X.; Wang, X.; Shi, X.; Wang, B.; Li, M.; Wang, Q.; Zhang, S. Antifungal Effect of Volatile Organic Compounds from Bacillus Velezensis CT32 against Verticillium Dahliae and Fusarium Oxysporum. *Processes* **2020**, *8* (12), 1674. https://doi.org/10.3390/pr8121674.

(74) Veselova, M. A.; Plyuta, V. A.; Khmel, I. A. Volatile Compounds of Bacterial Origin: Structure, Biosynthesis, and Biological Activity. *Microbiology* **2019**, *88* (3), 261–274. https://doi.org/10.1134/S0026261719030160.

(75) Tabares, M.; Ortiz, M.; Gonzalez, M.; Carazzone, C.; Vives Florez, M. J.; Molina, J. Behavioral Responses of Rhodnius Prolixus to Volatile Organic Compounds Released in Vitro by Bacteria Isolated from Human Facial Skin. *PLoS Negl. Trop. Dis.* **2018**, *12* (4), e0006423. https://doi.org/10.1371/journal.pntd.0006423.

(76) Fitzgerald, S.; Duffy, E.; Holland, L.; Morrin, A. Multi-Strain Volatile Profiling of Pathogenic and Commensal Cutaneous Bacteria. *Sci. Rep.* **2020**, *10* (1), 17971. https://doi.org/10.1038/s41598-020-74909-w.

(77) Ahle, C. M.; Stødkilde, K.; Poehlein, A.; Bömeke, M.; Streit, W. R.; Wenck, H.; Reuter, J. H.; Hüpeden, J.; Brüggemann, H. Interference and Co-Existence of Staphylococci and

Cutibacterium Acnes within the Healthy Human Skin Microbiome. *Commun. Biol.* **2022**, *5* (1), 923. https://doi.org/10.1038/s42003-022-03897-6.

(78) Nakatsuji, T.; Kao, M. C.; Zhang, L.; Zouboulis, C. C.; Gallo, R. L.; Huang, C.-M. Sebum Free Fatty Acids Enhance the Innate Immune Defense of Human Sebocytes by Upregulating β-Defensin-2 Expression. *J. Invest. Dermatol.* **2010**, *130* (4), 985–994. https://doi.org/10.1038/jid.2009.384.

(79) Stincone, A.; Prigione, A.; Cramer, T.; Wamelink, M. M. C.; Campbell, K.; Cheung, E.; Olin-Sandoval, V.; Grüning, N.; Krüger, A.; Tauqeer Alam, M.; Keller, M. A.; Breitenbach, M.; Brindle, K. M.; Rabinowitz, J. D.; Ralser, M. The Return of Metabolism: Biochemistry and Physiology of the Pentose Phosphate Pathway. *Biol. Rev.* **2015**, *90* (3), 927–963. https://doi.org/10.1111/brv.12140.

(80) Vishinkin, R.; Busool, R.; Mansour, E.; Fish, F.; Esmail, A.; Kumar, P.; Gharaa, A.; Cancilla, J. C.; Torrecilla, J. S.; Skenders, G.; Leja, M.; Dheda, K.; Singh, S.; Haick, H. Profiles of Volatile Biomarkers Detect Tuberculosis from Skin. *Adv. Sci.* **2021**, *8* (15), 2100235. https://doi.org/10.1002/advs.202100235.

(81) Saric-Bosanac, S.; Clark, A. K.; Sivamani, R. K.; Shi, V. Y. The Role of Hypothalamus-Pituitary-Adrenal (HPA)-like Axis in Inflammatory Pilosebaceous Disorders. *Dermatol. Online J.* **2020**, *26* (2). https://doi.org/10.5070/D3262047430.

(82) Rios-Navarro, A.; Gonzalez, M.; Carazzone, C.; Celis Ramírez, A. M. Why Do These Yeasts Smell So Good? Volatile Organic Compounds (VOCs) Produced by Malassezia Species in the Exponential and Stationary Growth Phases. *Molecules* **2023**, *28* (6), 2620. https://doi.org/10.3390/molecules28062620.

(83) Razo-Belmán, R.; Ángeles-López, Y. I.; García-Ortega, L. F.; León-Ramírez, C. G.; Ortiz-Castellanos, L.; Yu, H.; Martínez-Soto, D. Fungal Volatile Organic Compounds: Mechanisms Involved in Their Sensing and Dynamic Communication with Plants. *Front. Plant Sci.* **2023**, *14*, 1257098. https://doi.org/10.3389/fpls.2023.1257098.

(84) Moskaluk, A. E.; VandeWoude, S. Current Topics in Dermatophyte Classification and Clinical Diagnosis. *Pathogens* **2022**, *11* (9), 957. https://doi.org/10.3390/pathogens11090957.

(85) Coutinho-Abreu, I. V.; Jamshidi, O.; Raban, R.; Atabakhsh, K.; Merriman, J. A.; Akbari, O. S. Identification of Human Skin Microbiome Odorants That Manipulate Mosquito Landing Behavior. *Sci. Rep.* **2024**, *14* (1), 1631. https://doi.org/10.1038/s41598-023-50182-5.

(86) Zhang, H.; Zhu, Y.; Liu, Z.; Peng, Y.; Peng, W.; Tong, L.; Wang, J.; Liu, Q.; Wang, P.; Cheng, G. A Volatile from the Skin Microbiota of Flavivirus-Infected Hosts Promotes Mosquito Attractiveness. *Cell* **2022**, *185* (14), 2510-2522.e16. https://doi.org/10.1016/j.cell.2022.05.016.

(87) Bang, C.; Schmitz, R. A. Archaea Associated with Human Surfaces: Not to Be Underestimated. *FEMS Microbiol. Rev.* **2015**, *39* (5), 631–648. https://doi.org/10.1093/femsre/fuv010.

(88) Probst, A. J.; Auerbach, A. K.; Moissl-Eichinger, C. Archaea on Human Skin. *PLoS ONE* **2013**, *8* (6), e65388. https://doi.org/10.1371/journal.pone.0065388.

(89) Moissl-Eichinger, C.; Probst, A. J.; Birarda, G.; Auerbach, A.; Koskinen, K.; Wolf, P.; Holman, H.-Y. N. Human Age and Skin Physiology Shape Diversity and Abundance of Archaea on Skin. *Sci. Rep.* **2017**, *7* (1), 4039. https://doi.org/10.1038/s41598-017-04197-4.

(90) Umbach, A. K.; Stegelmeier, A. A.; Neufeld, J. D. Archaea Are Rare and Uncommon Members of the Mammalian Skin Microbiome. *mSystems* **2021**, *6* (4), 10.1128/msystems.00642-21. https://doi.org/10.1128/msystems.00642-21.

(91) Shetage, S. S.; Traynor, M. J.; Brown, M. B.; Raji, M.; Graham-Kalio, D.; Chilcott, R. P. Effect of Ethnicity, Gender and Age on the Amount and Composition of Residual Skin Surface Components Derived from Sebum, Sweat and Epidermal Lipids. *Skin Res. Technol.* **2014**, *20* (1), 97–107. https://doi.org/10.1111/srt.12091.

(92) Mahnert, A.; Dreer, M.; Perier, U.; Melcher, M.; Duller, S.; Lehnen, A.; Goessler, T.; Brunner, D.; Graier, T.; Wolf, P.; Ponce-Toledo, R. I.; Hodgskiss, L.; Kerou, M.; Moissl-Eichinger, C.; Schleper, C. Molecular Tracking and Cultivation Reveal Ammonia Oxidizing Archaea as Integral Members of the Human Skin Microbiome. August 5, 2024. https://doi.org/10.1101/2024.08.05.606590.

(93) Traxler, S.; Barkowsky, G.; Saß, R.; Klemenz, A.-C.; Patenge, N.; Kreikemeyer, B.; Schubert, J. K.; Miekisch, W. Volatile Scents of Influenza A and S. Pyogenes (Co-)Infected Cells. *Sci. Rep.* **2019**, *9* (1), 18894. https://doi.org/10.1038/s41598-019-55334-0.

(94) Essler, J. L.; Kane, S. A.; Nolan, P.; Akaho, E. H.; Berna, A. Z.; DeAngelo, A.; Berk, R. A.; Kaynaroglu, P.; Plymouth, V. L.; Frank, I. D.; Weiss, S. R.; Odom John, A. R.; Otto, C. M. Discrimination of SARS-CoV-2 Infected Patient Samples by Detection Dogs: A Proof of Concept Study. *PLOS ONE* **2021**, *16* (4), e0250158. https://doi.org/10.1371/journal.pone.0250158.

(95) Giraldo, D.; Rankin-Turner, S.; Corver, A.; Tauxe, G. M.; Gao, A. L.; Jackson, D. M.; Simubali, L.; Book, C.; Stevenson, J. C.; Thuma, P. E.; McCoy, R. C.; Gordus, A.; Mburu, M. M.; Simulundu, E.; McMeniman, C. J. Human Scent Guides Mosquito Thermotaxis and Host Selection under Naturalistic Conditions. *Curr. Biol.* **2023**, *33* (12), 2367-2382.e7. https://doi.org/10.1016/j.cub.2023.04.050.

(96) Moitinho-Silva, L.; Boraczynski, N.; Emmert, H.; Baurecht, H.; Szymczak, S.; Schulz, H.; Haller, D.; Linseisen, J.; Gieger, C.; Peters, A.; Tittmann, L.; Lieb, W.; Bang, C.; Franke, A.; Rodriguez, E.; Weidinger, S. Host Traits, Lifestyle and Environment Are Associated with Human Skin Bacteria. *Br. J. Dermatol.* **2021**, *185* (3), 573–584. https://doi.org/10.1111/bjd.20072.

(97) Yeoman, A. M.; Shaw, M.; Lewis, A. C. Estimating Person-to-person Variability in VOC Emissions from Personal Care Products Used during Showering. *Indoor Air* **2021**, *31* (4), 1281–1291. https://doi.org/10.1111/ina.12811.

(98) Willems, M. E. T.; Todaka, M.; Banic, M.; Cook, M. D.; Sekine, Y. Intake of New Zealand Blackcurrant Powder Affects Skin-Borne Volatile Organic Compounds in Middle-Aged and Older Adults. *J. Diet. Suppl.* **2022**, *19* (5), 603–620. https://doi.org/10.1080/19390211.2021.1908479.

(99) Du, J.; Gong, C.; Pei, X.; Zhao, H.; Xu, X. Analysis of Triacylglycerols in Castor Oil Through Liquid Chromatography–Mass Spectrometry Based on Fourier Transform–Ion Cyclotron Resonance–Mass Spectrometry and Gas Chromatography–Mass Spectrometry. *J. Chromatogr. Sci.* **2019**, *57* (2), 108–115. https://doi.org/10.1093/chromsci/bmy088.

(100) Zhou, Z.; Lakey, P. S. J.; Von Domaros, M.; Wise, N.; Tobias, D. J.; Shiraiwa, M.; Abbatt, J. P. D. Multiphase Ozonolysis of Oleic Acid-Based Lipids: Quantitation of Major Products and Kinetic Multilayer Modeling. *Environ. Sci. Technol.* **2022**, *56* (12), 7716–7728. https://doi.org/10.1021/acs.est.2c01163.

(101) VanderGiessen, M.; Tallon, A. K.; Damico, B.; Lahondère, C.; Vinauger, C. Soap Application Alters Mosquito-Host Interactions. *iScience* **2023**, *26* (5), 106667. https://doi.org/10.1016/j.isci.2023.106667.

(102) Finnegan, M.; Duffy, E.; Morrin, A. The Determination of Skin Surface pH via the Skin Volatile Emission Using Wearable Colorimetric Sensors. *Sens. Bio-Sens. Res.* **2022**, *35*, 100473. https://doi.org/10.1016/j.sbsr.2022.100473.

(103) Araviiskaia, E.; Berardesca, E.; Bieber, T.; Gontijo, G.; Sanchez Viera, M.; Marrot, L.; Chuberre, B.; Dreno, B. The Impact of Airborne Pollution on Skin. *J. Eur. Acad. Dermatol. Venereol.* **2019**, *33* (8), 1496–1505. https://doi.org/10.1111/jdv.15583.

(104) Karl, T.; Striednig, M.; Graus, M.; Hammerle, A.; Wohlfahrt, G. Urban Flux Measurements Reveal a Large Pool of Oxygenated Volatile Organic Compound Emissions. *Proc. Natl. Acad. Sci.* **2018**, *115* (6), 1186–1191. https://doi.org/10.1073/pnas.1714715115.

(105) Wakayama, T.; Ito, Y.; Sakai, K.; Miyake, M.; Shibata, E.; Ohno, H.; Kamijima, M. Comprehensive Review of 2-ethyl-1-hexanol as an Indoor Air Pollutant. *J. Occup. Health* **2019**, *61* (1), 19–35. https://doi.org/10.1002/1348-9585.12017.

(106) Curpen, S.; Francois-Newton, V.; Moga, A.; Hosenally, M.; Petkar, G.; Soobramaney, V.; Ruchaia, B.; Lutchmanen Kolanthan, V.; Roheemun, N.; Sokeechand, B. N.; Aumeeruddy, Z.; Ramracheya, R. D. A Novel Method for Evaluating the Effect of Pollution on the Human Skin under Controlled Conditions. *Skin Res. Technol.* **2020**, *26* (1), 50–60. https://doi.org/10.1111/srt.12763.

(107) De Boer, F.; Kezic, S.; Van Der Lelie, G.; Motazedi, E.; Rustemeyer, T.; Van Dijk, A.; Almasian, M.; Jakasa, I.; Van Der Molen, H. F. Effect of Repeated Low-Dose UVR Exposure on Skin Inflammation Threshold, Skin Biomarkers, and Vitamin D in Healthy Adults. *J. Invest. Dermatol.* **2025**, S0022202X2500106X. https://doi.org/10.1016/j.jid.2025.01.024.

(108) Fukuda, S.; Baba, S.; Akasaka, T. Psychological Stress Has the Potential to Cause a Decline in the Epidermal Permeability Barrier Function of the Horny Layer. *Int. J. Cosmet. Sci.* **2015**, *37* (1), 63–69. https://doi.org/10.1111/ics.12169.

(109) Martin, H. J.; Turner, M. A.; Bandelow, S.; Edwards, L.; Riazanskaia, S.; Thomas, C. L. P. Volatile Organic Compound Markers of Psychological Stress in Skin: A Pilot Study. *J. Breath Res.* **2016**, *10* (4), 046012. https://doi.org/10.1088/1752-7155/10/4/046012.

(110) Tsukuda, M.; Nishiyama, Y.; Kawai, S.; Okumura, Y. Identifying Stress Markers in Skin Gases by Analysing Gas Collected from Subjects Undergoing the Trier Social Stress Test and Performing Statistical Analysis. *J. Breath Res.* **2019**, *13* (3), 036003. https://doi.org/10.1088/1752-7163/ab0903.

(111) Katsuyama, M.; Narita, T.; Nakashima, M.; Kusaba, K.; Ochiai, M.; Kunizawa, N.; Kawaraya, A.; Kuwahara, Y.; Horiuchi, M.; Nakamoto, K. How Emotional Changes Affect Skin Odor and Its Impact on Others. *PLOS ONE* **2022**, *17* (6), e0270457. https://doi.org/10.1371/journal.pone.0270457.

(112) Araviiskaia, E.; Berardesca, E.; Bieber, T.; Gontijo, G.; Sanchez Viera, M.; Marrot, L.; Chuberre, B.; Dreno, B. The Impact of Airborne Pollution on Skin. *J. Eur. Acad. Dermatol. Venereol.* **2019**, *33* (8), 1496–1505. https://doi.org/10.1111/jdv.15583.

(113) Wu, T.; Müller, T.; Wang, N.; Byron, J.; Langer, S.; Williams, J.; Licina, D. Indoor Emission, Oxidation, and New Particle Formation of Personal Care Product Related Volatile Organic Compounds. *Environ. Sci. Technol. Lett.* **2024**, *11* (10), 1053–1061. https://doi.org/10.1021/acs.estlett.4c00353.

(114) Xiao, P.; Chen, D. The Effect of Sun Tan Lotion on Skin by Using Skin TEWL and Skin Water Content Measurements. *Sensors* **2022**, *22* (9), 3595. https://doi.org/10.3390/s22093595.

(115) Wang, H.; Wang, H.; Wang, K.; Xiong, J.; Huang, S.; Wolfson, J. M.; Koutrakis, P. Characterization of Chemical Transport in Human Skin and Building Material. *J. Hazard. Mater.* **2023**, *458*, 131917. https://doi.org/10.1016/j.jhazmat.2023.131917.

(116) Mogilnicka, I.; Bogucki, P.; Ufnal, M. Microbiota and Malodor—Etiology and Management. *Int. J. Mol. Sci.* **2020**, *21* (8), 2886. https://doi.org/10.3390/ijms21082886.

(117) Hamilton-Kemp, T.; Newman, M.; Collins, R.; Elgaali, H.; Yu, K.; Archbold, D. Production of the Long-Chain Alcohols Octanol, Decanol, and Dodecanol by Escherichia Coli. *Curr. Microbiol.* **2005**, *51* (2), 82–86. https://doi.org/10.1007/s00284-005-4469-x.

(118) Kabir, K. M. M.; Baker, M. J.; Donald, W. A. Micro- and Nanoscale Sensing of Volatile Organic Compounds for Early-Stage Cancer Diagnosis. *TrAC Trends Anal. Chem.* **2022**, *153*, 116655. https://doi.org/10.1016/j.trac.2022.116655.

(119) Agarwal, S. M.; Sharma, M.; Fatima, S. VOCC: A Database of Volatile Organic Compounds in Cancer. *RSC Adv.* **2016**, *6* (115), 114783–114789. https://doi.org/10.1039/C6RA24414A.

(120) Leemans, M.; Cuzuel, V.; Bauër, P.; Baba Aissa, H.; Cournelle, G.; Baelde, A.; Thuleau, A.; Cognon, G.; Pouget, N.; Guillot, E.; Fromantin, I.; Audureau, E. Screening of Breast Cancer from Sweat Samples Analyzed by 2-Dimensional Gas Chromatography-Mass Spectrometry: A Preliminary Study. *Cancers* **2023**, *15* (11), 2939. https://doi.org/10.3390/cancers15112939.

(121) Stinson, B.; Laguerre, A.; Gall, E. T. Per-Person and Whole-Building VOC Emission Factors in an Occupied School with Gas-Phase Air Cleaning. *Environ. Sci. Technol.* **2022**, *56* (6), 3354–3364. https://doi.org/10.1021/acs.est.1c06767.

(122) Tang, X.; Misztal, P. K.; Nazaroff, W. W.; Goldstein, A. H. Siloxanes Are the Most Abundant Volatile Organic Compound Emitted from Engineering Students in a Classroom. *Environ. Sci. Technol. Lett.* **2015**, *2* (11), 303–307. https://doi.org/10.1021/acs.estlett.5b00256.

(123) Rankin-Turner, S.; McMeniman, C. J. A Headspace Collection Chamber for Whole Body Volatilomics. *The Analyst* **2022**, *147* (22), 5210–5222. https://doi.org/10.1039/D2AN01227H.

(124) Zou, Z.; He, J.; Yang, X. An Experimental Method for Measuring VOC Emissions from Individual Human Whole-Body Skin under Controlled Conditions. *Build. Environ.* **2020**, *181*, 107137. https://doi.org/10.1016/j.buildenv.2020.107137.

(125) Wang, N.; Ernle, L.; Bekö, G.; Wargocki, P.; Williams, J. Emission Rates of Volatile Organic Compounds from Humans. *Environ. Sci. Technol.* **2022**, *56* (8), 4838–4848. https://doi.org/10.1021/acs.est.1c08764.

(126) Jha, S. Kr. Characterization of Human Body Odor and Identification of Aldehydes Using Chemical Sensor. *Rev. Anal. Chem.* **2017**, *36* (2). https://doi.org/10.1515/revac-2016-0028.

(127) Kimura, K.; Sekine, Y.; Furukawa, S.; Takahashi, M.; Oikawa, D. Measurement of 2-Nonenal and Diacetyl Emanating from Human Skin Surface Employing Passive Flux Sampler—GCMS System. *J. Chromatogr. B* **2016**, *1028*, 181–185. https://doi.org/10.1016/j.jchromb.2016.06.021.

(128) Wisthaler, A.; Weschler, C. J. Reactions of Ozone with Human Skin Lipids: Sources of Carbonyls, Dicarbonyls, and Hydroxycarbonyls in Indoor Air. *Proc. Natl. Acad. Sci.* **2010**, *107* (15), 6568–6575. https://doi.org/10.1073/pnas.0904498106.

(129) Zhou, Z.; Lakey, P. S. J.; Von Domaros, M.; Wise, N.; Tobias, D. J.; Shiraiwa, M.; Abbatt, J. P. D. Multiphase Ozonolysis of Oleic Acid-Based Lipids: Quantitation of Major Products and Kinetic Multilayer Modeling. *Environ. Sci. Technol.* **2022**, *56* (12), 7716–7728. https://doi.org/10.1021/acs.est.2c01163.

(130) Timm, C. M.; Lloyd, E. P.; Egan, A.; Mariner, R.; Karig, D. Direct Growth of Bacteria in Headspace Vials Allows for Screening of Volatiles by Gas Chromatography Mass Spectrometry. *Front. Microbiol.* **2018**, *9*, 491. https://doi.org/10.3389/fmicb.2018.00491.

(131) Duffy, E.; Albero, G.; Morrin, A. Headspace Solid-Phase Microextraction Gas Chromatography-Mass Spectrometry Analysis of Scent Profiles from Human Skin. *Cosmetics* **2018**, *5* (4), 62. https://doi.org/10.3390/cosmetics5040062.

(132) Yang, S.; Gao, K.; Yang, X. Volatile Organic Compounds (VOCs) Formation Due to Interactions between Ozone and Skin-Oiled Clothing: Measurements by Extraction-Analysis-Reaction Method. *Build. Environ.* **2016**, *103*, 146–154. https://doi.org/10.1016/j.buildenv.2016.04.012.

(133) Lin, W.-C.; Hsu, K.-C.; You, M.-F.; Lee, K.-H.; Chi, C.-H.; Chen, J.-Y. Octanoic Acid Promotes Clearance of Antibiotic-Tolerant Cells and Eradicates Biofilms of Staphylococcus Aureus Isolated from Recurrent Bovine Mastitis. *Biofilm* **2023**, *6*, 100149. https://doi.org/10.1016/j.bioflm.2023.100149.

(134) Jin, X.; Zhou, J.; Richey, G.; Wang, M.; Hong, S. M. C.; Hong, S. H. Undecanoic Acid, Lauric Acid, and N-Tridecanoic Acid Inhibit *Escherichia Coli* Persistence and Biofilm Formation. *J. Microbiol. Biotechnol.* **2021**, *31* (1), 130–136. https://doi.org/10.4014/jmb.2008.08027.

(135) Narayanan, A.; Baskaran, S.; Amalaradjou, M.; Venkitanarayanan, K. Anticarcinogenic Properties of Medium Chain Fatty Acids on Human Colorectal, Skin and Breast Cancer Cells in Vitro. *Int. J. Mol. Sci.* **2015**, *16* (3), 5014–5027. https://doi.org/10.3390/ijms16035014.

(136) Tsushima, S.; Wargocki, P.; Tanabe, S. Sensory Evaluation and Chemical Analysis of Exhaled and Dermally Emitted Bioeffluents. *Indoor Air* **2018**, *28* (1), 146–163. https://doi.org/10.1111/ina.12424.

(137) Shimizu, N.; Ito, J.; Kato, S.; Eitsuka, T.; Saito, T.; Nishida, H.; Miyazawa, T.; Nakagawa, K. Evaluation of Squalene Oxidation Mechanisms in Human Skin Surface Lipids and Shark Liver Oil Supplements. *Ann. N. Y. Acad. Sci.* **2019**, *1457* (1), 158–165. https://doi.org/10.1111/nyas.14219.

(138) Mochalski, P.; King, J.; Unterkofler, K.; Hinterhuber, H.; Amann, A. Emission Rates of Selected Volatile Organic Compounds from Skin of Healthy Volunteers. *J. Chromatogr. B* **2014**, *959*, 62–70. https://doi.org/10.1016/j.jchromb.2014.04.006.

(139) Sekine, Y.; Toyooka, S.; Watts, S. F. Determination of Acetaldehyde and Acetone Emanating from Human Skin Using a Passive Flux Sampler—HPLC System. *J. Chromatogr. B* **2007**, *859* (2), 201–207. https://doi.org/10.1016/j.jchromb.2007.09.033.

(140) Qu, Y.; Xie, D.; Liu, Y. Emissions of Volatile Organic Compounds from Human Occupants in a Student Office: Dependence on Ozone Concentration. *ACS Environ. Au* **2024**, *4* (1), 3–11. https://doi.org/10.1021/acsenvironau.3c00043.

(141) Amann, A.; Costello, B. D. L.; Miekisch, W.; Schubert, J.; Pleil, J.; Ratcliffe, N.; Risby, T. The Human Volatilome: Volatile Organic Compounds (VOCs) in Exhaled Breath,

Skin Emanations, Urine, Feces and Saliva. *J. Breath Res.* **2014**, *8* (3), 034001. https://doi.org/10.1088/1752-7155/8/3/034001.

(142) Ashrafi, M.; Novak-Frazer, L.; Bates, M.; Baguneid, M.; Alonso-Rasgado, T.; Xia, G.; Rautemaa-Richardson, R.; Bayat, A. Validation of Biofilm Formation on Human Skin Wound Models and Demonstration of Clinically Translatable Bacteria-Specific Volatile Signatures. *Sci. Rep.* **2018**, *8* (1), 9431. https://doi.org/10.1038/s41598-018-27504-z.

(143) Veselova, M. A.; Plyuta, V. A.; Khmel, I. A. Volatile Compounds of Bacterial Origin: Structure, Biosynthesis, and Biological Activity. *Microbiology* **2019**, *88* (3), 261–274. https://doi.org/10.1134/S0026261719030160.

(144) Ashrafi, M.; Bates, M.; Baguneid, M.; Alonso-Rasgado, T.; Rautemaa-Richardson, R.; Bayat, A. Volatile Organic Compound Detection as a Potential Means of Diagnosing Cutaneous Wound Infections. *Wound Repair Regen.* **2017**, *25* (4), 574–590. https://doi.org/10.1111/wrr.12563.

(145) Liu, Y.; Li, W.; Duan, Y. Effect of H_2 O_2 Induced Oxidative Stress (OS) on Volatile Organic Compounds (VOCs) and Intracellular Metabolism in MCF-7 Breast Cancer Cells. *J. Breath Res.* **2019**, *13* (3), 036005. https://doi.org/10.1088/1752-7163/ab14a5.

(146) De Jong, F. J. M.; Lilien, T. A.; Fenn, D. W.; Wingelaar, T. T.; Van Ooij, P.-J. A. M.; Maitland-van Der Zee, A. H.; Hollmann, M. W.; Van Hulst, R. A.; Brinkman, P. Volatile Organic Compounds in Cellular Headspace after Hyperbaric Oxygen Exposure: An In Vitro Pilot Study. *Metabolites* **2024**, *14* (5), 281. https://doi.org/10.3390/metabo14050281.

(147) Mohammadzadeh, R.; Mahnert, A.; Duller, S.; Moissl-Eichinger, C. Archaeal Key-Residents within the Human Microbiome: Characteristics, Interactions and Involvement in Health and Disease. *Curr. Opin. Microbiol.* **2022**, *67*, 102146. https://doi.org/10.1016/j.mib.2022.102146.

(148) De Lacy Costello, B.; Amann, A.; Al-Kateb, H.; Flynn, C.; Filipiak, W.; Khalid, T.; Osborne, D.; Ratcliffe, N. M. A Review of the Volatiles from the Healthy Human Body. *J. Breath Res.* **2014**, *8* (1), 014001. https://doi.org/10.1088/1752-7155/8/1/014001.

(149) Morrison, G. C.; Weschler, C. J.; Bekö, G.; Koch, H. M.; Salthammer, T.; Schripp, T.; Toftum, J.; Clausen, G. Role of Clothing in Both Accelerating and Impeding Dermal Absorption of Airborne SVOCs. *J. Expo. Sci. Environ. Epidemiol.* **2016**, *26* (1), 113–118. https://doi.org/10.1038/jes.2015.42.

(150) S., K.; Saquib, M.; Poojary, H.; Illanad, G.; Valavan, D.; M, S.; Nayak, R.; Mazumder, N.; Ghosh, C. Skin Emitted Volatiles Analysis for Noninvasive Diagnosis: The Current

Advances in Sample Preparation Techniques for Biomedical Application. *RSC Adv.* **2024**, *14* (17), 12009–12020. https://doi.org/10.1039/D4RA01579G.

(151) Yu, J.; Wania, F.; Abbatt, J. P. D. A New Approach to Characterizing the Partitioning of Volatile Organic Compounds to Cotton Fabric. *Environ. Sci. Technol.* **2022**, *56* (6), 3365–3374. https://doi.org/10.1021/acs.est.1c08239.

(152) Kramer, C.; Mochalski, P.; Unterkofler, K.; Agapiou, A.; Ruzsanyi, V.; Liedl, K. R. Prediction of Blood:Air and Fat:Air Partition Coefficients of Volatile Organic Compounds for the Interpretation of Data in Breath Gas Analysis. *J. Breath Res.* **2016**, *10* (1), 017103. https://doi.org/10.1088/1752-7155/10/1/017103.

(153) Green, M.; Feschuk, A. M.; Kashetsky, N.; Maibach, H. I. "Normal" TEWL-how Can It Be Defined? A Systematic Review. *Exp. Dermatol.* **2022**, *31* (10), 1618–1631. https://doi.org/10.1111/exd.14635.

(154) Pojmanová, P.; Ladislavová, N.; Škeříková, V.; Kania, P.; Urban, Š. Human Scent Samples for Chemical Analysis. *Chem. Pap.* **2020**, *74* (5), 1383–1393. https://doi.org/10.1007/s11696-019-00989-2.

(155) Eftekhari, A.; Morrison, G. C. A High Throughput Method for Measuring Cloth-Air Equilibrium Distribution Ratios for SVOCs Present in Indoor Environments. *Talanta* **2018**, *183*, 250–257. https://doi.org/10.1016/j.talanta.2018.02.061.

(156) Laing, R. M. Natural Fibres in Next-to-Skin Textiles: Current Perspectives on Human Body Odour. *SN Appl. Sci.* **2019**, *1* (11), 1329. https://doi.org/10.1007/s42452-019-1388-1.

(157) De Boer, F. L.; Van Der Molen, H. F.; Kezic, S. Epidermal Biomarkers of the Skin Barrier in Atopic and Contact Dermatitis. *Contact Dermatitis* **2023**, *89* (4), 221–229. https://doi.org/10.1111/cod.14391.

(158) Cuzuel, V.; Leconte, R.; Cognon, G.; Thiébaut, D.; Vial, J.; Sauleau, C.; Rivals, I. Human Odor and Forensics: Towards Bayesian Suspect Identification Using GC × GC–MS Characterization of Hand Odor. *J. Chromatogr. B* **2018**, *1092*, 379–385. https://doi.org/10.1016/j.jchromb.2018.06.018.

(159) Cuzuel, V.; Portas, E.; Cognon, G.; Rivals, I.; Heulard, F.; Thiébaut, D.; Vial, J. Sampling Method Development and Optimization in View of Human Hand Odor Analysis by Thermal Desorption Coupled with Gas Chromatography and Mass Spectrometry. *Anal. Bioanal. Chem.* **2017**, *409* (21), 5113–5124. https://doi.org/10.1007/s00216-017-0458-8.

(160) He, J.; Zou, Z.; Yang, X. Measuring Whole-Body Volatile Organic Compound Emission by Humans: A Pilot Study Using an Air-Tight Environmental Chamber. *Build. Environ.* **2019**, *153*, 101–109. https://doi.org/10.1016/j.buildenv.2019.02.031.

(161) Peng, X.; Wu, X.; Zhang, M.; Yuan, H. Metal–Organic Framework Coated Devices for Gas Sensing. *ACS Sens.* **2023**, *8* (7), 2471–2492. https://doi.org/10.1021/acssensors.3c00362.

(162) Torad, N. L.; Zhang, S.; Amer, W. A.; Ayad, M. M.; Kim, M.; Kim, J.; Ding, B.; Zhang, X.; Kimura, T.; Yamauchi, Y. Advanced Nanoporous Material–Based QCM Devices: A New Horizon of Interfacial Mass Sensing Technology. *Adv. Mater. Interfaces* **2019**, *6* (20), 1900849. https://doi.org/10.1002/admi.201900849.

(163) Arulvasan, W.; Chou, H.; Greenwood, J.; Ball, M. L.; Birch, O.; Coplowe, S.; Gordon, P.; Ratiu, A.; Lam, E.; Hatch, A.; Szkatulska, M.; Levett, S.; Mead, E.; Charlton-Peel, C.; Nicholson-Scott, L.; Swann, S.; Van Schooten, F.-J.; Boyle, B.; Allsworth, M. High-Quality Identification of Volatile Organic Compounds (VOCs) Originating from Breath. *Metabolomics* **2024**, *20* (5), 102. https://doi.org/10.1007/s11306-024-02163-6.

(164) Zhang, J. D.; Le, M. N.; Hill, K. J.; Cooper, A. A.; Stuetz, R. M.; Donald, W. A. Identifying Robust and Reliable Volatile Organic Compounds in Human Sebum for Biomarker Discovery. *Anal. Chim. Acta* **2022**, *1233*, 340506. https://doi.org/10.1016/j.aca.2022.340506.

(165) Ampong, I.; Zimmerman, K. D.; Nathanielsz, P. W.; Cox, L. A.; Olivier, M. Optimization of Imputation Strategies for High-Resolution Gas Chromatography–Mass Spectrometry (HR GC–MS) Metabolomics Data. *Metabolites* **2022**, *12* (5), 429. https://doi.org/10.3390/metabo12050429.

(166) Faquih, T.; Van Smeden, M.; Luo, J.; Le Cessie, S.; Kastenmüller, G.; Krumsiek, J.; Noordam, R.; Van Heemst, D.; Rosendaal, F. R.; Van Hylckama Vlieg, A.; Willems Van Dijk, K.; Mook-Kanamori, D. O. A Workflow for Missing Values Imputation of Untargeted Metabolomics Data. *Metabolites* **2020**, *10* (12), 486. https://doi.org/10.3390/metabo10120486.

(167) Liu, J.; Zhang, R.; Xiong, J. Machine Learning Approach for Estimating the Human-Related VOC Emissions in a University Classroom. *Build. Simul.* **2023**, *16* (6), 915–925. https://doi.org/10.1007/s12273-022-0976-y.

(168) Zhu, J.; Ren, Z.; Lee, C. Toward Healthcare Diagnoses by Machine-Learning-Enabled Volatile Organic Compound Identification. *ACS Nano* **2021**, *15* (1), 894–903. https://doi.org/10.1021/acsnano.0c07464.

Thesis Outline

The central goal of this work was to explore the current skin VOC sampling and analysis workflows to explore and strengthen their relationship to skin physiology (skin surface pH, skin hydration), across different participants. The work seeks to better understand factors inducing variance in volatile profiles, within a participant and across different participants. Using these insights, a method for testing VOC adsorbent materials was developed to a explore sorbent's ability of retaining compounds of relevance to the skin, from a gas headspace (HS). Moreover, this work introduces a simple, wearable skin VOC sample collection protocol. This work lays the groundwork for enabling near-future decentralised skin VOC collection, ultimately increasing skin VOC study cohorts for robust and reproducible results within this emerging field. Recent literature highlights a need for standardisation of skin VOC sampling and analysis protocols, while the myriad of these approaches likely intensifies the variance of skin VOC profiles reported. Addressing this, this present work explores skin emitted VOCs to overcome current challenges. Chapter 1 highlights interplay amongst metabolic processes, microbial activity, environmental conditions and their impacts on recovered VOCs, while exploring their sampling and analysis approaches.

Chapter 2 describes a study carried out as part of this work to explore skin VOC profile stability within and across different people over time, to understand factors influencing participant healthy skin volatile profiles. For this, headspace solid-phase microextraction (HS-SPME) fibres were used for non-invasive volar forearm skin VOC sampling coupled to gas-chromatography mass-spectrometry (GC-MS) analysis. Biophysical skin parameters thought to reflect skin health (skin surface pH, tissue dielectric constant, transepidermal water loss and stratum corneum hydration) were collected with VOC samples to investigate correlations. Collected data highlighted stability within a participant profile during the study, while principle component analysis revealed greater degree of profile variance across different participants.

Chapter 3 introduces a new skin VOC sampling method using planar films (instead of SPME fibres) with solvent extraction for GC-MS analysis. Merits to this approach include 'cost-effectiveness' and 'ease of use' compared to HS-SPME unit used by our group to date. 3 free-standing sorbent films (Tenax TA, Tenax TA/divinylbenzene and PDMS) were explored for their ability to retain common skin compounds from a gas HS. Skin VOC collection using these samplers was explored by adapting Tenax TA and PDMS films into a wearable format and applying on the volar forearm for skin VOC sampling and GC-MS analysis.

Chapter 4 evaluates conclusions from this thesis, summarising key findings and offers fresh perspectives contributing to this emerging field of skin metabolomics.

Chapter 2: Exploring the Stability of the Healthy Human Skin Volatile Profile

Abstract

This research will explore sampling and analysis of skin emitted VOCs using headspace solid-phase microextraction (HS-SPME) in conjunction with gas chromatography-mass spectrometry (GC-MS) from 3 different participants, over two different timescales. This was done towards establishing an understanding of factors contributing to the variability of skin volatile profiles, across people over time.

This work incorporates biophysical measurements (sspH, TDC, TEWL, SCH) used to assess the skin barrier function. By considering these variables in a single dataset, correlations were examined with respect to changes in skin emitted VOC abundances. This research aims to establish a more holistic understanding of the overall skin homeostasis.

Furthermore, an investigation is conducted on the role of originating participant, sampling duration (within a day and across days), skin acidity and hydration, towards forming the skin volatile profile. Incorporating these intrinsic and extrinsic parameters into the study aids standardisation of skin volatile collection when conducting studies across highly variable samples from different participants, body sites and health statuses.

Finally, the impact of topical applications of salicylic acid (SA) on the skin VOC profile was examined. Significant changes in the recovered skin profile included decrease in sspH, followed by up-regulations in acetic acid, a short chain fatty acid. Overall, this research contributes to the emerging understanding of skin emitted volatiles, considering skin barrier function, monitoring of ambient conditions and reliable analytical techniques (HS-SPME sampling with GC-MS based identification). The findings presented aim to deepen the knowledge of the complex interplay between the skin and its environment, opening avenues for advancements in dermatology and diagnostics of localised and systemic conditions.

2.1. Introduction

Heterogeneous in structure, the skin comprises of 3 main layers shown in Figure 2.1. From the bottom up; hypodermis, dermis and the outermost epidermis are found in varying thicknesses based on body location of skin tissue[1]. The epidermis is composed of five sublayers of differentiated cutaneous cells including keratinocytes, corneocytes, melanocytes and Langerhans cells[2], supported a non-uniform distribution of H_2O amongst corneocytes and skin lipids[2], forming the ECM. This layer also incorporates invaginations arising from hair follicles and various types of glands present in the dermal layer, inclusive of eccrine, sebaceous and apocrine glands[3,4]. These are colonised by skin resident microorganisms[4].

The uppermost sublayer of the epidermis, the stratum corneum (SC) is the primary barrier to pathogens and xenobiotics[5], consisting of a lipophilic ECM, that also functions as a sophisticated biosensor regulating metabolic activity in response to external stimuli[1,6,7]. This area is also colonised by the skin microbiome, capable of producing volatile compounds. These aspects of the skin, including strict sspH regulation, are in delicate balance supported by interplay amongst each other, contributing to overall skin homeostasis.

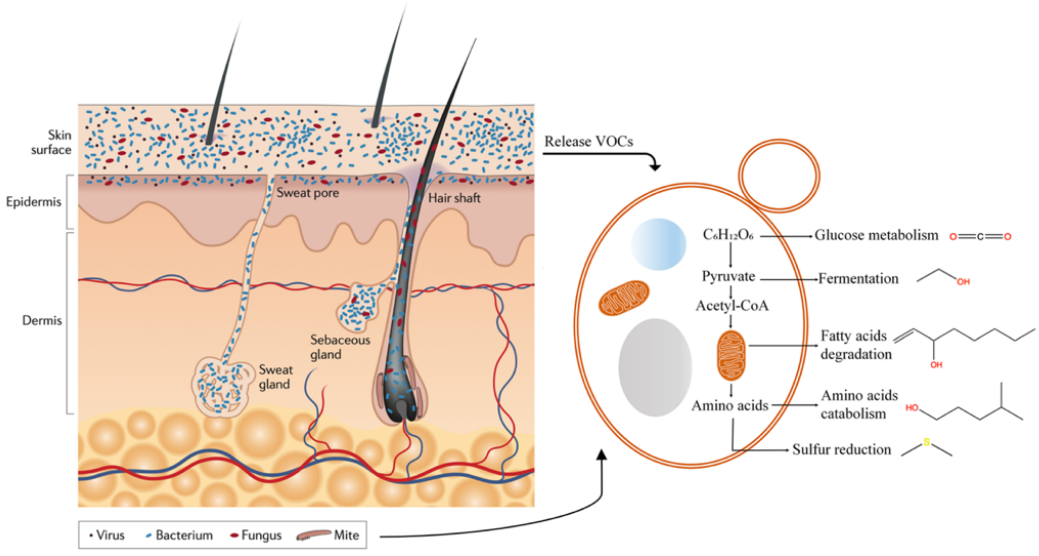

Figure 2.1. Schematic of human skin viewed in cross-section, with skin resident microbiota inhabiting the invaginations and appendages of the skin (right). Microorganism propagated skin VOC formation from available substrates found on the skin (left). Figure adapted from Grice and Segre (left)[8] and Rios-Navarro et al. (right)[9].

Reported factors for person-to-person variability of skin emitted volatiles is strikingly similar to RSSCs variation amongst explored populations[4]. When skin resident microorganisms metabolise this RSSC medium for energy, they produce volatile by- and end-stage metabolic products known as skin-derived VOCs[3,10–14]. Skin VOC emissions are often described as highly unique to a participant[15–17], due to the culmination of all unique interparticipant differences that are compounded by differences in the composition of each participant skin microbiome[4,11,14,18].

When these compounds are considered together, they form a subset of the healthy human volatilome containing 2746 unique compounds as detailed in the 2021 survey conducted by Drabińska et al[19]. The healthy skin was found to emit 623 of these VOCs[19] (consisting 22.7% of the overall human volatilome) comprising of a collection of compound classes inclusive of acids, aldehydes, ketones, alcohols, alkanes and alkenes. Emerging databases such as these[20,21], may be used to give non-invasive insight into a wide range of health aspects such as localised skin conditions[22,23], biological age[10,24], skin surface pH[12,18] and even systemic conditions such as psychological stress[25,26], tuberculosis[27,28] and cardiovascular disease[11,29].

An optimal skin barrier function is essential to maintain skin homeostasis, where if this balance is disturbed, skin infections[5], accelerated skin ageing[10,25], or skin inflammation[25] may occur. Healthy skin barrier function is generally comprised of 3 main processes including SC acidification (acid mantle)[6], SC lipid matrix forming a barrier decreasing trans-epidermal water loss (TEWL)[5], also contributing to the acid mantle, and SC hydration (SCH). SCH is governed by presence of free H_2O distributed throughout the SC with the aid of hydroscopic NMF[5,6].

SspH, TEWL and SCH are closely interlinked, where for instance, lipid barrier degradation causes an increase in TEWL, disrupting the barrier function subsequently resulting in the alkalinisation of the skin barrier[5,6,30]. Concomitant commensal bacteria of the epidermis favour an acidic pH and healthy skin barrier[13]. If these homeostatic conditions are disturbed, there may be an increased probability of pathogenic proliferation, such as *Streptococcus aureus* (*S. aureus*), a bacterial species that is associated with atopic dermatitis[6,13,31,32].

Similarly, an increased TEWL and decreased SCH was found to be a part of pathogenesis of psoriatic skin when compared to healthy skin[6,32]. Recently, Lucchi et al. evaluated the impact of psychological stress on these skin barrier parameters, where TEWL exhibited no significant changes, however a decrease in sspH was observed[25]. These results supported skin volatile emissions, stressing the importance of monitoring skin barrier function in conjunction with VOCs.

For this work, the main goal was to characterise the healthy skin barrier function and the corresponding skin volatile emissions, across 3 different participants to examine shared

trends and correlations of VOCs recovered with measurements of sspH, TDC, TEWL and SCH. Using the established HS-SPME skin VOC collection workflow, GC-MS analysis enabled comparison between skin VOCs common across participants, and those unique to individual participants. ‘Skin profiles’ were compared across participants and over time to elucidate profile variations. Finally, a treatment of 2% (w/w) SA was applied to the skin in an effort to temporarily perturb the skin barrier function and to examine if this perturbation influenced the skin VOC profile.

2.2. Materials and Methods

2.2.1. Chemicals

Salicylic acid (SA) (CAS: 69-72-7), ethanol (CAS: 64-17-5) and C_7-C_{30} standard saturated alkane mixture in hexane were purchased from Sigma-Aldrich, Ireland. HI-77400C pH Combination Buffer Solution Kit 4.01 & 7.01 was purchased from Hanna Instruments Bedfordshire, UK.

2.2.2. Participant recruitment

Ambient room temperature and humidity were monitored at 20-24°C and 35-50%, respectively, over the course of the study. 3 healthy participants (P1, P2, P3), aged 23-25 participated in this study, where 2 skin VOC samples were collected from the volar forearm, each day at 11:00 and 16:00, during the winter season of 2023/24. No special dietary regimens were imposed, however participants were asked to not apply any PCPs on their arms throughout the sampling period. P1 was then recruited for the second part of the study. Skin VOC samples were collected from the volar forearm throughout the study.

Participants were informed on the aim and purpose of the study and asked to provide written informed consent and complete a short questionnaire about their gender, age and cosmetic/fragrance use. The local ethics committee (Dublin City University Research Ethics Committee) approved the study on skin volatiles (Reference: DCUREC/2016/053) prior to commencement of the work, and the study was performed according to the Declaration of Helsinki.

2.2.3. Participant biophysical skin barrier function assessment

All probe-based measurements (sspH, TDC, TEWL, SCH), were collected from the same site (volar forearm, ca. 10 cm up from the wrist), where all measurements were performed in triplicate and averaged to account for SC heterogeneity. To avoid addition bias, dry contact measurements (TDC, SCH, TEWL) were taken prior to the pH measurement. Skin site was randomised between the left and right forearms for all participants.

TDC was measured using a MoistureMeter-D (Delfin Technologies Ltd., Kuopio, Finland) at 300 MHz with an effective measurement penetration depth of 0.5 mm. For reference, pure water has a value of approximately 78.5, where the display range for the MoistureMeter-D is 1-80[33].

TEWL and SCH were measured simultaneously using the GPSkin Barrier probe (GPOWER Inc., Seoul, Republic of Korea). This is a rapid, wireless probe where prior studies deemed this a reliable source of information about skin barrier function[34,35], compared to separate conventional devices. Briefly, TEWL measurements are taken using a pseudo-closed chamber, for minimizing interfering humidity and pressure, where the water loss sensor is inside the chamber. SCH measurements are based on 2 probes measuring contact bioelectrical impedance at a frequency of 1 kHz[35], in contrast to TDC measurements, using a frequency of 300 MHz, allows a greater effective measuring depth.

SspH was measured using a calibrated HALO flat glass probe (HI14142, Hanna Instruments, Bedfordshire, UK), shown in Figure 2.2. (a). After each measurement, the skin sampling site was gently wiped (Kleenex® Medical Wipes) to remove any excess remaining moisture.

2.2.4. Participant skin volatile emission sampling

Following the collection of skin barrier measurements (sspH, TDC, SCH, TEWL), skin volatile samples were collected from the volar forearm of all participants as shown in Figure 2.1. (b). Skin sampling was randomised also between the left and right forearms for all participants. HS-SPME fibres were employed for sampling as per our group's previously established workflow[23,36]. The SPME fibres used were comprised of 50/30/20 μm DVB/Carboxen/PDMS Stableflex (2 cm) assemblies (57348-U, Supelco Corp., Bellefonte, PA, USA). The HS affixed to the volar forearm isolates the SPME fibre and skin surface from the external laboratory environment.

This HS was affixed to the volar forearm with Leukosilk surgical tape (BSN Medical GmbH, Hamburg, Germany). SPME fibres were exposed to the enclosed HS for 15 min, after which the fibre was removed and transferred into the GC injector for 2 minute thermal desorption. A sampling time of 15 min was employed based on sampling time optimisation deployed by our group[23].

Blank air samples (prior to skin exposure) were collected using the same HS vial used to sample skin. The HS was wrapped in aluminium foil to seal the HS and the HS sampled as before using SPME. Prior to this, both the glass HS and foil were thermally treated overnight at 70°C.

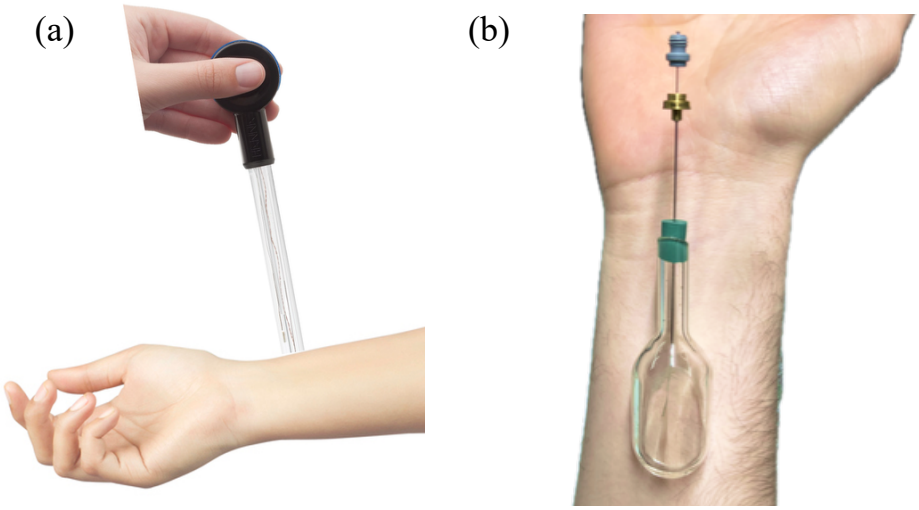

Figure 2.2. (a) Hanna Instruments HALO flat glass probe measuring skin surface pH at the volar forearm and **(b)** SPME fibre housed in a glass headspace affixed to the volar forearm.

2.2.5. 2% salicylic acid solution preparation and application

P1 was then recruited for the second part of the study where the impact of the topical treatment of 2% SA was investigated. Applying a low concentration salicylic acid solution (2% w/w), skin VOC samples were collected at intervals; prior to application, after 5, 60, 120, 180, 240 min. Note that sampling time was 15 min and so for example, where 5 min timeline is stated, this sampling took place from 5 min after application of SA solution. This study was performed in June 2024 (n=3), and in May 2025 (n=3). The collected data was combined for analysis.

1.00 g of pharmacopeia grade SA was dissolved in 50 cm^3 water/ethanol carrier solution. The carrier was made of 63% (w/w) water and 35% (w/w) ethanol[37]. This was done to resemble commercially available SA 2% (w/w) solutions. The final concentration of the prepared SA solution was calculated to be 0.13 mol/L. The solution was stored at 4°C, and was let to come to room temperature before use. 10 µL of this 2% (w/w) SA solution was pipetted onto the volar forearm where the HS was subsequently affixed for skin HS-SPME sampling.

After topical application, the skin was allowed to air dry for 5 min, and the glass HS affixed above the site for sampling (n=3) for 15 min at intermittent times over 4 h.

Blank (laboratory air samples (n=9) and control skin samples without SA application (n=9) were also collected, as detailed in the previous section. These were collected in the same

time period as SA treated skin samples. The HS above the 2% SA solution was sampled using SPME. Briefly, 1 μL of the 2% SA solution was added to a sealed 20 cm^3 HS vial. SPME fibres (DVB/CAR/PDMS) were pierced the cap after 5 min. The fibre was exposed to the HS above the solution for 15 min. The SPME fibre was desorbed in the GC inlet at 270°C for 2 min.

2.2.6. Gas chromatography-mass spectrometry

An Agilent 7820A gas chromatograph connected to an Agilent 5977B mass selective detector (Agilent Technologies, Inc., Santa Clara, CA, USA) was utilized. The GC column employed was of the type SLB-5 MS (30 m × 0.25 mm × 0.25 μm df; Supelco). Helium carrier gas was used with a constant flow rate of 1 mL min^{-1}. The system was equipped with a SPME Merlin Microseal (Merlin Instrument Company, Newark, DE, USA), and the inlet held at 250°C.

Splitless injection mode was used for all samples and each SPME fibre desorbed in SPME inlet for 2 minutes. The GC oven temperature was held at 40°C for 5 followed by a ramp rate of 10°C min^{-1} until a temperature of 270°C was reached. The MS was operated at a scan rate of 3.94 s^{-1}, with a scan range of 35-400 m/z, ion source temperature 230°C and ionising energy of 70 eV.

2.2.7. Data analysis

Agilent MassHunter Quantitative Analysis 10.0 software was used to analyse raw chromatographic data. Peak acquisition and the respective peak area (abundance) data were calculated by using chromatogram deconvolution compound mining algorithms, where a peak filter of ≥10 000 counts was set. A Level 2 putative identification of compounds and structures was performed using the National Institute of Standards and Technology (NIST17) library, and was supported by a visual comparison of the unknown mass spectra, with previous literature reports and with retention index (RI) matching with a tolerance of ±15 RI units.

A standard mixture of saturated alkanes (C_7–C_{30}; Sigma Aldrich, Ireland) was used for RI matching. Compounds thought to be contaminants (such as siloxanes likely arising from SPME fibres and column bleed) were excluded from the data set. Prism (v10.0.0) was used for all data exploration and visualisation. A non-parametric Wilcoxon based t-test was used to determine significant differences. P-values < 0.1 were deemed to be statistically significant.

2.3. Results and discussion

2.3.1. Characterising the healthy human skin barrier function

Biophysical measurements from the skin were collected from each participant where they were all assessed for time-related variations on two timescales (within a day and across days). Described in Figure 2.3., no significant change with respect to AM/PM sampling was observed for any of the three participants, for any of the collected skin barrier parameters, indicating good skin barrier function stability over a day.

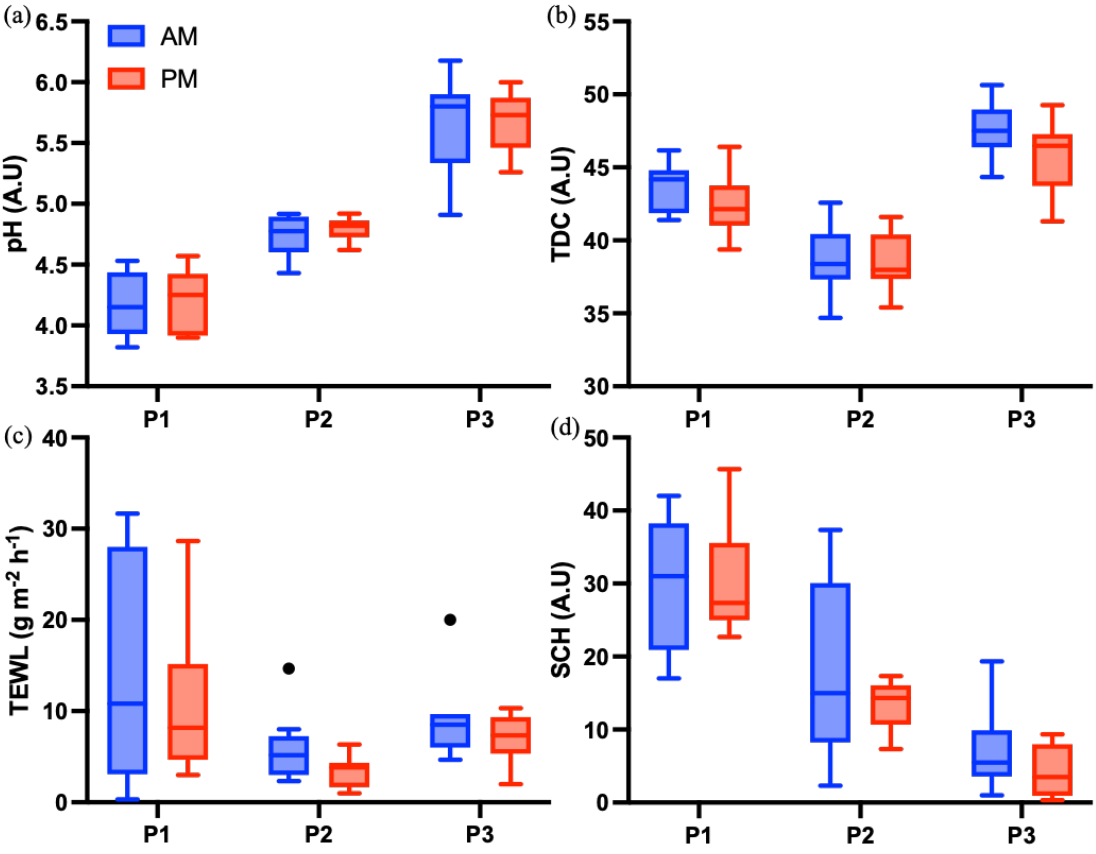

Figure 2.3. **(a)** Volar forearm sspH measurements, **(b)** TDC measurements, **(c)** TEWL measurements and **(d)** SCH measurements in box plots comparing every AM and every PM sample, per participant. Box and whiskers are calculated using the Tukey method. P values are shown in Table A2.1. due to no significant trends shared across all participants.

Following this, variability across days was assessed (Figure 2.4). The cutaneous healthy baseline and functional barrier states of the skin may be assessed through the measurements of

these parameters. These are influenced by a range of endogenous (genetic, age, skin thickness, skin phototype)[6,10,38] and exogenous (environmental, diurnal/seasonal variations, PCP usage)[39–41] factors, following a similar set influences as was established for RSSCs and subsequent skin VOC emissions.

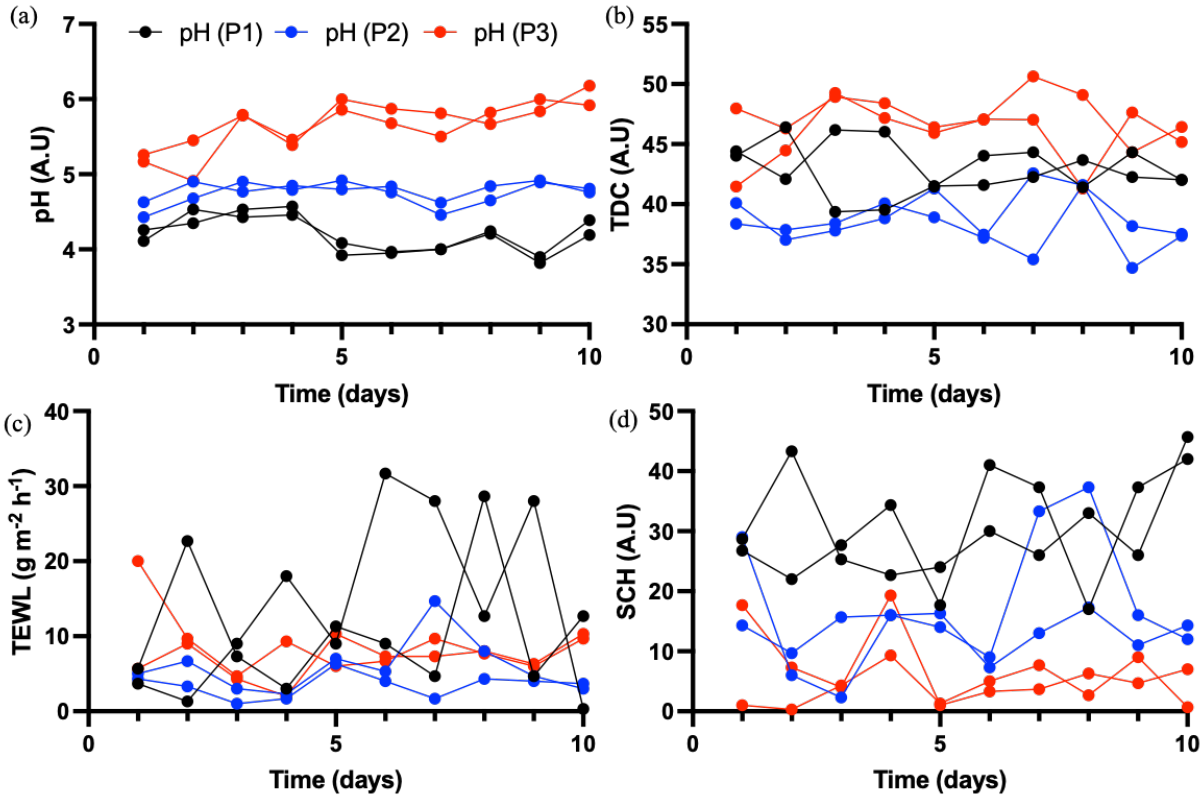

Figure 2.4. (a) Volar forearm sspH measurements, **(b)** TDC measurements, **(c)** TEWL measurements and **(d)** SCH measurements per participant collected on volar forearm daily over 10 days of study. Error bars represent the SD of the replicate data within each sampling day.

SspH of all participants was observed to be between 4 and 6 pH units, while not exceeding SD of 0.32 pH units, across all samples. This indicates acid mantle stability over the course of the study. Reported healthy ranges for the skin acid mantle match this observation[6,12].

TDC assesses local dermal layer tissue hydration levels through electrode-skin contact impedance measurements[33]. Diurnal changes in TDC have been shown previously[42], however in this study significance with respect to sampling times for the participants. TDC was observed to be more variable than sspH (average SD of 2) across participants.

Ideally healthy skin barrier exhibits low a TEWL and high SCH[43], however these values are reported to have participant-specific healthy ranges, and are difficult to determine across participants. TEWL (expressed in $g\ m^{-2}\ h^{-1}$) is used as a measure for epidermal permeability barrier function[30,44]. High TEWL and SCH variability was generally observed particularly for P1, where P2 and P3 were observed to be more stable over time.

As with TDC, SCH measurements help to assess barrier function of the skin through SC capacitance measurements[34,35,43,44], evaluating the water holding capacity of the SC. Governed by ECM lipids and NMF of the SC matrix[1,5], SCH provides surface level analysis into water content within the surface SC[45], whereas TDC probes deeper hydration within the subcutaneous tissues.

For certain skin conditions such as psoriasis, skin barrier function is perturbed[6] and TEWL has been used as a tool to evaluate severity, along with grading rosacea[32]. As suggested by Kleesz et al., cofactors such as eccrine sweat gland activity may contribute to a highly fluctuating TEWL[44]. As such precaution should be taken during the interpretation of TEWL measurements. TEWL and SCH are prone to high variability derived from various human exposomal factors, such as psychological stress or physical activity[25,31].

In this study, TEWL and SCH are observed as highly variable both within a day and across days as they are both surface hydration parameters, they are likely influenced by local skin temperatures, humidity, ventilation, applied PCPs and physical activity levels[33,42,45,46]. Overall however, sspH and TDC are more stable throughout the duration of the study, while TEWL and SCH are highly variable. This skin hydration and water loss variance does not appear to follow any systematic change across all participants, therefore TEWL and SCH were not considered for further analysis. Once the skin barrier function was assessed for time-based variations (within and across days), recovered skin derived VOC emission was subsequently examined in the same manner.

2.3.2. Characterising skin volatile emissions across the 3 healthy participants

The stability of surface skin-derived volatile emissions was investigated from the volar forearm of the 3 healthy participants. Consistent with other published studies[10,12,18], a variety of compound classes including carboxylic acids, aldehydes, ketones, alcohols, ethers, esters were recovered from skin, shown in Figure 2.5. (a). The largest number of unique compounds recovered was identified for P1 (blue), followed by P2 (cyan) and then P3 (purple) with the least. Additionally shown in Figure 2.5. (a)., while following the same sampling approach employed for skin samples, VOCs were recovered from blank air samples (red) within an enclosed 3 mL glass HS.

Through a filtering of 30% appearance frequency thresholds for the collected data, the abundance information of a smaller subset of reliability identified compounds was collected and shown in Figure 2.5. (b). Furthermore, a smaller subset of compounds thought to be derived endogenously from skin was identified across the 3 participants shown in comparative box plots of Figure 2.6. This subset of compounds was considered for downstream correlation analysis and skin VOC profile construction.

Amongst these compounds deemed to be derived from skin, acetic acid and nonanal were detected in the blank air samples (red), however in lower frequencies and abundances, compared to the recovered skin samples of Figure 2.6.

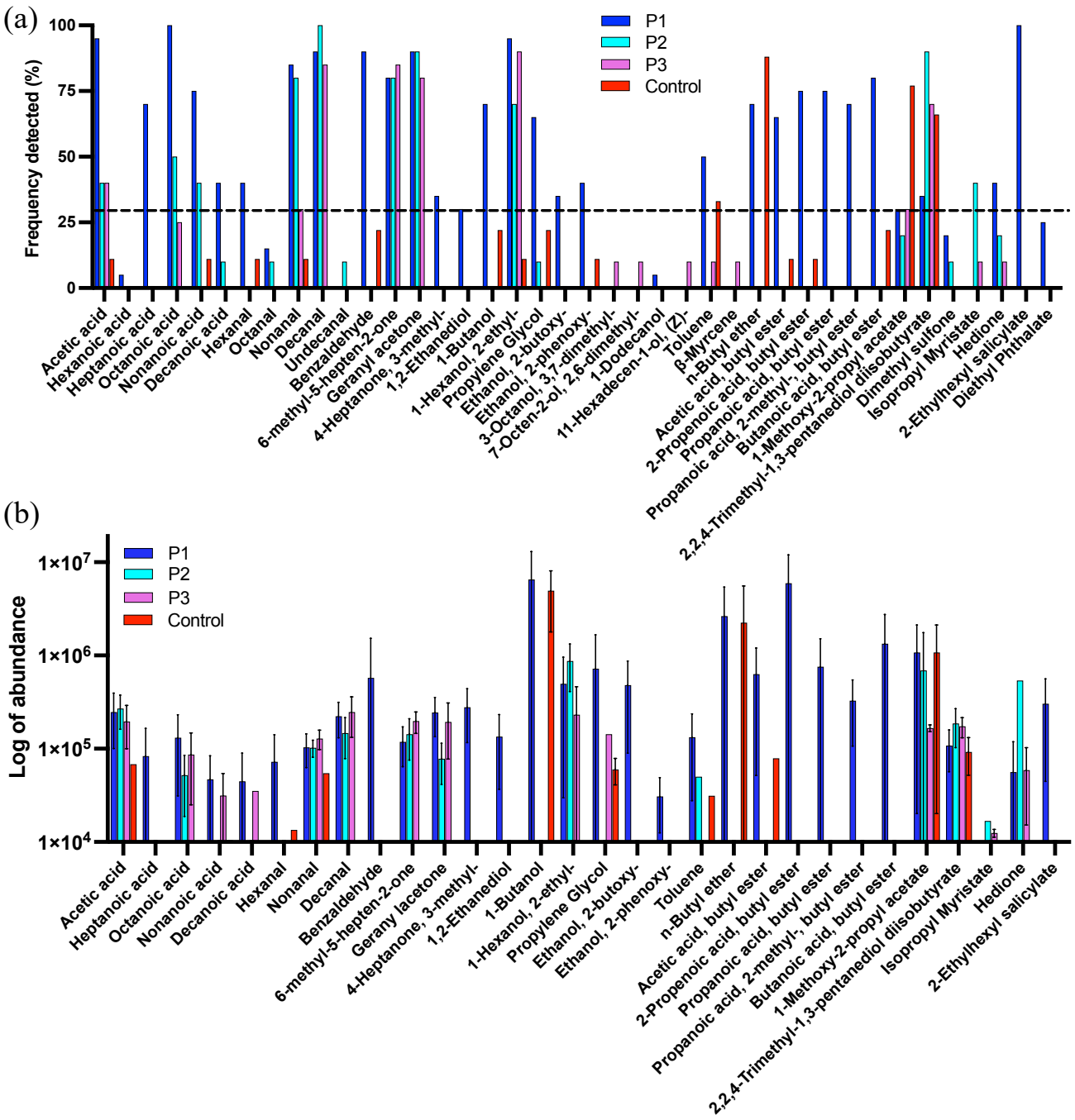

Figure 2.5. Bar charts of (**a)** % frequency of each VOC recovered (n=20) recovered from P1, P2 and P3, **(b)** Mean abundance of each recovered VOC per participant (log scale). Bar chart **(b)** only displays abundances for VOCs detected > 30% frequency. Error bars represent the SD of mean abundances recovered.

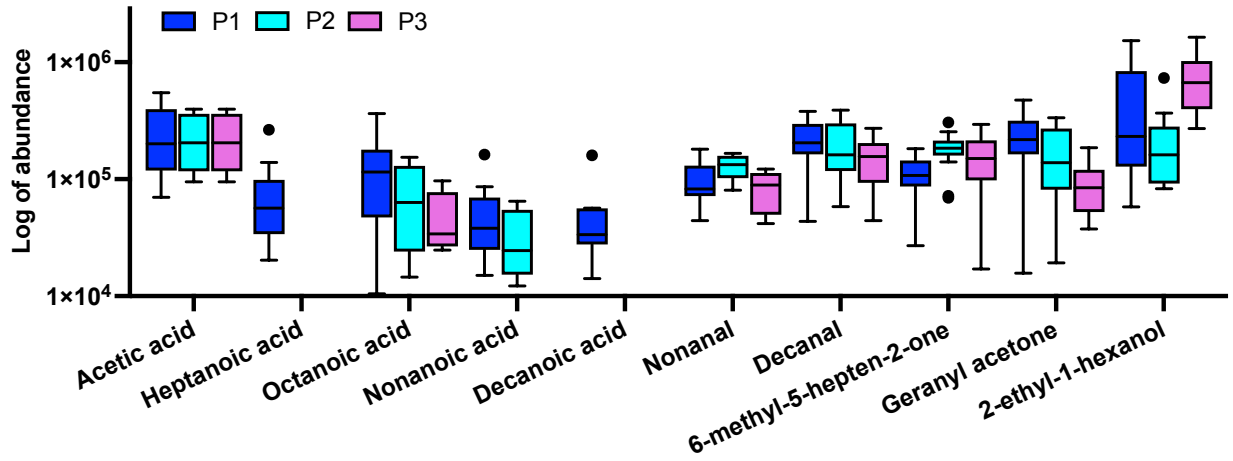

Figure 2.6. Box and whisker plot of each recovered VOC abundance from Figure 2.5 that was considered endogenous (log scale). Box and whisker plots calculated using the Tukey method.

Overall, 10 compounds were deemed endogenous as recovered for P1, 7 for P2 and 6 for P3, across all samples collected. Among these, are regularly reported skin volatiles including acetic-, octanoic-, and nonanoic acid, nonanal, decanal, 6-methyl-5-hepten-2-one (6-MHO), geranyl acetone (GA) and 2-ethyl-1-hexanol (2-EH)[12,19,24,47,48].

Acetic acid, a commonly identified metabolite of microbial activity[3,10,19,49], was recovered in high frequencies for P1 (95%). Lower appearance frequencies were observed for P2 and P3 (<45%). Many studies report acetic acid as a highly abundant component of the skin volatile emissions[10,12,19,49,50]. This SCFA has been shown to be an indicator of the function of the skin barrier function[12] and considered as an end-stage metabolite of resident skin microorganism activity[14,24,49]. Interestingly, recovered abundances of this SCFA are similar across samples when observed, despite having different recovery frequencies across participants, shown in Figure 2.5 (a) and Figure 2.6. This observation suggests different participants may have varying acid mantle activity and different compositions of the skin microbiome, as proposed by other studies[51,52].

Medium chained saturated volatile fatty acids (MCFAs) were also recovered and included heptanoic-, octanoic-, nonanoic- and decanoic acid. These MCFAs are established free fatty acid components of sebum, derived from the sebaceous gland microenvironment[38,53,54]. Interestingly, heptanoic acid was recovered in high frequency (>60%) from only 1 of 3 participants suggesting variability in skin surface lipid or skin microbiome compositions across participants. This is corroborated by previous studies evaluating inter- and

intra-participant variability of skin sebum composition finding the latter to be more consistent between samples[51,52].

Nonanal and decanal were recovered at high frequencies across all participants (>80% decanal for all participants) indicating high aldehyde emission stability. Similarly, the ketones 6-MHO and GA were recovered across all participants in high frequencies (>70%). These volatile carbonyl compounds have been suggested to originate from lipid peroxidation pathways, where skin surface lipids interact with ROS present at the skin surface. This may be induced by external oxidative stimuli such as photo-oxidation from sunlight or auto-oxidation originating from interactions of pollutants (PFAS, NO_2, O_3) with surface skin lipids[41,51,55]. Finally, the alcohol, 2-EH is a previously reported skin derived volatile[4,49] and has been linked to microbial degradation of plasticisers. This compound is also potentially present in indoor air from building material VOC emissions[47] or can be added during the manufacture of topical PCPs[10,56]. Given its persistence amongst VOC emissions from the skin during the study and an uncertainty regarding its origin it remained within the collected dataset.

2.3.3. Correlation and cluster analysis of temporal skin VOC and barrier function data

To assess skin volatile emission temporal stability, two timescales were investigated. Here, skin barrier function data together with abundances of the 10 recovered VOC collected over time are considered simultaneously through Spearman correlation analysis (Figure 2.7.) and principal component analysis (PCA) shown in Figure 2.8. Spearman analysis provides a means of non-parametric correlation visualisation through using a matrix where the strength of the relationship between two variables is described through the spearman co-efficient, *r*. The outputs are ranged between +1 (to describe strong correlations) and -1 (to describe lack of correlations).

Figure 2.7 shows the spearman correlation matrices for P1 (a), P2 (b) and P3 (c). These matrices guide the data analysis to identify which areas to focus on. To make the analysis stronger, data will be considered primarily if it shares correlational trends across multiple participants. Spearman for each participant reveals correlations applicable to a single participant, and these deserve to be addressed in future work.

(a)

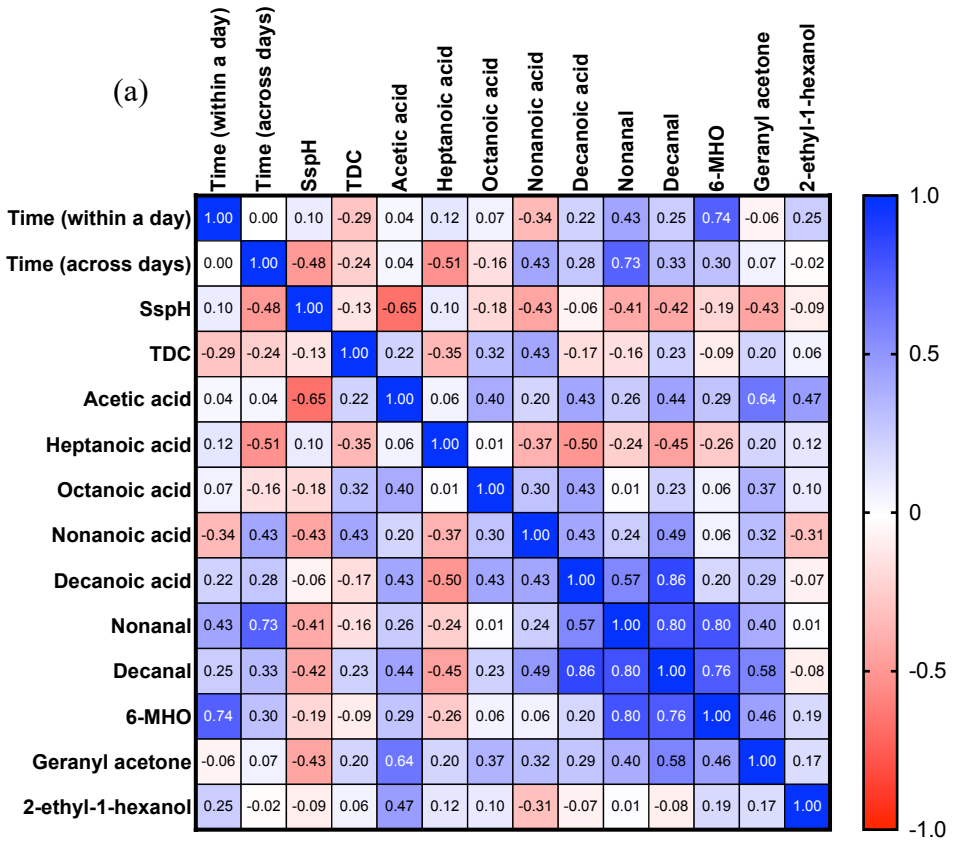
Time (within a day) 1.00 0.00 0.10 -0.29 0.04 0.12 0.07 -0.34 0.22 0.43 0.25 0.74 -0.06 0.25
Time (across days) 0.00 1.00 -0.48 -0.24 0.04 -0.51 -0.16 0.43 0.28 0.73 0.33 0.30 0.07 -0.02
SspH 0.10 -0.48 1.00 -0.13 -0.65 0.10 -0.18 -0.43 -0.06 -0.41 -0.42 -0.19 -0.43 -0.09
TDC -0.29 -0.24 -0.13 1.00 0.22 -0.35 0.32 0.43 -0.17 -0.16 0.23 -0.09 0.20 0.06
Acetic acid 0.04 0.04 -0.65 0.22 1.00 0.06 0.40 0.20 0.43 0.26 0.44 0.29 0.64 0.47
Heptanoic acid 0.12 -0.51 0.10 -0.35 0.06 1.00 0.01 -0.37 -0.50 -0.24 -0.45 -0.26 0.20 0.12
Octanoic acid 0.07 -0.16 -0.18 0.32 0.40 0.01 1.00 0.30 0.43 0.01 0.23 0.06 0.37 0.10
Nonanoic acid -0.34 0.43 -0.43 0.43 0.20 -0.37 0.30 1.00 0.43 0.24 0.49 0.06 0.32 -0.31
Decanoic acid 0.22 0.28 -0.06 -0.17 0.43 -0.50 0.43 0.43 1.00 0.57 0.86 0.20 0.29 -0.07
Nonanal 0.43 0.73 -0.41 -0.16 0.26 -0.24 0.01 0.24 0.57 1.00 0.80 0.80 0.40 0.01
Decanal 0.25 0.33 -0.42 0.23 0.44 -0.45 0.23 0.49 0.86 0.80 1.00 0.76 0.58 -0.08
6-MHO 0.74 0.30 -0.19 -0.09 0.29 -0.26 0.06 0.06 0.20 0.80 0.76 1.00 0.46 0.19
Geranyl acetone -0.06 0.07 -0.43 0.20 0.64 0.20 0.37 0.32 0.29 0.40 0.58 0.46 1.00 0.17
2-ethyl-1-hexanol 0.25 -0.02 -0.09 0.06 0.47 0.12 0.10 -0.31 -0.07 0.01 -0.08 0.19 0.17 1.00
Time (within a day)
Time (across days)
SspH
TDC
Acetic acid
Heptanoic acid
Octanoic acid
Nonanoic acid
Decanoic acid
Nonanal
Decanal
6-MHO
Geranyl acetone
2-ethyl-1-hexanol
1.0
0.5
0
-0.5
-1.0

(b)

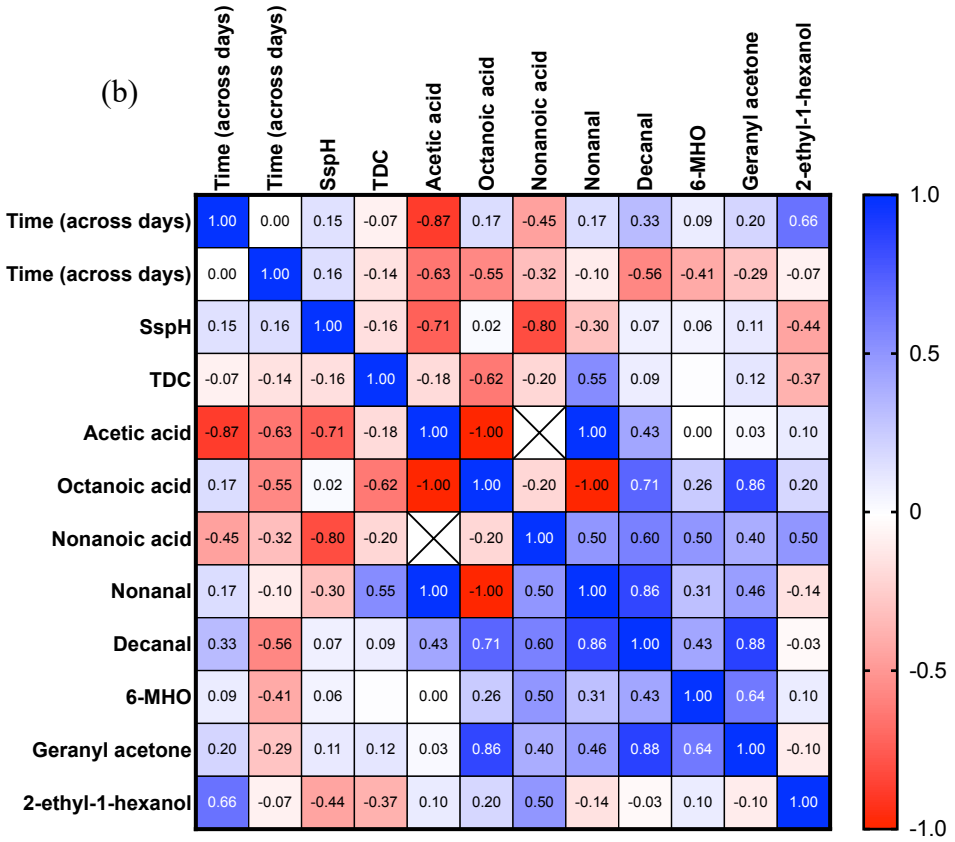
Time (across days) 1.00 0.00 0.15 -0.07 -0.87 0.17 -0.45 0.17 0.33 0.09 0.20 0.66
Time (across days) 0.00 1.00 0.16 -0.14 -0.63 -0.55 -0.32 -0.10 -0.56 -0.41 -0.29 -0.07
SspH 0.15 0.16 1.00 -0.16 -0.71 0.02 -0.80 -0.30 0.07 0.06 0.11 -0.44
TDC -0.07 -0.14 -0.16 1.00 -0.18 -0.62 -0.20 0.55 0.09 0.12 -0.37
Acetic acid -0.87 -0.63 -0.71 -0.18 1.00 -1.00 1.00 0.43 0.00 0.03 0.10
Octanoic acid 0.17 -0.55 0.02 -0.62 -1.00 1.00 -0.20 -1.00 0.71 0.26 0.86 0.20
Nonanoic acid -0.45 -0.32 -0.80 -0.20 -0.20 1.00 0.50 0.60 0.50 0.40 0.50
Nonanal 0.17 -0.10 -0.30 0.55 1.00 -1.00 0.50 1.00 0.86 0.31 0.46 -0.14
Decanal 0.33 -0.56 0.07 0.09 0.43 0.71 0.60 0.86 1.00 0.43 0.88 -0.03
6-MHO 0.09 -0.41 0.06 0.00 0.26 0.50 0.31 0.43 1.00 0.64 0.10
Geranyl acetone 0.20 -0.29 0.11 0.12 0.03 0.86 0.40 0.46 0.88 0.64 1.00 -0.10
2-ethyl-1-hexanol 0.66 -0.07 -0.44 -0.37 0.10 0.20 0.50 -0.14 -0.03 0.10 -0.10 1.00
Time (across days)
Time (across days)
SspH
TDC
Acetic acid
Octanoic acid
Nonanoic acid
Nonanal
Decanal
6-MHO
Geranyl acetone
2-ethyl-1-hexanol
1.0
0.5
0
-0.5
-1.0

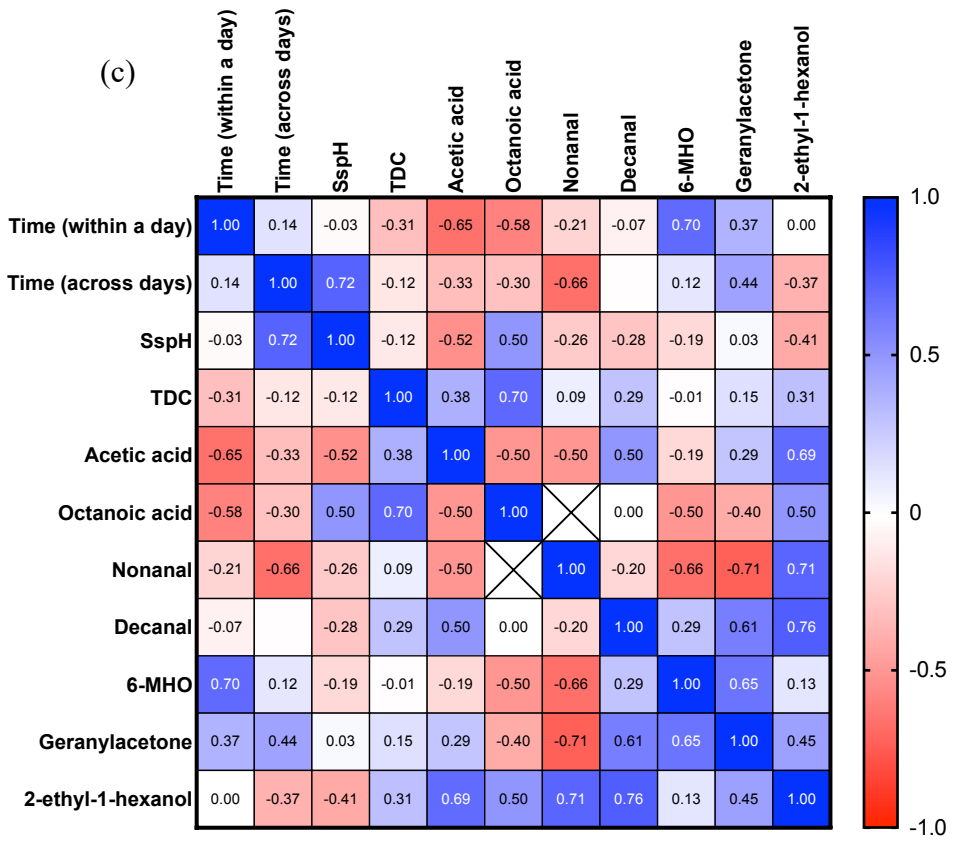

Figure 2.7. (a) Correlation matrix for each variable collected from P1 skin (n=20) **(b)** Correlation matrix for each variable collected from P2 skin (n=20) **(c)** Correlation matrix for each variable collected from P3 skin (n=20). Blue indicates a positive correlation and red indicates a negative correlation, with Spearman correlation coefficient (*r*) inside each box. Boxes with X represent missing data, indicating an absence of correlational analysis.

Furthermore, during PCA the originating participant is also used by the software for principal component regression modelling. PCA is a multivariate unsupervised machine learning approach which is conducted to inspect similarities (clustering) between multiple datasets taken from a single individual, as well as investigating if samples taken from different individuals are clustering apart from each other (dissimilarities)[46,57,58]. The plot of principal components (PC) scores in Figure 2.8. (a) visualises sample separation along two different axes. Corresponding loadings vectors of Figure 2.8. (b) show the strength and direction that each of the investigated variables is having on the data.

In total, 47.34% of the sum variance was explained through PCA, with 33.50% in the first dimension (PC1) and a further 13.84% in the second dimension (PC2). The analysis demonstrated a degree of clustering data between samples collected from different participants, in addition to discrimination between the samples collected from the same participant. Based on the PCA it is interpreted that PC1 broadly represents the inter-participant (across participants) variability and PC2 broadly represents intra-participant (within a participant) variability.

From the scores plot of Figure 2.5. (b), it is apparent that the two different timescales investigated, along with the measured TDC and 2-EH emissions are influencing the combined dataset to a lesser degree compared to sspH, acidic compounds and carbonyl containing compounds. As a result, further analysis will briefly evaluate if any trends are shared across participants, then consider the significance of the recovered acid and carbonyl compounds across the participants, in greater detail.

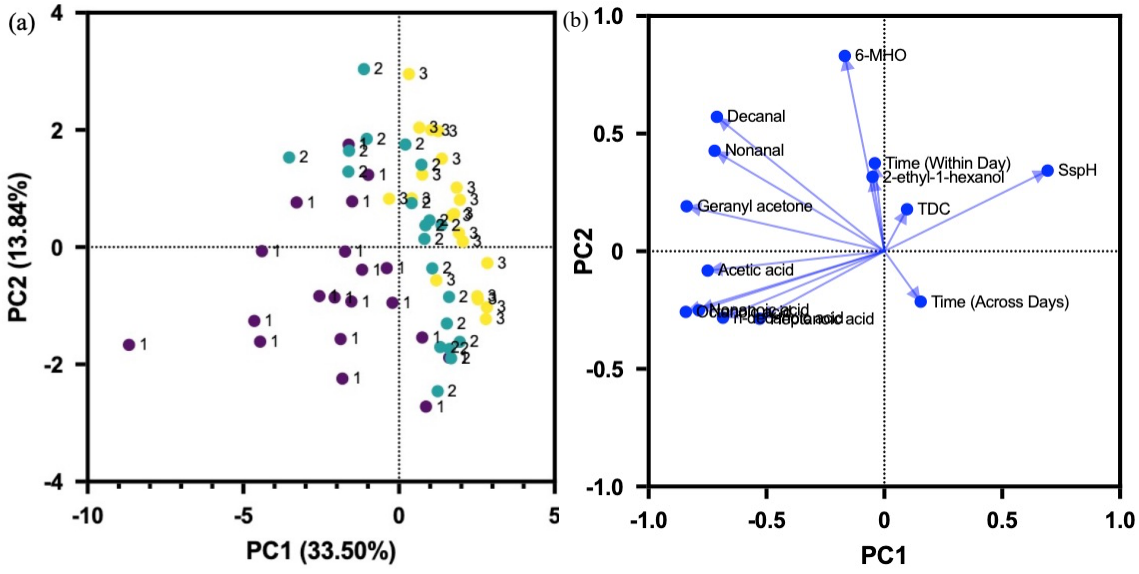

Figure 2.8. (a) Scores plot PC1 and PC2 for collected skin data of each participant (n=60) and **(b)** its corresponding loadings plot. Normalised data and the correlation matrix were used for the PCA. Each sample in **(a)** is coloured and labelled according to the participant from which the data is collected. The length and direction of the arrows in **(b)** represent the contribution of each variable onto each point in the scores plot. The tabulated output is provided in Table A2.2.

Given the findings of non-significant variations in the skin barrier function, individual VOCs become of lower importance within a correlational context. Shown in Figure 2.8. (b), both 6-MHO and 2-EH exhibit arrows in the same direction suggesting a positive correlation with sample collection time (within a day). The significant spearman correlation coefficients between identified skin VOCs and the sampling time (AM/PM) are highlighted for each participant. 6-MHO showed a positive correlation for both P1 and P3 (r=0.74, r=0.70 and p=0.0037, p=0.0037, respectively) while 2-EH showed positive correlation for P2 (r=0.66, p=0.0556).

Overall, these correlations are not shared across all three participants. Additionally, the length of the arrows indicates these variables do not influence the data to a large degree and are relatively stable over the course of this study. Alternatively, variables of short arrow lengths may be modelled noise, or be subject to noisy data. This may indicate the emissions of these compounds from the skin is stable throughout a day, given no major insults to the skin barrier function. Table A2.5. lists the variance of the samples collected per each participant.

The healthy range for diurnal variance of a skin profile remains a challenge to quantify, largely due to a high number of variables influencing data collection and statistical analysis. To explore this variance across days, samples were collected twice daily, for 10 consecutive working days. The variance of the skin barrier function across days was explored in Section 2.3.1. With this in mind, a specific skin emitted VOC following shared trends across all participants was statistically unidentifiable for this study.

Overall, the constructed skin profiles remained relatively stable over the explored timescales of this study. PCA has shown some correlations in the collected dataset across the 3 participants, therefore this will be examined to explore the stronger influencing factors, in greater depth. Firstly, the acid compounds emitted from the skin will be investigated in conjunction to sspH, given opposite locations distributed in quadrants 2 and 3. Secondly, the carbonyl profile of the skin will be investigated, given a broad clustering of these compounds situated in quadrant 1.

2.3.4. Influence of acidic compounds on skin volatile profiles

SspH measurements were taken prior VOC sampling for all participants, where all values measured are within expected normal pH range associated with a healthy skin barrier function (4 – 6). Variance across different participants was interpreted to be broadly described by PC1, where interestingly, the skin barrier function parameter contributing the greatest was sspH. To examine this closer a heatmap was constructed, shown in Figure 2.9., to help visualise the activity of acid VOC emissions per participant. P1 had the most diverse acid profile and the lowest sspH, while P2 and P3 were observed to show elevated sspH concurrent to lower diversities of acid compounds.

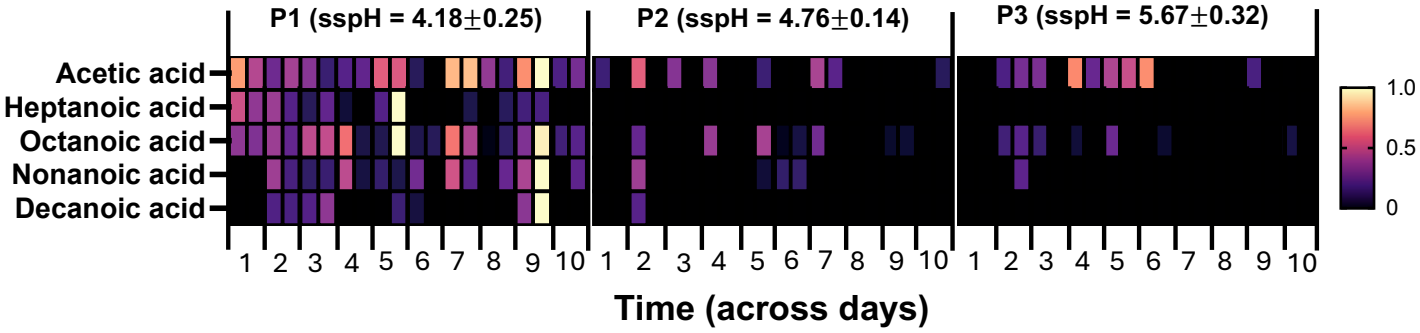

Figure 2.9. Heatmap showing the normalised peak area of each acid VOC recovered from the volar forearm in AM samples (LHS) and PM samples (RHS) across days of the study, for each participant (n=60). SspH and its SD across the 3 participants is shown above each heatmap. The legend shows a bright colour as the maximum abundance recovered in the study for that compound while a darker colour indicates a lower or absent abundance value for that compound, within a day.

The main compounds in this study responsible for inter-participant dissimilarities are documented in published literature[10,12,19,24,41,47,49,50,55] and were identified as acetic-, heptanoic-, octanoic-, nonanoic- and decanoic acid. These acids contributed strongly to PC1 while sharing the influence direction in Figure 2.8 (b)., suggesting these are candidate compounds to aid an identification of inter-participant dissimilarities. Furthermore, this direction of influence was inverse to sspH. Interestingly, this may reflect metabolic elements of a unique skin microbiome, as skin commensal microorganisms excrete acidic compounds[7]. Based on this observation, further investigation into the skin acid mantle with respect to the corresponding acid VOCs is carried out and described in the scatter plots of Figure 2.10.

The SCFA and volatile acids (C_2, C_7-C_{10}) recovered in this study have been previously linked to skin surface acidity by our group[10–12,18,23,36] and others[19,25,50,55,59]. Figure 2.10. (a) highlights a strongly correlated increase in acetic acid VOC emissions concurrent to sspH decreases. A degree of correlation was also observed between total acid emissions (TAcid) and sspH across the 3 participants in Figure 2.10 (b). Acetic acid (C_2) was recovered above the set thresholds for all participants and is the only comparable acidic compound recovered reliably across the 3 participants in this study. Simple linear regression (SLR) analysis was performed for both recovered acetic acid abundances and TAcid abundances, as a function of sspH. Strong linear correlations were found with respect to sspH for 2 out of 3 participants (P1 r^2=0.53, p=0.0004 and P2 r^2=0.72, p=0.0163).

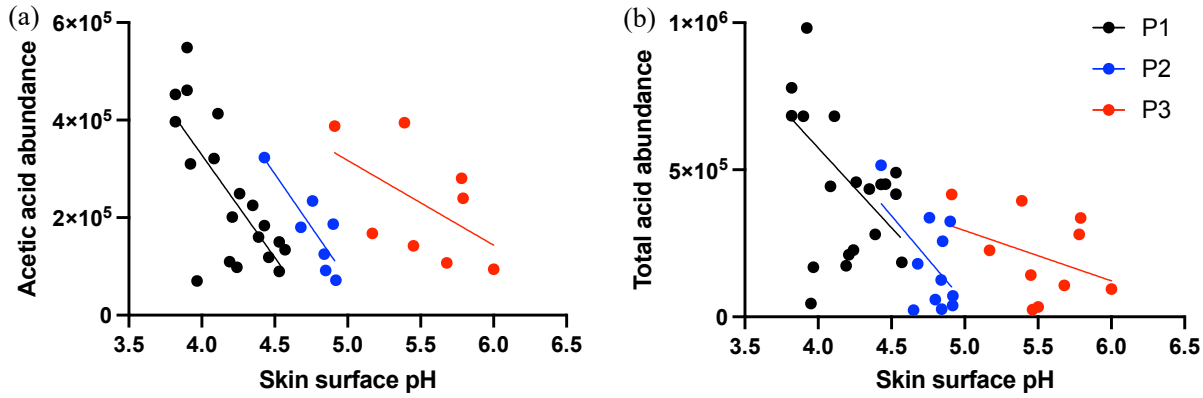

Figure 2.10. (a) Scatter plots of acetic acid abundance as a function of sspH per each participant. **(b)** Scatter plots of total acid abundance as a function of sspH per each participant. Simple linear regression output is shown in Table A2.3. and Table A2.4.

FFAs abundant as part of skin ECM and RSSCs substantially contribute to the skin barrier function and overall skin homeostasis. These likely contribute to the recovered skin volatile emissions as well. As previously proposed by our group[12], this association may be amplified due to the equilibrium vapor pressure of FFAs and skin surface H^+ ion concentration, amongst other factors. Based on the correlation shown in Figure 2.10., it is thought that acid VOC emissions from the skin may alter in both diversity (number of unique volatile acid compounds) and abundance (peak area per unique compound) with inter-participant sspH variations.

Supporting these observations are the large negative slopes calculated through SLR and shown in Table A2.2. and Table A2.3. These are highlighted along with corresponding significance values for P1 (p=0.0004) and P2 (p=0.0163). This significance is not observed for P3, which was also observed to have the highest sspH out of all participants. This corresponded with the skin profile with least 'active' acid volatile emissions, visualised in Figure 2.9. Despite FFAs being just one of several mechanisms contributing to SC acidity, it is clear that skin FFA abundance and variety, as measured by volatile acid emissions, may be a key indicator for skin surface acidity[12]. These findings could be translated into non-invasive biodiagnostic and monitoring of cutaneous diseases and treatment protocols involving sspH[22,60].

2.3.5. Influence of carbonyl compounds on skin volatile profiles

The carbonyl containing compounds recovered in this study all lie in the opposite quadrant to TDC in the PCA. Interestingly however, no significant correlations were statistically identified between skin TDC and the carbonyl containing VOCs across the 3 participants. In a pilot study, TDC was indicated to correlate with free radical intensity induced by UV radiation, which was identified to cause a decrease for TDC in mice skin samples[61]. The presence of this correlation is not prominent in the conducted PCA, although this is highly unlikely to be a prominent correlation for healthy skin barrier function, therefore this was not considered for further analysis.

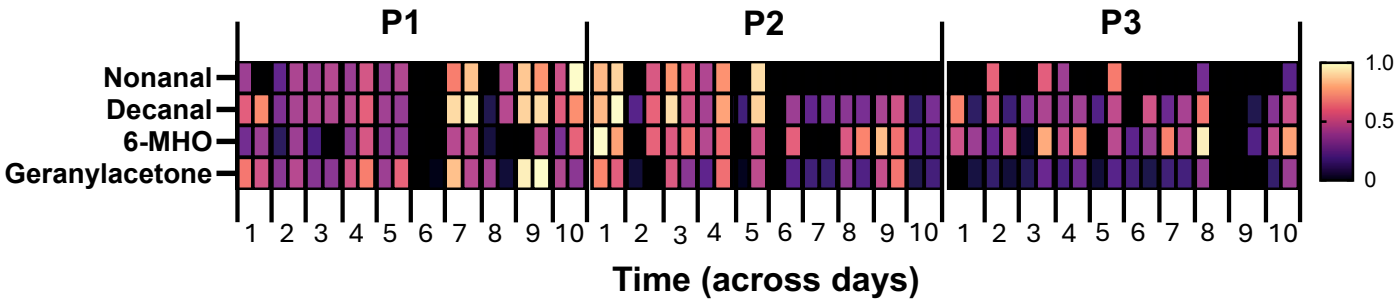

Figure 2.11. Heatmap showing the normalised peak area of each labelled VOC recovered from the volar forearm in AM samples (LHS) and PM samples (RHS) across the 3 participants (n=60). The legend shows a bright colour as the maximum abundance recovered in the study for that compound while a darker colour indicates a lower or absent abundance value for that compound, within a day.

The carbonyl compounds identified in this study are thought to be highly interlinked with oxidative events. Given the >80% observed occurrence frequencies of decanal, 6-MHO and GA across the 3 participants shown in Figure 2.5. (b), it could be interpreted that all participants are experiencing oxidation of their skin surface lipids. All participants are assumed to share common precursors to these compounds found in human skin oil. These oxidative stressors initiate a chain of processes which may induce ROS emergence at the skin surface or within skin tissues[10,41,62,63]. Inclusive of recovered 6-MHO and GA, these compounds are referred to as secondary oxidation products of SQ[41,62,63]. Further research into this relationship could result in meaningful holistic health insights or even lead to skin oil oxidation continuous monitoring. This is because throughout a day, the skin is generally exposed to greater instances of pollutants and other oxidising stimuli, compared to night time exposures. Table A2.5. lists the variance in skin profiles across participants.

Moreover, oxidation of triglycerides or unsaturated FFAs present in skin leads to the formation of volatile aldehydes (nonanal, decanal, undecanal, dodecanal) as prominent carbonyl containing products[10,19,24,49,50,64]. As mentioned before, 6-MHO had some shown some diurnal variability in the carbonyl compound profiles for 2 out of 3 participants. This observation be due to them experiencing different rates of skin oxidation throughout the duration of each day of the study, for myriad reasons contributing to oxidation as discussed.

2.3.6. Influence of 2% salicylic acid skin treatments on the skin volatile profile

Aspects of the skin barrier function were found to be linked to skin volatile emissions in the first part of this study. To explore this further in the second part of this study, a series of skin barrier perturbations were chemically induced using a 2% (w/w) SA solution. Skin barrier function parameters (sspH, TDC, TEWL, SCH) were collected as previously described, before and after topical treatments to investigate their impact on the skin volatile profile. SA was selected as an intervention to study because of its well documented mode of action in the skin. Furthermore at 2% (w/w), topical treatments of SA is not found to induce skin irritation or toxicity over a prolonged period of time, exceeding what was explored in this study[37,65].

Following this same sampling method employed for skin samples and shown in Figure 2.12. (a), acetic acid, nonanoic acid, decanal, 6-MHO and 2-EH were detected in the blank laboratory air samples (red), however in lower abundances and frequencies (<30%), compared to average abundances recovered from skin. A control HS-SPME sample of 10 μL of the 2% SA (w/w) solution inside a 20 cm^3 HS vial (see Methods) (orange) is shown where amounts of

octanoic acid, nonanoic acid, SA, nonanal, decanal 2-EH were recovered. Other than nonanal, nonanoic acid and SA, these VOCs may have been in the HS above the solution as opposed to be from the solution itself, recovered in low frequencies (n = 1/3). Nonanoic acid was recovered in from all samples with abundances comparable those recovered from the skin. It was kept in the dataset for further analysis because of uncertainty regarding its behaviour at the skin surface. This will be considered further during interpretation of the data.

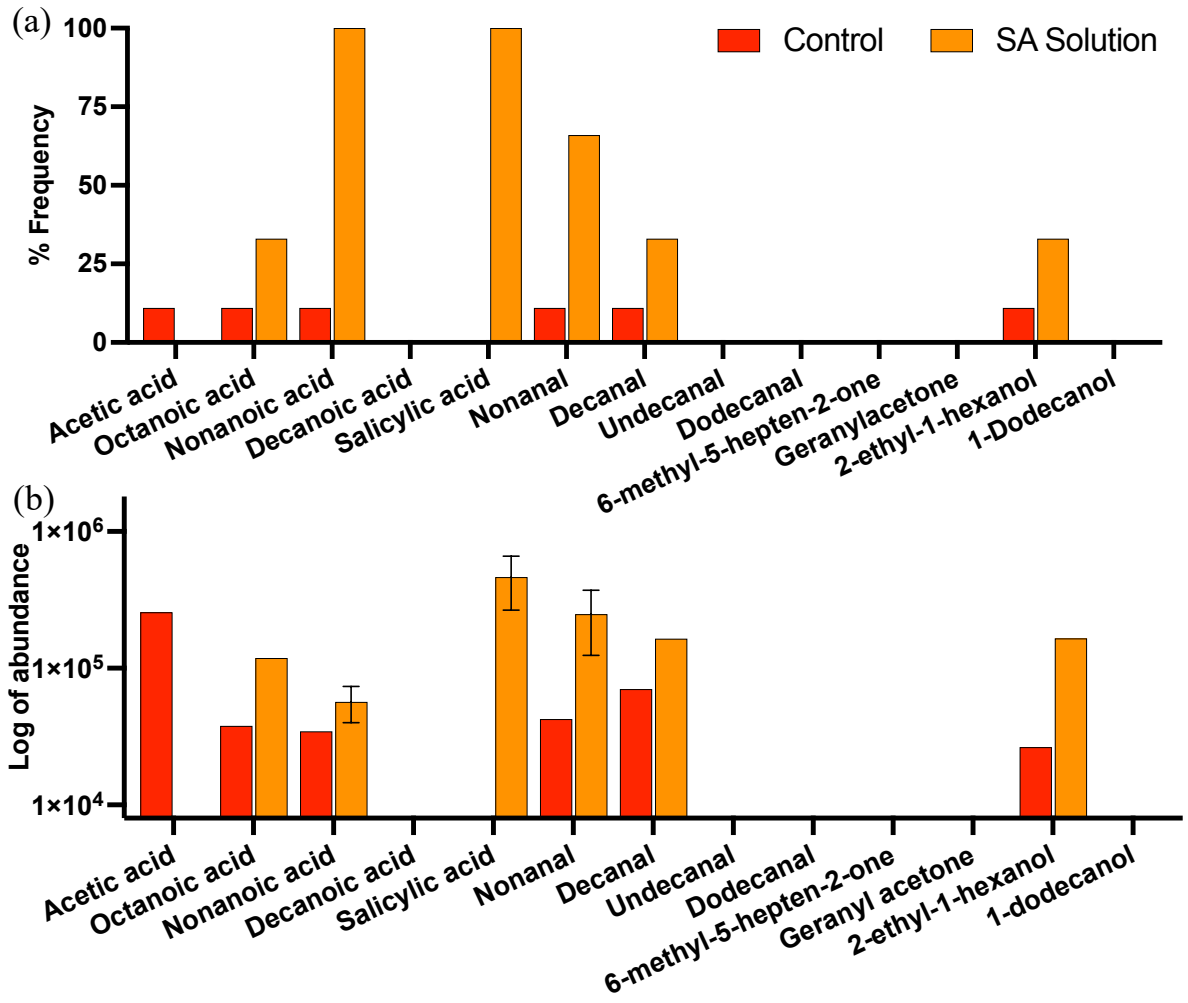

Figure 2.12. (a) % Frequency of each VOC recovered from laboratory HS air control samples (red, n=9) and SA solution HS (orange, n=3) samples. **(b)** Abundance of each VOC recovered from laboratory HS air control samples (red, n=9) and SA solution HS (orange, n=3) samples (log scale). Error bars represent SD of mean abundances per each compound recovered.

2.3.6.1. Characterising the skin volatile profile after 2% (w/w) SA treatment

Volatile emissions were collected from the volar forearm (P1) before any carrier solution application or SA skin treatment (t=0 min). Then, 10 µL of the carrier solution only and 10 µL of 2% (w/w) SA in carrier solution were applied onto the skin. HS-SPME was performed 5 min after carrier solution application or SA skin treatment (sampling time: 15 min).

Sampling was repeated after 1h, 2h, 3h and 4h after carrier solution application or SA skin treatment. This was performed a total of 3 times with no treatments (blue), 6 times using the carrier solution (light brown) and 6 times using the SA solution (dark brown). Figure 2.13. shows that samples collected from SA treated skin, show a shift in volatile emissions compared to untreated skin. The bar charts in Figure 2.13. (b) compare the mean abundances of VOCs recovered from unperturbed skin (blue), skin 5 min after carrier solution used was applied skin (light brown) and skin 5 min after SA treatment (dark brown).

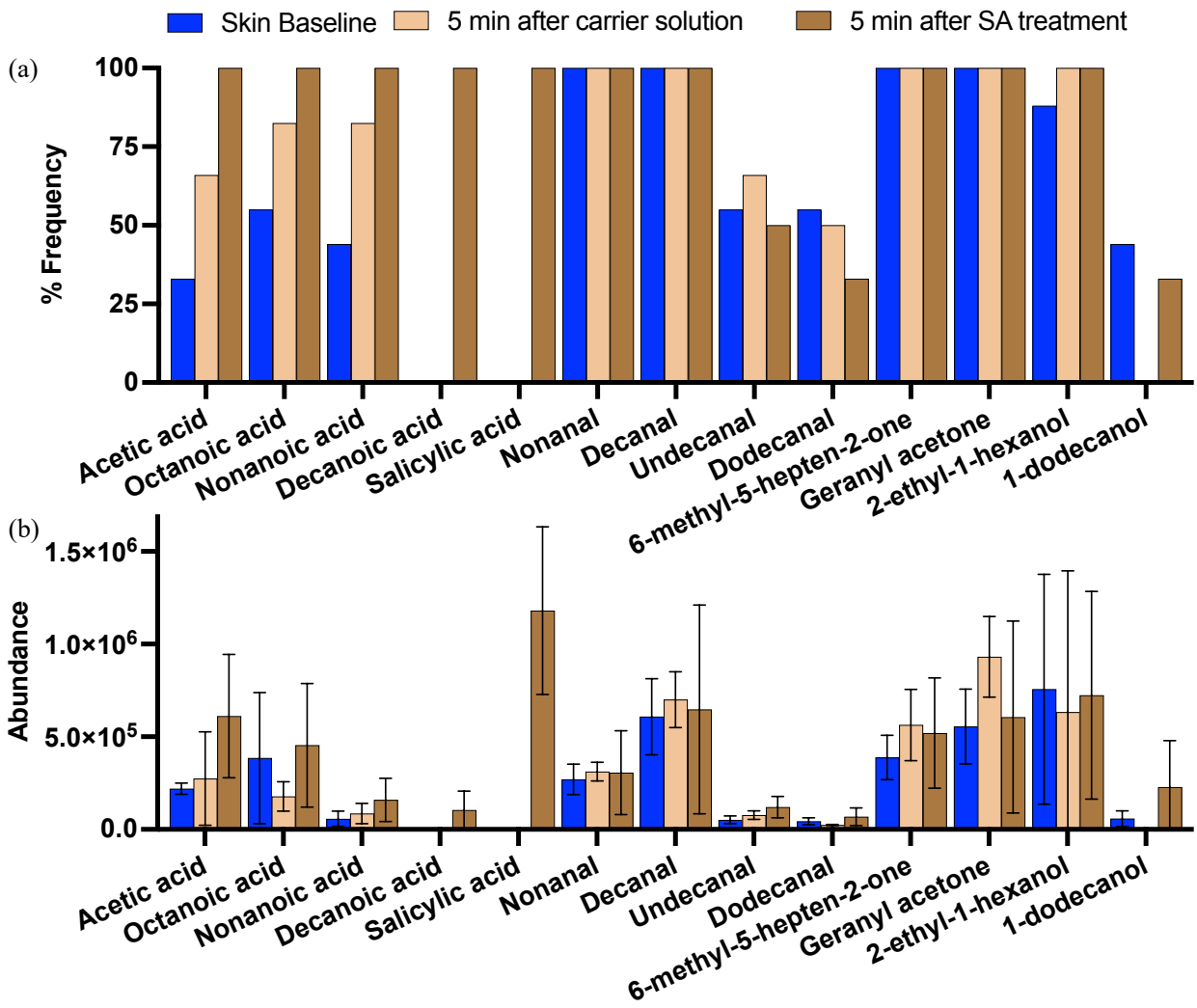

Figure 2.13. (a) % Frequency of each VOC recovered from P1 skin samples (blue, n=9), skin samples 5 min after carrier solution (light brown, n=6) and 5 min after 2% (w/w) SA treatment (dark brown, n=6). **(b)** Mean abundance of each VOC recovered from P1 skin samples (blue, n=9), skin samples collected 5 min after carrier solution (light brown, n=6) and skin samples collected 5 min after 2% (w/w) SA treatment (dark brown, n=6), in log scale. Error bars represent SD of mean abundances for each compound.

Overall, 13 compounds were identified for P1 when comparing unperturbed skin samples (t=0) and skin samples 5 min after each topical treatment. Among these, are the previously reported skin derived volatiles acetic-, octanoic-, nonanoic- and decanoic acid, nonanal, decanal, 6-MHO, GA and 2-EH. Compounds emitted from P1 skin, where these were not identified in the first part of the study, include salicylic acid, undecanal, dodecanal, and 1-dodecanol.

SA was identified as part of skin volatile emissions for P1, only after the skin was treated with 10 µL 2% (w/w) SA aliquots. These emissions were observed to subside once unperturbed skin of the same participant was sampled the following day. Small topical carrier solution treatments of a water/ethanol mixture were thought to have negligible and transient impact on the skin barrier function, due to no significant differences observed in this study for skin barrier function or skin volatiles after treatment. Acetic acid, being the most polar analyte recovered, showed a greater degree of SD in abundances, after the carrier solution was applied, compared to the unperturbed skin. However, this effect is thought to be transient as the carrier solution quickly evaporates. SA is less volatile compared to the carrier solution, therefore it concentrates at the skin surface as the carrier solution evaporates. Then, SA is adsorbed into the superficial layers of the skin, where it potentially can undertake its keratolytic functions[37,65].

Decanoic acid, SA and 1-dodecanol were recovered consistently from skin samples 5 min after 2% (w/w) SA treatments shown in Figure 2.13. (b). These VOCs were not identified in skin samples taken before topical treatment of 2% (w/w) SA (t=0), or after the carrier solution was applied onto the skin. This was observed in SA treated skin samples, where SA was found to persist in skin emissions throughout the rest of the experimental run. To better understand the impact of SA on the overall skin profile, the skin barrier response was considered alongside the collected skin volatile emissions.

2.3.6.2. Influence of salicylic acid on the skin barrier function and volatile emissions

Comparative box plots in Figure 2.14. examine the median spread of all variables collected in this part of the study for P1 skin, before treatment (blue, n=9) and 5 min after 2% (w/w) SA treatment (dark brown, n=6). Topical 2% (w/w) SA treatments were consistently observed to decrease sspH with respect to sampling times, highlighted in Figure 2.14. (a) and Figure 2.15. (a). The average unperturbed sspH was compared to average sspH 5 min after applications using Wilcoxson ranked sum testing, showing a significant down-regulation ($p=0.0001$) 5 min after 2% (w/w) SA skin treatment.

TDC, TEWL, and SCH were observed to remain relatively stable with respect to both carrier solution and 2% (w/w) SA treatments, for the sampling durations examined, shown in Figure 2.14 (a). This was observed through no significant differences between P1 untreated skin and skin 5 min after SA treatment. Given the lack of significance in the first part of the study, corroborated by the lack of observed significance in the second part of the study, these measurements were not considered for the data analysis in this section.

Compared to P1 skin VOC emissions before any treatments, the total acid (TAcids) emissions were observed to significantly up-regulate ($p=0.0021$), for 2% (w/w) SA treated skin, shown in Figure 2.14 (b). When the data is considered together, this trend was not observed for any of the other recovered compound classes or for TVOCs.

The volatile emissions was collected over a sampling interval of 5 min after topical applications. 5 min was deemed enough time for the solvent to volatilise away, and for the SA to induce changes within the skin. Sampling was avoided immediately before, as large ethanol peak would make acetic acid detection difficult. This was found to be the case for sampling SA solution during controls. The samples collected 5 min after treatments were selected for a detailed characterisation and comparison to samples collected before treatments, as these are chromatographs with the largest differences and closest in time to samples taken at (t=0). Concurrent to the observed decrease in sspH, acetic acid emissions were observed to significantly increase ($p=0.0131$) induced through a 2% (w/w) SA treatment onto the skin, shown in Figure 2.14 (c).

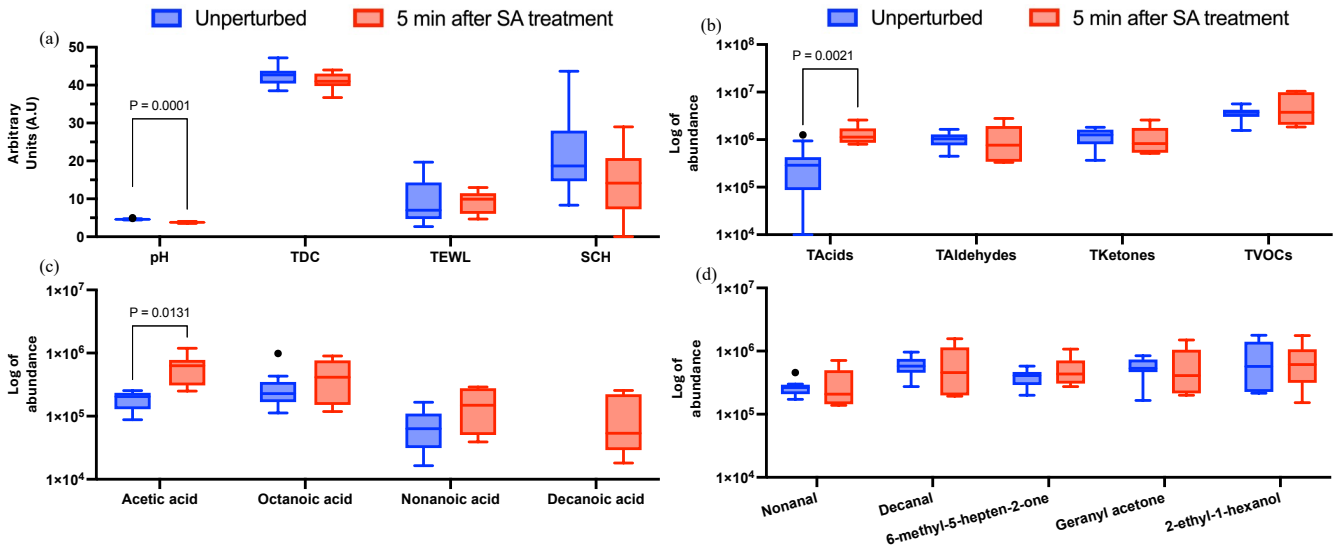

Figure 2.14. Box and whisker plots comparing skin volatile emissions and skin barrier function before and 5 min after 2% (w/w) SA treatment. **(a)** Compared to unperturbed skin, 2% (w/w) SA treatment significantly decreases sspH (p=0.0001), **(b)** significantly up-regulates total acid (TAcid) VOC emissions (p=0.0021) **(c)** up-regulates volatile acids recovery (abundances), particularly for acetic acid, significant up-regulation in emissions (p=0.0131) is observed. **(d)** Volatile aldehydes, ketones and alcohol VOC emissions remained undisturbed with no significant differences before and after 2% (w/w) SA application. Boxes and whiskers were calculated using the Tukey method.

2.3.6.3. Characterising salicylic acid treated skin volatile emissions over time

By accelerating corneocyte turnover and altering the composition of surface lipids[65], SA is thought to increase availability of lipid precursors for skin VOC emissions, including non-volatile precursors to volatile acids, aldehydes, and ketones. When examined in the form of connecting scatterplots, a repeatable skin emission response for TVOCs and the recovered volatile acids is revealed in Figure 2.15 (a) and (b), 5 min after 2% (w/w) SA treatment.

5 min after the 2% (w/w) SA treatment, skin emissions show a general up-regulation of the recovered acids, shown in Figure 2.15 (c). This trend was not observed for untreated skin, or skin 5 min after carrier solution applications, however it must be noted nonanoic acid presence in the solution may induce additive effects.

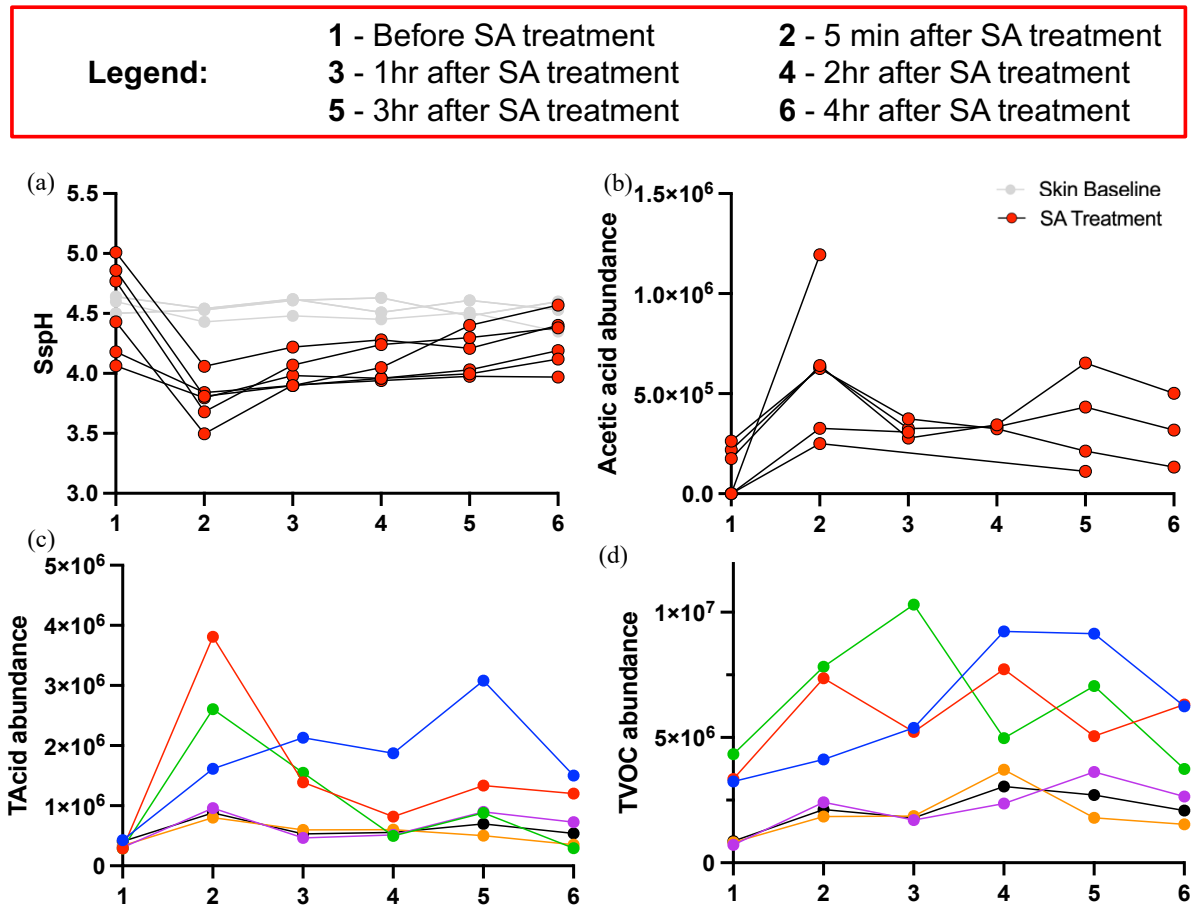

Figure 2.15. (a) Connected scatterplots of sspH measurements over time for P1 untreated skin (grey, n=6) and during 2% (w/w) SA treatments (red, n=6). **(b)** Acetic acid abundance during 2% (w/w) SA treatments (n=6). **(c)** TAcid abundance during 2% (w/w) SA treatments (n=6), in log scale. **(d)** TVOC abundance during 2% (w/w) SA treatments (n=6), on a log scale. Each unique colour represents data collected during each of the n=6 SA treatment experiments.

SA's activity increases substrate availability for lipid peroxidation (SQ, FFAs, phospholipid cell membranes) and accelerates corneocyte turnover. These newly oxidisable substrates react with the atmosphere are thought to up-regulate TAcid and TVOC skin emissions, for the examined duration. The skin appears to begin a homeostatic response shortly after SA treatments. Shown in Figure 2.15 (c) and (d) as a subtle time-dependant decreased in abundances, the skin barrier appears to being re-establishment of homeostasis, broadly interpreted through the systematic down-regulations in volatile emissions.

After inducing a skin barrier perturbation through this application, the skin barrier may respond in some way, in an effort to re-establish homeostasis. At 4 hours after 2% (w/w) SA treatments TAcid emissions appear closer to their baseline, compared to TVOCs at the same

time points. Unfortunately, the sampling duration was not long enough to observe a complete return to the baseline, however the process of returning to homeostasis appears to occur to a degree. These observations show that for future experiments, skin should be monitored for a duration extending 4 hours, to allow the volatile emissions to return to their unperturbed skin baseline emissions.

Overall, 10 µL topical additions of a water/ethanol mixture were unable to be determined statistically if it alters the skin barrier function or the associated VOC emissions. Notably, the VOCs analysed mostly unchanged (no significant up- or down-regulations), as ethanol has not been shown to accelerate corneocyte turnover or the rates of lipid peroxidation, as is the case with SA. Acetic acid showed an elevated variance in abundance compared to untreated skin, likely through a dissolution into the carrier solution, although due to this high SD, statistical comparison was not possible.

Conversely, skin 2% (w/w) SA treatments induced molecular and structural alterations in the SC, shown through sspH changes and systematic trends in volatile emissions. Theoretically, these alterations are thought to be increased rates of desquamation and corneocyte turnovers[37,65]. In this study, these effects manifested in a change in the skin barrier function (sspH decrease, $p=0.0001$) concurrent to up-regulations in TAcid emissions ($p=0.0021$) and acetic acid emissions ($p=0.0131$), deviating away from untreated skin emissions.

2.4.Conclusion

This research investigates and highlights the potential bio-diagnostic and cutaneous bio-monitoring capabilities of skin derived volatile emissions, with support of volar collected skin barrier function parameters (sspH, TDC, TEWL, SCH). Skin VOC profiles were constructed from an AM and PM sample per each day, collected from the volar forearms of 3 healthy participants, over a duration of 10 days. Several common VOCs were identified across all participants, while certain VOCs were observed to be consistently present in specific individuals.

Spearman correlation analysis and PCA strengthened findings of the literature linking the skin barrier and VOCs, highlighting the nature of the correlational relationship of skin surface acidity and acetic acid emissions, across different participants. Lastly, skin barrier disturbances were induced using a prepared 2% (w/w) SA solution, readily present in PCPs at this concentration. This treatment resulted in repeated deviations away from untreated skin surface pH ($p=0.0001$) in addition to total acid VOC emissions ($p=0.0021$) and acetic acid emissions ($p=0.0131$).

Future research should further elucidate the temporal dynamics of skin barrier disruptions and repair following topical treatments through an extended monitoring time. Subsequently, preventative measures towards large variance amongst the skin barrier function measurements should be implemented more stringently to isolate effects of temporal variance, if there are any.

Furthermore, an SA concentration-response relationship should be constructed to explore and quantify this skin volatile response to a more accurate degree. Prospective work should additionally repeat this study with a larger participant cohort, while investigating a broader range of skin perturbation mechanisms, including a series of treatments at different concentrations.

2.5. References

(1) Starr, N. J.; Khan, M. H.; Edney, M. K.; Trindade, G. F.; Kern, S.; Pirkl, A.; Kleine-Boymann, M.; Elms, C.; O'Mahony, M. M.; Bell, M.; Alexander, M. R.; Scurr, D. J. Elucidating the Molecular Landscape of the Stratum Corneum. *Proc. Natl. Acad. Sci.* **2022**, *119* (12), e2114380119. https://doi.org/10.1073/pnas.2114380119.

(2) Mojumdar, E. H.; Sparr, E. The Effect of pH and Salt on the Molecular Structure and Dynamics of the Skin. *Colloids Surf. B Biointerfaces* **2021**, *198*, 111476. https://doi.org/10.1016/j.colsurfb.2020.111476.

(3) Coutinho-Abreu, I. V.; Jamshidi, O.; Raban, R.; Atabakhsh, K.; Merriman, J. A.; Akbari, O. S. Identification of Human Skin Microbiome Odorants That Manipulate Mosquito Landing Behavior. *Sci. Rep.* **2024**, *14* (1), 1631. https://doi.org/10.1038/s41598-023-50182-5.

(4) Haertl, T.; Owsienko, D.; Schwinn, L.; Hirsch, C.; Eskofier, B. M.; Lang, R.; Wirtz, S.; Loos, H. M. Exploring the Interrelationship between the Skin Microbiome and Skin Volatiles: A Pilot Study. *Front. Ecol. Evol.* **2023**, *11*, 1107463. https://doi.org/10.3389/fevo.2023.1107463.

(5) Choi, E. H.; Kang, H. Importance of Stratum Corneum Acidification to Restore Skin Barrier Function in Eczematous Diseases. *Ann. Dermatol.* **2024**, *36* (1), 1. https://doi.org/10.5021/ad.23.078.

(6) Baker, P.; Huang, C.; Radi, R.; Moll, S. B.; Jules, E.; Arbiser, J. L. Skin Barrier Function: The Interplay of Physical, Chemical, and Immunologic Properties. *Cells* **2023**, *12* (23), 2745. https://doi.org/10.3390/cells12232745.

(7) Haertl, T.; Owsienko, D.; Schwinn, L.; Hirsch, C.; Eskofier, B. M.; Lang, R.; Wirtz, S.; Loos, H. M. Exploring the Interrelationship between the Skin Microbiome and Skin Volatiles: A Pilot Study. *Front. Ecol. Evol.* **2023**, *11*, 1107463. https://doi.org/10.3389/fevo.2023.1107463.

(8) Grice, E. A.; Segre, J. A. The Skin Microbiome. *Nat. Rev. Microbiol.* **2011**, *9* (4), 244–253. https://doi.org/10.1038/nrmicro2537.

(9) Rios-Navarro, A.; Gonzalez, M.; Carazzone, C.; Celis Ramírez, A. M. Why Do These Yeasts Smell So Good? Volatile Organic Compounds (VOCs) Produced by Malassezia Species in the Exponential and Stationary Growth Phases. *Molecules* **2023**, *28* (6), 2620. https://doi.org/10.3390/molecules28062620.

(10) Finnegan, M.; Fitzgerald, S.; Duroux, R.; Attia, J.; Markey, E.; O'Connor, D.; Morrin, A. Predicting Chronological Age via the Skin Volatile Profile. *J. Am. Soc. Mass Spectrom.* **2024**, jasms.3c00315. https://doi.org/10.1021/jasms.3c00315.

(11) Duffy, E.; Morrin, A. Endogenous and Microbial Volatile Organic Compounds in Cutaneous Health and Disease. *TrAC Trends Anal. Chem.* **2019**, *111*, 163–172. https://doi.org/10.1016/j.trac.2018.12.012.

(12) Shetewi, T.; Finnegan, M.; Fitzgerald, S.; Xu, S.; Duffy, E.; Morrin, A. Investigation of the Relationship between Skin-Emitted Volatile Fatty Acids and Skin Surface Acidity in Healthy Participants—a Pilot Study. *J. Breath Res.* **2021**, *15* (3), 037101. https://doi.org/10.1088/1752-7163/abf20a.

(13) Swaney, M. H.; Nelsen, A.; Sandstrom, S.; Kalan, L. R. Sweat and Sebum Preferences of the Human Skin Microbiota. *Microbiol. Spectr.* **2023**, *11* (1), e04180-22. https://doi.org/10.1128/spectrum.04180-22.

(14) Fitzgerald, S.; Duffy, E.; Holland, L.; Morrin, A. Multi-Strain Volatile Profiling of Pathogenic and Commensal Cutaneous Bacteria. *Sci. Rep.* **2020**, *10* (1), 17971. https://doi.org/10.1038/s41598-020-74909-w.

(15) Colón-Crespo, L. J.; Herrera-Hernández, D.; Holness, H.; Furton, K. G. Determination of VOC Marker Combinations for the Classification of Individuals by Gender and Race/Ethnicity. *Forensic Sci. Int.* **2017**, *270*, 193–199. https://doi.org/10.1016/j.forsciint.2016.09.011.

(16) Cuzuel, V.; Leconte, R.; Cognon, G.; Thiébaut, D.; Vial, J.; Sauleau, C.; Rivals, I. Human Odor and Forensics: Towards Bayesian Suspect Identification Using GC × GC–MS Characterization of Hand Odor. *J. Chromatogr. B* **2018**, *1092*, 379–385. https://doi.org/10.1016/j.jchromb.2018.06.018.

(17) Thurn, B.; Deo, A.; Patel, D.; Sunnucks, E.; Forbes, S.; Stuart, B. H.; Su, S.; Ueland, M. Ante- and Post-Mortem Human Volatiles for Disaster Search and Rescue. *Forensic Chem.* **2024**, *40*, 100596. https://doi.org/10.1016/j.forc.2024.100596.

(18) Finnegan, M.; Duffy, E.; Morrin, A. The Determination of Skin Surface pH via the Skin Volatile Emission Using Wearable Colorimetric Sensors. *Sens. Bio-Sens. Res.* **2022**, *35*, 100473. https://doi.org/10.1016/j.sbsr.2022.100473.

(19) Drabińska, N.; Flynn, C.; Ratcliffe, N.; Belluomo, I.; Myridakis, A.; Gould, O.; Fois, M.; Smart, A.; Devine, T.; Costello, B. D. L. A Literature Survey of All Volatiles from Healthy Human Breath and Bodily Fluids: The Human Volatilome. *J. Breath Res.* **2021**, *15* (3), 034001. https://doi.org/10.1088/1752-7163/abf1d0.

(20) Agarwal, S. M.; Sharma, M.; Fatima, S. VOCC: A Database of Volatile Organic Compounds in Cancer. *RSC Adv.* **2016**, *6* (115), 114783–114789. https://doi.org/10.1039/C6RA24414A.

(21) Arulvasan, W.; Chou, H.; Greenwood, J.; Ball, M. L.; Birch, O.; Coplowe, S.; Gordon, P.; Ratiu, A.; Lam, E.; Hatch, A.; Szkatulska, M.; Levett, S.; Mead, E.; Charlton-Peel, C.; Nicholson-Scott, L.; Swann, S.; Van Schooten, F.-J.; Boyle, B.; Allsworth, M. High-Quality Identification of Volatile Organic Compounds (VOCs) Originating from Breath. *Metabolomics* **2024**, *20* (5), 102. https://doi.org/10.1007/s11306-024-02163-6.

(22) Fitzgerald, S.; Holland, L.; Ahmed, W.; Piechulla, B.; Fowler, S. J.; Morrin, A. Volatilomes of Human Infection. *Anal. Bioanal. Chem.* **2024**, *416* (1), 37–53. https://doi.org/10.1007/s00216-023-04986-z.

(23) Duffy, E.; Jacobs, M. R.; Kirby, B.; Morrin, A. Probing Skin Physiology through the Volatile Footprint: Discriminating Volatile Emissions before and after Acute Barrier Disruption. *Exp. Dermatol.* **2017**, *26* (10), 919–925. https://doi.org/10.1111/exd.13344.

(24) Owsienko, D.; Goppelt, L.; Hierl, K.; Schäfer, L.; Croy, I.; Loos, H. M. Body Odor Samples from Infants and Post-Pubertal Children Differ in Their Volatile Profiles. *Commun. Chem.* **2024**, *7* (1), 53. https://doi.org/10.1038/s42004-024-01131-4.

(25) Lucchi, G.; Crépin, M.; Chambaron, S.; Peltier, C.; Gilbert, L.; Guéré, C.; Vié, K. Effects of Psychological Stress on the Emission of Volatile Organic Compounds from the Skin. *Sci. Rep.* **2024**, *14* (1), 7238. https://doi.org/10.1038/s41598-024-57967-2.

(26) Fukuda, S.; Baba, S.; Akasaka, T. Psychological Stress Has the Potential to Cause a Decline in the Epidermal Permeability Barrier Function of the Horny Layer. *Int. J. Cosmet. Sci.* **2015**, *37* (1), 63–69. https://doi.org/10.1111/ics.12169.

(27) Vishinkin, R.; Busool, R.; Mansour, E.; Fish, F.; Esmail, A.; Kumar, P.; Gharaa, A.; Cancilla, J. C.; Torrecilla, J. S.; Skenders, G.; Leja, M.; Dheda, K.; Singh, S.; Haick, H. Profiles of Volatile Biomarkers Detect Tuberculosis from Skin. *Adv. Sci.* **2021**, *8* (15), 2100235. https://doi.org/10.1002/advs.202100235.

(28) Makhubela, P. C. K.; Rohwer, E. R.; Naudé, Y. Detection of Tuberculosis-Associated Compounds from Human Skin by GCxGC-TOFMS. *J. Chromatogr. B* **2023**, *1231*, 123937. https://doi.org/10.1016/j.jchromb.2023.123937.

(29) Yokokawa, T.; Sato, T.; Suzuki, S.; Oikawa, M.; Yoshihisa, A.; Kobayashi, A.; Yamaki, T.; Kunii, H.; Nakazato, K.; Ishida, T.; Takeishi, Y. Feasibility of Skin Acetone Analysis in Patients with Cardiovascular Diseases. *FUKUSHIMA J. Med. Sci.* **2018**, *64* (2), 60–63. https://doi.org/10.5387/fms.2018-03.

(30) Proksch, E. pH in Nature, Humans and Skin. *J. Dermatol.* **2018**, *45* (9), 1044–1052. https://doi.org/10.1111/1346-8138.14489.

(31) Chang, Y.; Wang, X. Sweat and Odor in Sportswear – A Review. *iScience* **2023**, *26* (7), 107067. https://doi.org/10.1016/j.isci.2023.107067.

(32) Montero-Vilchez, T.; Segura-Fernández-Nogueras, M.-V.; Pérez-Rodríguez, I.; Soler-Gongora, M.; Martinez-Lopez, A.; Fernández-González, A.; Molina-Leyva, A.; Arias-Santiago, S. Skin Barrier Function in Psoriasis and Atopic Dermatitis: Transepidermal Water Loss and Temperature as Useful Tools to Assess Disease Severity. *J. Clin. Med.* **2021**, *10* (2), 359. https://doi.org/10.3390/jcm10020359.

(33) Mayrovitz, H. N.; Bernal, M.; Brlit, F.; Desfor, R. Biophysical Measures of Skin Tissue Water: Variations within and among Anatomical Sites and Correlations between Measures. *Skin Res. Technol.* **2013**, *19* (1), 47–54. https://doi.org/10.1111/srt.12000.

(34) Logger, J. G. M.; Driessen, R. J. B.; De Jong, E. M. G. J.; Van Erp, P. E. J. Value of GPSkin for the Measurement of Skin Barrier Impairment and for Monitoring of Rosacea Treatment in Daily Practice. *Skin Res. Technol.* **2021**, *27* (1), 15–23. https://doi.org/10.1111/srt.12900.

(35) Ye, L.; Wang, Z.; Li, Z.; Lv, C.; Man, M. -Q. Validation of GPSkin Barrier for Assessing Epidermal Permeability Barrier Function and Stratum Corneum Hydration in Humans. *Skin Res. Technol.* **2019**, *25* (1), 25–29. https://doi.org/10.1111/srt.12590.

(36) Duffy, E.; Albero, G.; Morrin, A. Headspace Solid-Phase Microextraction Gas Chromatography-Mass Spectrometry Analysis of Scent Profiles from Human Skin. *Cosmetics* **2018**, *5* (4), 62. https://doi.org/10.3390/cosmetics5040062.

(37) Davis, D. A. P.; Kraus, A. L.; Thompson, G. A.; Olerich, M.; Odio, M. R. Percutaneous Absorption of Salicylic Acid after Repeated (14-Day) In Vivo Administration to Normal, Acnegenic or Aged Human Skin. *J. Pharm. Sci.* **1997**, *86* (8), 896–899. https://doi.org/10.1021/js960496b.

(38) Shetage, S. S.; Traynor, M. J.; Brown, M. B.; Galliford, T. M.; Chilcott, R. P. Application of Sebomics for the Analysis of Residual Skin Surface Components to Detect Potential Biomarkers of Type-1 Diabetes Mellitus. *Sci. Rep.* **2017**, *7* (1), 8999. https://doi.org/10.1038/s41598-017-09014-6.

(39) Wang, N.; Müller, T.; Ernle, L.; Bekö, G.; Wargocki, P.; Williams, J. How Does Personal Hygiene Influence Indoor Air Quality? *Environ. Sci. Technol.* **2024**, *58* (22), 9750–9759. https://doi.org/10.1021/acs.est.4c01698.

(40) Weschler, C. J.; Nazaroff, W. W. Human Skin Oil: A Major Ozone Reactant Indoors. *Environ. Sci. Atmospheres* **2023**, *3* (4), 640–661. https://doi.org/10.1039/D3EA00008G.

(41) Morrison, G. C.; Eftekhari, A.; Majluf, F.; Krechmer, J. E. Yields and Variability of Ozone Reaction Products from Human Skin. *Environ. Sci. Technol.* **2021**, *55* (1), 179–187. https://doi.org/10.1021/acs.est.0c05262.

(42) Mayrovitz, H. N.; Berthin, T. Assessing Potential Circadian, Diurnal, and Ultradian Variations in Skin Biophysical Properties. *Cureus* **2021**. https://doi.org/10.7759/cureus.17665.

(43) Jansen Van Rensburg, S.; Franken, A.; Du Plessis, J. L. Measurement of Transepidermal Water Loss, Stratum Corneum Hydration and Skin Surface pH in Occupational Settings: A Review. *Skin Res. Technol.* **2019**, *25* (5), 595–605. https://doi.org/10.1111/srt.12711.

(44) Kleesz, P.; Darlenski, R.; Fluhr, J. W. Full-Body Skin Mapping for Six Biophysical Parameters: Baseline Values at 16 Anatomical Sites in 125 Human Subjects. *Skin Pharmacol. Physiol.* **2012**, *25* (1), 25–33. https://doi.org/10.1159/000330721.

(45) Gidado, I. M.; Qassem, M.; Triantis, I. F.; Kyriacou, P. A. Review of Advances in the Measurement of Skin Hydration Based on Sensing of Optical and Electrical Tissue Properties. *Sensors* **2022**, *22* (19), 7151. https://doi.org/10.3390/s22197151.

(46) Xiao, P.; Chen, D. The Effect of Sun Tan Lotion on Skin by Using Skin TEWL and Skin Water Content Measurements. *Sensors* **2022**, *22* (9), 3595. https://doi.org/10.3390/s22093595.

(47) Irga, Peter. J.; Mullen, G.; Fleck, R.; Matheson, S.; Wilkinson, Sara. J.; Torpy, Fraser. R. Volatile Organic Compounds Emitted by Humans Indoors– A Review on the Measurement, Test Conditions, and Analysis Techniques. *Build. Environ.* **2024**, *255*, 111442. https://doi.org/10.1016/j.buildenv.2024.111442.

(48) Finnegan, M.; Fitzgerald, S.; Duroux, R.; Attia, J.; Markey, E.; O'Connor, D.; Morrin, A. Predicting Chronological Age via the Skin Volatile Profile. *J. Am. Soc. Mass Spectrom.* **2024**, jasms.3c00315. https://doi.org/10.1021/jasms.3c00315.

(49) Rankin-Turner, S.; McMeniman, C. J. A Headspace Collection Chamber for Whole Body Volatilomics. *The Analyst* **2022**, *147* (22), 5210–5222. https://doi.org/10.1039/D2AN01227H.

(50) Mitra, A.; Choi, S.; Boshier, P. R.; Razumovskaya-Hough, A.; Belluomo, I.; Spanel, P.; Hanna, G. B. The Human Skin Volatolome: A Systematic Review of Untargeted Mass Spectrometry Analysis. *Metabolites* **2022**, *12* (9), 824. https://doi.org/10.3390/metabo12090824.

(51) Géhin, C.; Tokarska, J.; Fowler, S. J.; Barran, P. E.; Trivedi, D. K. No Skin off Your Back: The Sampling and Extraction of Sebum for Metabolomics. *Metabolomics* **2023**, *19* (4), 21. https://doi.org/10.1007/s11306-023-01982-3.

(52) Shetage, S. S.; Traynor, M. J.; Brown, M. B.; Chilcott, R. P. Sebomic Identification of Sex- and Ethnicity-Specific Variations in Residual Skin Surface Components (RSSC) for Bio-Monitoring or Forensic Applications. *Lipids Health Dis.* **2018**, *17* (1), 194. https://doi.org/10.1186/s12944-018-0844-z.

(53) Girod, A.; Ramotowski, R.; Weyermann, C. Composition of Fingermark Residue: A Qualitative and Quantitative Review. *Forensic Sci. Int.* **2012**, *223* (1–3), 10–24. https://doi.org/10.1016/j.forsciint.2012.05.018.

(54) Ludovici, M.; Kozul, N.; Materazzi, S.; Risoluti, R.; Picardo, M.; Camera, E. Influence of the Sebaceous Gland Density on the Stratum Corneum Lipidome. *Sci. Rep.* **2018**, *8* (1), 11500. https://doi.org/10.1038/s41598-018-29742-7.

(55) Mochalski, P.; Wiesenhofer, H.; Allers, M.; Zimmermann, S.; Güntner, A. T.; Pineau, N. J.; Lederer, W.; Agapiou, A.; Mayhew, C. A.; Ruzsanyi, V. Monitoring of Selected Skin- and Breath-Borne Volatile Organic Compounds Emitted from the Human Body Using Gas Chromatography Ion Mobility Spectrometry (GC-IMS). *J. Chromatogr. B* **2018**, *1076*, 29–34. https://doi.org/10.1016/j.jchromb.2018.01.013.

(56) Wakayama, T.; Ito, Y.; Sakai, K.; Miyake, M.; Shibata, E.; Ohno, H.; Kamijima, M. Comprehensive Review of 2-ethyl-1-hexanol as an Indoor Air Pollutant. *J. Occup. Health* **2019**, *61* (1), 19–35. https://doi.org/10.1002/1348-9585.12017.

(57) Wold, S.; Esbensen, K.; Geladi, P. Principal Component Analysis. *Chemom. Intell. Lab. Syst.* **1987**, *2* (1–3), 37–52. https://doi.org/10.1016/0169-7439(87)80084-9.

(58) Belinato, J. R.; Silva, E.; De Souza, D. S.; Março, P. H.; Valderrama, P.; Do Prado, R. M.; Bonugli-Santos, R. C.; Pilau, E. J.; Porto, C. Rapid Discrimination of Fungal Strains Isolated from Human Skin Based on Microbial Volatile Organic Profiles. *J. Chromatogr. B* **2019**, *1110–1111*, 9–14. https://doi.org/10.1016/j.jchromb.2019.02.007.

(59) Gallagher, M.; Wysocki, C. J.; Leyden, J. J.; Spielman, A. I.; Sun, X.; Preti, G. Analyses of Volatile Organic Compounds from Human Skin. *Br. J. Dermatol.* **2008**, *159* (4), 780–791. https://doi.org/10.1111/j.1365-2133.2008.08748.x.

(60) Zouboulis, C. C.; Coenye, T.; He, L.; Kabashima, K.; Kobayashi, T.; Niemann, C.; Nomura, T.; Oláh, A.; Picardo, M.; Quist, S. R.; Sasano, H.; Schneider, M. R.; Törőcsik, D.; Wong, S. Y. Sebaceous Immunobiology - Skin Homeostasis, Pathophysiology,

Coordination of Innate Immunity and Inflammatory Response and Disease Associations. *Front. Immunol.* **2022**, *13*, 1029818. https://doi.org/10.3389/fimmu.2022.1029818.

(61) Faisal, M.; Juswono, U. P.; Santoso, D. R. The Dielectric Properties of Skin Damage and Its Correlation to Free Radical Intensity Caused by UVA/UVB Radiation Impact. *J. Phys. Conf. Ser.* **2022**, *2165* (1), 012053. https://doi.org/10.1088/1742-6596/2165/1/012053.

(62) Ishikawa, A.; Ito, J.; Shimizu, N.; Kato, S.; Kobayashi, E.; Ohnari, H.; Sakata, O.; Naru, E.; Nakagawa, K. Linoleic Acid and Squalene Are Oxidized by Discrete Oxidation Mechanisms in Human Sebum. *Ann. N. Y. Acad. Sci.* **2021**, *1500* (1), 112–121. https://doi.org/10.1111/nyas.14615.

(63) Shimizu, N.; Ito, J.; Kato, S.; Eitsuka, T.; Saito, T.; Nishida, H.; Miyazawa, T.; Nakagawa, K. Evaluation of Squalene Oxidation Mechanisms in Human Skin Surface Lipids and Shark Liver Oil Supplements. *Ann. N. Y. Acad. Sci.* **2019**, *1457* (1), 158–165. https://doi.org/10.1111/nyas.14219.

(64) Thurn, B.; Deo, A.; Patel, D.; Sunnucks, E.; Forbes, S.; Stuart, B. H.; Su, S.; Ueland, M. Ante- and Post-Mortem Human Volatiles for Disaster Search and Rescue. *Forensic Chem.* **2024**, *40*, 100596. https://doi.org/10.1016/j.forc.2024.100596.

(65) Zhou, C.; Hua, C.; Liang, Q.; Al Rudaisat, M.; Chen, S.; Song, Y.; Zhu, J.; Cheng, H. 0.5–5% Supramolecular Salicylic Acid Hydrogel Is Safe for Long-Term Topical Application and Improves the Expression of Genes Related to Skin Barrier Homeostasis in Mice Models. *Drug Des. Devel. Ther.* **2023**, *Volume 17*, 1593–1609. https://doi.org/10.2147/DDDT.S397541.

Chapter 3: Exploring Sorbent Materials as Planar Films towards Wearable Skin VOC Sampling Platforms with GC-MS Analysis

Abstract

Human skin emitted volatile organic compounds (VOCs) have been increasing in popularity as non-invasive information probes for physiological statuses, disease diagnostics, and environmental exposure biomonitoring. Currently, solid-phase microextraction (SPME) is one of the primary approaches for skin emitted VOC sampling, coupled with gas chromatography (GC-MS) analysis. This passive diffusive based collection utilises the equilibrium partitioning of VOCs between the skin and a coated fibre. The SPME sampling method for skin VOCs is constrained by a complex procedure with common prerequisite for the subject's presence at the sampling site.

These limitations restrict the potential of SPME for a higher throughput collection of skin VOCs from a wider participant cohort, one which does not need to be situated at the same site as analysis. Furthermore, comfort during sampling is hindered, especially for prolonged wearable VOC sampling durations. This is important towards achieving sampling standardisation, where 15 minute sampling durations may be significantly impacted by healthy temporal variations of skin VOC emissions. Prolonged sampling durations provide a time averaged snapshot of VOCs, therefore is more resistant to transient and rapid changes in a skin volatile profile.

Addressing this, the present work investigates a move towards flexible, wearable sorbent materials, optimised towards longer durations for VOC sampling. The sorbent materials chosen for this work include Tenax TA, Tenax TA/divinylbenzene (DVB) and PDMS. While SPME relies on partition co-efficients prioritising rapid equilibrium and saturation, these sorbents may exhibit higher K values for skin derived VOCs, over longer sampling durations. This may enable sustained, time-weighted accumulation of emitted VOCs. Moreover, these materials could be further modified towards targeted analyte collection workflows, thus working towards establishing a process to evaluate $K_{Sorbent\text{-}Air}$ values for skin relevant VOCs is of high analytical value.

3.1. Introduction

Human skin continuously emits a diverse range of VOCs[1–3]. Considering the substantial variability within each individual skin microbiome[4–6] and various other personal factors[1,7,8], accurately determining the composition of person-to-person skin VOC emissions presents a significant challenge. Healthy skin VOC emissions can exhibit substantial variations in composition and abundance across individuals, and even greater across populations[9,10]. Consequently, sorbent materials designed towards efficiently collecting these volatile compounds from the skin face a unique obstacle, in terms of untargeted VOC adsorption[11].

This means that sorbent materials must possess a broad enough polarity range to accommodate various untargeted scenarios for general skin VOC screening. Alternatively, they must exhibit high selectivity towards a pre-determined skin VOC, or set of VOCs, with established associations for a specific health objective. These two biomonitoring scenarios likely merit two different approaches. Given the emergent state of the skin volatiles field, untargeted collection should be prioritised as reliable skin emitted biomarkers have yet to be established across a sufficiently large population[11,12].

Different sorbent materials demonstrate varying affinities for specific chemical classes of VOCs. For example, SPME (DVB/CAR/PDMS) fibres exhibit excellent retention of a wide range of skin derived volatile compounds[2,13,13], even in the presence of humidity in the HS. This polymer coating is formed from compounds of different polarities, aimed at a complimentary effect to enable a bipolar adsorption phase[3,14] (sorbent interacts with slightly polar and very non-polar compounds simultaneously). This indicates DVB and PDMS areas of the polymer are likely optimised for adsorbing non-polar compounds, while CAR (Carboxen molecular sieve) areas provide an excellent adsorbent site for very small compounds. Given its carbon-sieve type structure, this includes small compounds with more polar characteristic than most VOCs, such as acetic acid or acetone.

PDMS is a porous polymer consisting of repeating dimethyl siloxane units, resulting in a non-polar character and affinity for VOC adsorption[3,15]. PDMS patches have been previously used in a direct coupling method where semi- and low-volatile compounds were found to be more effectively adsorbed[3,16]. Notably, PDMS material may swell on VOC adsorption, where absorption into the deeper polymer network is also possible given enough time. This effect can also occur at a high humidity for a prolonged period of time, however interestingly, the presence of water may alter the process of which PDMS may adsorb VOCs.

Tenax TA is a porous polymer consisting of repeating 2,6-diphenyl-p-phenylene oxide units and has been used as a VOC collection medium extensively, finding the most prevalent

use for thermal desorption tubes[17–19]. It is commercially available and its high surface is shown in Figure 3.1. The high hydrophobicity of Tenax TA theoretically prevents humidity induced analytical problems associated with carbon-based materials, while still retaining compatibility with a wide range of molecular weights for effective VOC capture (C_7–C_{26}). Degradation products formed include benzene derivatives such as benzaldehyde and acetophenone from Tenax[17,20].

Divinylbenzene (DVB) consists of a benzene ring substituted with two vinyl (ethenyl) groups. DVB is commonly as a cross-linker in polymer chemistry for forming poly-DVB-co-polymer networks with other compounds[21]. The presence of two vinyl groups allows it to form highly cross-linked polymers, usually impacting their thermal and chemical stabilities[22]. For VOC adsorption this means the sorbent material may partake in increased dipole-dipole interactions, compared to an adsorbent material not containing DVB in its structure.

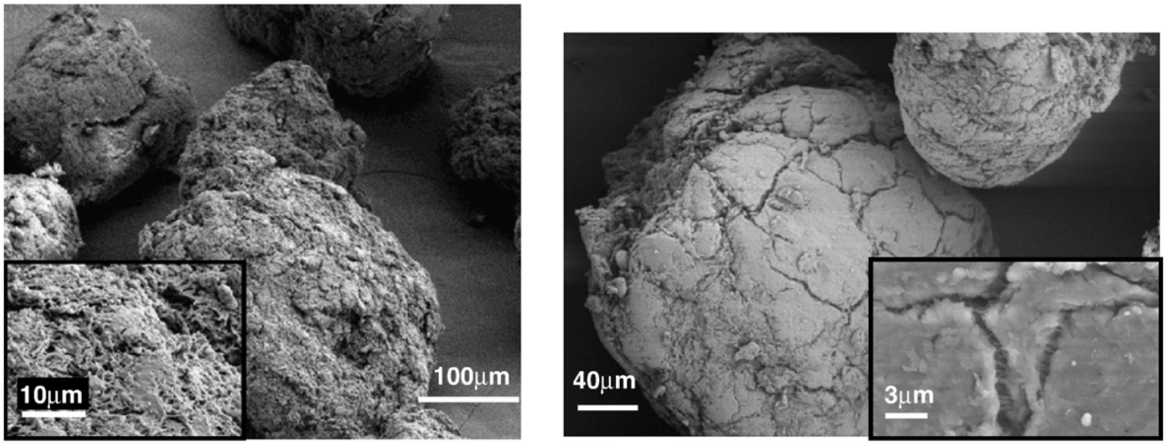

Figure 3.1. SEM micrographs of Tenax TA beads, highlighting high surface areas optimised for VOC adsorption capabilities. Figure reproduced from Alfeeli et al.[18].

The current research has focused on developing a method for the simultaneous sampling of a range of volatile compounds of relevance to the human skin, from a gas HS. Three different sorbent materials were selected (Tenax TA, Tenax TA/DVB and PDMS) and prepared into planar polymer film format to investigate their ability to adsorb gas phase VOCs. This mixture of volatile compound had to be relatively complex to facilitate a system where many unique compounds are mixed in the gas phase, reflecting the myriad of biochemical pathways to skin VOC emissions.

A solution composed of a mixture of 15 skin relevant compounds was made, where the selected compounds are readily identified in literature and in the past work of this Thesis, as skin derived. As present in healthy skin VOC emissions, this solution is comprised of a series of carboxylic acids, aldehydes, ketones and alcohols. Using the neat solution of these VOC (NS_{VOC}), in other words, a mixture of equal masses of each compound, stock solution in water (SS_{aq}) was made. These compounds then were collected from dilutions of this SS_{aq} in an enclosed HS through the robust SPME technique, correlating the masses of each compound added into each air-water system, to the abundances for each compound.

These sorbent materials (Tenax TA, Tenax TA/DVB and PDMS) were tested for their ability to adsorb VOCs from a closed, static 850 cm^3 chamber from the same SS_{aq}, as was characterised by SPME sampling. The results indicated Tenax TA/DVB film recovered the greatest VOC abundances for the aldehydes and ketones, at the lowest concentrations tested in chamber, out of the 3 different sorbent materials used. Interestingly, the acids were not recovered after the solvent extraction of any sorbent film employed.

Crucially, these static headspace adsorption techniques operate on the principle of chemical equilibrium partitioning[3]. For skin VOC monitoring, the aim is to establish an equilibrium balance between the skin and the sorbent, so that extracted abundances of identified compounds from the sorbent is closely related to those abundances present in the skin[18].

Finally, these insights were applied to non-invasive human skin VOC sampling, where the Tenax TA and PDMS films were adapted into a wearable format and worn on P1 volar forearm for a duration of 8 hours.

3.2. Materials and methods

3.2.1. Materials

Hexane (CAS: 110-54-3), heptanoic acid (CAS: 111-14-8), octanoic acid (CAS: 124-07-2), nonanoic acid (CAS: 112-05-0), decanoic acid (CAS: 334-48-5), dodecanoic acid (CAS: 143-07-7), octanal (CAS: 124-13-0), nonanal (CAS: 124-19-6), decanal (CAS: 112-31-2), 6-methyl-5-hepten-2-one (CAS: 110-93-0), 2-ethyl-1-hexanol (CAS: 104-76-7), TENAX®-Trapping Agent (Tenax TA) porous polymer adsorbent (80-100 mesh) and divinylbenzene (CAS: 1321-74-0) were purchased from Sigma-Aldrich, Ireland. Undecanal (CAS: 112-44-7), dodecanal (CAS: 112-54-9), 1-dodecanol (CAS: 112-53-8) and 6,10-dimethyl-5,9-undecandien-2-one (CAS: 796-70-1, E and Z mixture) were purchased from Fischer Scientific (Dublin, Ireland). All chemicals were acquired from commercial suppliers and were used as received unless otherwise stated. SPME fibres (50/30/20 µm DVB/CAR/PDMS Stableflex (2 cm) assemblies (Supelco Corp., Bellefonte, PA, USA) were purchased from Sigma-Aldrich, Ireland.

3.2.2. HS-SPME of skin volatiles

To determine a mixture of VOCs suitable towards reflecting skin emissions, at relevant concentrations, volar forearm VOC collection was carried out. Briefly, SPME fibres (DVB/CAR/PDMS) were exposed to an enclosed 3 cm^3 HS affixed onto the volar forearm for 15 min. Immediately after sampling, fibres were desorbed in the GC inlet at 270°C for 2 min for GC-MS analysis as per Section 3.2.11. All experiments were conducted at ambient temperature and humidity. The room temperature was monitored 3 times daily and remained 22.90°C (±1.02°C) throughout the duration of the study. Ambient laboratory room humidity was monitored 3 times daily throughout the duration of the study and remained 35.63% (±6.34%). All samples in this study were collected from January to May 2025.

3.2.3. Neat VOC standard solution preparation

15 frequently identified, abundantly recovered and skin-emitted VOCs were selected to be included in a standard VOC mixture (Table 3.1). 200 mg of each VOC were added into an amber glass vial (20 cm^3) glass vial and vortexed for 2 min. The vial was sealed, stored at 4°C, and is referred to as the Neat Solution (NS_{VOC}). The NS_{VOC} was vortexed for 2 min prior to each use, to ensure homogeneity.

3.2.4. Standard calibration solutions preparation for HS-SPME sampling

10 μL of the NS_{VOC} was transferred into 15 cm^3 H_2O in 20 cm^3 glass HS vial to prepare the aqueous stock solution (SS_{aq}). Serial dilutions (x4 and x5, respectively) using a dilution factor of 1:15 were performed using H_2O as the solvent. Prior to each serial dilution the standard vortexed for 2 minutes to ensure homogeneity. Masses of all VOCs for the solutions analysed (1/3375 and 1/50,675 dilutions) are listed in Table 3.1.

HS-SPME sampling was conducted on a 1 cm^3 aliquot of the diluted solutions, inside 20 cm^3 capped HS vials, following the Methods Section 3.2.2. Briefly, a SPME fibre (DVB/CAR/PDMS) was used to the pierce 20 cm^3 HS vial cap, where it was held in place. The fibre was exposed to the HS above 1 cm^3 of VOC standard aqueous solution for 15 min at room temperature. The HS of a 20 cm^3 vial containing 1 cm^3 standard solution was sampled for 15 min at room temperature. The fibre was then transferred into the GC inlet at 270°C for 2 min desorption.

For this VOC sampling approach, based on thermodynamic conditions and physicochemical properties of each VOC, a fraction of the VOC mass will partition into the HS based on the distribution of VOCs across the 2 phases and will reach equilibrium after a given time. Calculating the concentrations of each VOC in the HS was considered outside the scope of this study, therefore abundances recovered from GC-MS were the main guideline used for the interpretation of results.

Table 3.1. Densities and masses of each VOC in the SS_{aq}. Using serial dilutions, 1/3375 dilution and 1/50,625 dilutions of the SS_{aq} were selected for triplicate 20 cm^3 HS-SPME analysis and comparison to HS-SPME skin samples. Bolded values represent importance towards results.

VOC	SS_{aq} (mg VOC)	1/3375 dilution (µg VOC)	1/50,625 dilution (ng VOC)
Acetic acid	0.699	**0.17**	10.62
Heptanoic acid	0.611	**0.15**	9.38
Octanoic acid	0.606	**0.15**	9.38
Nonanoic acid	0.600	**0.15**	9.38
Decanoic acid	0.595	**0.15**	9.38
Dodecanoic acid	0.583	**0.14**	8.75
Octanal	0.547	0.13	**8.12**
Nonanal	0.551	0.13	**8.12**
Decanal	0.552	0.14	**8.75**
Undecanal	0.551	0.13	**8.12**
Dodecanal	0.554	0.14	**8.75**
6-methyl-5-hepten-2-one	0.570	0.14	**8.75**
6,10-dimethyl-5,9-undecadien-2-one	0.582	0.14	**8.75**
2-ethyl-1-hexanol	0.553	0.14	**8.75**
1-dodecanol	0.553	0.14	**8.75**

3.2.5. Standard calibration solutions preparation for liquid injection

5 µL of the NS_{VOC} was pipetted into 100 cm^3 hexane to prepare the stock solution (SS_{Hex}). The composition of the SS_{Hex} and the masses of each VOC in a 5 µL NS_{VOC} aliquot is listed in Table 3.2. The SS_{Hex} was used to make calibration solutions of 7 different concentrations, to evaluate the relationship between mass of VOC and corresponding GC-MS abundance. The concentration of each compound in the calibration solutions was calculated precisely for each VOC, depending of density but were ≈3, 2, 1.7, 1.3, 1, 0.6 and 0.3 mg/L. This concentration range was then analysed using GC-MS. The masses of VOC corresponding to each concentration is described in Table 3.2. and Table 3.3.

Table 3.2. Densities and calculated masses of VOC in NS_{VOC} and SS_{Hex}, and concentrations of all VOCs in SS_{Hex}.

VOC	Density ($g\ cm^{-3}$)	Mass of VOC in NS_{VOC} (mg VOC)	Mass of VOC in SS_{Hex} (mg VOC)	Concentration of VOC in SS_{Hex} (mg/L)
Acetic acid	1.049	200	0.350	3.500
Heptanoic acid	0.920	200	0.303	3.030
Octanoic acid	0.910	200	0.303	3.020
Nonanoic acid	0.905	200	0.298	2.980
Decanoic acid	0.893	200	0.294	2.940
Dodecanoic acid	0.883	200	0.274	2.740
Octanal	0.821	200	0.276	2.760
Nonanal	0.827	200	0.277	2.770
Decanal	0.830	200	0.279	2.790
Undecanal	0.838	200	0.281	2.810
Dodecanal	0.844	200	0.274	2.740
6-methyl-5-hepten-2-one	0.823	200	0.293	2.930
6,10-dimethyl-5,9-undecadien-2-one	0.880	200	0.278	2.780
2-ethyl-1-hexanol	0.833	200	0.277	2.770
1-dodecanol	0.830	200	0.277	2.770

Table 3.3. Masses of each VOC/L for each specified dilution of SS_{Hex}.

VOC	1/1.5 dilution of SS_{Hex} (mg/L)	1/1.8 dilution of SS_{Hex} (mg/L)	1/2.3 dilution of SS_{Hex} (mg/L)	1/3 dilution of SS_{Hex} (mg/L)	1/4.5 dilution of SS_{Hex} (mg/L)	1/10 dilution of SS_{Hex} (mg/L)
Acetic acid	2.34	1.95	1.55	1.17	0.77	0.35
Heptanoic acid	2.02	1.69	1.34	1.01	0.67	0.30
Octanoic acid	2.02	1.68	1.34	1.01	0.66	0.30
Nonanoic acid	1.99	1.66	1.32	0.99	0.66	0.29
Decanoic acid	1.96	1.64	1.30	0.98	0.65	0.29
Dodecanoic acid	1.83	1.53	1.22	0.91	0.60	0.27
Octanal	1.84	1.54	1.22	0.92	0.61	0.28
Nonanal	1.85	1.54	1.23	0.92	0.61	0.28
Decanal	1.86	1.56	1.24	0.93	0.61	0.28
Undecanal	1.88	1.56	1.25	0.94	0.62	0.28
Dodecanal	1.83	1.53	1.22	0.91	0.60	0.27
6-methyl-5-hepten-2-one	1.95	1.63	1.30	0.98	0.65	0.29
6,10-dimethyl-5,9-undecadien-2-one	1.86	1.55	1.23	0.93	0.61	0.28
2-ethyl-1-hexanol	1.85	1.54	1.23	0.92	0.61	0.28
1-dodecanol	1.85	1.54	1.23	0.92	0.61	0.28

3.2.6. Tenax TA and Tenax TA/divinylbenzene planar film preparation

Glass petri dishes (8 cm diameter), were used as film-casting substrates. Before use, substrates were cleaned with ethanol washings, acetone washings, followed by H_2O washings, all performed three times. Substrates were then oven dried at 80°C overnight, and maintained at this temperature, until immediately prior use.

1000 mg of Tenax TA was dissolved in 100 cm^3 of dichloromethane (DCM) using sonication to give a final Tenax TA concentration of 10 mg cm^{-3}. 10 cm^3 of this solution was pipetted into the glass petri dish and placed into a vacuum desiccator overnight. The substrates were removed from the desiccator and 5 cm^3 of GC grade methanol was pipetted onto the dried films. These were placed in an 80°C oven for 5 min, to aid removal of the film from the glass substrate. Once removed, the films were placed back into an 80°C oven overnight, to dry and thermally help remove excess methanol or Tenax TA based residual VOCs. A representative film is shown in Figure 3.2 (a).

To prepare the Tenax TA/DVB polymer films, 2 cm^3 DVB was transferred into 98 cm^3 of DCM. This solution was homogenised and then used to dissolve 1000 mg Tenax TA, as used for the other batch of planar films (10 mg Tenax TA/18.28 mg DVB per cm^{-3}). The rest of the film preparation procedure was repeated as described for the Tenax TA films. A representative film is shown in Figure 3.2 (b).

3.2.7. Polydimethylsiloxane film preparation

Silicone elastomer PDMS sheets (0.50 μm thickness) were purchased from Limitless Shielding Ltd., Essex, UK. PDMS discs (38 mm diameter) were cut from PDMS sheets using a circular stamping press. A representative prepared disc is imaged in Figure 3.2 (c). The prepared PDMS discs were washed for 5 min in 10 cm^3 methanol, three times, then thermally treated at 80°C,overnight. PDMS discs were kept at this temperature until immediately prior to use.

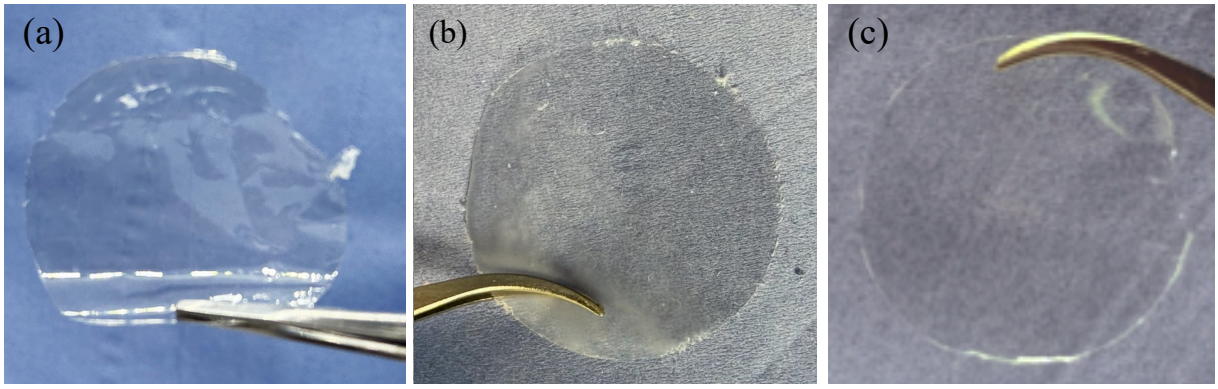

Figure 3.2. Freshly prepared **(a)** Tenax TA film cutting, **(b)** Tenax TA/DVB film cutting and **(c)** PDMS film cutting. All were cut using a 38 mm diameter circular stamping press.

3.2.8. Sorbent film evaluation in the HS of standard VOC solutions

The 3 sorbent materials (Tenax TA, Tenax TA/DVB, PDMS) were investigated for their ability to adsorb a mixture of 15 standard VOCs in an aqueous solution, from HS (850 cm^3), using the chamber shown in Figure 3.3. (a). Each film was placed in between two pieces of planar stainless-steel mesh (10 x 10 cm), herein referred to as 'VOC sampler'.

The VOC sampler was placed on top of a clean aluminium foil stage (7 x 4 x 3 cm) in the chamber. 10 cm^3 of VOC-containing aqueous solutions (5 different concentrations were added to the chamber and closed immediately for sampling. After 2 h at room temperature, the chamber was opened to remove the sorbent film. The sorbent film was solvent extracted immediately after, following the procedure in Section 3.2.9. All sampling experiments was repeated in triplicate for each sorbent material.

In terms of the VOC solutions described used in this testing, the NS_{VOC} mixture of 15 compounds was used to prepare the solutions for these experiments. The final concentrations of these solutions in water were calculated and reported as % (volume/volume) (Table 3.4.).

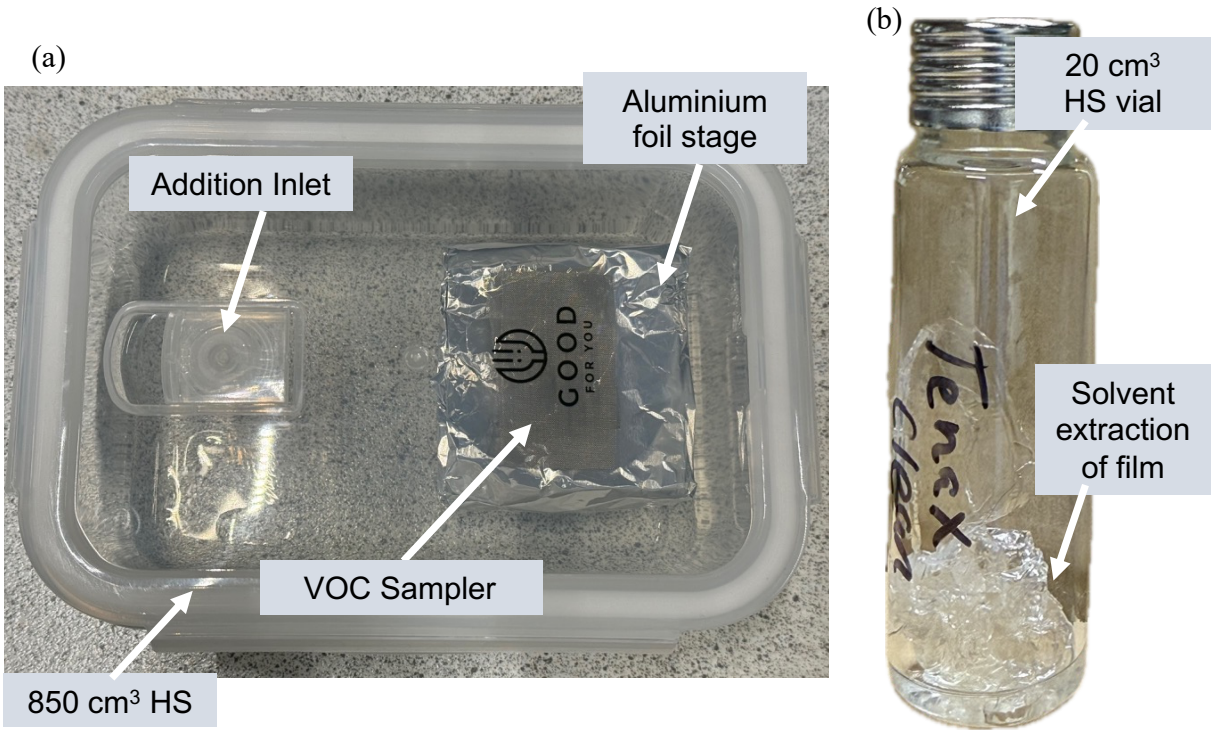

Figure 3.3. (a) Experimental set-up in chamber for testing sorbent films and **(b)** glass HS vial (20 cm^3) used for solvent extraction from the sorbent films following exposure. Solvent: 2 cm^3 hexane.

Table 3.4. Masses of each VOC in each of the NS_{aq} solutions (10 cm^3) used to test the different sorbent films. Solutions (10 cm^3) were added to the chamber (850 cm^3) with a specified sorbent film. Films were left for 2 h in the chamber before solvent extraction and GC-MS analysis.

VOC	Control (H_2O only) (mg VOC)	0.10% (v/v) NS_{aq} (mg VOC)	0.25% (v/v) NS_{aq} (mg VOC)	0.50% (v/v) NS_{aq} (mg VOC)	0.75% (v/v) NS_{aq} (mg VOC)	1% (v/v) NS_{aq} (mg VOC)
Acetic acid	-	**0.70**	1.75	3.49	5.24	6.99
Heptanoic acid	-	**0.61**	1.53	3.05	4.58	6.11
Octanoic acid	-	**0.61**	1.52	3.03	4.55	6.06
Nonanoic acid	-	**0.60**	1.50	3.00	4.50	6.00
Decanoic acid	-	**0.60**	1.49	2.97	4.46	5.95
Dodecanoic acid	-	**0.58**	1.46	2.91	4.37	5.83
Octanal	-	**0.55**	1.37	2.73	4.10	5.47
Nonanal	-	**0.55**	1.38	2.75	4.13	5.51
Decanal	-	**0.55**	1.38	2.76	4.14	5.52
Undecanal	-	**0.55**	1.38	2.75	4.13	5.51
Dodecanal	-	**0.55**	1.39	2.77	4.15	5.54
6-methyl-5-hepten-2-one	-	**0.57**	1.43	2.85	4.27	5.70
6,10-dimethyl-5,9-undecadien-2-one	-	**0.58**	1.46	2.91	4.36	5.82
2-ethyl-1-hexanol	-	**0.55**	1.38	2.76	4.14	5.53
1-dodecanol	-	**0.55**	1.38	2.76	4.15	5.53

3.2.9. Solvent extraction

Immediately after HS sampling in the chamber, the sorbent film was removed using tweezers, transferred into 2 cm^3 GC-grade hexane in a 20 cm^3 HS vial and capped. The vial was vortexed for 5 min and then rested for 15 min, before being vortexed again for 1 min. A representative solvent extraction vial is shown in Figure 3.3. (b). The vial was opened and the sorbent film was removed. The remaining hexane was transferred into a 2 cm^3 GC autosampling vial for liquid injection onto the GC-MS. Control HS experiments (water only) were run in triplicate for each sorbent and liquid extracted following the same method as described.

3.2.10. Skin VOC sampling using sorbent films

To test these films for their ability to recover VOCs directly from skin, sorbent films were placed between 2 stainless steel mesh films (thickness: 60 μm, hole diameter: 0.075 mm) and incorporated into an adherent wound dressing (12 x 12 cm), secured to the dressing using the adhesive edges of the dressing (Figure 3.4.).

The volar forearm was selected as the sampling area. As the HS volume is likely smaller compared to the 3 cm^3 HS used for SPME, and skin contact with the film more likely, the steel mesh was cut to cover the entire planar film area (9 x 9 cm), as shown in Figure 3.4. The dressing was applied to the volar forearm and was worn by a participant for 8 h. After this, the dressing was removed and the sorbent film was transferred into 2 cm^3 hexane for solvent extraction as described in Section 3.2.9. The hexane was transferred to the GC via liquid injection and GC-MS analysis carried out as per Section 3.2.11.

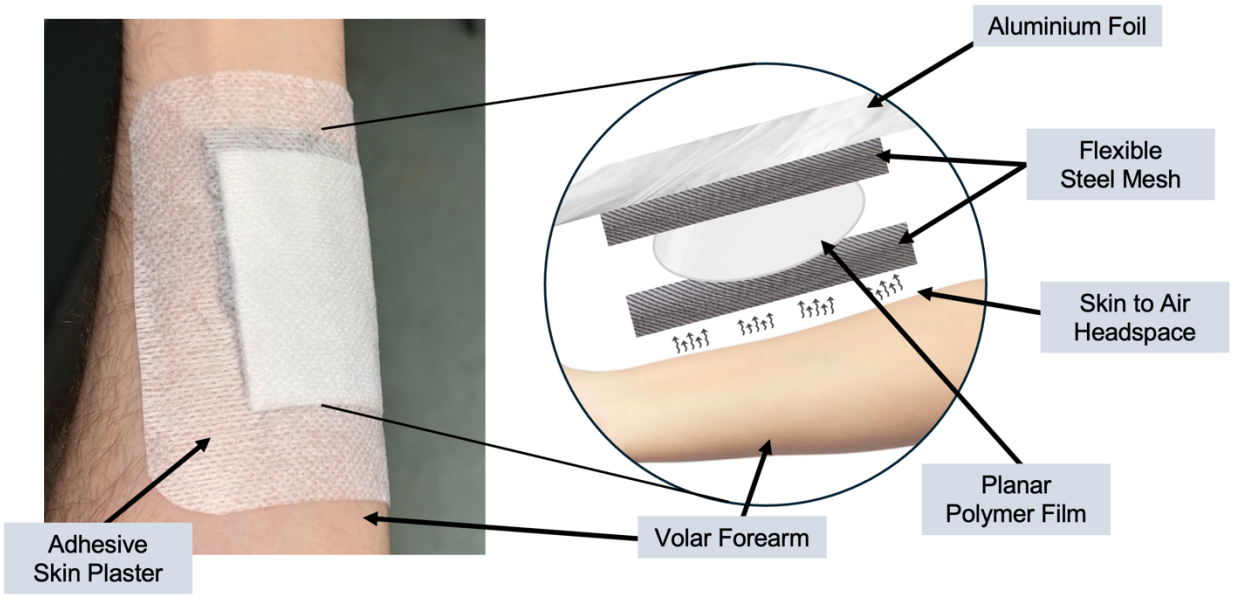

Figure 3.4. Image of the VOC sampler worn on the participant volar forearm during the study (left) for wearable skin VOC collection and the corresponding schematic of the VOC sampler structure underneath the worn plaster (right).

3.2.11. Gas chromatography-mass spectrometry

An Agilent 7820A gas chromatograph connected to an Agilent 5977B mass selective detector (Agilent Technologies, Inc., Santa Clara, CA, USA) was used for all analyses. Separations were carried out on an SLB-5 MS column (30 m × 0.25 mm × 0.25 µm diameter; Supelco). Helium was used as the carrier gas throughout all experiments, maintaining a constant flow rate of 1 cm^3 min^{-1}. Splitless injection was used for all SPME fibre-based and liquid-based samples.

For SPME fibre-based samples, the system was equipped with a SPME Merlin Microseal (Merlin Instrument Company, Newark, DE, USA), and the inlet was maintained at a temperature of 270°C. The fibre was desorbed for 2 min within a SPME inlet liner (Supelco).

For liquid samples, the system was equipped with an Agilent 7693A automatic liquid sampler (ALS). For each sample, 1 cm^3 of the solution that is to be analysed was added to an ALS-GC vial. The standard injection volume was set to 1 µL. The corresponding liquid injection GC method had a solvent delay set to 6.5 min. Its initial GC oven temperature was 40°C for 5 min after which the oven was programmed at a rate of 10°C min^{-1} to 270°C. Once 28 min elapsed, the oven was programmed to increase to 300°C to finish the GC run at 30 min total.

The MS was operated at a scan rate of 3.94 s^{-1}, with a scan range of 35-400 m/z, ion source temperature 230°C and ionising energy of 70 eV, for all runs. The GC-MS chromatographic component area output is described in this work in absolute abundance values.

3.2.12. Data analysis

Qualitative analysis of raw chromatographic data was performed using Agilent MassHunter Quant-My-Way Analysis 10.0 software. Peak acquisition and peak abundance data were identified by employing a chromatogram deconvolution mining algorithm. A peak filter of ≥8,000 counts was applied.

A Level 2 putative identification of compounds and structures was performed using the National Institute of Standards and Technology 2023 (NIST23) library. This was supported by a visual comparison of the unknown mass spectra with previous literature reports and by matching retention index (RI) values with a tolerance of ±15 RI units.

A standard mixture of saturated alkanes (C_7–C_{30}) in hexane was utilised for RI matching (Sigma Aldrich, Ireland). Furthermore, compounds deemed to be background species or contaminants (e.g., siloxanes likely originating from SPME and column bleed) were explored and subsequently excluded from the data set, except for results discussing the prepared PDMS films.

Data processing, exploration and visualisation were all conducted using RStudio (v2025.05.0). Principal component analysis (PCA) was conducted on the normalised Tenax TA/DVB dataset obtained using R packages 'FactoMineR' and 'factoextra'. All other R packages employed included: 'tidyverse', 'readr', 'terra', 'purrr', 'RcolorBrewer', 'ggplot2', 'scales', 'gridExtra', 'patchwork' and 'ggfortify'.

3.3. Results and Discussion

3.3.1. HS-SPME standard VOC sampling

The analytical functionality of planar films used as VOC samplers was explored in this work. Using a standard method in skin VOC collection as a comparison (triple phase HS-SPME), the sorbent materials investigated included Tenax TA, Tenax TA/DVB and PDMS. Using a range of concentrations of a standard VOC mixture within closed static HS, skin relevant VOCs were adsorbed onto VOC samplers from the gas phase.

Towards testing the sorbent films ability to retain gas phase compounds in a closed static chamber, the mass of each VOC present in the chamber was a key consideration for this part of the work. A need to broadly establish the masses of skin relevant compounds per an air-water system that induced a similar GC abundance response was apparent. Addressing this, Table 3.5. compares the average recovered abundances of these 15 compounds from a static air-water system, using the HS-SPME sampling technique. These results of the air-water system were compared to the abundances observed from skin, through this same non-invasive sampling approach.

To do this, a stock solution was first prepared in water (NS_{aq}) comprising of 15 compounds that were selected on the basis that they are regularly recovered from skin using our HS-SPME method. These prepared solutions are described in Table 3.1. and were prepared according to the Methods Section 3.2.4. Through these serial dilutions of the NS_{aq}, two different concentrations were selected for triplicate HS-SPME sampling, due to their similarities to P1 skin samples. These concentrations were reported as 1/3375 dilution and 1/50,625 dilution of the SS_{aq}, and the masses of each compound present in these dilutions was listed in Table 3.1.

All 15 of the compounds added into the air-water system were simultaneously recovered from this 20 cm^3 HS including carboxylic acids, aldehydes, ketones and alcohols, as per healthy human skin emissions[2,13,23,24]. To compare to these results, a representative HS-SPME skin chromatogram is shown in Figure 3.5. As anticipated, the average abundances obtained from an in-vivo skin sample corresponds to very small masses of VOC, considering low concentrations of skin emitted VOCs[16,25,26] and the high pre-concentration efficiency of the SPME fibre[2,3,27]. These masses were found to be in the range of micrograms (µg) for the acids and in nanograms (ng) for the aldehydes and ketones. Table 3.5. lists the recovered abundances from each of these discussed samples.

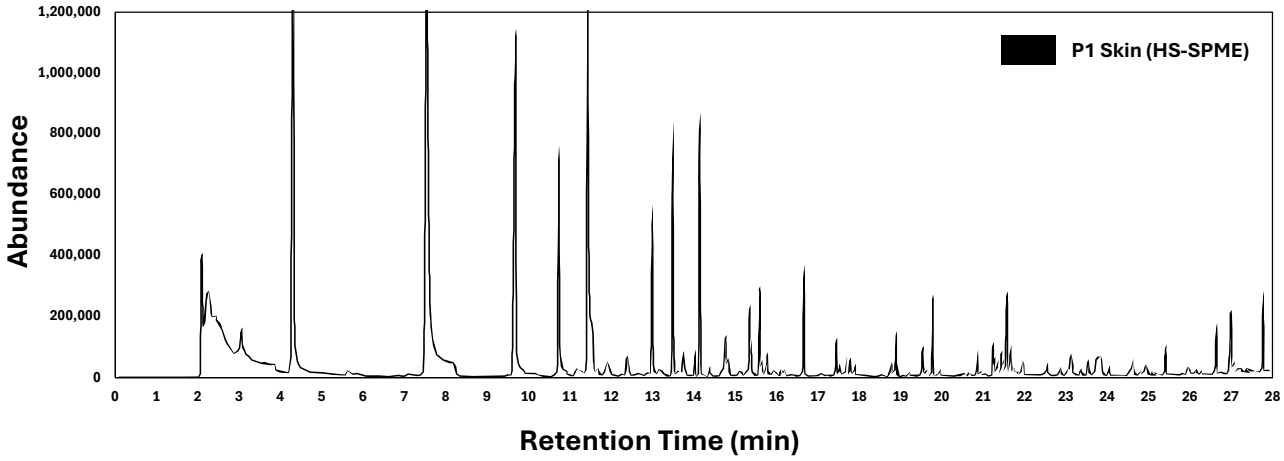

Figure 3.5. A representative raw chromatograph obtained from P1 volar forearm HS-SPME skin sample. Table 3.5. lists the identified compounds from (n=3) SPME P1 skin samples.

The peak abundances induced by HS-SPME volar forearm skin VOC samples compared to peak abundances of standard analyte solutions revealed the mass to HS volume ratio required for the selected compounds. The triplicate HS-SPME volar forearm skin chromatograms (a representative of these is shown in Figure 3.5.) were selected as a model for evaluating these compounds. It was important this was collected and analysed shortly before the rest of the experiment as GC abundance is known to be affected by time sensitive factors such as environmental or instrumental conditions. This is especially important with regards to the extracted data in an effort to keep standard deviations (SD), or experimental variance, as small as possible.

In general, carboxylic acids dissolve more readily into aqueous environments compared to aldehydes or ketones[23], therefore an inherent limitation of this method is a partial retention of carboxylic acids in the aqueous solution used to facilitate the transfer and sampling of these compounds. This is likely partially the case with alcohol VOCs as well, albeit the particular compounds selected for these experiments are fatty alcohols (2-ethyl-1-hexanol and 1-dodecanol), they still have H-bonding ability (-OH group). To explore their properties further, a stock solution was prepared in hexane comprising of 15 compounds that were selected on the basis that they are regularly recovered from skin using our HS-SPME method.

Table 3.5. Average abundances and SD of VOCs recovered from the HS above skin, collected via HS-SPME sampling (HS volume 3cm^3; n=3), and average abundances of VOCs recovered from the HS above NS_{aq} solutions (1 cm^3) at 2 dilutions (HS volume 20 cm^3; n=3). Bolded values indicate the abundance values closest to those recovered from skin.

VOC	RT (min)	Abundances recovered from skin	Abundances recovered from 1/50,625 NS_{aq} dilution	Abundances recovered from 1/3375 NS_{aq} dilution
Acetic acid	3.14	**408 136**	n/d	**341 493**
Heptanoic acid	13.40	n/d	n/d	n/d
Octanoic acid	14.95	**197 368 ±202 312**	n/d	**118 412 ±18 702**
Nonanoic acid	16.33	**168 304 ±159 739**	n/d	**207 987 ±10 603**
Decanoic acid	17.63	n/d	n/d	**n/d**
Dodecanoic acid	20.12	n/d	n/d	**n/d**
Octanal	11.85	n/d	**188 946 ±82 961**	601 715 ±779 699
Nonanal	13.71	**183 242 ±34 521**	**174 116 ±99 227**	254 716 ±180 416
Decanal	15.35	**245 592 ±51 814**	**548 389 ±290 596**	1 542 774 ±1 967 127
Undecanal	16.85	**n/d**	**305 253 ±222 284**	1 504 239 ±2 029 715
Dodecanal	18.24	**n/d**	**425 073 ±410 546**	3 184 121 ±4 346 516
6-methyl-5-hepten-2-one	11.49	**132 929 ±58 013**	**92 643 ±19 361**	2 018 795 ±942 712
6,10-dimethyl-5,9-undecadien-2-one	18.63	**161 98 ±155 208**	**72 627 ±56 849**	1 086 881 ±724 719
2-ethyl-1-hexanol	12.35	**191 952 ±110 787**	**151 091 ±97 709**	1 713 915 ±1 888 849
1-dodecanol	19.09	n/d	n/d	533 387

3.3.2. GC-MS analysis of skin emitted compounds

These SS_{Hex} solutions are described in Table 3.2. and Table 3.3. These were prepared according to the Methods Section 3.2.5. Then each of the solutions were analysed by GC-MS using liquid injection for 7 different concentrations (0.3-3 ppm for each compound). Hexane was the solvent of choice as it was the solvent used later for solvent extraction from the candidate sorbent films and thus the idea was that the masses of sorbent-adsorbed VOCs that were solvent extracted could potentially be extrapolated using these calibration plots. The lower concentration range chromatograms are shown, overlaid, in Figure 3.6.

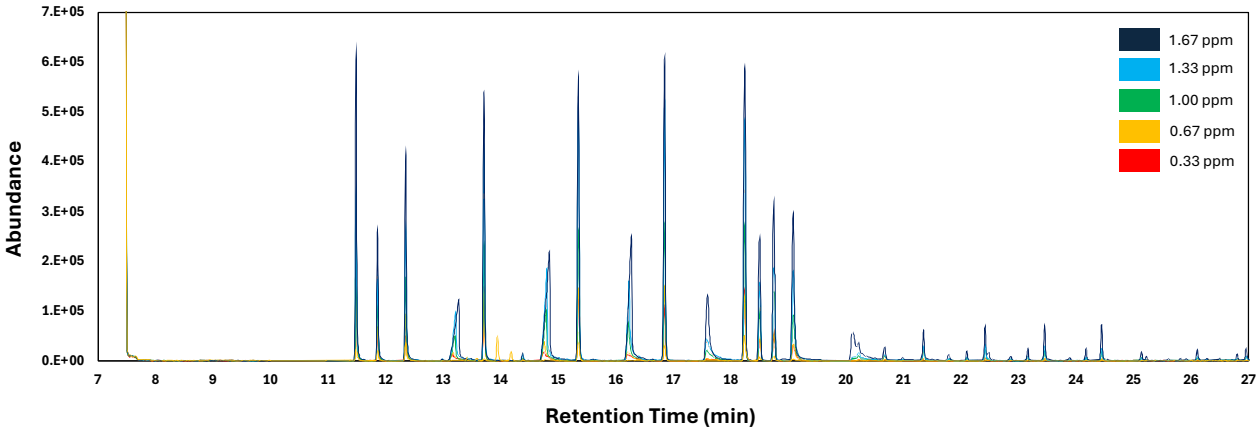

Figure 3.6. Overlaid raw chromatographs obtained for 5 lowest concentrations prepared from dilutions of SS_{Hex}. Upper concentrations were excluded for clarity in the lower range of the Y-axis.

Shown in the overlaid chromatograms of Figure 3.6., the peak shapes for all aldehydes, ketones and 2-EH (RT=13.35 min) are very sharp and narrow. Compared to a degree of peak tailing for heptanoic acid (RT=13.10 min) and octanoic acid (RT=14.95 min), followed by a degree of peak fronting for nonanoic acid (RT=16.33 min) and decanoic acid (RT=17.50 min), these peaks are not as sharp as their aldehyde and ketone counterparts.

This, concurrent to the lower abundances of each of the analysed carboxylic acids and 1-dodecanol (RT=19.10 min), indicates that the method used is intrinsically less sensitive to these compounds. Albeit these are still considered aliphatic ‘fatty’ compounds, their ability to form hydrogen bonds may play a bigger role in the way they interact with stationary phases. These insights are applied to the latter part of the study and examined further.

The chromatographs of Figure 3.6. were used towards the construction of calibration plots, shown in Figure 3.7., where the recovered abundances for each compound were plotted against concentration (ppm). Linear regression resulted in satisfactory coefficients of determination (R^2), generally greater than 0.950. Due to the method used with a solvent delay of 6.5 min, longer than the RT of acetic acid, acetic acid was not recovered in the chromatographs. However, all other VOCs were detected.

Dodecanoic acid exhibited poor responses over the concentration range examined where it was only recovered for the highest concentration analysed (2.94 ppm). Interestingly, 1-dodecanol followed a similar trend, where it was more difficult to identify in the chromatographs due to a small and broad peak, albeit for analysis, it showed satisfactory linearity (R^2=0.944).

These results show the linear relationship between the abundance (peak area) and mass of the corresponding compound identified with the support of MS data. The abundance for our GC-MS system is measured in total ion count (TIC) intensity, as a function of column retention time (RT)[2,28], which also helps to confirm the presence of that compound. The peak shape of each compound on the chromatograph indicates its affinity to the column, related to the compounds breakthrough volume for this DB-5ms column.

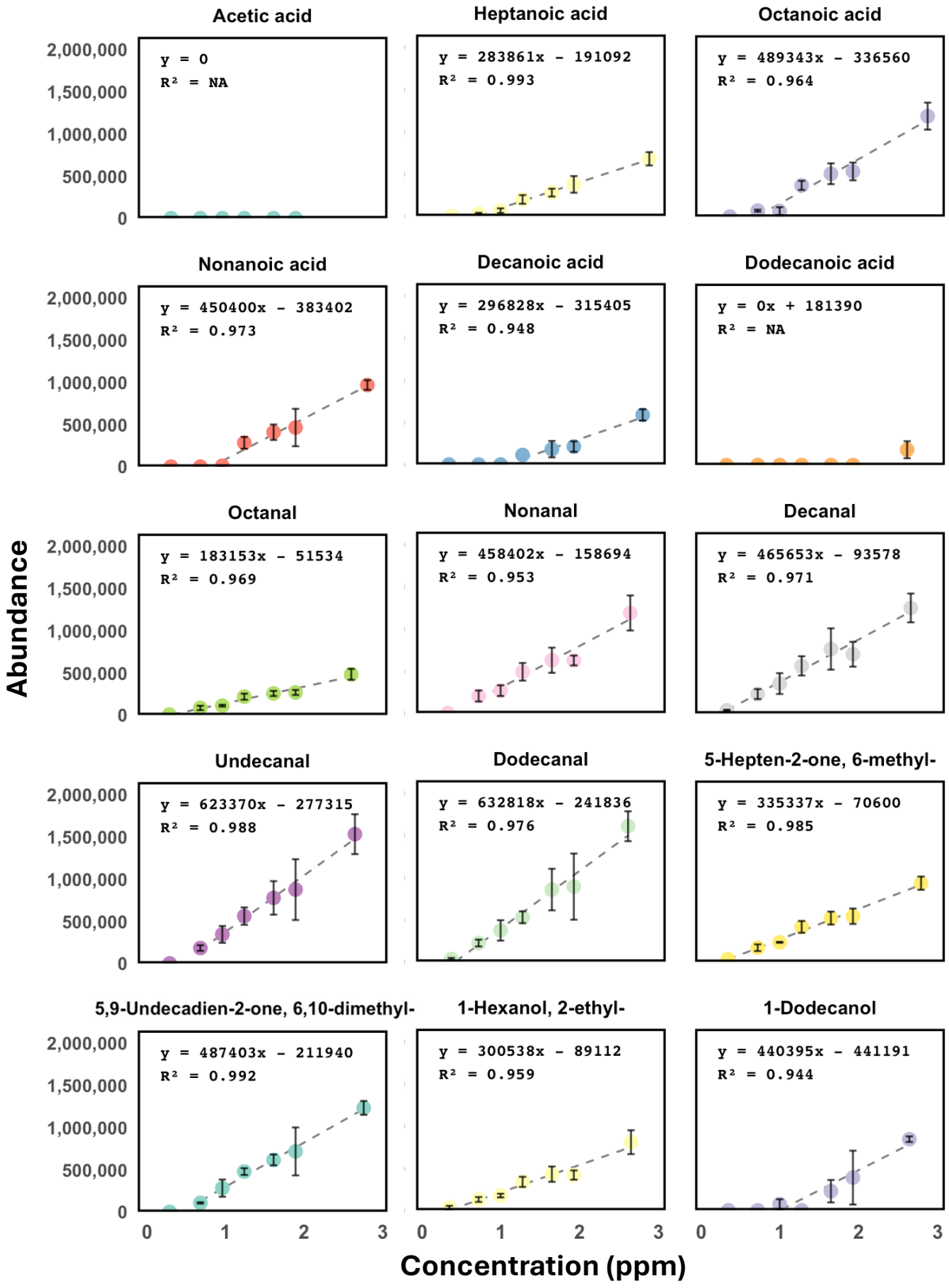

Figure 3.7. Scatterplots and applied linear regressions for VOC abundances recovered from mixed VOC solutions prepared from SS_{Hex} at 7 different concentrations.

3.3.3. Tenax TA sorbent film testing

Tenax TA films were prepared as described in the Methods Section 3.2.6. Following thermal treatment, each prepared Tenax TA planar film was weighed an analytical mass balance. Average film masses were recorded to be 94.95 ±4.60 mg. These planar films were explored for their ability to adsorb NS_{aq} at five different concentrations (in water) (Table 3.4.).

The mixture of 15 skin representative compounds from a high humidity HS inside a 850 cm^3 chamber, shown in Figure 3.3. (a). The HS was considered high humidity due to observed condensation forming on the walls of the chamber. This was a trend that was observed to occur across both, 3cm^3 HS-SPME skin sampling and these 850 cm^3 chamber experiments. The RH of the HS was unable to be measured using an instrument, therefore the %RH was not able to be quantified and reported.

Solvent extraction was carried out in hexane and direct injection of the hexane onto GC-MS resulted in the identification of only one compound - octamethyl-cyclotetrasiloxane (RT=11.37 min). This was the only compound to pass criteria specified in the Methods and is associated with the siloxane-based GC column. This shows the workflow employed is clean and free of contaminants that may interfere with the study. All prepared sorbent materials were subject to solvent extraction, after 2-hour exposure to ambient laboratory air to explore their by-products and inspect for contaminants. For the Tenax TA film, a small range of benzene derivatives were present in the extracted solutions when analysed with ALS-GC-MS. This was found to not interfere significantly with the collection of the 15 selected compounds collection analysis as these compounds did not overlap in terms of RT, for example, benzene, 1,4-diethenyl- (RT=14.18 min) or tetracosane (RT=28.36 min).

15 skin representative compounds were prepared as NS_{aq} at five different concentrations for each experiment inside a 850 cm^3 chamber. These concentrations were calculated to be 0.10% (v/v), 0.25% (v/v), 0.50% (v/v), 0.75% (v/v) and 1% (v/v), respectively. Each of their masses are listed in Table 3.6. Firstly, the single-phase Tenax TA film sorption performance was examined.

Overall, 7 out of 15 standard VOCs (octanal, nonanal, decanal, undecanal, dodecanal, 6-methyl-5-heptan-2-one, geranyl acetone) were recovered from the chamber containing the NS_{aq} solutions using the Tenax TA film at 0.10% (v/v) concentrations for 2-hour sampling. Subsequently, starting from concentration 0.25% (v/v), 2-ethyl-1-hexanol was recovered from the chamber onwards using the Tenax TA film. For the highest NS_{aq} concentration examined, 9 out of 15 standard VOCs (heptanoic acid, octanal, nonanal, decanal, undecanal, dodecanal, 6-methyl-5-heptan-2-one, geranyl acetone, 2-ethyl-1-hexanol) were recovered. Interestingly,

1-dodecanol was not recovered during any of these experiments. All compounds recovered were identified n=2 or more chromatographs where this, and the abundances for each compound are shown in Figure 3.8.

All 5 aldehydes and 2 ketones were successfully collected from the NS_{aq} in the chamber, at all solution concentrations examined. In terms of the alcohols and the acids, only 1 out of the 2 alcohols were recovered, albeit more inconsistently when compared to the aldehydes and ketones. For all concentrations, the alcohol, 1-dodecanol, and all the present acids, were not observed in any chromatographs after solvent extraction, except heptanoic acid (RT=13.10 min). With the average abundance of heptanoic acid average being approx. 31,000 at 1%, this indicates recovery for concentrations much lower than 1% (v/v) would not be possible for this method. Furthermore, using $y = 283861x - 191092$ from the linear regression (Figure 3.7.), this can be used to estimate that approx. 0.785 ppm heptanoic acid was present in the solvent extract (2 cm^3 hexane). This 0.785 mg/L concentration equates to a mass of 0.0016 mg heptanoic acid in 2 cm^3 hexane.

Similar behaviour for Tenax TA was observed by Zou et al., where acid and alcohols were not recovered from Tenax TA thermal desorption tubes[29]. Stated by manufacturers and supported by experimental observations, Tenax TA exhibits strong hydrophobic characteristics due to its aromatic backbone and is excellent at adsorbing non-polar compounds in the range of C_7–C_{26}[30]. Alcohols and acids form extensive hydrogen-bonding networks with a high degree of dipole-dipole moments. The surface of Tenax TA likely lacks ability to facilitate these forms of intermolecular bonding, therefore exhibiting ineffective recoveries for the acids in this study.

Alcohols and acids form extensive hydrogen-bonding networks in the vapor phase, with a high degree of dipole-dipole moments. The surface of Tenax TA appears to lack ability to effectively facilitate these forms of intermolecular bonding, therefore exhibiting ineffective adsorption recoveries for the acids explored in this study.

Moreover, given that the current work presents a method performed at room temperature, this should be considered when interpreting results. Interestingly, the chromatographs of the Tenax films exposed to the ambient air for 2-hour sampling show the absence of a large quantity of Tenax TA degradation products. This indicates that this solvent extraction method offers a unique advantage. Unlike standard high temperature thermal desorption of VOCs, this extraction does not involve heat, which likely minimises production of Tenax TA degradation products.

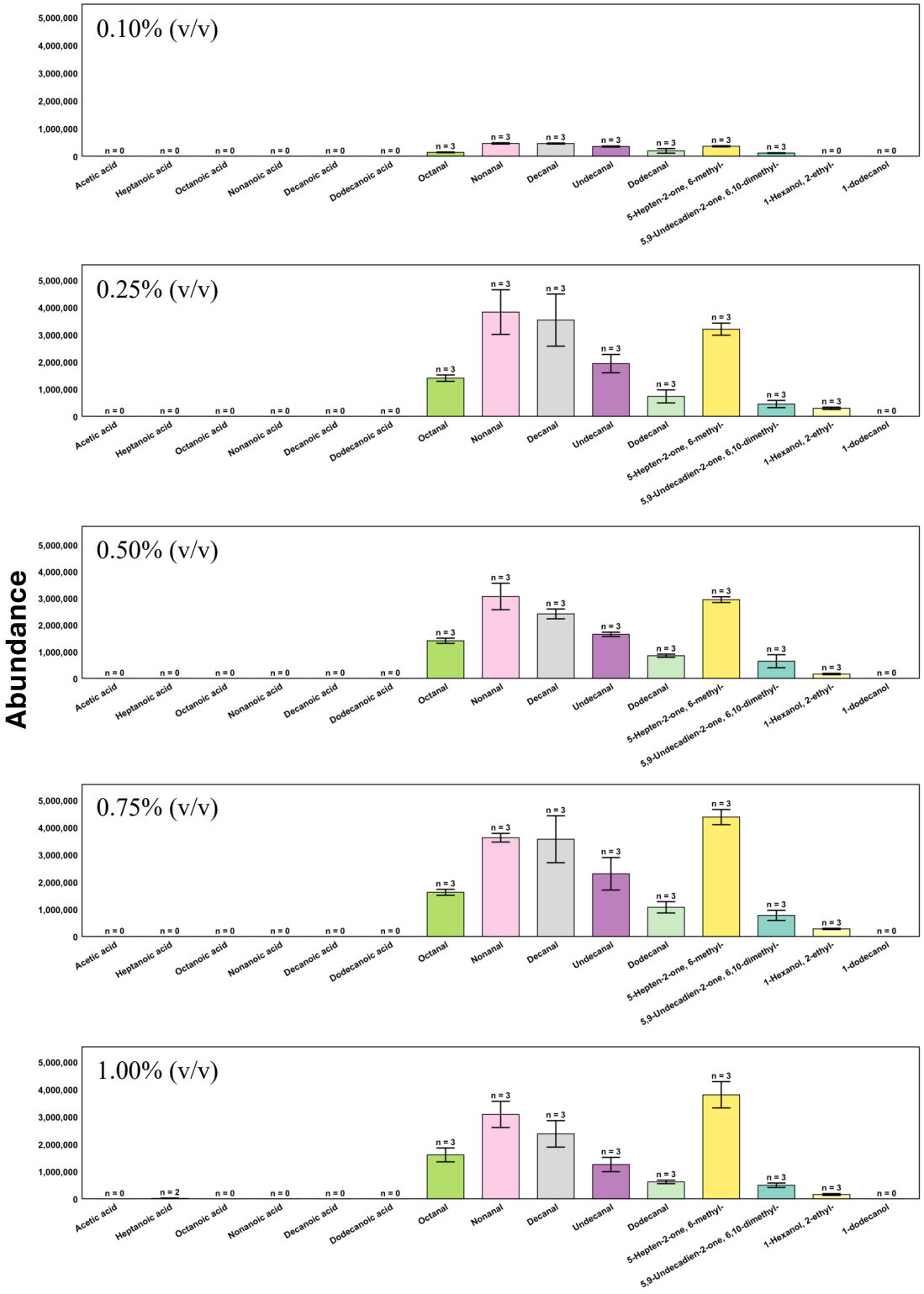

Figure 3.8. Bar charts of each VOC abundance recovered from each of the NS_{aq} solutions (10 cm^3) used to test Tenax TA sorbent film (n=3). Solutions (10 cm^3) were added to the chamber (850 cm^3) with a specified sorbent film. Films were left for 2 h in the chamber before solvent extraction and GC-MS analysis.

Table 3.6. Average abundances and SD of VOCs recovered from each of the NS_{aq} solutions (10 cm^3) used to test Tenax TA sorbent film (n=3). Solutions (10 cm^3) were added to the chamber (850 cm^3) with a specified sorbent film. Films were left for 2 h in the chamber before solvent extraction and GC-MS analysis. n/d=not detected.

VOC	RT (mins)	Abundances for Control (H_2O only)	Abundances for 0.10% (v/v) NS_{aq}	Abundances for 0.25% (v/v) NS_{aq}	Abundances for 0.50% (v/v) NS_{aq}	Abundances for 0.75% (v/v) NS_{aq}	Abundances for 1% (v/v) NS_{aq}
Acetic acid	3.14	n/d	**n/d**	n/d	n/d	n/d	n/d
Heptanoic acid	13.40	n/d	**n/d**	n/d	n/d	n/d	31 709 ±12 970
Octanoic acid	14.95	n/d	**n/d**	n/d	n/d	n/d	n/d
Nonanoic acid	16.33	n/d	**n/d**	n/d	n/d	n/d	n/d
Decanoic acid	17.63	n/d	**n/d**	n/d	n/d	n/d	n/d
Dodecanoic acid	20.12	n/d	**n/d**	n/d	n/d	n/d	n/d
Octanal	11.85	n/d	**154 303 ±13 403**	1 418 792 ±116 151	1 423 507 ±96 537	1 637 285 ±107 985	1 620 771 ±253 995
Nonanal	13.71	n/d	**477 584 ±23 295**	3 843 846 ±818 876	3 082 365 ±494 893	3 639 854 ±158 604	3 099 064 ±478 853
Decanal	15.35	n/d	**474 651 ±19 418**	3 548 171 ±957 288	2 429 804 ±183 421	3 584 710 ±860 378	2 390 048 ±482 834
Undecanal	16.85	n/d	**366 332 ±19 734**	1 952 614 ±336 187	1 665 500 ±79 879	2 317 290 ±596 085	1 268 508 ±263 444
Dodecanal	18.24	n/d	**208 421 ±83 370**	748 740 ±238 277	864 211 ±57 569	1 086 824 ±208 208	633 591 ±63 554
6-methyl-5-hepten-2-one	11.49	n/d	**373 420 ±20 111**	3 216 824 ±222 100	2 962 893 ±107 856	4 396 683 ±278 159	3 816 614 ±480 390
6,10-dimethyl-5,9-undecadien-2-one	18.60	n/d	**129 870 ±11 087**	468 517 ±132 103	657 767 ±243 493	792 652 ±186 527	512 153 ±80 473
2-ethyl-1-hexanol	12.35	n/d	**n/d**	311 143 ±41 993	178 356 ±25 202	293 864 ±21 491	173 586 ±32 604
1-dodecanol	19.10	n/d	**n/d**	n/d	n/d	n/d	n/d

Furthermore, these results indicate the sorption capacity of this Tenax TA film is reached by 0.25% (v/v). After this, the recovered abundances appears to remain relatively consistent and no change in response was observed after this. To explore this mass range, the concentration of each VOC in the extracted solution recovered from 0.25% (v/v) was extrapolated using the calibrations curves of Figure 3.7. This estimated sorption capacity was then broadly approximated to be 40 mg, when all of the VOCs recovered with the Tenax TA film were applied using these linear equations, however this is an estimation, likely followed by a high SD.

3.3.4. Tenax TA/divinylbenzene sorbent film testing

To enhance the performance and reliability of the previously prepared Tenax TA sorbent films, DVB was then added into the Tenax TA solution at approximately 2% (see Methods Section 3.2.6) and films prepared in a similar manner. Following thermal treatment of these films, Tenax TA/DVB films were weighed, and an average mass of 101.25±6.00 mg was recorded for all prepared films. Here, a dual-phase sorbent material Tenax TA/DVB as planar films were explored for their ability to adsorb NS_{aq} at five different concentrations (in water) (Table 3.2).

This will also be compared to the single-phase Tenax TA films to explore any advantages or disadvantages. As performed for the Tenax TA films, 15 skin representative compounds were prepared as NS_{aq} at five different concentrations for each experiment inside each 850 cm^3 chamber. These NS_{aq} concentrations were calculated to be 0.10% (v/v), 0.25% (v/v), 0.50% (v/v), 0.75% (v/v) and 1% (v/v), respectively.

All prepared sorbent materials were subject to solvent extraction, after 2-hour exposure to ambient laboratory air to explore their by-products and inspect for contaminants. For the Tenax TA/DVB film, a small range of benzene derivative peaks and a large 1,2-divinylbenzene (RT=13.94 min) peak were present in the extracted solutions when analysed with ALS-GC-MS. This was found to not interfere significantly with the collection of the 15 selected compounds as these compounds did not overlap in terms of RT.

Overall, 8 out of 15 standard VOCs (octanal, nonanal, decanal, undecanal, dodecanal, 6-methyl-5-hepten-2-one, geranyl acetone and 2-ethyl-1-hexanol) were recovered using the Tenax TA/DVB film at NS_{aq} 0.10% (v/v) concentrations. Interestingly, compared to the single-phase film, heptanoic acid was not detected at 1% (v/v). Instead, heptanoic acid was identified for all samples at concentrations 0.50% (v/v) and 0.75% (v/v). This does not appear to follow

a reliable concentration dependant trend, and is therefore excluded from further discussion. All species reported as recovered were identified in n=2 or more chromatographs and this is highlighted in Figure 3.9. and Table 3.7.

The acids examined were described as slightly polar chemical compounds due to strongly polarised carbonyl (C=O) and hydroxyl (O-H) groups by Jha and Hayashi et al[31]. These results suggested that acids partake in H bonding with other compounds or sorbent phases capable in H-bonding with greater affinity compared to other VOCs such as the aldehydes, ketones, alcohols.

Taking this into consideration, consistent HS recovery of all standard aldehydes, ketones and 1 out of 2 alcohols examined indicates an uptake mechanism other than H bonding, for this sorbent material. This is supported by weak, almost entirely, below LOD recoveries, of all organic acids, at all examined NS_{aq} solution concentrations examined in this work.

Notably, high humidity is likely an interferent species here, occupying any residual H-bonding sites[19]. Combined with a degree of acid dissolution and retention in the NS_{aq}[23], this method is likely not optimised towards efficient recoveries of the carboxylic acids.

This subsequently leads to poor pre-concentration efficiencies for VOCs with acid or alcohol functional groups. This data helps to show this sorbent materials sensitivity for these compounds, however, the 0.10% (v/v) concentration examined appears to be largely above limits of detection (LOD) and quantification (LOQ) for this method. This is indicated by a high change in abundances of recovered VOCs between the control sorbent films and corresponding sorbents from 2-hour sampling at 0.10% (v/v) concentrations. The magnitude of this difference indicates this material has pre-concentration abilities for aldehyde and ketone concentrations lower than 0.10% (v/v) concentrations. In future work, a lower concentration range of the same compounds should be explored to establish accurate sorbent LODs, for this method.

Furthermore, the results indicate that the sorption capacity of the film is reached by 0.50% (v/v). After this, the recovered abundances are observed to remain relatively consistent and no significant change in response was observed after this. To explore this mass range, the concentration of each VOC in the extracted solution recovered from 0.50% (v/v) of Figure 3.9. was extrapolated using the calibrations curves in Figure 3.7. This estimated sorption capacity was then broadly approximated to be 32 mg, when all of the VOCs recovered with the Tenax TA/DVB film were applied using these linear equations. Compared to the Tenax TA film, these are likely within an error % margin of each other, however interestingly, this occurred at 0.50% (v/v).

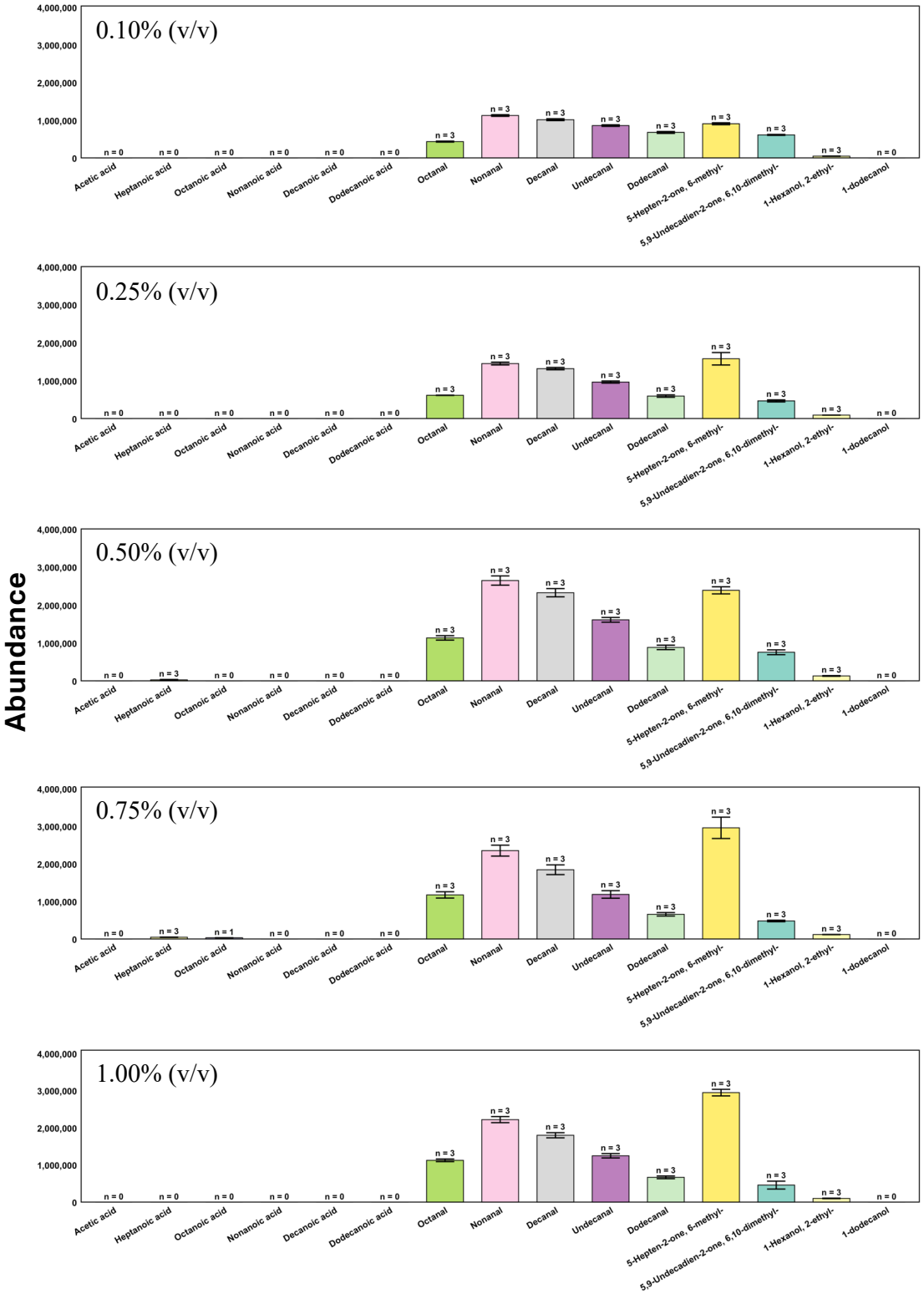

Figure 3.9. Bar charts of each VOC abundance recovered from each of the NS_{aq} solutions (10 cm^3) used to test Tenax TA/DVB sorbent film (n=3). Solutions (10 cm^3) were added to the chamber (850 cm^3) with a specified sorbent film. Films were left for 2 h in the chamber before solvent extraction and GC-MS analysis.

Table 3.7. Average abundances and SD of VOCs recovered from each of the NS_{aq} solutions (10 cm^3) used to test Tenax TA/DVB sorbent film (n=3). Solutions (10 cm^3) were added to the chamber (850 cm^3) with a specified sorbent film. Films were left for 2 h in the chamber before solvent extraction and GC-MS analysis. n/d=not detected.

VOC	RT (mins)	Abundances for Control (H_2O only)	Abundances for 0.10% (v/v) NS_{aq}	Abundances for 0.25% (v/v) NS_{aq}	Abundances for 0.50% (v/v) NS_{aq}	Abundances for 0.75% (v/v) NS_{aq}	Abundances for 1% (v/v) NS_{aq}
Acetic acid	3.14	n/d	**n/d**	n/d	n/d	n/d	n/d
Heptanoic acid	13.40	n/d	**n/d**	n/d	37 945 ±10 204	58 426 ±3 926	n/d
Octanoic acid	14.95	n/d	**n/d**	n/d	n/d	n/d	n/d
Nonanoic acid	16.33	n/d	**n/d**	n/d	n/d	n/d	n/d
Decanoic acid	17.63	n/d	**n/d**	n/d	n/d	n/d	n/d
Dodecanoic acid	20.12	n/d	**n/d**	n/d	n/d	n/d	n/d
Octanal	11.85	n/d	**445 130 ±13 176**	625 543 ±4 054	1 145 624 ±58 600	1 185 904 ±84 061	1 138 014 ±35 724
Nonanal	13.70	n/d	**1 138 512 ±21 991**	1 463 008 ±36 334	2 659 542 ±122 663	2 364 548 ±145 095	2 233 384 ±81 585
Decanal	15.35	n/d	**1 027 947 ±24 623**	1 329 325 ±30 152	2 338 164 ±108 203	1 856 371 ±130 088	1 812 302 ±69 037
Undecanal	16.85	n/d	**870 962 ±21 261**	975 130 ±28 316	1 622 547 ±62 469	1 198 347 ±100 706	1 260 383 ±58 689
Dodecanal	18.24	n/d	**688 644 ±24 496**	605 251 ±31 431	894 941 ±58 393	669 233 ±46 118	679 640 ±36 242
6-methyl-5-hepten-2-one	11.50	n/d	**919 609 ±25 473**	1 589 758 ±164 250	2 400 651 ±93 488	2 971 769 ±284 672	2 960 165 ±88 186
6,10-dimethyl-5,9-undecadien-2-one	18.60	n/d	**623 089 ±12 313**	477 673 ±27 342	766 105 ±63 269	491 754 ±20 556	470 109 ±106 434
2-ethyl-1-hexanol	12.35	n/d	**58 522 ±3 649**	102 463 ±755	141 471 ±9 052	129 897 ±2 947	112 031 ±6 504
1-dodecanol	19.10	n/d	**n/d**	n/d	n/d	n/d	n/d

3.3.5. PDMS planar film sorption testing

PDMS films were prepared as described in the Methods Section 3.2.7. Following thermal treatment, each PDMS film was weighed using an analytical mass balance. Average film masses were recorded to be 140.60 ±3.10 mg. The prepared PDMS films were subjected to VOC adsorption experiments, following the NS_{aq} concentration range shown in Table 3.4.

A control PDMS film were subject to solvent extraction, after 2-hour exposure to ambient laboratory air to explore their by-products and inspect for contaminants. From these results, only the hexane solvent peak was visible on the chromatograph. No compounds were identified that passed criteria set in the Methods, nor were there any peaks after the solvent peak which remained unidentified.

15 skin representative compounds were prepared as NS_{aq} at five different concentrations for each experiment inside a 850 cm^3 chamber. These concentrations were calculated to be 0.10% (v/v), 0.25% (v/v), 0.50% (v/v), 0.75% (v/v) and 1% (v/v), respectively. Finally, the single-phase PDMS film sorption performance was examined.

Overall, for the two-hour chamber NS_{aq} solution sampling at all concentrations investigated, no compounds were successfully recovered using the PDMS film. This was the same for the control experiment, where a blank HS was sampled. This result was not expected, as for other reported VOC sampling work[15], PDMS has been deemed a suitable sorbent material. The PDMS films used here however were demonstrated to be unsuitable for sampling the skin VOC standard mixture (sampling duration 2 h at room temperature).

As these films were commercially produced, it may be that some additional processing steps for these sheets were used, impeding their ability to adsorb VOCs. Thus future work should investigate casting PDMS films and investigating for this purpose as other researchers have found good recoveries of skin VOCs, in-vivo. Published PDMS materials include rolling stir bars[32], polymer strips[33], wearable polymer loops[15], and direct contact skin patches[34–36].

The selected 2-hour sampling duration may not have allowed enough time for a passive diffusive adsorption process to occur onto the PDMS films. Additionally, PDMS flexibility and swelling properties are reported to enable good performance in humid HS, given its siloxane-based polymer backbone. However, compared to Tenax TA, chemically engineered towards high surface areas[18], PDMS elastomer surface areas are lower, often necessitating sampling durations of days, at minimum[33].

3.3.6. Comparison of film sorption between Tenax TA and Tenax TA/DVB

The lowest concentrations tested using Tenax TA and Tenax TA/DVB sorbents were compared to each other to examine their adsorbent performance using this method. These concentrations were determined to be 0.10% (v/v) of NS_{aq}. A comparison between these two solvent extracted sorbent films and their recovered abundances is explored as part of Table 3.8.

At the same NS_{aq} concentrations per each air-water system the total recovered compounds (TVOC) were calculated as a sum of all recovered compounds. The average abundance of TVOC for Tenax TA (≅2,184,581) films was observed to be significantly greater when DVB was present in the adsorbent (≅5,772,415). The abundances increased a magnitude of 2.64x for the compound peak areas in terms of TVOC average abundances, when the Tenax TA/DVB film is used, compared to the Tenax TA film. A Wilcoxson signed rank-test indicates that compound abundances using Tenax TA films were statistically lower than those recovered using the Tenax TA/DVB films, in every single paired comparison (p=0.0156). This significance represented VOCs recovered by both sorbent materials, therefore excluding 2-ethyl-1-hexanol abundances.

Table 3.8. lists the relative standard deviation (%RSD) for 6 aldehyde and 2 ketone compounds recovered using both of these sorbents, respectively. This shows that the relative errors were mostly within 9% for both sorbent materials, indicating that this experiment had a degree of repeatability and comparability, for these recovered aldehydes and ketones.

Furthermore, the presence of DVB within the sorbent matrix significantly enhanced this reproducibility. This is shown as roughly 50% decrease in %RSD values, for all aldehyde and ketone compounds, compared to when DVB was absent from the sorbent phase. Additionally, the recovery of 2-ethyl-1-hexanol becomes feasible at these 0.10% (v/v) concentrations, highlighted by a RSD of 6.24% for n=3 samples. Using this average recovered abundance of 2-ethyl-1-hexanol as approximately 58,522 while using $y = 300538x - 89112$ of Figure 3.5., this corresponding concentration is calculated to be approximately 0.49 ppm 2-ethyl-1-hexanol.

Keeping these results in mind, the optimal sorbent of these three appears to be Tenax TA/DVB, to apply these insights onto testing these on skin. However, given the persistence and uncertainly regarding DVB and its interaction with skin, this was avoided and reserved for future method development. Instead, the biocompatible PDMS film and the prepared Tenax TA film were adapted into a wearable format to test in contactless VOC sampling from the skin, in the second part of this study.

Table 3.8. Comparison of average abundances of recovered compound, between the prepared Tenax TA and Tenax TA/DVB films. PDMS films are not shown, due to lack of compound identifications from their chromatographs.

VOC	RT (mins)	0.10% (v/v) NS_{aq} abundance for Tenax TA film	%RSD for Tenax TA film	0.10% (v/v) NS_{aq} abundance for Tenax TA/DVB film	%RSD for Tenax TA/DVB film
Acetic acid	3.14	n/d	-	n/d	-
Heptanoic acid	13.40	n/d	-	n/d	-
Octanoic acid	14.95	n/d	-	n/d	-
Nonanoic acid	16.33	n/d	-	n/d	-
Decanoic acid	17.63	n/d	-	n/d	-
Dodecanoic acid	20.12	n/d	-	n/d	-
Octanal	11.85	154 303 ±13 403	**8.69%**	445 130 ±13 176	**2.96%**
Nonanal	13.71	477 584 ±23 295	**4.88%**	1 138 512 ±21 991	**1.93%**
Decanal	15.35	474 651 ±19 418	**4.09%**	1 027 947 ±24 623	**2.40%**
Undecanal	16.85	366 332 ±19 734	**5.39%**	870 962 ±21 261	**2.44%**
Dodecanal	18.24	208 421 ±83 370	**40.00%**	688 644 ±24 496	**3.56%**
6-methyl-5-hepten-2-one	11.49	373 420 ±20 111	**5.39%**	919 609 ±25 473	**2.77%**
6,10-dimethyl-5,9-undecadien-2-one	18.63	129 870 ±11 087	**8.54%**	623 089 ±12 313	**1.98%**
2-ethyl-1-hexanol	12.35	n/d	-	58 522 ±3 649	**6.24%**
1-dodecanol	19.09	n/d	-	n/d	-

3.3.7. Sorbent film testing on skin

In the second part of the experiment, P1 volar forearm was non-invasively sampled using Tenax TA and PDMS films. 3 samples were collected using Tenax TA films, while 3 samples were collected using PDMS films. These sorbent films were adapted into a wearable format described as part of Figure 3.4.

Briefly, sorbent films were incorporated into an adherent wound dressing and secured with adhesive. The flexible steel mesh was cut to cover the entire planar film area (9 cm x 9 cm) to prevent direct contact with the skin surface. After 8-hour sampling, the dressing was removed, and the sorbent film was transferred to 2 cm^3 hexane for solvent extraction as per Section 3.3.9.

For the Tenax TA film in wearable format, peaks of benzene-derivatives were present in the chromatographs, as was found for the solvent extracted controls. 4 of these relatively prominent peaks are shown in black in Figure 3.10. (between RT=13 min and 14.50 min). Unfortunately, no skin derived VOCs were recovered from the volar forearm skin for the sampling duration of 8 hours. This may have been a result of an incomplete closure on the HS by the wound dressing, allowing VOC removal, therefore this should be optimised for future experiments.

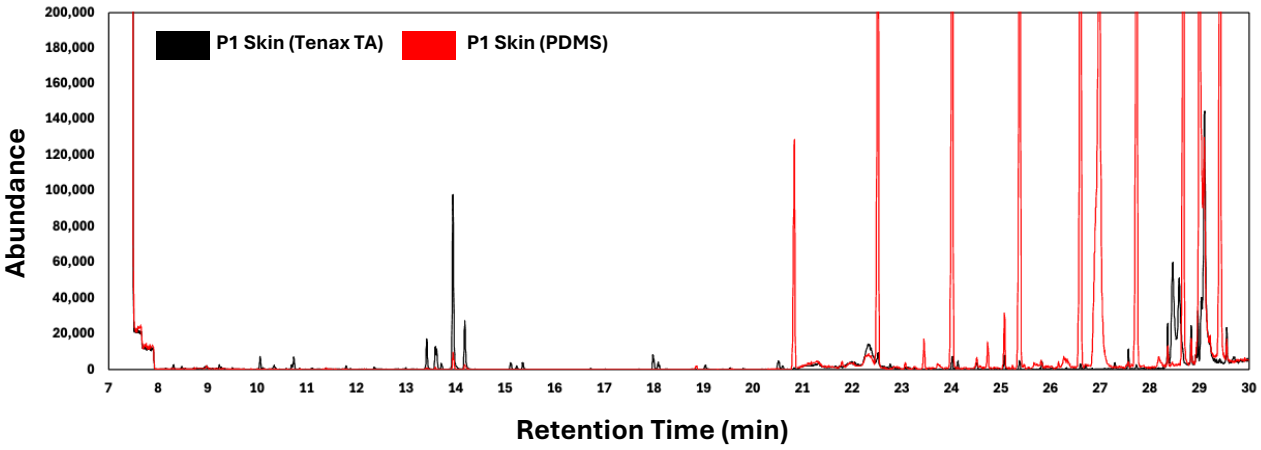

Figure 3.10. A representative raw chromatograph obtained from P1 volar forearm wearable Tenax TA skin sample (black) and P1 volar forearm wearable PDMS skin sample (red). The sampling duration used for both films was 8 h. The films were solvent extracted immediately after sampling using 2 cm^3 hexane for ALS-GC-MS analysis (n=3).

Using PDMS films in wearable format, isopropyl palmitate (RT=25.10 min) was successfully recovered from P1 volar forearm skin, listed in Table 3.9. Although this is not thought to be endogenous, it is likely to be derived from an applied personal care product. There were several highly abundant siloxane peaks appearing in the latter part of the chromatograph, however none of these peaks passed the set criteria from the Methods. A representative chromatograph was shown in red overlaid in Figure 3.10. This chromatographic feature of abundant siloxanes was not present in any of the controls or NS_{aq} collection experiments performed using the PDMS film.

Examining the volar forearm HS-SPME skin sampling conducted in this study, isopropyl palmitate was recovered in 2 out of 3 samples. This compound was not found in blank SPME fibre chromatographs, nor was it found in the PDMS film controls.

The average abundance recovered from HS-SPME approach was approximately 15,000 for 15 min, compared to an average abundance of approximately 47,000 for 8 hours. Furthermore, unidentifiable yet prominent peaks appeared in the latter part of the chromatograph at RT=27 min and RT=29 min, respectively. These could indicate less volatile compounds adsorbed to the PDMS from the skin, or from the wound dressing employed.

Table 3.9. Comparison of recovered isopropyl palmitate from P1 volar forearm HS-SPME skin and from the solvent extraction of a PDMS film worn on P1 volar forearm. GC chromatographs were obtained through a 2 min SPME desorption in the GC inlet or through direct liquid injections with ALS. No SD is shown due to n=2 samples.

Method	RT (min)	Identified VOC	Match Factor (%)	Average absolute abundance (n=2)
P1 skin 3cm^3 HS-SPME	25.10	Isopropyl palmitate	71	14 765
P1 skin PDMS film and solvent extraction	25.07	Isopropyl palmitate	77	47 112

To enable a greater degree of accuracy and to lower LODs, this procedure should be repeated using solventless extraction techniques for input into GC-MS analysis. Extraction techniques such as thermal desorption have merit over solvent based techniques, as they avoid additional solvation effects associated with using a large variety of solvents, and the interactions with those solvents. Dutta et al. has also proposed that the optimal adsorption for small aldehydes occurs under sub-zero temperatures, whilst increasing the desorption temperatures of sorbent materials lowers any analyte losses[19]. Thermal desorption units are usually fitted with cold traps to harness these effects, resulting in increased chromatographic resolutions and LODs.

3.4 Conclusion

Through replicating skin VOC emission sampling, a range of three sorbent materials (Tenax TA, Tenax TA/DVB and PDMS), in planar film format, were assessed for their ability to collect VOCs from static gas HS. Exploring alternatives past commercially available HS-SPME skin VOC sampling approaches is a primary goal towards enlarging study participant cohorts, for more accessible and high quality skin VOC sampling.

Supported by future development, these findings may be integrated into wider scale wearable skin VOC samplers, given performance parity with current HS-SPME VOC collection techniques. In future, to optimise VOC collection, a lower range of headspace concentrations, in addition to a wider array of sorbent materials, should be explored following the developed method for sorbent material testing. Overall, a multi-adsorbent type approach offered higher sensitivity and better reproducibility for skin relevant aldehydes and ketones, compared to single phase sorbents (Tenax TA or PDMS alone). Finally, having integrated these materials into a wearable format, volar forearm skin VOC collection abilities were evaluated and compared to the HS-SPME approach, predominantly used to date.

Extraction and GC-MS analysis of the wearable VOC sampler using the Tenax TA film did not show any compounds collected from the volar forearm. The PDMS based wearable sampler likely showed a degree of affinity to lower volatility compounds, although these were not able to be reliably identified, possibly due to our GC-MS method optimised towards more volatile compound analysis. Future work should also include repeating this experimental method using solventless extraction techniques such as exploring performance of this method through thermal desorption VOC extraction approach and comparing the sensitivity to the developed and described method of this work.

3.5. References

(1) Morrison, G. C.; Eftekhari, A.; Majluf, F.; Krechmer, J. E. Yields and Variability of Ozone Reaction Products from Human Skin. *Environ. Sci. Technol.* **2021**, *55* (1), 179–187. https://doi.org/10.1021/acs.est.0c05262.

(2) Finnegan, M.; Fitzgerald, S.; Duroux, R.; Attia, J.; Markey, E.; O'Connor, D.; Morrin, A. Predicting Chronological Age via the Skin Volatile Profile. *J. Am. Soc. Mass Spectrom.* **2024**, jasms.3c00315. https://doi.org/10.1021/jasms.3c00315.

(3) S., K.; Saquib, M.; Poojary, H.; Illanad, G.; Valavan, D.; M, S.; Nayak, R.; Mazumder, N.; Ghosh, C. Skin Emitted Volatiles Analysis for Noninvasive Diagnosis: The Current Advances in Sample Preparation Techniques for Biomedical Application. *RSC Adv.* **2024**, *14* (17), 12009–12020. https://doi.org/10.1039/D4RA01579G.

(4) Baker, P.; Huang, C.; Radi, R.; Moll, S. B.; Jules, E.; Arbiser, J. L. Skin Barrier Function: The Interplay of Physical, Chemical, and Immunologic Properties. *Cells* **2023**, *12* (23), 2745. https://doi.org/10.3390/cells12232745.

(5) Oh, J.; Byrd, A. L.; Park, M.; Kong, H. H.; Segre, J. A. Temporal Stability of the Human Skin Microbiome. *Cell* **2016**, *165* (4), 854–866. https://doi.org/10.1016/j.cell.2016.04.008.

(6) Moissl-Eichinger, C.; Probst, A. J.; Birarda, G.; Auerbach, A.; Koskinen, K.; Wolf, P.; Holman, H.-Y. N. Human Age and Skin Physiology Shape Diversity and Abundance of Archaea on Skin. *Sci. Rep.* **2017**, *7* (1), 4039. https://doi.org/10.1038/s41598-017-04197-4.

(7) Wang, N.; Müller, T.; Ernle, L.; Bekö, G.; Wargocki, P.; Williams, J. How Does Personal Hygiene Influence Indoor Air Quality? *Environ. Sci. Technol.* **2024**, *58* (22), 9750–9759. https://doi.org/10.1021/acs.est.4c01698.

(8) Hiramoto, T.; Kakumu, Y.; Sato, S.; Sekine, Y. Deodorising Garlic Body Odour by Ingesting Natural Food Additives Containing Phenolic Compounds and Polyphenol Oxidase. *Appl. Sci.* **2024**, *14* (21), 9631. https://doi.org/10.3390/app14219631.

(9) Weschler, C. J.; Nazaroff, W. W. Human Skin Oil: A Major Ozone Reactant Indoors. *Environ. Sci. Atmospheres* **2023**, *3* (4), 640–661. https://doi.org/10.1039/D3EA00008G.

(10) Zhang, H.; Zhu, Y.; Liu, Z.; Peng, Y.; Peng, W.; Tong, L.; Wang, J.; Liu, Q.; Wang, P.; Cheng, G. A Volatile from the Skin Microbiota of Flavivirus-Infected Hosts Promotes Mosquito Attractiveness. *Cell* **2022**, *185* (14), 2510-2522.e16. https://doi.org/10.1016/j.cell.2022.05.016.

(11) Ampong, I.; Zimmerman, K. D.; Nathanielsz, P. W.; Cox, L. A.; Olivier, M. Optimization of Imputation Strategies for High-Resolution Gas Chromatography–Mass Spectrometry (HR GC–MS) Metabolomics Data. *Metabolites* **2022**, *12* (5), 429. https://doi.org/10.3390/metabo12050429.

(12) Arulvasan, W.; Chou, H.; Greenwood, J.; Ball, M. L.; Birch, O.; Coplowe, S.; Gordon, P.; Ratiu, A.; Lam, E.; Hatch, A.; Szkatulska, M.; Levett, S.; Mead, E.; Charlton-Peel, C.; Nicholson-Scott, L.; Swann, S.; Van Schooten, F.-J.; Boyle, B.; Allsworth, M. High-Quality Identification of Volatile Organic Compounds (VOCs) Originating from Breath. *Metabolomics* **2024**, *20* (5), 102. https://doi.org/10.1007/s11306-024-02163-6.

(13) Shetewi, T.; Finnegan, M.; Fitzgerald, S.; Xu, S.; Duffy, E.; Morrin, A. Investigation of the Relationship between Skin-Emitted Volatile Fatty Acids and Skin Surface Acidity in Healthy Participants—a Pilot Study. *J. Breath Res.* **2021**, *15* (3), 037101. https://doi.org/10.1088/1752-7163/abf20a.

(14) Forbes, S. L.; Rust, L.; Trebilcock, K.; Perrault, K. A.; McGrath, L. T. Effect of Age and Storage Conditions on the Volatile Organic Compound Profile of Blood. *Forensic Sci. Med. Pathol.* **2014**, *10* (4), 570–582. https://doi.org/10.1007/s12024-014-9610-3.

(15) Roodt, A. P.; Naudé, Y.; Stoltz, A.; Rohwer, E. Human Skin Volatiles: Passive Sampling and GC × GC-ToFMS Analysis as a Tool to Investigate the Skin Microbiome and Interactions with Anthropophilic Mosquito Disease Vectors. *J. Chromatogr. B* **2018**, *1097–1098*, 83–93. https://doi.org/10.1016/j.jchromb.2018.09.002.

(16) Jiang et al. - 2013 - A Non-Invasive Method for in Vivo Skin Volatile Compounds Sampling.

(17) Axel Clausen, P.; Wolkoff, P. Degradation Products of Tenax TA Formed during Sampling and Thermal Desorption Analysis: Indicators of Reactive Species Indoors. *Atmos. Environ.* **1997**, *31* (5), 715–725. https://doi.org/10.1016/S1352-2310(96)00230-0.

(18) Alfeeli, B.; Taylor, L. T.; Agah, M. Evaluation of Tenax TA Thin Films as Adsorbent Material for Micro Preconcentration Applications. *Microchem. J.* **2010**, *95* (2), 259–267. https://doi.org/10.1016/j.microc.2009.12.011.

(19) Dutta, T.; Kim, K.-H.; Brown, R. J. C.; Kim, Y.-H.; Boukhvalov, D. Metal-Organic Framework and Tenax-TA as Optimal Sorbent Mixture for Concurrent GC-MS Analysis of C1 to C5 Carbonyl Compounds. *Sci. Rep.* **2018**, *8* (1), 5033. https://doi.org/10.1038/s41598-018-23391-6.

(20) Klenø, J. G.; Wolkoff, P.; Clausen, P. A.; Wilkins, C. K.; Pedersen, T. Degradation of the Adsorbent Tenax TA by Nitrogen Oxides, Ozone, Hydrogen Peroxide, OH Radical, and Limonene Oxidation Products. *Environ. Sci. Technol.* **2002**, *36* (19), 4121–4126. https://doi.org/10.1021/es025680f.

(21) Poliquit, B. Z.; Burn, P. L.; Shaw, P. E. Properties of PDMS-Divinylbenzene Based Pre-Concentrators for Nitroaromatic Vapors. *J. Mater. Chem. C* **2020**, *8* (47), 16967–16973. https://doi.org/10.1039/D0TC03228J.

(22) Lepró, X.; Ehrmann, P.; Menapace, J.; Lotscher, J.; Shin, S.; Meissner, R.; Baxamusa, S. Ultralow Stress, Thermally Stable Cross-Linked Polymer Films of Polydivinylbenzene (PDVB). *Langmuir* **2017**, *33* (21), 5204–5212. https://doi.org/10.1021/acs.langmuir.7b01403.

(23) Uebi, T.; Hariyama, T.; Suzuki, K.; Kanayama, N.; Nagata, Y.; Ayabe-Kanamura, S.; Yanase, S.; Ohtsubo, Y.; Ozaki, M. Sampling, Identification and Sensory Evaluation of Odors of a Newborn Baby's Head and Amniotic Fluid. *Sci. Rep.* **2019**, *9* (1), 12759. https://doi.org/10.1038/s41598-019-49137-6.

(24) Drabińska, N.; Flynn, C.; Ratcliffe, N.; Belluomo, I.; Myridakis, A.; Gould, O.; Fois, M.; Smart, A.; Devine, T.; Costello, B. D. L. A Literature Survey of All Volatiles from Healthy Human Breath and Bodily Fluids: The Human Volatilome. *J. Breath Res.* **2021**, *15* (3), 034001. https://doi.org/10.1088/1752-7163/abf1d0.

(25) Mochalski, P.; King, J.; Unterkofler, K.; Hinterhuber, H.; Amann, A. Emission Rates of Selected Volatile Organic Compounds from Skin of Healthy Volunteers. *J. Chromatogr. B* **2014**, *959*, 62–70. https://doi.org/10.1016/j.jchromb.2014.04.006.

(26) Mochalski, P.; Wiesenhofer, H.; Allers, M.; Zimmermann, S.; Güntner, A. T.; Pineau, N. J.; Lederer, W.; Agapiou, A.; Mayhew, C. A.; Ruzsanyi, V. Monitoring of Selected Skin- and Breath-Borne Volatile Organic Compounds Emitted from the Human Body Using Gas Chromatography Ion Mobility Spectrometry (GC-IMS). *J. Chromatogr. B* **2018**, *1076*, 29–34. https://doi.org/10.1016/j.jchromb.2018.01.013.

(27) Goryński, K.; Goryńska, P.; Górska, A.; Harężlak, T.; Jaroch, A.; Jaroch, K.; Lendor, S.; Skobowiat, C.; Bojko, B. SPME as a Promising Tool in Translational Medicine and Drug Discovery: From Bench to Bedside. *J. Pharm. Biomed. Anal.* **2016**, *130*, 55–67. https://doi.org/10.1016/j.jpba.2016.05.012.

(28) Finnegan, M.; Duffy, E.; Morrin, A. The Determination of Skin Surface pH via the Skin Volatile Emission Using Wearable Colorimetric Sensors. *Sens. Bio-Sens. Res.* **2022**, *35*, 100473. https://doi.org/10.1016/j.sbsr.2022.100473.

(29) Zou, Z.; He, J.; Yang, X. An Experimental Method for Measuring VOC Emissions from Individual Human Whole-Body Skin under Controlled Conditions. *Build. Environ.* **2020**, *181*, 107137. https://doi.org/10.1016/j.buildenv.2020.107137.

(30) Chu, L.; Deng, S.; Zhao, R.; Deng, J.; Kang, X. Comparison of Adsorption/Desorption of Volatile Organic Compounds (VOCs) on Electrospun Nanofibers with Tenax TA for Potential Application in Sampling. *PLOS ONE* **2016**, *11* (10), e0163388. https://doi.org/10.1371/journal.pone.0163388.

(31) Jha, S. K.; Hayashi, K. A Quick Responding Quartz Crystal Microbalance Sensor Array Based on Molecular Imprinted Polyacrylic Acids Coating for Selective Identification of Aldehydes in Body Odor. *Talanta* **2015**, *134*, 105–119. https://doi.org/10.1016/j.talanta.2014.09.049.

(32) Soini, H. A.; Bruce, K. E.; Klouckova, I.; Brereton, R. G.; Penn, D. J.; Novotny, M. V. In Situ Surface Sampling of Biological Objects and Preconcentration of Their Volatiles for Chromatographic Analysis. *Anal. Chem.* **2006**, *78* (20), 7161–7168. https://doi.org/10.1021/ac0606204.

(33) Gibson, L. T.; Ewlad-Ahmed, A.; Knight, B.; Horie, V.; Mitchell, G.; Robertson, C. J. Measurement of Volatile Organic Compounds Emitted in Libraries and Archives: An Inferential Indicator of Paper Decay? *Chem. Cent. J.* **2012**, *6* (1), 42. https://doi.org/10.1186/1752-153X-6-42.

(34) Riazanskaia, S.; Blackburn, G.; Harker, M.; Taylor, D.; Thomas, C. L. P. The Analytical Utility of Thermally Desorbed Polydimethylsilicone Membranes for In-Vivo Sampling of Volatile Organic Compounds in and on Human Skin. *The Analyst* **2008**, *133* (8), 1020. https://doi.org/10.1039/b802515k.

(35) Martin, H. J.; Reynolds, J. C.; Riazanskaia, S.; Thomas, C. L. P. High Throughput Volatile Fatty Acid Skin Metabolite Profiling by Thermal Desorption Secondary Electrospray Ionisation Mass Spectrometry. *The Analyst* **2014**, *139* (17), 4279–4286. https://doi.org/10.1039/C4AN00134F.

(36) Martin, H. J.; Turner, M. A.; Bandelow, S.; Edwards, L.; Riazanskaia, S.; Thomas, C. L. P. Volatile Organic Compound Markers of Psychological Stress in Skin: A Pilot Study. *J. Breath Res.* **2016**, *10* (4), 046012. https://doi.org/10.1088/1752-7155/10/4/046012.

(37) Tan, E. K. W.; Rughoobur, G.; Rubio-Lara, J.; Tiwale, N.; Xiao, Z.; Davidson, C. A. B.; Lowe, C. R.; Occhipinti, L. G. Nanofabrication of Conductive Metallic Structures on Elastomeric Materials. *Sci. Rep.* **2018**, *8* (1), 6607. https://doi.org/10.1038/s41598-018-24901-2.

Chapter 4: Conclusions and future work

4.1. Conclusion and future work

Skin-emitted volatile compounds are increasingly identified as useful probes for non-invasive health monitoring. However, these measurements provide limited robust health insights due to a lack of standardised methods and small study cohort sizes. Keeping this in mind, Chapter 1 reviews the recent research to reveal a complex mixture of compounds from different sources, underscoring the importance of understanding skin VOC biochemical origin. The composition of skin VOC emissions was reported to change with respect to the anatomy of the skin, while an expansive skin microbiome, comprising resident and transient microbes, supported person-to-person variance in skin VOC emissions. The myriad of approaches for skin VOC capture was explored highlighting the range of analysis techniques used in the field currently.

The primary aim of this work was to comparatively characterise the skin volatile profile of different participants using current and robust skin VOC workflows. Through non-invasively harnessing the volatile emissions of the skin, which is continually and passively emitted from skin, tremendous biomonitoring and diagnostic applications became apparent. Further research across larger participant cohorts is the next step to enrich this field. Contributing to this endeavour, this work evaluates the correlation of skin volatile emissions to the skin barrier function, across different subjects. Looking to adapt this skin sampling technique into a simple and low-cost platform, adsorbent materials were evaluated for their ability to retain a similar set of compounds from the gas phase. A mixture of aldehydes, ketones and an alcohol was simultaneously retained from the gas HS using the prepared adsorbents, and identified using gas chromatography-mass spectrometry (GC-MS). Finally, this work introduces a simple and wearable skin VOC sample collection protocol and highlights its potential to scale sampling of skin VOCs for larger cohorts.

Chapter 2 uses the robust HS-SPME technique for sampling skin VOCs with GC-MS analysis to measure skin VOC emissions of 3 different participants, over a period of 10 days, twice daily (n=60). Supporting this data, collected probe-based biophysical parameters (skin surface pH, tissue dielectric constant, transepidermal water loss and stratum corneum hydration) revealed a correlation between skin acidity and subject skin volatile acid emissions, across the participants. Furthermore, through constructed skin profiles and statistical analysis techniques, participant data over the study period were comprehensively visualised to reveal clustering. This showed the stability within each respective volatile profile while demonstrating a consistency across person-to-person variance in profiles as well.

Chapter 3 aims to overcome the need for the expensive and complex HS-SPME technique by exploiting the continual, passive emission from the skin and developing wearable planar film VOC samplers. A simple and scalable adsorbent film-based VOC sampling platform is developed, along with the method to test its performance. 3 different materials (Tenax TA, Tenax TA/DVB and PDMS) were tested for their ability to collect gaseous compounds, of relevance to the skin. The testing revealed the best performing material to be Tenax TA/DVB, reliably recovering a range of aldehydes, ketones and an alcohol from a gas HS. Adapting these films into a wearable format, the worn PDMS sampler showed overlap with a volatile recovered from the skin using the HS-SPME technique. The sensitivity of these samplers when worn must be addressed in future work to realise the full potential of this skin VOC collection approach.

Looking to the near future, the contributions of this work to skin volatile research are important to address. Further study into the biochemical origins of skin VOCs will enrich the choices available for sampling and analysis approaches, so researchers can make more informed decisions. Robustly identifying a set of target compounds from skin, for a large population cohort study is the next step for VOCs becoming meaningful probes of non-invasive health information[1]. Toward this goal, the current HS-SPME technique has many merits, yet requires complex sampling protocol, coupled with its expensive cost, may be unsuitable for larger scale sample collection[2].

Building on this work to develop lower cost sampling approaches in planar film format the next goal should be modifying the method used to transfer the retained compounds. Solventless, thermal extraction techniques have been reported to increase LOD of such transfer of compounds for trace analysis, compared to solvent extraction[3]. This, in conjunction with further optimising the material properties, should increase the platforms sensitivity, in an effort to improve the recovered compound performance while worn on the volar forearm.

DVB has a great ability to form a variety of complex co-polymer networks[4,5]. Combined with robust surface analysis and binding site optimisation, DVB may be further used to develop a sampling material, whose VOC sorbent performance exceeds the developments in this work. Lastly, further optimisation and effort to enclose the worn VOC sampler HS completely, while not sacrificing comfort during wear, is of paramount importance, apparent in this work. Improving these identified areas may improve the performance of the introduced wearable platform, harnessing the full potential of skin VOC sampling across large populations.

4.2. References

(1) Arulvasan, W.; Chou, H.; Greenwood, J.; Ball, M. L.; Birch, O.; Coplowe, S.; Gordon, P.; Ratiu, A.; Lam, E.; Hatch, A.; Szkatulska, M.; Levett, S.; Mead, E.; Charlton-Peel, C.; Nicholson-Scott, L.; Swann, S.; Van Schooten, F.-J.; Boyle, B.; Allsworth, M. High-Quality Identification of Volatile Organic Compounds (VOCs) Originating from Breath. *Metabolomics* **2024**, *20* (5), 102. https://doi.org/10.1007/s11306-024-02163-6.

(2) S., K.; Saquib, M.; Poojary, H.; Illanad, G.; Valavan, D.; M, S.; Nayak, R.; Mazumder, N.; Ghosh, C. Skin Emitted Volatiles Analysis for Noninvasive Diagnosis: The Current Advances in Sample Preparation Techniques for Biomedical Application. *RSC Adv.* **2024**, *14* (17), 12009–12020. https://doi.org/10.1039/D4RA01579G.

(3) Finnegan, M.; Fitzgerald, S.; Duroux, R.; Attia, J.; Markey, E.; O'Connor, D.; Morrin, A. Predicting Chronological Age via the Skin Volatile Profile. *J. Am. Soc. Mass Spectrom.* **2024**, jasms.3c00315. https://doi.org/10.1021/jasms.3c00315.

(4) Poliquit, B. Z.; Burn, P. L.; Shaw, P. E. Properties of PDMS-Divinylbenzene Based Pre-Concentrators for Nitroaromatic Vapors. *J. Mater. Chem. C* **2020**, *8* (47), 16967–16973. https://doi.org/10.1039/D0TC03228J.

(5) Poliquit, B. Z.; Burn, P. L.; Shaw, P. E. Understanding the Mechanism of Nitroaromatic Vapour Uptake in PDMS-Based Pre-Concentrators Using 4-Nitrotoluene. *Sens. Diagn.* **2022**, *1* (4), 821–828. https://doi.org/10.1039/D2SD00045H.

Appendix

Chapter 2

Table A2.1. Wilcoxon ranked sum test p values for AM/PM differences (Figure 2.3.) per each collected skin barrier function variable, for each participant.

	P1	P2	P3
SspH	0.3594	0.1602	0.9219
TDC	0.3105	0.8457	0.0840
TEWL	0.6035	0.0098	0.4766
SCH	0.9805	0.4062	0.3223

Table A2.2. Input variables and their corresponding value output from PCA, in addition to principal component regression (PCR) model p values of each corresponding input variable.

Input Variable	**PCA Eigenvector Output**		**PCR p-value**
	PC1	PC2	MLR and PCA models
Time (Across Days)	0.049	-0.172	<0.0001
Time (Within a Day)	-0.001	0.284	0.0055
pH	0.327	0.186	<0.0001
TDC	0.036	-0.042	<0.0001
TEWL	-0.132	-0.362	0.0031
SCH	-0.293	-0.246	<0.0001
Acetic acid	-0.318	-0.025	0.0183
Heptanoic acid	-0.227	-0.110	0.0003
Octanoic acid	-0.362	-0.086	<0.0001
Nonanoic acid	-0.349	-0.132	<0.0001
Decanoic acid	-0.288	-0.079	<0.0001
Nonanal	-0.300	0.302	0.0339
Decanal	-0.288	0.401	0.5880
6-MHO	-0.042	0.555	<0.0001
Geranyl acetone	-0.351	0.205	<0.0001
2-ethyl-1-hexanol	-0.011	0.124	<0.0001

Table A2.3. Tabular results of simple linear regression for Figure 2.10. (a)

SLR Output	P1	P2	P3
Correlation Coefficient (R^2)	0.53	0.72	0.28
Significance (p value)	0.0004	0.0163	0.1810
Linear equation	Y = -420 566x + 2010973	Y = -433 846x + 2242100	Y = -173 681x + 1185789

Table A2.4. Tabular results of simple linear regression for Figure 2.10. (b)

SLR Output	P1	P2	P3
Correlation Coefficient (R^2)	0.21	0.29	0.14
Significance (p value)	**0.0450**	**0.0892**	0.2876
Linear Equation	y = -542343x + 2743907	y = -170786x + 1147223	y = -590377x + 3000484

Table A2.5. Tabulated results of PCA variance for each PC and the corresponding SD for all sample collected per each participant (n=20). A higher SD represents a more variable volatile profile observed throughout the duration of the study.

Participant	PC1	PC2	SD
1	2.1850	1.3702	3.5552
2	1.3475	1.7000	3.0475
3	0.9031	1.0853	1.9884